

# THE INTERFEROMETRY OF REVERSED AND NON-REVERSED SPECTRA

By CARL BARUS

*Hazard Professor of Physics and Dean of the Graduate Department  
in Brown University*



PUBLISHED BY THE CARNEGIE INSTITUTION OF WASHINGTON  
WASHINGTON, 1916

CARNEGIE INSTITUTION OF WASHINGTON  
PUBLICATION No. 249

PRINTED BY J. B. LIPPINCOTT COMPANY  
AT THE WASHINGTON SQUARE PRESS  
PHILADELPHIA, U. S. A.

# CONTENTS.

| CHAPTER I.— <i>The Interferences of Crossed Spectra.</i>  |  | PAGE |
|---|--|------|
| 1. Introductory.....  |  | 7    |
| 2. Coincident spectra with one reversed on a given Fraunhofer line. Figs. 1, 2, 3...  |  | 8    |
| 3. The same. Further experiments.....   |  | 11   |
| 4. Coincident spectra with one reversed on a given longitudinal axis. Figs. 4, 5, 6...                                      |  | 12   |
| 5. Interference of the corresponding first-order spectra of the grating, in the absence of rotation. Figs. 7, 8, 9, 10..... |  | 14   |
| 6. Conclusion.....  |  | 16   |
| CHAPTER II.— <i>Further Study of the Interference of Reversed Spectra.</i>  |  |      |
| 7. Apparatus with one grating. Figs. 11, 12, 13, <i>a, b</i> .....  |  | 19   |
| 8. Observations and experiments with a single grating. Fig. 14.....   |  | 22   |
| 9. Inferences. Fig. 15, <i>a, b</i> .....   |  | 24   |
| 10. Apparatus with two gratings. Figs. 16, 17, 18.....  |  | 26   |
| 11. Experiments continued. New interferometer. Figs. 19, 20.....  |  | 30   |
| 12. Experiments continued. Homogeneous light.....   |  | 32   |
| 13. Experiments continued. Contrast of methods.....   |  | 33   |
| 14. Experiments continued. Rotation, etc., of grating. Figs. 21, 22.....  |  | 33   |
| 15. Tentative equations. Figs. 23, 24, 25.....  |  | 36   |
| 16. Experiments continued. Analogies. Figs. 26, 27.....   |  | 38   |
| 17. Subsidiary diffractions. Figs. 28, 29.....  |  | 43   |
| 18. Conclusion.....   |  | 45   |
| CHAPTER III.— <i>The Interferences of Non-reversed Spectra of Two Gratings.</i>   |  |      |
| 19. Introduction. Method. Figs. 30, 31.....   |  | 46   |
| 20. White light. Colored fringes. Tables 1, 2, 3. Figs. 32, 33, 34, 35.....   |  | 47   |
| 21. Homogeneous light. Wide slit. Transverse axes coincident. Tables 4, 5. Fig. 36...                                       |  | 52   |
| 22. Homogeneous light. Fine slit. Transverse axes not coincident. Table 6. Fig. 37.   |  | 54   |
| 23. Homogeneous light. Slit and collimator removed. Table 7. Fig. 38.....   |  | 55   |
| 24. Inferences. Figs. 39, 40.....   |  | 56   |
| 25. Rotation of colored fringes. Non-reversed spectra. Figs. 41, 42.....  |  | 58   |
| 26. Final treatment of reversed spectra. Hypothetical case. Figs. 43, 44, 45, 46....  |  | 60   |
| 27. Case of reflecting grating. Homogeneous light. Figs. 47, 48.....  |  | 64   |
| 28. Non-symmetrical positions. Fore-and-aft motion. Fig. 49.....  |  | 67   |
| CHAPTER IV.— <i>The Distance Between Two Parallel Transparent Plates.</i>   |  |      |
| 29. Introductory.....   |  | 69   |
| 30. Apparatus. Figs. 50, 51.....  |  | 69   |
| 31. Equations. Figs. 52, 53.....  |  | 70   |
| 32. Method.....   |  | 72   |
| 33. Observations and corrections. Preliminary work. Figs. 54, 55.....   |  | 73   |
| CHAPTER V.— <i>Interferometers for Parallel and for Crossed Rays.</i>   |  |      |
| 34. Introduction. Methods. Figs. 56, 57.....  |  | 78   |
| 35. Experiment. Reflecting grating. Parallel rays. Fig. 58.....   |  | 79   |
| 36. Experiments. Transmitting grating. Parallel rays.....   |  | 81   |
| 37. Experiments. Transmitting grating. Crossed rays. Figs. 59, 60, 61, <i>a, b</i> .....                                    |  | 82   |
| 38. The same. The linear phenomenon. Fig. 62.....   |  | 85   |
| 39. The same. Inferences. Figs. 63, 64, 65.....   |  | 87   |
| 40. Experiments. Reflecting grating. Crossed rays. Figs. 66, 67.....  |  | 88   |
| 41. The same. Compensators.....   |  | 91   |
| 42. Miscellaneous experiments. Fringes with mercury light.....  |  | 91   |
| 43. Inferences. Figs. 68, 69.....   |  | 92   |

CHAPTER VI.—*Channeled Spectra Occurring in Connection with the Diffraction of Reflecting Gratings.*

|   |     |
|---|-----|
| 44. Introductory.....                       | 95  |
| 45. Apparatus. Fig. 70.....                 | 95  |
| 46. Scattering.....                         | 95  |
| 47. Fringes with white light.....           | 96  |
| 48. Fringes with sodium light.....          | 97  |
| 49. Grating on a spectrometer. Fig. 71..... | 98  |
| 50. Inferences.....                         | 100 |

CHAPTER VII.—*Prismatic Methods in Reversed and Non-reversed Spectrum Interferometry.*

|  |     |
|--|-----|
| 51. Purpose.....                                     | 102 |
| 52. Method and apparatus. Figs. 72, 73.....          | 102 |
| 53. The same. Crossed rays.....                      | 103 |
| 54. Another method. Fig. 74.....                     | 104 |
| 55. Methods using prismatic dispersion. Fig. 75..... | 105 |
| 56. Methods with paired prisms. Fig. 76.....         | 106 |

CHAPTER VIII.—*The Linear Type of Displacement Interferometers.*

|  |     |
|--|-----|
| 57. Introductory.....                              | 107 |
| 58. Apparatus. Fig. 77.....                        | 107 |
| 59. Film grating. Adjustment. Figs. 78, 79.....    | 109 |
| 60. Michelson's interferences.....                 | 110 |
| 61. Film grating. Another adjustment. Fig. 80..... | 111 |
| 62. Equations.....                                 | 111 |

CHAPTER IX.—*The Use of Compensators Bounded by Curved Surfaces.*

|   |     |
|---|-----|
| 63. Introduction.....   | 113 |
| 64. Lens systems.....   | 113 |
| 65. Effective thickness of the lenticular compensator. Fig. 81.....                   | 115 |
| 66. Observations largely with weak lenses and short interferometer. Figs. 82, 83..... | 116 |
| 67. Remarks. Fig. 84.....   | 118 |
| 68. Observation with lens systems on both sides. Figs. 85, 86.....                    | 119 |
| 69. Telescopic interferences. Figs. 87, 88, 89, 90, 91.....                           | 120 |

CHAPTER X.—*The Dispersion of Air.*

|  |     |
|--|-----|
| 70. Introduction. Table 8.....   | 124 |
| 71. Observations with arc lamp.....  | 124 |
| 72. Observations with sunlight. Single tube. Table 9.....                  | 125 |
| 73. Two (differential) refraction tubes. Table 10. Fig. 92.....            | 127 |
| 74. Differential and single refraction tubes. Sunlight. Tables 11, 12..... | 129 |
| 75. Distortion of glass absent.....  | 131 |
| 76. Further observations with sunlight. Table 13.....                      | 131 |
| 77. Conclusion.....  | 132 |

CHAPTER XI.—*The Refraction of Air with Temperature.*

|  |     |
|--|-----|
| 78. Apparatus. Fig. 93. Table 14.....                                | 133 |
| 79. Observations.....  | 134 |
| 80. Computation.....   | 135 |
| 81. Final experiments at 100°. Table 15.....                         | 136 |
| 82. Experiments at red heat.....                                     | 137 |
| 83. Further experiments at high temperatures. Fig. 94. Table 16..... | 139 |
| 84. Flames.....  | 140 |
| 85. Conclusion.....  | 141 |

CHAPTER XII.—*Adiabatic Expansion Observed with the Interferometer.*

|   |     |
|---|-----|
| 86. Introductory. Table 17.....                                       | 142 |
| 87. Experiments with short, bulky air-chambers.....                   | 143 |
| 88. Effect of strained glass.....                                     | 145 |
| 89. Equations.....  | 146 |
| 90. Experiments with long tubes. Diameter, 1 inch. Table 18.....      | 148 |
| 91. The same. Diameter of tube, 2 inches. Table 19.....               | 150 |
| 92. The same. Diameter of tube, 4 inches. Tables 20, 21. Fig. 95..... | 151 |

CHAPTER XIII.—*Miscellaneous Experiments.*

|  |     |
|--|-----|
| 93. Effect of ionization on the refraction of a gas.....   | 154 |
| 94. Mach's interferences. Fig. 96.....   | 155 |
| 95. A Rowland spectrometer for transmitting and reflecting gratings, plane or concave. Figs. 97, 98, 99..... | 156 |

## PREFACE.

The following account of my experiments has been given chronologically. Although many of the anomalous features, in which the interferences of superposed coördinated spectra first presented themselves, were largely removed in the later work, yet the methods used in the several papers, early and later, are throughout different. It therefore seemed justifiable to record them, together with the inferences they at first suggested. The pursuit of the subject as a whole was made both easier and more difficult by the unavoidable tremors of the laboratory in which I am working; for it is possibly easier to detect an elusive phenomenon if it is in motion among other similar stationary phenomena. But it is certainly difficult, thereafter, to describe it when found.

It will be convenient to refer to the cases in which one of the two coincident spectra from the same source is rotated  $180^\circ$  with reference to the other on a transverse axis (*i.e.*, an axis parallel to the Fraunhofer lines), under the term *reversed spectra*; while the term *inverted spectra* is at hand for those cases in which one of the paired spectra is turned  $180^\circ$  relative to the other on a longitudinal axis (*i.e.*, an axis parallel to the  $r-v$  length of the spectrum). In this book the latter are merely touched upon, briefly, in Chapter I, but they are now being investigated in detail and give promise of many interesting results. The chapter contains a full account of what may be seen with a single grating—the linear phenomenon, as I have called it, and which, if it stood alone, would be difficult to interpret.

In Chapter II, therefore, the interferences of reversed spectra are treated by the aid of two gratings, in virtue of which a multitude of variations are inevitably introduced. The phenomena are thus exhibited in a way leading much more smoothly to their identification.

This endeavor is given greater promise in Chapter III, which contains a comparison of the interferences of reversed and non-reversed spectra, the latter produced in a way quite different from those in my earlier work. Naturally these in their entirety are even more bewilderingly varied, and become particularly so when, as in Chapter IV, an intermediate reflection of one spectrum is admitted. But with this I was on more familiar ground, as I have hitherto, in these publications, given such investigations particular attention.

The flexibility of the new methods is well shown in Chapter V, where separated component beams can with equal facility be made to run in parallel, or across each other at any angle, and perhaps both, with the double result visible in the field of the telescope. In case of crossed rays a remarkable phenomenon is shown, in which very small differences in wave-length imply a remarkably large difference in rotational phase (virtually resolving power) of the two interesting groups of interference fringes due to each wave-length.

Spectra obtained with two, or at times even with one grating, are often annoyingly furrowed with large transverse fringes. These are investigated in Chapter VI, and referred to diffractions resulting from residual errors in the rulings. In Chapter VII, finally, several examples of new methods of investigation are given. They show the important bearing of the diffraction at the slit of the collimator on all these experiments. The cleavage of a field of diffracted rays as an essential preliminary is here put in direct evidence.

In Chapters VIII to XIII I have returned to my older experiments with the displacement interferometer. The subjects adduced, like the dispersion of air at low and high temperatures, the adiabatic expansion of air, etc., are pursued less with the object of reaching results of precision than of testing the limits of the displacement method and developing it.

My thanks are due to Miss Abbie L. Caldwell for very efficient assistance in preparing the manuscript and drawings for the press.

CARL BARUS.

BROWN UNIVERSITY, *Providence, Rhode Island.*

## CHAPTER I.

### THE INTERFERENCES OF CROSSED SPECTRA.

**1. Introductory.**—If two component spectra from the same source coincide throughout their extent the elliptic interferences will be spread over the whole surface, provided, of course, the respective glass and air-path differences of the two component rays are not so great as to throw the phenomenon beyond the range of visibility. In the usual method of producing these interferences, where the corresponding reflections and transmissions of the two component rays take place at the same points of the same plane surface, the interference pattern is automatically centered, or nearly so. This is not the case when, as in the following experiments, the interfering beams are separated in some other way; and the problem of centering is often one of the chief difficulties involved; and if the beams are to be treated independently, it is difficult to obviate this annoyance.

Suppose, now, that one of the spectra is rotated around an axis normal to both, by a small angle. Will the interferences at once vanish, or is there a limiting angle below which this is not the case? In other words, how far can one trench with light-waves upon the case of musical beats, or of interferences not quite of the same wave-length?

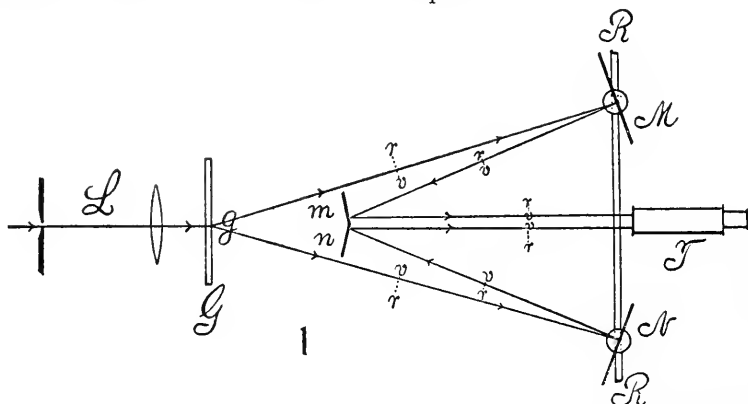
Instead of approaching the question in this form, in which it would be exceedingly difficult, experimentally, I have divided it into two component parts. Let one of the spectra be rotated  $180^\circ$  around a *longitudinal* axis, parallel to the red-violet length of the spectrum and normal to the Fraunhofer lines. In such a case, interference should be possible only along the infinitely thin longitudinal axis of rotation to which both spectra are symmetrical, one being the mirror image of the other. One would not expect these interferences to be visible. It is rather surprising, however, that this phenomenon (as I have found) may actually be observed, along a definite longitudinal band in the spectrum, about twice the angular width of the distance between the sodium lines and symmetrical with respect to the axis of rotation. It is independent of the width of the slit, provided this is narrow enough to show the Fraunhofer lines to best advantage.

Again, let one spectrum be rotated  $180^\circ$  about a given Fraunhofer line (transverse axis), the nickel or mean *D* line, for instance. The two coplanar spectra are now mutually reversed, showing the succession red-violet and violet-red, respectively. Interference should take place only along the mean *D* line and be again inappreciable. Experimentally, I was not at first able to find any interferences for this case in the manner shown below, but this may have been due to inadequacies in the experimental means employed, for the dispersion was insufficient and the reflecting edge of the paired mirrors too rough. Improving the apparatus, I eventually found the phenomenon,

but appearing as a single line, vividly colored above the brightness of the spectrum; or, again, more jet-black than the Fraunhofer lines and located in the position of the coincident wave-lengths of the two superimposed spectra.

It is possible, however, as will be shown in § 4, to obtain two spectra in such a way that if their longitudinal axes coincide the Fraunhofer lines intersect at a small angle, and *vice versa*. In such a case, for coincident Fraunhofer lines, interference occurs in a band around these lines and is absent in the rest of the spectrum; whereas, if the longitudinal axes are coincident, the interferences are arranged with reference to these axes. These results seem to bear on the question, but it is difficult to clearly resolve them.

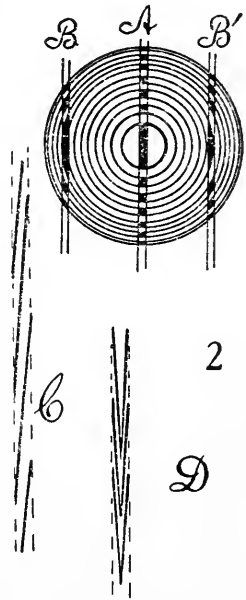
The methods used in this paper consist chiefly in bringing the two first-order spectra of a grating, or the second-order spectra or their equivalents, to interfere. In this respect they contain an additional method of interferometry which may be useful, if for any reason it is necessary that the two component beams are not to retrace their paths.



**2. Coincident spectra with one reversed on a given Fraunhofer line.**—In figure 1,  $L$  is a narrow vertical sheet (subsequently broadened by the diffraction of the slit) of white sunlight or arc light from a collimator,  $G$  the transparent grating ruled on the side  $g$ , from which the first or second order of spectra  $gM$  and  $gN$  originate.  $M$  and  $N$  are opaque mirrors mounted adjustably on a firm rail,  $RR$ , each of them with three adjustment screws relative to horizontal and vertical axes.  $M$  is provided with a slide micrometer (not shown). From  $M$  and  $N$  the beams pass to the smaller paired mirrors,  $m$  and  $n$ , which should meet in a fine vertical line at a very obtuse angle. A silvered biprism would here be far preferable, but none having the required angle was available. From  $n, m$ , the beams pass into the telescope  $T$ . As the spectra are each divergent after issuing from  $g$ , they can be made to overlap on leaving  $n, m$ , by aid of the adjustment screws on  $M$  and  $N$ . Moreover, as the spectra are mirror images of each other, as suggested in figure 1, any spectrum lines (as, for instance, the  $D$ ) may be put in coincidence on using one of the adjustment screws specified. It is necessary that the telescope  $T$  be sufficiently near  $M$  in order that the micrometer may be manipulated.

The *D* lines placed in coincidence are obviously opposites, each line being paired with the mate of the other. A fine wire must be drawn across the slit of the collimator, in order that the vertical coincidence may be tested. One should expect the interferences to appear between the *D* lines on gradually moving the micrometer mirror *M*, parallel to itself, into the required position. As stated above, I did not at first succeed in finding the interferences, but the experiment is a delicate one. In a repetition with first-order spectra, it would be advisable to replace the plane mirrors *m*, *n*, by slightly concave mirrors, about 2 meters in focal distance, and to replace the telescope *T* by a strong eyepiece. This is the method used in the next paragraph, and it was more easily successful.

Later I returned to the experiment with the same adjustment, except that the plane mirrors *m*, *n*, were placed *beyond* the grating, with the object of using the equivalent of second-order spectra to get more dispersion. This plan did not fail, and, having once obtained the interferences, the reproduction seemed quite easy, as they remained visible while the micrometer *M* was moved over about 5 mm. or more, a very important observation. Their appearance with a *small* telescope was that of a single fine line, alternately flaming yellow (very bright on the yellow background of the surrounding part of the spectrum) and jet black as compared with the *D* lines, between which the interferential line was situated, and on an enhanced yellow ground. The flicker is referable to the tremor of the laboratory, which makes it impossible to keep these interferences quiet. Shutting off the light from either mirror, *M* or *N*, naturally quenches the interferences, but leaves the yellow part of the spectrum behind.



Obviously, coincidence of the longitudinal axes of the spectra alone is needed. Therefore, upon moving the two double *D* lines apart, by aid of the adjustment screws on the mirror *M* and *N*, symmetrically to the ends of the yellow field in the telescope, the interferences were isolated and located midway between the *D* doublets of each spectrum, *i.e.*, in the center of the field of the telescope. They could now be observed to better advantage. In the small telescope there is apparently but one dark line. If stationary, its ultimate character, when centered, would be surmised to be given by the intersection of a vertical diameter with a series of confocal ellipses, successively bright and dark, as indicated in figure 2. The light and dark parts alternate or flicker. On moving the micrometer, the vertical intersector *A* takes a more and more lateral position like *B*, so that the trembling interferences would soon be invisible, as they rapidly become finer and hair-like (not shown).

On using higher magnification (larger telescope), two black lines bordering

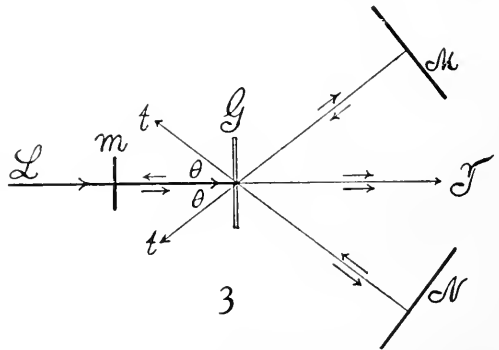
a bright line, or a black line between two bright lines, seemed to be visible; but the interferences would have to be stationary to be definitively described, since the width of the pattern is not more than one-third to one-half of the distance between the sodium lines.<sup>1</sup> The interferences, moreover, did not now readily conform to the design *B*, figure 2, anticipated, but were more of the type *C*, with long, dark lines slightly oblique to the vertical, and vibrating within a vividly yellow band. Sometimes these were heavier, with two or three faint lines on one side.

Further experiment showed that the phenomenon is not influenced by the width of the slit, except that it is clearest and sharpest with the narrowest slit possible and vanishes when the slit is made so wide that the Fraunhofer lines disappear. It may easily be produced by the modified method following, in any wave-length red, yellow, green, etc., with no essential difference except in size. It is present, moreover, in all focal planes, *i.e.*, the ocular of the telescope may be inserted or pulled out to any distance, yet the same phenomena persist on the vague, colored background. A number of observations were made to detect the change

of the pattern of the interference, between its entrance into the field and its eventual evanescence, in case of the continuous displacement of the mirror *M* over 5 mm. In figure 2 this would be equivalent to a passage of *B* into *B'* through *A*, and the fringes for a distant center should therefore rotate, as they actually do in the experiments of the next paragraph.

But in the present case the type *C* persists; the lines may become longer or all but coalesce and their inclination may change somewhat. They nevertheless remain fine and nearly vertical, until they vanish completely and there is no rotation. Nor could the phenomenon be found again within the length of the given micrometer screw. Hence it is improbable that these interferences conform at once to the ordinary elliptic type for which figure 2 applies, even if the ellipse is considered exceptionally eccentric. The use of two slits, one following the other, does not change the pattern.

The modified method of experiment was one of double diffraction. In figure 3, *L* is the blade of light from the collimator, which passing *under* the plane mirror, *m*, penetrates the grating *G*, whence the diffracted first-order beams reach the opaque mirrors *M* and *N*. These return the beams, nearly normally but with an *upward* slant, so that the color selected intersects the



<sup>1</sup>The use of the  $D_1 D_2$  distance of the sodium lines for the measurement of the breadth of the interference phenomenon is a mere matter of convenience in describing it. It will be shown in the next report that the breadth of the strip carrying interference fringes is quite independent of the dispersion of the optic system.

grating at a higher level than  $L$ . A second diffraction takes place at about the same angle,  $\theta$ , to the direct ray  $t$ , and the coincident rays now impinge on the mirror  $m$ . They are thence reflected into the telescope at  $T$ . This method admits of easier adjustment, as everything is controlled by the adjustment screws on  $M$  and  $N$ . Plane mirrors  $M$ ,  $N$ , and  $m$  only are needed, the latter being on a horizontal axis to accommodate  $T$ . The direct (white) beam is screened off after transmission through the grating, if necessary. But it rarely enters the telescope.

**3. The same. Further experiments.**—In place of the plane mirror,  $m$ , a slightly concave mirror (2 meters in focal distance, say) may be used with advantage and the telescope  $T$  replaced by a strong eyepiece. In this way I obtained the best results.

It is to be noticed that the apparatus (fig. 3) may serve as a spectrometer, provided the wave-length  $\lambda$  of one line and the grating space  $D$  are known, and the mirror,  $M$ , is measurably revolvable about a vertical axis. In this case any unknown wave-length,  $\lambda'$ , is obtained by rotating  $M$  until  $\lambda'$  is in coincidence with  $\lambda$ . Supposing the  $\lambda$ 's of the two spectra to have been originally in coincidence and that  $\theta$  is the angle of  $M$  which now puts  $\lambda'$  in coincidence with  $\lambda$ , it is easily shown that

$$\lambda' - \lambda = \lambda (2 \sin^2 \theta / 2 + \sqrt{D^2 / \lambda^2 - 1} \sin \theta)$$

Angles must in such a case be accurately measurable, *i.e.*, to about 0.1 minute of arc per Ångström unit, if the grating space  $D = 351 \times 10^{-6}$ , as above. Counter-rotation of the mirror  $N$  till the  $\lambda$ 's coincide would double the accuracy. The usual grating, however, has greater dispersion and would require less precision in  $\theta$ .

Finally, a still simpler and probably more efficient device consists in combining the mirror  $m$  and the plane grating  $G$ , or of proceeding, in other words, on the plan of Rowland's method for concave reflecting gratings. In such a case the light would enter in the direction  $TG$ , figure 3, be reflected along  $GM$ , back along  $MG$ , and then return along  $GT$  at a slightly higher or lower level than on entering. The equation just given would still apply, and many interesting modifications are suggested. Experiments of this kind are to be tested. Moreover, in case of the plane-transmitting grating and plane mirror, as above shown, the same simplification is possible if the lens is replaced by the telescope at  $T$ . But in this case the spectra are intersected by strong, stationary interferences due to reflections from front and rear faces and consequently not conveniently available. A reflecting grating and telescope would not encounter this annoyance. In general, however, as in the disposition adopted in figure 3, the light enters opposite the observer, and, as the light directly transmitted can be screened off, this is a practical convenience in favor of the transparent grating. The reflected spectra used may be placed at any level by rotating the mirror  $m$  on a horizontal axis.

On further repeating the work by the use of the concave mirror  $m$ , a strong eyepiece at  $T$ , figure 3, and using a compensator, I eventually succeeded in

erecting the interference design *C*, figure 2. It then took the form given at *D*, and this seems to furnish the final clue to the subject. In other words, the design consists of a new type of extremely eccentric ellipses, with their long axes parallel to the Fraunhofer lines, each end having the outline of a needle-point, possibly even concave outward. Only one end of the long, closed curves is obtainable. These jet-black lines dance on the highly colored background of less than half the width between the two sodium lines. The interference design would, therefore, be the same (apart from color) as that which would be obtained if the spectrum containing ordinary elliptic interferences were to shrink longitudinally from red to violet, till it occupied less than half the space between the two *D* lines. In fact, I have at other times obtained just such patterns, with all the colors present, but *not in the pure yellow*, as in the present case. Vertically, the path-difference is always due to more or less obliquity of the rays passing through the plate of the grating. Horizontally, however, the equivalent path-difference is complicated, in the present case, by the fact that one wave-length of a pair has increased, whereas the other has diminished, while both may pass through the same thickness of glass and air.

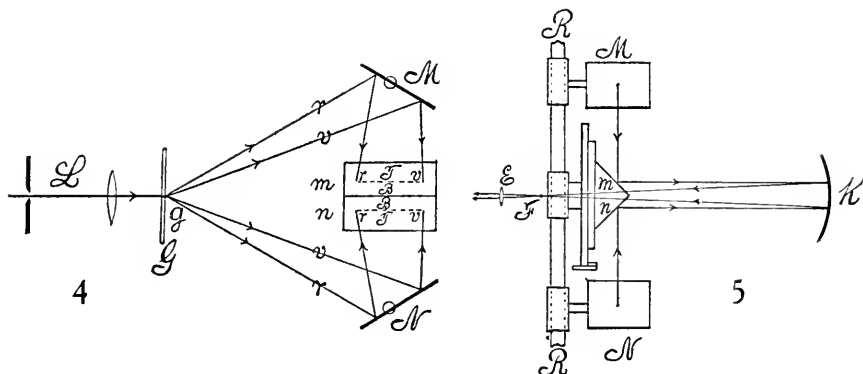
**4. Coincident spectra with one reversed on a given longitudinal axis.**—For this experiment it is necessary to reflect the first-order spectra issuing at the grating *G*, figure 4, from the ruled face *g* (a narrow, preferably horizontal, blade of white light is here furnished by the collimator *L* with a horizontal slit, and the rulings of the grating are also horizontal and parallel to it), twice in succession and preferably from mirrors *M* and *N* and *m* and *n*, reflecting normally to each other and inclined at an angle of, roughly,  $45^\circ$ . Each of the mirrors *M* and *N* must be revolvable about a horizontal axis parallel to the slit and furnished with three adjustment screws relatively to axes normal to each other, one of which is horizontal. The mirrors *m*, *n* are the silvered faces of a prism right-angled at the edge. It is, moreover, to be placed on the slide of a Fraunhofer micrometer so that the prism may be moved, gradually up and down, for the adjustment of distances.

On leaving the mirror *m*, *n*, the two spectra are carried by nearly horizontal and parallel sheets of divergent rays, which pass outward from the diagram. But it will be seen that one of the two spectra reaching the observer is reversed on the longitudinal axis relatively to the other; *i.e.*, if one is in the position

$$\text{red} \left\{ \begin{array}{c} \text{top} \\ \text{bottom} \end{array} \right\} \text{violet, the other will be red} \left\{ \begin{array}{c} \text{bottom} \\ \text{top} \end{array} \right\} \text{violet.}$$

The subsequent passage of the rays is shown in figure 5, which is the side elevation and therefore at right angles to the preceding figure. The rays from *m* and *n* impinge on a distant, slightly concave mirror *K* (about 1.74 meters in focal distance), placed somewhat obliquely, so that when the rays come to a focus at *F* near the micrometer they may just avoid it. The partially overlapping spectra at *F* are viewed by a strong eyepiece, *E*. The observer at *E* can then control the Fraunhofer micrometer by which *m*, *n* is raised and lowered, and the three adjustment screws of *M*.

The adjustment consists in first roughly placing all parts in symmetry with sunlight, until the two spectra appear at *E*. The lens may be removed. There should be a bright, narrow spectrum band on each side of and near the edge of the prism *mn*; for it is clear that after passing the lens *E*, corresponding rays from *M* and *N* must both enter the pupil of the eye to be seen together. To make the spectrum parallel, the mirror *mn* is rotated, as a whole, around a vertical axis. The three screws on the mirrors *M* and *N* then assist in completing the adjustment; the rotation around the horizontal axis brings



the sodium lines in coincidence (both must be clearly seen and sharp and at an appreciable distance apart); that around the oblique axis gives rise to more or less overlapping, as required. The need of a sharp coincidence of the sodium lines is very *essential* in all these experiments.

After proper vertical position of *mn* has been found by slowly moving the micrometer screw up and down, the fringes appear. They are usually very fine lines, possibly indicating distant centers of the ellipses to which they belong. The appearance is roughly suggested in figure 6. They are thus totally different from the preceding set, § 3. They pass from the type *a* through *b*



(contraction toward the violet end was not noticed) into the type *c*, when the mirrors *mn* move in a given direction. The center of the ellipses is in the vertical through the field of view for the adjustment *b*, in which case the lines pass from end to end of the spectrum as a narrow band near the longitudinal axis of actual coincidence of spectra, symmetrically.

The height or breadth of the longitudinal interference band, *d* in figure 6, is not greater than 1.5 to 2 times the distance apart of the sodium lines at right angles to the band. From this the angular divergence of the breadth of the band may be found, since  $\lambda = D \sin \theta$ , where  $\lambda$  is the wave-length of light, *D* the grating space, and  $\theta$  the angle of diffraction. Hence for the two sodium lines

$$\Delta\theta = \Delta\lambda / D \cos \theta$$

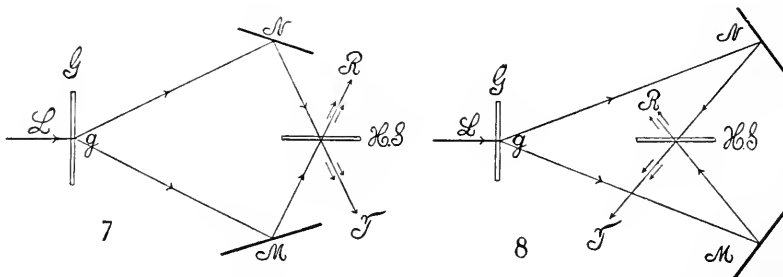
Since  $D = 351 \times 10^{-6}$ ,  $\cos \theta = .986$ , and  $\Delta\lambda = 6 \times 10^{-8}$ ; therefore  $\Delta\theta = 1.7 \times 10^{-4}$  radians. Since the width of the band is about twice this, it will be 68 seconds of arc, or, roughly, about a minute in breadth. Within the strip, when the fringes are horizontal, I counted about five of them, so that their distance apart would be about 14 seconds of arc.

It appears, therefore, that rays of a given color, say of the wave-length at  $D$ , which leave the grating at a given point and at an angle of about one minute in the plane of the  $D$  line, are still in a condition to interfere; whereas one would anticipate that only those rays which lie in the common longitudinal axis of rotation of the two coincident spectra, symmetrical to this, should be in this condition. Such interference should not be appreciable, since the white rays are independent and apparently come from two different points of the slit. If we consider the angular deviation of pencils of parallel rays crossing the grating to be equivalent to the divergence of their respective optical axes at the collimating lens (about 45 cm. in focal distance), the distance apart of two points of the slit, the rays of which are still able to produce interference, is

$$x = 45 \times \Delta\theta = 45 \times 1.7 \times 10^{-4} = 7.6 \times 10^{-3} \text{ cm.}$$

or nearly 0.1 mm. Hence points of white light in the slit about 0.1 mm. apart along its length are included in the band of interferences in question, extending in colored light from red to violet. This seemingly anomalous result will be fully interpreted at another opportunity.

**5. Interference of the corresponding first-order spectra of the grating, in the absence of rotation.**—This apparatus seemed to be of special interest, since the rays used do not retrace their path and are thus available for experi-



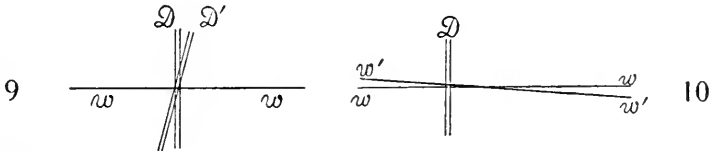
ments in which rays traveling in one direction only, are needed.\* I have tried both the adjustments given in figures 7 and 8, the latter, since the rays are more nearly normally reflected at the mirrors  $M$  and  $N$ , having some advantages; but the other succeeds nearly as well. The difficulty encountered is a curious one of adjustment, which was not anticipated. In other words, if the longitudinal axes of two identical spectra are in coincidence, the Fraunhofer lines are likely to be at a small angle to each other and complete inter-

\* Cf. Am. Journal of Sci., XXXIV, p. 101, 1912, on the interferometry of an air column carrying electrical current.

ference is therefore impossible. Again, if the spectrum lines are in coincidence, the longitudinal axes usually diverge by a small angle. Furthermore, the interferences are almost always eccentric and the lines hair-like, indicating distant centers. I have not succeeded in making a perfect adjustment, systematically; but the discrepancies indicated are themselves interesting in their bearing on the subject of this paper.

In figures 7 and 8,  $L$  is a vertical blade of white light from a collimator with fine slit, and  $G$  is the grating. The two first-order spectra leaving the ruled face at the line  $g$  strike the opaque mirrors  $M$  and  $N$ , the former on a micrometer moving the mirror parallel to itself. From  $M$  and  $N$  the rays reach the half-silvered plate of glass  $HS$ , where one is transmitted and the other reflected into the telescope  $T$ . The coincident rays  $R$  are superfluous.

After placing the parts and roughly adjusting them for symmetry with sunlight, the finer adjustment may be undertaken. It may be noticed that the two systems  $M$  and  $N$ , and  $G$  as well as  $HS$ , can be used for further adjustment separately. All are provided with adjustment screws relatively to rectangular axes. To put the mirrors  $M$  and  $N$  in parallel and in the vertical plane with the grating  $G$ , the half-silvered plate should be removed



and replaced by a small white vertical screen of cardboard, placed at right angles to the direction of  $HS$  in figure 7 and receiving both spectra. A fine wire is drawn across the slit to locate the longitudinal axis, and an extra lens may be added to the collimator and properly spaced until the doublet insures sharp focussing. Both mirrors,  $M$  and  $N$ , are now rotated on horizontal axes, until the longitudinal black lines in their spectra cease to diverge and coincide accurately.  $G$ ,  $M$ ,  $N$ , may now be considered in adjustment. On returning the half-silvered plate,  $HS$ , it in turn is to be carefully rotated around horizontal and vertical axes, until the horizontal black line in the spectrum and the sodium line (always incidentally present in the arc lamp) both coincide. But, as a rule, it will be found that if the longitudinal axes,  $ww$ , figure 9, coincide, the  $D$  lines cross each other at a small angle, exaggerated in the figure. The interferences, when found by moving the micrometer at  $M$ , are usually coarse, irregular lines, indicating a center not very distant and located on the level of a band where the  $D$  lines cross.

On the other hand, if the  $D$  lines are brought to coincidence by moving the adjustment screws on  $M$  and  $N$  (which throws them out of parallel), the longitudinal axes  $ww$ ,  $w'w'$ , figure 10, diverge at a small angle and the interferences are found in a vertical band where the lines  $ww$  and  $w'w'$  cross. This band is relatively wide, however, as compared with the cases in paragraphs 2 and 3. Nevertheless, I have looked upon these results as additional proof

of the possibility of interference; for in neither case ought they to occur if the spectra are not quite coincident horizontally and vertically. If they do occur, it would at first sight seem that a certain small latitude of wave-length adjustment is permitted even with light-waves.

I was at first inclined to refer the cause of this lack of simultaneous parallelism to the grating itself, as it occurred with an Ames grating ruled on glass, with a Michelson reflecting grating, and with a film grating, in about the same measure. But subsequently, on adopting the method of figure 8, the divergence was largely removed and the interferences were now visible throughout the whole of the spectrum. The discrepancy is probably due to insufficient normality of the plate of the grating to the incident white ray, since one of the rays is twice reflected. In any case the adjustment of the coincident sodium lines must be very accurate if the fringes are to be sharp; certainly as little as half their distance apart will obscure the phenomenon.

Though the spectra are bright, the interferences are not as good as with the usual method (paragraph 1); *i.e.*, the dark lines are not black. Neither have I found an available or systematic method for centering the fringes, so that the lines obtained are usually delicate. Again, the position of the collimator, both as regards slit and lens, is here of very serious importance. Any micrometric horizontal motion of either, in its own plane, will throw the fringes out. Finally, the whole spectrum travels with the motion of the micrometer mirror *M*. The apparatus is thus too difficult to adjust for use, to be of practical interest when simpler methods are at hand. The effect of tremors acting prejudicially on so many parts is exaggerated.

**6. Conclusion.**—The phenomena of paragraphs 2, 3, and 4, showing definite and characteristic interference in case of two coincident spectra crossed either on a longitudinal or transverse axis, represent the chief import of the present chapter. These results can not be directly due to the diffraction of a slit (regarding the line of coincidence as such), owing to their relatively small magnitudes and their independence of the breadth of the slit. Since there is in each case but a single line of points or axis, the disturbance of which comes from identical sources, we might regard the image of this line in the telescope to be modified by the diffraction of its objective. But if the interferences originated in this way, the Fraunhofer lines of the spectrum should show similar characteristics and the diffraction pattern should differ from those observed. Thus the conclusion is apparently justified that distinct and independent points of the narrow slit whose distance apart on its length is not greater than 0.1 mm. contribute rays to the field of interference in each of the colors of the spectrum (longitudinal axes coinciding).

The phenomenon of inversion is virtually one of homogeneous light, the same type of interference occurring in each color from red to violet. When the fringes are horizontal, homogeneous light and a correspondingly broad slit would replace the spectrum. They belong, moreover, to the elliptic category, being of the same nature, apart from their limitations, as those

used in displacement interferometry. With the exception of the points lying on the longitudinal axis of rotation or of coincidence, all the pairs of points of the two coincident spectra owe the major part of their light to different sources; *i.e.*, the points of the superposed spectra are not colored images of one and the same point in the slit.

Again, in case of rotation of one of the coincident spectra around a transverse axis (Fraunhofer line), colors which differ in wave-length by about half the distance apart of the two sodium lines seem also to admit of interference. This permissible difference of wave-length is thus relatively about

$$\frac{\Delta\lambda}{\lambda} = \frac{.5 \times 6 \times 10^{-8}}{59 \times 10^{-6}} = 5 \times 10^{-4}$$

or less than 0.1 per cent. The character of these interferences is distinctive. They are not of the regular elliptic type, but arise and vanish in a succession of nearly vertical (parallel to slit), regularly broken lines. Later observation, however, revealed as their true form a succession of long spindles or needle-shaped designs. The chief peculiarity observed is their almost scintillating mobility, which in the above text has been referred to the inevitable tremors of the laboratory. It is, however, interesting to inquire into the conditions of the possibility of observable beating light-waves. For two waves, very close together, of frequency  $n$  and  $n'$  and wave-lengths  $\lambda$  and  $\lambda'$ , if  $V$  is the velocity of light, the number of beats per second would be

$$n' - n = V \left( \frac{1}{\lambda'} - \frac{1}{\lambda} \right) = V \frac{\Delta\lambda}{\lambda^2}$$

Therefore in case of the two sodium lines, for instance,

$$n' - n = 3 \times 10^{10} \times 6 \times 10^{-8} / 3480 \times 10^{-12} = 5 \times 10^{11}$$

*i.e.*, about  $5 \times 10^{10}$  beats per 0.1 second, the physiological interval of flickering. Naturally this seems to be out of all question, even if one is confronting a source which is an approach to a mathematical line. The endeavor will have to be made to produce these interferences under absolutely quiet surroundings. Their appearance is altogether singular and not like the case of paragraph 4, where there is also perceptible tremor, or with the general case of trembling interference patches, with which I am, unfortunately, all too familiar.

In this place, however, it is my sole purpose to present, at its face value, an observation which is spatial, independent of time consideration; and the laterally cramped character of the new interference, with its long, hair-like lines thrust into a strip less than half the distance apart of the sodium lines, is the only evidence submitted. If the coincident path of two rays of slightly different wave-lengths,  $\lambda$  and  $\lambda'$ , which interfere, is  $x$ , then there are  $x/\lambda$  and  $x/\lambda'$ , complete waves in the given path, and, in case of original identity in phase, instantaneous reënforcement will occur when

$$x \left( \frac{1}{\lambda} - \frac{1}{\lambda'} \right) = 1, 2, 3, \dots n$$

In other words, at the  $n$ th reënforcement

$$\Delta\lambda = n\lambda^2/x$$

Hence, since  $\lambda^2$  is very small and  $x$  relatively very large, the small value of  $\Delta\lambda$  (*i.e.*, the very thin strip of spectrum within which the phenomenon occurs) is apparent. In the above experiments the estimates, in round numbers, were  $\Delta\lambda = 2.4 \times 10^{-8}$ ,  $\lambda^2 = 36 \times 10^{-10}$ . Hence if  $n = 1$ ,

$$x = 36 \times 10^{-10} / 2.4 \times 10^{-8} = .15 \text{ cm.}$$

so that one reënforcement would have to occur about at each 1.5 mm. along the rays. Nevertheless, the formidable difficulty remains to be investigated, *viz.*, why these nominally beating wave-trains, with an infinitesimal group period ( $10^{-11}$  sec.), could be recognized at all.

The characteristic feature of the new phenomenon is this, that apart from intensity it *persists, without variation, through a path-difference of over 5 millimeters; i.e.*, through 15,000 or 20,000 wave-lengths. It follows, since the optical paths grating-mirror-grating are alone significant, that two individual light-waves of the same ray over 15,000 wave-lengths apart are still appreciably identical. Beyond that the waves under consideration no longer correspond in orientation and can not interfere in a way to produce alternations of accentuated brightness and darkness.

## CHAPTER II.

---

### FURTHER STUDY OF THE INTERFERENCE OF REVERSED SPECTRA.

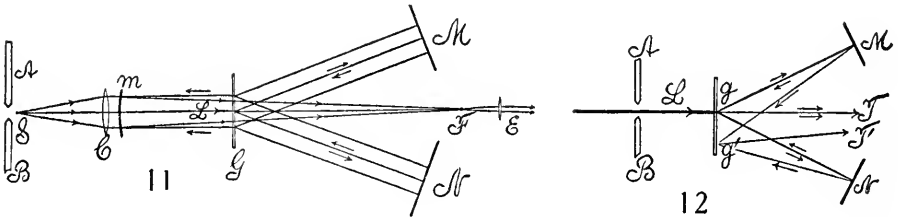
**7. Apparatus with one grating.**—The different methods suggested in paragraph 3 were each tried in succession, but none of them were found equally convenient or efficient in comparison with the method finally used in the preceding paper. To begin with the annoyances encountered in the use of a reflecting grating, it was found that the impinging light from the collimator and the reflected doubly diffracted beam from the grating lie too close together, even if all precautions are taken, to make this method of practical value. The use of Rowland's concave grating without a collimator is out of the question, since the spectra formed on the circular locus of condensation, if reflected back, will again converge into a white image of the slit, colored if part of the spectrum is reflected. The plane-reflecting grating, though not subject to this law, requires a collimator, and, since marked obliquity of rays is excluded, it will hardly be probable that the elusive phenomena can be obtained in this way. A compromise method, in which both the reflecting and the transmitting grating are used, will be described in paragraph 10. Though apparently the best adapted of all the methods used, it has only after difficult and prolonged research led to results. These, however, proved very fruitful in their bearing on the phenomena.

For first-order spectra, where there is abundance of light (it is often difficult to exclude all the whitish glare in the field of the telescope completely), the method of figure 11, which shows normal rays only, is still preferable. Here the impinging collimated beam  $L$  passes below the opaque mirror  $m$  and through the lower half of the grating  $G$ . The diffracted pencil is reflected nearly normally but slightly upward, by the mirrors  $M$  and  $N$  (the former carried on a micrometer slide), to be again diffracted at the grating and therefore to impinge as definitely colored light on the lower edge of the concave mirror  $m$  (about 1.5 to 2 meters in focal distance), whence it is brought to a focus at  $F$  and viewed by the strong eyepiece  $E$ . Considerable dispersion and magnification is obtained in this way; indeed, the two  $D$  lines stand far apart and the nickel line is distinctly visible between them. There must be a fine hair wire across the slit so that the longitudinal axes of the spectra may be accurately adjusted. The mirror  $m$  above the impinging beam must be capable of rotation about a vertical and a horizontal axis in order that the focus  $F$  may be appropriately placed between  $M$  and  $N$ . With  $G$  at 1 meter and  $m$  at 2 meters from  $F$ , the disposition is good. The micrometer  $M$  is easily at hand. Though the direct beam may be screened off, the glare reflected back from the grating and the glare from the objective of the collimator are not excluded, as stated. In fact, it was eventually found necessary

to carry this pencil in an opaque tube reaching from the objective of the collimator, as far as the grating.

With first-order spectra this method always succeeded satisfactorily, and in case of a ruled grating the phenomenon is exhibited brilliantly, if the paths  $GM$  and  $GN$  are optically nearly equal. After some experience it is fairly easy to find it. I have not, however, been able to obtain it with a film grating, even after using a variety of excellent samples. This is not remarkable, for the film grating is hardly sufficiently plane to produce clear regular reflection, and the corresponding paths  $GM$  and  $GN$  would not, therefore, be definite.

Second-order spectra are too faint and can not be seen, unless the glare is excluded in the manner stated. All modifications of the method seemed without avail, until finally the light was led from the collimator objective  $C$ , figure 11, to the grating  $G$ , in a cylindrical tube, whereupon both the glare from the objective and the rearward reflection from the grating were effectively screened off. This tube must, of course, lie below the returning pencil, *i.e.*, it must not (in section) cover more than the lower half of the grating. In this case the second-order spectra, though faint, were seen clearly; but



the scintillating interferences could not be observed until the very weak eyepiece,  $E$ , was used with the concave mirror  $m$ ; or a weak telescope with a plane mirror. It was then detected, but showed no essential difference from the case of first-order spectra. The larger dispersion, in other words, was unavailable. The phenomenon was seen most distinctly by drawing out the eyepiece of the telescope, as the light is thereby concentrated, although the Fraunhofer lines vanish. Second-order spectra are therefore not necessarily advantageous. The phenomenon is very hard to find, and the experiments were persisted in only to obtain the result under different conditions.

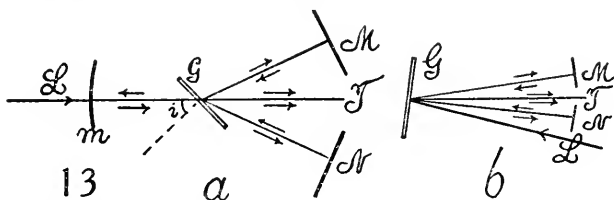
The tube-like light conductor referred to above is, of course, advantageous in case of first-order spectra. If the concave mirror is used, the phenomenon may even be seen brilliantly with the naked eye.

An alternative method of half-silvering the ruled face of the grating and then using it as a reflector was tried with success. The beam of parallel rays from the collimator  $L$ , figure 12, is transmitted by the grating (ruled, half-silvered face,  $g$  toward the mirrors  $M$  and  $N$ ) and the two diffracted beams then returned by the opaque mirrors  $M$  and  $N$ , to be in turn diffracted by reflection into the telescope  $T$ . In fact, this method succeeds with the unsilvered grating; for the rays diffracted, by reflection, from the ruled face (toward the telescope), but not very well. The reflection from the rear face

of the grating is so cut up by the strong, stationary interferences that it is unavailable. The grating plate must, of course, be slightly wedge-shaped, otherwise all the spectra would be superposed. In case the ruled face is half-silvered, however, the stationary interferences are practically absent, while two strong spectra are reflected from the silvered side. The phenomenon may then be produced at all distances of  $G$  from  $M$  and  $N$  (2 meters and less), but best at distances within 1 meter. It is, however, frequently hard to find unless different distances apart of the mean  $D$  lines are tested. This may be due to the fact that the silver film is not quite equally thick.

Besides the symmetrical position,  $gT$ , figure 12, the two corresponding unsymmetrical positions  $g'T'$  were tested with success; and it appeared that while in the case  $gT$  the phenomenon is virtually linear, dark or bright, like a Fraunhofer line, a succession of dark lines inclined to the vertical may appear for the unsymmetrical position  $g'T'$ . Dark lines are apt to be broadened.

Questions relative to the effect of oblique incidence were also tested by aid of the concave-mirror method shown in figure 11, the white light from  $C$  to  $G$  being conducted in an inch tube of pasteboard, immediately under the concave mirror,  $m$ . Figure 13,  $a$ , shows the general disposition of apparatus.



The angle of incidence  $i$  is gradually increased, until the return rays from  $N$  meet the grating at nearly grazing incidence. No essential difference in the phenomenon was observed, however, except that it was apt to be broader in the non-symmetrical positions and to suggest fine new lines in parallel with the old. In a return to the symmetrical position, sharp lines were especially distinct, usually showing one dark and two bright lines, while two dark and one bright occurred less frequently. It could be seen quite vividly with the naked eye. When the telescope was used and the ocular drawn far forward, the multilinear form was often suggested. On broadening the slit the black lines vanish first and a flickering band remains after the Fraunhofer lines are gone. Finally, the phenomenon could be seen even when the longitudinal axes of the spectra were not quite coincident, but it rapidly became fainter in intensity.

Figure 13,  $b$ , suggests a method of using a reflecting grating, either plane or (possibly, if the incident light is parallel) concave, for the production of the phenomenon.  $G$  is the grating, receiving the collimated white light,  $L$ , which is diffracted toward  $M$  and  $N$ , thence reflected (at a different elevation) back to  $G$ , to be again diffracted towards  $T$ , above or below the direct beam, where it is observed. I have not, however, been able to obtain results with these methods owing to subsidiary difficulties.

8. **Observations and experiments with a single grating.**—On considering figure 11, it will be seen that the doubly reflected, doubly diffracted rays are also in a condition to interfere. Thus the rays *GMNG* and *GNGMG* have identical path-length, or at least path-difference; but it is improbable that superimposed on the strong spectra this effect could be seen, for the reflection from the ruled face of the grating is very slight and the divergent spectra have weakened seriously. The scintillating interferences, on the other hand, are much brighter than the superposed spectra. Such interferences, also, should be independent of the play of the micrometer *M*, since the path-difference of these beams is not changed thereby, each being identically lengthened or shortened. Furthermore, the interposition of a thick plate-glass compensator in *GM* should have no effect. Neither of these interferences applies for the phenomenon in question, which persists for a definite displacement of *M*, only, and the introduction of a compensator requires the usual equivalent displacement of *M*, within the range of the phenomenon. Finally, the interferences relatively to a phenomenon produced by double diffraction would not be modified.

Many experiments were made to ascertain the path-difference within which the phenomenon is visible. This can not be accurately determined, since it is a question of stating when an observation, which is becoming rapidly less distinct, has actually vanished. Moreover, any imperfection of the micrometer throws out the coincidence of longitudinal spectrum axes, while a readjustment breaks the continuity of the micrometer displacement, or reading. Results were obtained as follows, for example,  $\Delta N$  being the displacement of the mirror *M*:

|   |                                   |
|---|-----------------------------------|
| With telescope.....                     | $\Delta N = 0.34, 0.45, 0.41$ cm. |
| With concave mirror and lens.....       | 0.45, 0.35, 0.41 cm.              |
| With concave mirror and adjustment..... | 0.50 to 0.60 cm.                  |

The low readings are due to the micrometric wabbling of the micrometer slide. Since  $\Delta N$  is the double path-difference, the number of wave-lengths in question may be put

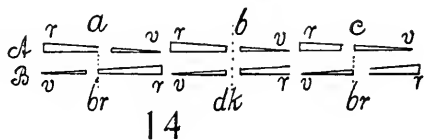
$$\frac{2 \times .45}{60 \times 10^{-6}} = 1.5 \times 10^4$$

*i.e.*, the distances along the ray are 15,000 to 20,000 wave-lengths apart, about as estimated in the above paper. This is the characteristic feature of the phenomenon.

Between its extreme ranges of visibility the appearance of the phenomenon scarcely changes. It ceases to be visible rather suddenly; and this is to be expected, since we are dealing directly with two wave-trains displaced relatively to each other. It is visible for a wide slit even after the Fraunhofer lines vanish. It disappears by decreasing in width, when the slit is closed. If the ocular of the telescope is drawn out, the phenomenon may even be observed after the Fraunhofer lines have vanished, in the dark, stringy spectrum of an extremely fine slit. When the longitudinal axis of the spectrum is indicated by a fine wire across the slit, the adjustment consists in bringing

the black longitudinal lines of the two spectra together. The question thus arises how close this coincidence is to be. When the phenomenon is sharp, it has been found possible to displace the two black lines so that a fine, bright strip of spectrum may just be seen between, without quite destroying the interferences. Naturally they are then much weaker. This result is in harmony with the observations made on rotating one spectrum, on a longitudinal axis,  $180^\circ$  with reference to the other.

Since the phenomenon was originally produced with sunlight, it might be supposed that the edges of the Fraunhofer line, under conditions of tremor, would interfere with each other as indicated in figure 14, where *A* is one and *B* the other of the two superposed spectra. The change of wave-length is suggested by the slant of lines on the diagram. In such a case, whereas the conditions *a* and *c* would show bright overlapping spectra, the dark line would appear under condition *b*. But even in this case, lines of slightly different wave-length would have to interfere with each other. The crucial test was made by using an arc-lamp spectrum, and it was then found that the phenomenon appeared as well as with sunlight.



A further question at issue is the breadth of spectrum needed to produce the phenomenon; for the observed breadth would be influenced by the quiver of the apparatus. With this end in view, different lines of the spectrum were placed in full coincidence, and it was found that for none of the secondary lines in the orange-yellow spectrum was it extinguished or even modified. If, however, the corresponding *D* lines of the spectra ( $D_1D_1'$ ;  $D_2 D_2'$ ) were superposed, the phenomenon in these experiments played like a wavy strip at their edges only. Sometimes a bright line flashed through the middle of the coincident lines. One would conclude, therefore, that the part of the spectrum used in producing these interferences is not much broader than either the  $D_1$  or  $D_2$  lines, while the other marked lines in the orange-yellow are too narrow to appreciably influence it. These results will be greatly amplified in the work done with two gratings below.

A corresponding experiment was now made with *sodium light*. To obtain a sufficiently intense source, solid caustic soda was volatilized between the carbons of the electric arc, *A* and *B*, figure 12, or the corresponding case in figure 11. On drawing the carbons apart, strong *D* lines were seen, in the entire absence of an arc spectrum, at first so broad as to be self-reversing. Gradually they became finer and eventually reached the normal appearance of the  $D_1, D_2$  lines. In order to facilitate adjustment and with the object of obtaining cases correlative with the results for the dark-line spectrum, a beam of sunlight (as at *L*, figure 12) was introduced between the carbons and the phenomenon established faultlessly in the usual way. The pencil of sunlight was then screened off and the arc light substituted, or the two were used together.

These observations seemed to show that when the normal  $D_1$  or  $D_2$  lines were placed in coincidence, the thread-like phenomenon fails to appear with

all the characteristics visible in the case of sunlight. When the slit is broadened an alternation of brightness, or flicker of light, may be detected vaguely. With a slit of proper width to show the Fraunhofer lines all this seemed to vanish. The actual phenomenon was therefore apparently not reproduced or improved either by homogeneous light or by widening the slit. Such experiments alternating with sunlight were made at considerable length, but the adaptation of methods for two gratings discussed in paragraph 10 will nevertheless throw out this conclusion.

If the narrow sodium line is broadened by adding fresh sodium at the carbon, so that the yellow spectrum is again self-reversed, the phenomenon plays with extreme vividness around either of the reversed and coincident  $D_1$  or  $D_2$  lines, or even within the black line in question, if narrow. But here the light is no longer homogeneous. Sometimes when the solar spectrum is used, a black line preponderates; in other adjustments a flashing bright line is in place; but the reason for this can not be detected by the present method.

**9. Inferences.**—If the wave-length of the two spectra is laid off in terms of the angle of diffraction,  $\theta$ , measured in the same direction in both cases, the graph will show two loci as in figure 15, *a*, intersecting in the single point of coincident wave-lengths  $\lambda_0$ . It appears, however, as if the wave-lengths at  $\varphi_1$  and  $\varphi_3$ ,  $\varphi_2$  and  $\varphi_4$ , are still in a condition to interfere. The phases  $\varphi_1$  and  $\varphi_2$ ,  $\varphi_3$  and  $\varphi_4$ , differ because of path-difference introduced for instance at the micrometer, the phases  $\varphi_1$   $\varphi_3$ ,  $\varphi_2$   $\varphi_4$  differ because of color differences, having passed through refracting media of glass and air. Probably the phase-difference  $\varphi_1 - \varphi_3 = \varphi_2 - \varphi_4$ , these having the same color-difference; and  $\varphi_1 - \varphi_2 = \varphi_3 - \varphi_4$ , having the same path-difference. At  $\lambda_0$ ,  $\theta_0$ , the two phases  $\varphi_0$  are due to path-difference only.

To allude again to the *question of beats*: if ten beats per second are discernible, the beating wave-trains in the case of the given grating would be only  $6 \times 10^{-10}$  second of arc apart in the spectrum. If the phenomenon has a breadth of  $3 \times 10^{-8}$  cm. in wave-length, as observed, then the number of beats in question will be  $2.5 \times 10^{11}$  per second. All this is out of the question, so far as the phenomenon appreciable to the eye is concerned. If beats were due to a difference of *velocity* resulting from the dispersion of air, and if  $T$  is the period of the beats,  $\lambda$  the mean wave-length,  $\delta \frac{1}{\mu}$  the difference of the reciprocal indices of refraction, we may write

$$T_1 = \frac{\lambda}{v \delta (1/\mu)}$$

If, furthermore,  $\mu = A - B/\lambda^2$ , where  $B = 1.34 \times 10^{-14}$ ,  $\delta \lambda = 2.4 \times 10^{-8}$ ,

$$T_1 = \frac{\lambda^4}{2vBd\lambda} = \frac{1.3 \times 10^{-17}}{2 \times 3 \times 10^{10} \times 1.34 \times 10^{-14} \times 2.4 \times 10^{-8}} = .7 \times 10^{-6} \text{ sec.}$$

or

$$N_1 = 1.4 \times 10^6 \text{ beats per sec.}$$

which would also be inappreciable.

If both the difference of wave-length and wave-velocity are considered, we should have for the first spectrum  $v$  and  $n$ , and for the second spectrum  $v$  and  $n'$ . The conditions would be left unchanged, if the second velocity is taken equal to the first and the frequency  $n'(v'/v)$  replaced by  $n'$ . From this it follows that the number of beats  $N$  is nearly

$$N = v \left( \frac{1}{\mu\lambda} - \frac{1}{\mu'\lambda'} \right) = -v \left( \frac{\delta\lambda}{\mu\lambda^2} + \frac{\delta\mu}{\lambda\mu^2} \right)$$

If  $\delta\lambda$  is considered negative, if  $\mu = A - B/\lambda^2$  and the multipliers  $\mu$  and  $\mu^2$  be neglected,

$$N = v\delta\lambda \left( \frac{1}{\lambda^2} - \frac{2B}{\lambda^4} \right)$$

which is the difference of the two cases above computed. As the first is very large compared with the second, the visibility of the phenomenon is not changed.

The theory of group waves usually introduces a factor 2. Thus if  $\lambda_1, v_1, n_1$ , be the group wave-length, velocity, and frequency,

$$\lambda_1 = 2\lambda^2/\delta\lambda \qquad v_1 = v \delta(\mu\lambda)/(\mu^2\delta\lambda) \qquad n_1 = v\delta(\mu\lambda)/(2\mu^2\lambda^2)$$

or,

$$n_1 = \frac{v\delta\lambda}{2} \left( \frac{1}{\mu\lambda^2} - \frac{2B}{\lambda^4} \right)$$

or with the above data

$$n_1 = \frac{1}{2} (2.0 \times 10^{11} - 1.4 \times 10^6)$$

results otherwise like the above and without bearing here. There is a possible question whether differences of wave-length due to velocity and not to period can be treated as dispersion.

The occurrence of *forced vibrations* has also been looked to as an explanation. Though here again, even if the spectra are almost always of unequal intensity, the reason for the preponderance of one would have to be stated. True, equal mean strength is not equivalent to equal instantaneous strength. In the case of forced vibrations, however, if the harmonic forces of one spectrum are  $F = A \cos pt$  (forced,  $T = 2\pi/p$ ), of the other  $F = A' \cos qt$ , (free,  $T = 2\pi/q$ ) and there is no friction, the resulting harmonic motion will be given by

$$y = \frac{A}{q^2 - p^2} \cos pt$$

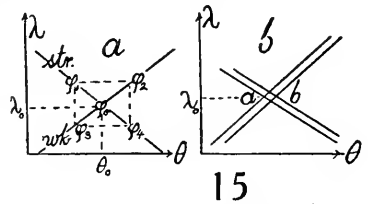
Now if we regard the case of figure 15, on one side of the line of coincidence  $\lambda_0, q^2 > p^2$ ; on the other side,  $p^2 > q^2$ . Hence, whenever a brilliant line flashes out due to coincident phases, there should also be a black line due to opposition; and, in fact, when the phenomenon is produced under conditions of perfect symmetry of the component beams, this seems to be its character; *i.e.*, the enhanced line cuts vertically across the breadth of the spectrum. The case  $q^2 = p^2$ , being of infinitely small breadth, would not be visible. It is not to be overlooked, however, that in certain adjustments, particularly in

the non-symmetrical case of figure 13, more than two black lines frequently occur. (Cf. § 15.) These accessory lines are ordinarily very thin and crowded on one side of the phenomenon only. It is thus merely the prevalent occurrence of paired dark and bright lines that are here brought to mind. Again, the suggestion of many oblique lines has occurred in some of the observations. These would be quite unaccounted for.

Finally, many attempts were made to find whether the phenomenon would occur again beyond its normal range of about  $2 \times 0.5$  cm. of displacement. But, though the micrometer screw actuating the mirror  $M$  was effectively  $2 \times 3$  cm. long, no recurrence could be found. At the ends of its range the phenomenon drops off rather abruptly.

None of the inferences put forward adequately account for the phenomenon as seen with a single grating, as a whole. In this dilemma I even went so far as to suppose that a new property of light might be in evidence. One feature, it is true, has been left without comment, and that is the width of the slit-image. If  $ab$ , figure 15  $b$ , is the angular width ( $d\theta$ ) of this image, the case of figure 15  $a$  should be additionally treated in terms of figure 15  $b$ .

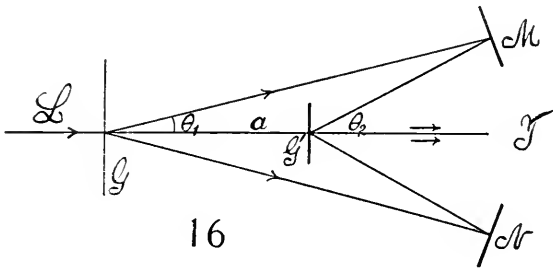
But within the limits of the present method of experiment, with but one grating, this circumstance seems to offer no clue. If, for instance, the spectra actually coincide in color throughout their extent, as in ordinary interferences, the interference patterns should be enormous, for the path-difference may be zero. The invariability of the present phenomena as to size within its long range of presence, the occurrence of intensely sharp and bright or dark single lines, with a distance ( $d\theta$ ) much less than the distance apart of the  $D_1, D_2$  lines, is in no way suggested by the width of slit-image. Moreover, in spite of its persistence, the interference phenomenon of reversed spectra has the sensitiveness of all interferences. Slight tapping on the massive table throws it out altogether. Clearly, therefore, a modification of method is essential if new light is to be thrown on the phenomenon, and from this viewpoint a *separation* of the two diffractions seems most promising.



**10. Apparatus with two gratings.**—All the varied experiments described in the preceding paragraph failed to show any essential modification of the linear interference pattern obtained. In a measure this was to be anticipated, inasmuch as both diffractions take place at the same grating. It therefore seemed promising to modify this limitation of the experiments, although the difficulty of finding the phenomena would obviously be greatly increased. The separation of the two diffractions, however, seemed to be alone capable of resolving the phenomenon into intelligible parts.

In the present method the glass grating  $G$ , figure 16, receives the white beam  $L$  from the collimator, which is then diffracted to the opaque mirror  $M$

(on a micrometer slide) and  $N$ , thence to be reflected to the reflecting grating  $G'$ , plane or curved. Here the two beams of the identically colored light selected are again diffracted to the telescope or lens at  $T$ . Since the gratings  $G$ ,  $G'$ , rarely have the same grating constant, their proper position must be found by computation and trial. In my work the distances to the line of mirrors  $NM$  were 165 cm. for  $G$  and 90 cm. for  $G'$ . This method automatically excludes the direct beam  $a$  and all glare, and gives excellent spectra both in the first and second orders. The use of two gratings, however, introduces the difficulties of adjustment specified, as the two  $D$  doublets corresponding to  $N$  and  $M$  will not, as a rule, be parallel and normal to the longitudinal axes of the spectrum, unless all cardinal features, like the rulings and their planes, are quite parallel. If the grating is not normal to the impinging beam, the axis of the corresponding spectrum is a curved line. The spectra are, moreover, likely to be unequally intense, a condition not infrequent even in the preceding method. It is possible that this may be due to the grating itself, but probably unequal parts of the corresponding beams are

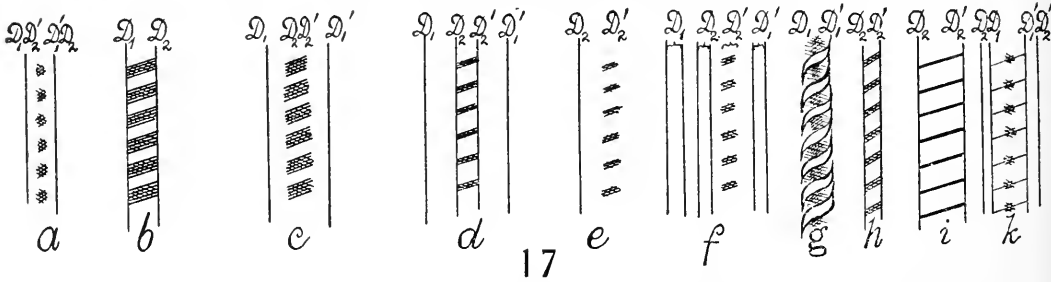


used in the two cases, or the mirrors are unequally good. As a result, in my earlier work I was not able to produce the phenomena with two gratings, after many trials, in spite of the clearness of the overlapping spectra; but the same serious difficulties are encountered whenever interferences are produced from two independent surfaces.

Later, having added a number of improvements to facilitate adjustments, I returned to the search again and eventually succeeded. There are essentially four operations here in question, supposing the grating  $G$  approximately in adjustment. By aid of the three adjustment screws on each of the mirrors  $M$  and  $N$ , figure 16, the fine wire drawn across the slit may be focussed on the grating, if an extra lens is added to the collimator and the black horizontal shadows of that wire, across the corresponding spectra, placed in coincidence. The grating  $G'$  is then to be moved slowly fore and aft, normal to itself, on the slide, so that the position in which the sodium lines are nearly in coincidence to an eye placed at the telescope,  $T$ , may be found. The grating  $G'$  is next to be slowly rotated on a line (parallel to  $LT$ ) normal to its surface, to the effect that the black axes of both spectra (*i.e.*, the spectra as a whole) may coincide. This must be done *accurately*, and the last small adjustments may be made at the screws controlling  $M$  and  $N$ . Finally, the micrometer

slide carrying  $M$  is to be moved fore and aft until the interferences appear. These operations are difficult even to an experienced observer. The fringes are very susceptible to tremors, and only under quiet surroundings do they appear sharply. At other times they move, as a whole, up and down and intermittently vanish.

The fringes so obtained, figure 17, were totally different from the preceding and consisted of short, black, equidistant, nearly horizontal lines across the active yellow strip of spectrum, at the axis of coincidence. The strip was about of the same width as above. Thus the pattern presented the general appearance of a barber's pole in black and yellow, the width being less than the sodium interval,  $D_1, D_2$ , and the distance apart of fringes usually smaller. They were visually in motion up and down, rarely quiet, no doubt owing to tremor. Since the fringes were nearly horizontal! or less than 30 degrees in inclination, it was possible to enlarge the width of the slit without destroying them, as in case of the hair-like vertical fringes in paragraph 2 above. In this way a breadth of strip greater than the distance  $D_1, D_2$ , could be obtained with sunlight or arc light, though a moderately fine slit was still desirable.



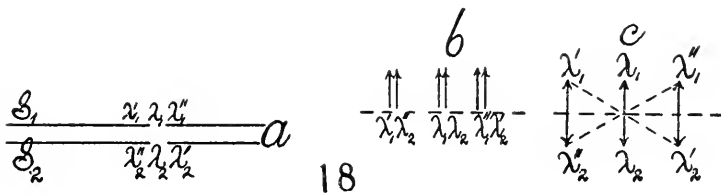
In general, the characteristics noted above were again observed. Thus on moving the micrometer screw controlling  $M$ , the interferences appeared rather abruptly. They vanished in a similar manner, after about 0.4 cm. or more of the micrometer screw had been passed over. In other words, the fringes remain identical for a path-difference of about  $2 \times 0.4$  cm., or nearly 15,000 wave-lengths.

If we call the four  $D$  lines available in the two solar spectra  $D_1, D_2, D'_1, D'_2$ , respectively, a number of curious results were obtained on placing them variously in approximate coincidence. Thus figure 17 a, when each  $D$  line of one spectrum coincides with the mate of the other ( $D_1, D'_2; D'_1, D_2$ ), equidistant dots, surrounded apparently by yellow luminous circles, appeared between the two doublets. On widening the slit the dots changed to a grating of nearly horizontal lines covering the strip  $D_1, D_2$ , figure 17 b. The lines in one part of the slit seemed to slope upward and in another to slope downward. With a large telescope the phenomenon was more dim and quiet, apparently. The fringes often lie in more definite focal planes and cease to be visible when the ocular of the telescope is far outward, differing from the case above.

The phenomenon of chief interest, however, was observed (figure 17 c) in placing two identical  $D$  lines in coincidence ( $D_1; D_2, D'_2; D'_1$ ). The fringes

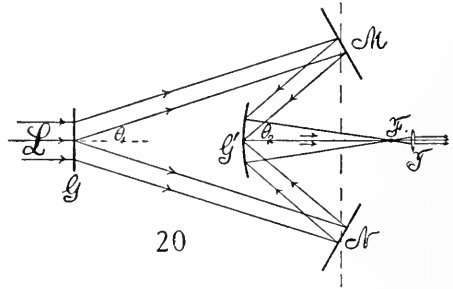
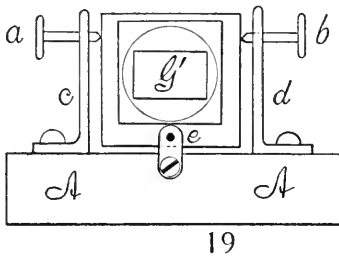
were then seen across the coincident lines, now no longer visible, quite independent of the absence of light. This would seem to mean that the otherwise quiet ether within the black line is stimulated into vibration by the identical harmonic motions of the bright fields at and beyond the edges of the line (diffraction). The question will presently be broached again in a different way. Here I may note that in the above cases of transverse lines (§ 8) it is often possible to observe a very fine parallel yellow line within the coincident  $D_2, D'_2$ , or  $D_1, D'_1$ , doublets, excited, therefore, in the dark space and splitting the line.

The experiments were now repeated with the sodium arc, and these also gave some striking results. Thus in the case of figure 17 *d* the lines were separated, but the yellow striations seemed to show across the dark space between  $D_2$  and  $D'_2$ . When the yellow light was too weak, cross-hatchings were seen only across  $D'_2$ , as in figure 17 *e*. Frequently the phenomenon figure 17 *f* occurred on broadening the slit, in which  $D_2$  and  $D'_2$  interfered, but only  $D'_2$  was marked. Screening off  $D_2$  (left mirror) at once removed the fringes. I have interpreted this observation as the result of parallax, due to the fact that the lines and the interferences are seen in different focal planes.



On the basis of these results one might with some plausibility adduce the following remarks in explanation of the phenomenon: In figure 18 *a*, let  $S_1$  and  $S_2$  be the overlapping reversed spectra and let the line of symmetry be at  $\lambda_1, \lambda_2$ . Then if identical ether vibrations can react on each other across a narrow ether gap, rays as far as  $\lambda'_1, \lambda'_2$  and  $\lambda''_1, \lambda''_2$  being of identical source and wave-length, respectively, are still in a condition to interfere. There would then be three groups of interferences,  $\lambda_1 \lambda_2, \lambda'_1 \lambda'_2, \lambda''_1 \lambda''_2$ . If, figure 18 *b*, all are in phase, we should have a brilliant line; if all are in opposite phases, a dark line on the principle of figure 18 *c*. Naturally, if wave-trains react on each other across an ether gap, small as compared with the  $D_1, D_2$  interval, the assumption made above relative to interference of different wave-lengths is superfluous. My misgiving in the matter arises from the misfortune of having taken down the original apparatus, for modification, and having since been unable to reproduce them with anything like the decisiveness with which they were at first apparently observed. I can not now be certain whether what occurred was actually what I seemed to see, or whether the broad illumination of the sodium flash (broad individual lines,  $D_1$  to  $D_2$ , virtually a continuous spectrum) may not have misled me. The experiments were continued, as follows.

**11. Experiments continued. New interferometer.**—At the outset it was necessary to ascertain the reason for the difference of the phenomena, as obtained with one grating in paragraph 8 and with two gratings in paragraph 10. As the probable cause is a lack of parallelism of the rulings in the latter case, it was necessary to remount the second grating  $G'$  in the manner shown in figure 19. Here  $AA$  is a baseboard, capable of sliding right or left and of rotating on a horizontal axis parallel to the grating. The latter (in a suitable frame) is held at the bottom by the axle,  $e$ , normal to the grating and by the two set-screws  $a$  and  $b$  carried by the standards  $c$  and  $d$ . Thus the grating could be rotated around an axis normal to its plane. At first a Michelson plane-reflecting grating  $G'$  and a telescope were used, as in figure 16; but it was found preferable (fig. 20) to use a Rowland concave reflecting grating  $G'$ , with the strong lens at  $T$ , the grating receiving a beam of parallel rays of light for each color from the collimator and first grating  $G$ . In this case, with sufficiently high dispersion, a large, strong field was obtained, in which even the very fine lines of the solar spectrum were quite sharp. Rotating grating  $G'$  around a parallel horizontal axis, like  $AA$ , figure 19, made little



difference, relatively speaking; but rotation around the axis  $e$ , normal to its plane, carried out by actuating  $a$  and  $b$  in opposite directions, made fundamental differences in the appearance of the phenomenon and eventually suggested a new interferometer for homogeneous light.

The adjustments are the same as in case of figure 16,  $G$  being the transparent grating, except that  $G'$  is now a concave grating and  $T$  a strong eyepiece. The distances  $G'T$  and  $GT$  were of the order of 1 and 2 meters.

On rotating the grating  $G'$  on an axis normal to its face, from a position of slight inclination of the rulings toward the left, through the vertical position, to slight inclination to the right, the fringes passed through a great variety of forms, to be described in detail in § 13 below. Difference of focal planes between the Fraunhofer lines and the interferences were common, so that effects of parallax were apt to occur. Thus when  $D_2$  and  $D'_2$  coincide, the ladder-like phenomenon may lie between  $D'_2$  and  $D'_1$ ; or the ladder may pass obliquely between the  $D_2 D_1$  and  $D'_1 D'_2$  doublets. The first experiment with the new and powerful apparatus (plane transparent grating  $G$ , grating space  $351 \times 10^{-6}$  cm., and the concave reflecting grating  $G'$ , grating space  $173 \times 10^{-6}$  cm., fig. 20) was made with the object of verifying, if possible, the

reaction of parallel ether wave-trains on each other across a very narrow ether gap. The sodium arc lamp was used as a source of light. The results as a whole were negative, or at least conflicting. Usually when strong interferences were observed for coincident positions of  $D_2, D'_2$ , for instance, there was no passage of fringes across the dark space when  $D_2$  and  $D'_2$  were slightly separated. At the beginning of the work (possibly as the result of lines broadened by a flash of sodium light) the stretch of interference fringes across the dark space was certain; but such evidence is not quite trustworthy, for a continuous spectrum (*i.e.*, lines broadened by the flash) would necessarily produce the striations. With a very fine slit the coincident  $D_1, D'_1$  or  $D_2, D'_2$  was frequently much broadened by a sort of burr of fringed interferences. When the lines are self-reversed, superposition of  $D_1, D'_1$ , etc., frequently showed vivid interferences across the intensely black middle line. This and the passage of the bright and dark lines across the superposed  $D_1, D'_1$  lines of the solar spectrum are thus the only evidence of the reaction of separated light-rays on each other across an ether gap observed in the new experiments, and the above results could not be repeated.

On introducing a refined mechanism to establish the sharpest possible coincidence of the  $D_1, D'_1$  or  $D_2, D'_2$  lines, it seemed as if these lines could at times be brought to overlap with precision, without the simultaneous appearance of the interferences around them; but on drawing out the ocular of the telescope or the lens the cross-hatching invariably appears. If the coincidence is not quite sharp, the phenomenon is usually very strong in the isolated bright strip. Horizontal fringes are best for the test.

An additional series of experiments was made some time later by *screening* off parts of the concave grating  $G'$ , in order to locate the seat of the phenomenon at the grating. Screening the transmitting grating  $G$  was without consequence; but on reducing the area  $G'$  to all but the middle vertical strip about 5 mm. wide, a very marked intensification of the phenomenon followed. Although the spectrum as a whole was darker, the interferences stood out from it, relatively much sharper, stronger, and broader than before. The Fraunhofer lines were still quite clear. Thus the pattern, *g*, figure 17, was now very common, both with sunlight and with sodium light. For a given slit the phenomenon began with a strong burr *c*, figure 17, completely obliterating and widening the superposed  $D_2, D'_2$  lines. When these lines were moved apart, the striations followed them, as in figure 17, *h* and *i*, to a limit depending on the width of the slit. A still more interesting pattern is shown in figure 17 *k*, in which the interferences proper are strong and marked between the two  $D_1 D'_1$  doublets, but much fainter striations are also evident, reaching obliquely across and obviously with the same period.

With this improvement I again tested the ether-gap phenomenon, using the sodium arc, and to my surprise again succeeded.  $D_1 D'_1$  lines of half the breadth of the doublets apart induced strong fringes between them, and the experiments were continued with the same results for a long time. Several days after, however, with another adjustment, it in turn failed. Clearly

there is some variable element involved that escaped me, and it will hardly be worth while to pursue the question further with the given end in view, without a radical change of method.

Screening middle parts of the grating (in relation to § 15) did not lead to noteworthy results here, but such experiments will become of critical importance below.

A word may be added in relation to Fresnellian interferences in the present work. These would be liable to occur if the observations had been made *outside* of the principal focus, with the sodium lines blurred. In all the experiments on the excitation of a narrow ether gap, however, the  $D$  lines were clearly in sight and sharp, so that the phenomena of non-reversed spectra and homogeneous light (in the next section) are not here in question. True, such interferences may often be found in the case of reversed spectra, when the sodium lines are purposely blurred, by pushing the ocular toward the front or to the rear.

**12. Experiments continued. Homogeneous light.**—To turn to a second class of experiments: very important results were obtained with homogeneous light (sodium arc) on placing the  $D_1D'_1$  or  $D_2D'_2$  lines in coincidence and then broadening the slit indefinitely or even removing it altogether. A new type of interferences was discovered, linear and parallel in character and intersecting the whole yellow field. These lines could (as above) be made to pass from a grid of very fine, hair-like, nearly horizontal lines to relatively broad, vertical lines, on changing the orientation of the grating  $G'$ , figure 16. Small changes of position of the grating produced a relatively large rotation and enlargement of the lines of the interference pattern. The fringes, when vertical and large, are specially interesting. The distances between successive fringes obtained were about the same (accidentally) as the  $D_1D_2$  distance of the sodium lines. They are quiet in the absence of tremor. If  $D_1D'_1$  or  $D_2D'_2$  were only present, the field would be an alternation of yellow and black striations; but as both doublets are present, the interferences overlap the flat (non-interfering) yellow field of the lines not in coincidence. The fringes are nevertheless quite distinct. A single homogeneous line (like the green mercury line) would give better results. It is necessary that the line selected (say  $D_1D'_1$ ) should coincide horizontally and vertically before the slit is broadened. Otherwise no fringes appear in the yellow ground, or at least not in the principal focal plane. On using a thin mica compensator, it is easy to make these fringes move while the mica film is rotated; and they pass from right to left and then back again from left to right, as the mica vane passes through the normal position of minimum effective thickness. Thus this is a new form of interferometer with homogeneous light. The fringes remain identical in size, from their inception till they vanish, while the micrometer  $M$ , figure 16, passes (as above) over about 15,000 wave-lengths. In this respect the new interferometer differs from all other types, the two air-paths,  $GMG'$  and  $GNG'$ , alone being in question. The condition of occurrence will be investigated in paragraph 13.

**13. Experiments continued. Contrast of methods.**—As these fringes were produced with a concave reflecting grating, the question may be put whether they would also appear in case of the plane reflecting grating,  $G'$ , in the adjustment of figure 16. The experiment was therefore repeated with a wide slit, or with no slit at all, and there was no essential difference in the two classes of results.

On the contrary, when the method of but one grating and sodium light was used (fig. 11), the interferometer fringes, in case of a very wide slit or the absence of a slit, could not be produced over the yellow field, as a whole. There appeared, however, an obviously pulsating flicker in parts of the field, on reducing the width of the slit till the sodium lines were each about the width of a  $D_1D_2$  space, with either  $D_1D'_1$  or  $D_2D'_2$  superposed. The sharply outlined slit showed an irregular, rhythmic brightening and darkening over certain parts of its length. These broad pulsations were very violent, very much in character with the linear phenomenon above. This behavior is very peculiar, recalling the appearance of a bright yellow ribbon undulating, or flapping fore and aft, so as to darken parts of its length rhythmically. The pulsations, moreover, were quite as active if seen at night, when the tremors of the laboratory were certainly reduced to minimum. Nevertheless, I am now convinced that such tremor only is in question.

Regarding the phenomenon as a whole, one may argue that in case of the wide slit and single grating, in which the lines for both diffractions are therefore rigorously parallel, the interference fringes are on so large a scale as to cover the whole field of view and thus to escape detection; *i.e.*, that a single vague, quivering shadow of a flickering field is all that may be looked for, in the limited field of view of the eyepiece.

Returning to the case of two gratings and the wide vertical interference fringes and, in turn, all but closing the slit (vertical interferences and sodium arc light), the pulsating phenomenon simply narrowed in width. The two or three sharp vibrating lines, alternating in black and yellow of the original phenomenon (Chapter I), did not appear. The cause of this is now to be investigated.

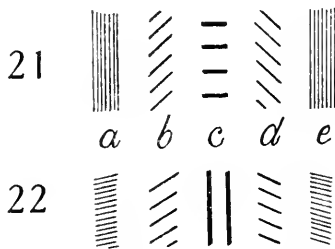
**14. Experiments continued. Rotation, etc., of grating.**—The method of two gratings (fig. 16 or 20, plane transmitting and concave reflecting) was first further improved by perfecting the fore-and-aft motion of the grating  $G'$  ( $G'$  movable in the direction  $G'T$  on a slide), as well as the precision of the independent rotation of  $G'$  normal to its face; *i.e.*, around  $G'T$ . These adjustments led to further elucidation of the phenomenon. To begin with the fore-and-aft motion of the concave grating  $G'$  (*i.e.*, displacements in the directions  $G'T$ , fig. 20), it was found that the fringes, figure 21,  $a, b, c, d, e$ , in any good adjustment, pass from extremely fine, sharp, vertical striations, which gradually thicken and incline to relatively coarse, horizontal lines, finally with further inclination in the same direction into fine vertical lines again, while  $G'$  continually moves (through about 5 cm.) on the slide normal to the face

of the grating. It was not at all difficult to follow the continuous tilt of these lines through the horizontal, occurring on careful and continuous front-and-rear motions of the grating  $G'$  through the limiting positions. The fringes usually vanish vertically merely because of their smallness.

Again, on rotating the grating  $G'$  around an axis normal to its face, the fringes merely vary in size, without changing their inclination. Thus if the horizontal fringes (which were here always closer than the inclined set) are in view, these will pass from extremely small-sized, fine, hair-like striations, through a maximum (which is a mere shadow, as a single fringe probably fills the field) back into the fine lines again. Only a few degrees of rotation of the grating suffice for the complete transformation. The maximum is frequently discernible only in consequence of a flickering field. An oblique set of fringes is equally available, remaining oblique as they grow continually coarser and in turn finer with the continuous rotation of the grating.

When the very large horizontal fringes are produced by this method, the change into vertical fringes by fore-and-aft motion of  $G'$  is very rapid, so that relatively wide, nearly vertical forms may be obtained. All these effects may be produced by solar or by arc light, around the line of symmetry of the overlapping spectra; or with sodium light when either  $D_1D'_1$  or  $D_2D'_2$  coincide.

The fine vertical or inclined lines appear as such when the slit is widened, either in case of white or of sodium light. These are the interferometer fringes seen above (§ 6), coarse or fine. With sodium light any width of slit, or no slit at all, is equally admissible. The same is true for the narrow maxima. Lines nearly horizontal were sometimes obtained, pointing, as a whole, toward a center.



Finally (and this is the important result) the extremely large horizontal maxima, when a single fringe fills the field, can not be seen apart from pulsations, in the case of a wide slit. With a very narrow slit, such as is suited for the Fraunhofer lines, these horizontal fringes appear as intensely bright or very dark images of the slit. In other words, the normal phenomenon of overlapping symmetrical spectra as described in Chapter I is merely the vertical strip of an enormous horizontal interference fringe, made sharp and differentiated by its narrowness. This case occurs at once when the rulings of the two gratings  $G$  and  $G'$  are all but parallel, and hence it is the regular phenomenon when but a single grating is used for the two diffractions, as in figures 11 and 12.

In later experiments on the effect of the rotation of the grating,  $G'$ , around a normal axis, the above results were found to be incomplete. If the rotation is sufficient in amount (a few degrees, always very small), it appears that, after enlarging, the fringes also rotate. But the rotation in this case corresponds to a *vertical* maximum, as indicated in figure 22, the vertical set being

the coarsest possible for a given fore-and-aft position of the grating  $G'$ . In the figure, the sequence  $a, b, c, d, e$  is obtained for a continuous rotation of the grating (in one direction around a normal axis).

It now became interesting to ascertain how the vertical set  $c$ , figure 22, would behave with the fore-and-aft motion. The experiments showed that there was no further rotation, but that, while  $G'$  passes normally to itself over about 1.5 cm. on the slide, the vertical fringes pass from extreme fineness at the limit of visibility, through an infinite vertical maximum (a single vague shadow pulsating in the field), back to extreme fineness again, without any rotation. If the edges of the corresponding yellow strips (superposed  $D_1, D'_1$  lines) did not quite coincide, the fringes were seen outside of the principal focal plane, as usual. Probably the vertical and horizontal maxima are identical in occurrence and appear in case of parallelism in the rulings of the two gratings  $G$  and  $G'$ , and the absence of path-difference. Hence if a single grating is used, as in the original method, the interferometer fringes are not obtainable. This is an important and apparently final result, remembering that fore-and-aft motion is probably equivalent to a rotation around a vertical axis, parallel to the grating.

With regard to the rotation in case of fore-and-aft motion of  $G'$ , it is well to remark that in approaching the position  $c$ , figure 24, it is apt to be very rapid as compared with the displacement, precisely as in the case of the picket-fence analogy.

Hence the original phenomenon, consisting of single lines, can not be manifolded by increasing the width of slit. It vanishes for a wide slit into an indiscernible shadow. The phenomenon is a strip cut across an enormous black or bright horizontal fringe, by the occurrence of a narrow slit. Moreover, the scintillations variously interpreted above are now seen to be due to tremors, however different from such an effect they at first appear; *i.e.*, the enormously broad, horizontal fringe changes from dark to bright, *as a whole*, by any half wave-length displacement of any part of the apparatus. It is thus peculiarly sensitive to tremors. On the other hand, oblique or fine vertical fringes are always recognizable for any size of slit. The inquiry is finally pertinent as to why the phenomenon is so remarkably sharpened by a narrow slit; but this must be left to the following experiments.

To be quite sure that the concave grating  $G'$  had no fundamental bearing on the phenomenon, I again replaced it by the Michelson plane reflecting grating (fig. 16,  $G$  transmitting,  $G'$  reflecting). In the same way I was able to rotate the fringes, continuously, through a horizontal maximum of size by fore-and-aft motion of  $G'$ . Rotation of  $G'$  in its own plane increased or decreased the breadth and distance apart of the fringes through a maximum, coinciding with the parallelism of the rulings of the two gratings. Here I also showed decisively that as the rungs of the interference ladder (fig. 21  $c$ ) thickened and receded from each other, the design passed, in the transitional case, through the original phenomenon of the single vertical line dark or brilliant yellow, for a slit showing the Fraunhofer lines clearly. The phenome-

non vanishes with the spectrum lines as the slit is widened, but, on the other hand, persists as far as the interference of light for a narrow slit. Finally, the apparent occurrence of more than one line is referable to the presence of more than one *nearly* horizontal wide band in the field of the telescope. Thus, for instance, cases between *b* and *c* near *c* and between *c* and *d* near *c*, figure 24, are the ones most liable to occur when both diffractions take place at a single grating. This result will be used in paragraph 15.

**15. Tentative equations.**—In the first place, the actual paths (apart from the theory of diffraction) of the two component rays, on the right and left sides of the line of symmetry,  $II'Z$ , figure 23, will be of interest. The computation may be made for the method of two gratings at once, as the result (if the distance apart of the gratings is  $C=0$ ) includes the method with one grating; *i.e.*, the more complicated figure 23, where  $G$  is the transmitting and  $G'$  the reflecting grating, resolves itself into a case of figure 24, with but one grating,  $G$ .  $M$  and  $M'$  are the two opaque mirrors,  $I$  the normally incident homogeneous ray. Supposing, for simplicity, that the grating planes  $G$  and  $G'$  are parallel and symmetrically placed relatively to the mirrors  $M$  and  $M'$ , as in the figure, the ray  $Y$  diffracted at the angle  $\theta_1$  is reflected into  $X$  at an angle  $\theta_2 - \theta_1$  and diffracted into  $Z$  normally, at an angle  $\theta_2$ , on both sides. Under the condition of symmetry assumed  $X + Y - (X' + Y') = 0$ , or without path-difference. Let  $N$  be the normal from  $I$  to  $M$ , and  $n$  the normal from  $I'$  to  $M'$ , with a similar notation on the other side. Hence if  $I$  be given an inclination,  $di$ ,  $\theta_1$  is incremented by  $d\theta_1$ ,  $Y + X$  passes into  $y_1 + y + x$ ,  $Y' + X'$  into  $y'_1 + y' + x'$ , decremented at an angle  $d\theta'_1$ , while both are diffracted into  $Z'$ . Since generally

$$\sin \theta_1 - \sin i = \lambda/D \qquad \cos \theta_1 d\theta_1 = \cos \theta'_1 d\theta'_1$$

for homogeneous light and the same  $di$ . Hence  $d\theta_1 = d\theta'_1 = d\theta$ , say. If  $\delta = \theta_2 - \theta_1$ , and  $\sigma = \theta_2 + \theta_1$ , the auxiliary equations

$$X + Y = C \frac{\sin \theta_1 + \sin \theta_2}{\sin \delta} \qquad C = \frac{N - n}{\cos (\sigma/2)}$$

are useful. From a consideration of the  $yC$  and  $yx$  triangles, moreover, the relations follow:

$$y + y_1 = \frac{N}{\cos (\delta/2 - d\theta)} \qquad y_1 = \frac{N - n}{\cos (\sigma/2) \cos (\theta_1 + d\theta)} \qquad x = y \frac{\cos (\theta_1 + d\theta)}{\cos (\theta_2 - d\theta)}$$

and from the  $y'_1C$  and  $y'x$  triangles, similarly,

$$y' + y'_1 = \frac{N}{\cos (\delta/2 + d\theta)} \qquad y'_1 = \frac{N - n}{\cos (\sigma/2) \cos (\theta_1 - d\theta)} \qquad x' = y' \frac{\cos (\theta_1 - d\theta)}{\cos (\theta_2 + d\theta)}$$

Hence, after some reduction, the path on one side is

$$x + y + y_1 = \frac{2N \cos (\sigma/2)}{\cos (\theta_2 - d\theta)} - \frac{N - n}{\cos (\sigma/2) \cos (\theta_2 - d\theta)}$$

which may be further simplified to

$$x+y+y_1 = \frac{N \cos \sigma + n}{\cos(\theta_2 - d\theta) \cos(\sigma/2)}$$

From this the path on the other side will be

$$x'+y'+y'_1 = \frac{N \cos \sigma + n}{\cos(\theta_2 + d\theta) \cos(\sigma/2)}$$

The path-difference,  $\Delta P$ , thus becomes, nearly,

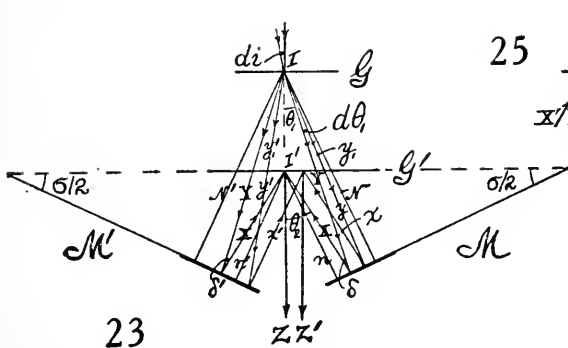
$$\Delta P = N \frac{\cos \sigma + n}{\cos(\sigma/2)} \left( \frac{1}{\cos(\theta_2 + d\theta)} - \frac{1}{\cos(\theta_2 - d\theta)} \right) = \frac{N \cos \sigma + n}{\cos(\sigma/2)} \frac{2 \sin \theta_2}{\cos^2 \theta_2} d\theta$$

This is perhaps the simplest form attainable. If, apart from diffraction, this should result in interference, the angular breadth of an interference fringe would be ( $\Delta P = \lambda$ )

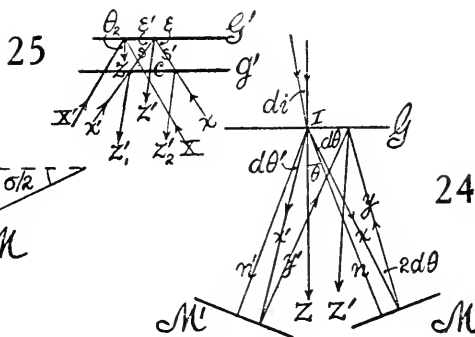
$$d\theta = \frac{\lambda \cos^2 \theta_2}{2 \sin \theta_2} \frac{\cos(\sigma/2)}{N \cos \sigma + n}$$

and if  $D$  is the grating space and  $\sin \theta = \lambda/D'$ ,

$$d\theta = \frac{(D'^2 - \lambda^2) \cos(\sigma/2)}{2D'(N \cos \sigma + n)}$$



23



24

In case of a single grating

$$\sigma/2 = \theta_2 = \theta \quad N = n \quad \cos \sigma = 2 \cos^2 \theta - 1$$

or

$$\Delta P = \frac{2N \cos^2 \theta}{\cos \theta} \frac{2 \sin \theta}{\cos^2 \theta} d\theta = 4N \tan \theta d\theta$$

a result which may be reduced more easily from figure 24. Hence, the angular distance apart of the fringes would be ( $\Delta P = \lambda$ )

$$d\theta = \frac{\lambda}{4N \tan \theta} = \frac{D \cos \theta}{4N} = \frac{\sqrt{D^2 - \lambda^2}}{4N}$$

if  $D$  is the grating space. To find the part of the spectrum ( $d\lambda$ ) occupied by a fringe in the case postulated, since  $\sin \theta = \lambda/D$ ,

$$\frac{d\theta}{\cos \theta} = \frac{d\lambda}{D \cos^2 \theta} = \frac{D}{4N}$$

and from the preceding equations, finally,

$$d\lambda = \frac{D^2 - \lambda^2}{4N}$$

where  $d\lambda$  would be the wave-length breadth of the fringe, remembering that the fringes themselves are homogeneous light.

In the grating used

$$D = 351 \times 10^{-6} \text{ cm.} \quad \lambda = 60 \times 10^{-6} \text{ cm.} \quad n = 100 \text{ cm.}$$

or

$$d\lambda = \frac{1200}{400} 10^{-10} = 3 \times 10^{-10} \text{ cm.}$$

This is but  $1/200$  of the distance,  $d\lambda = 6 \times 10^{-8}$  cm., between the  $D$  lines. Hence such fringes would be *invisible*. Moreover,  $d\theta \propto 1/N$ ; the fringes, therefore, should grow markedly in size as  $N$  is made smaller. Experiments were carried out with this consideration in view, by the single-grating and concave-mirror method,  $N$  being reduced from nearly 2 meters to 20 cm., without any observable change in the breadth or character of the phenomenon. It showed the same alternation of one black and one or two bright linear fringes, or the reverse, throughout. Hence, it seems improbable that the phenomenon, *i.e.*, the interference fringes, are referable to such a plan of interference as is given in figure 24.

Similarly, for the case of two gratings, figure 23,

$$d\theta = \frac{\cos(\sigma/2) (D'^2 - \lambda^2)}{2D'(N \cos \sigma + n)}$$

where, if we insert the data  $\theta_1 = 9^\circ 40'$  and  $\theta_2 = 19^\circ 55'$

$$D' = 173 \times 10^{-6} \text{ cm.} \quad N = 162 \text{ cm.} \quad n = 82 \text{ cm.} \quad \lambda = 58.9 \times 10^{-6} \text{ cm.}$$

then

$$d\theta = \frac{.967 \times 10^{-10} \times 263}{10^{-6} \times 346 \times (162 \times .87 + 82)} = .33 \times 10^{-6} \text{ radians.}$$

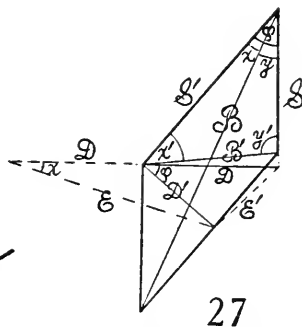
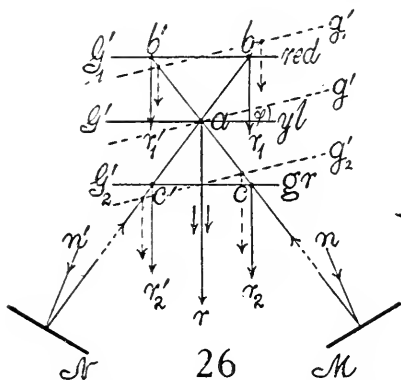
Thus  $d\theta$  is about of the same small order of values as above, *i.e.*, less than one-tenth second of arc or  $1/1000$  of the  $D_1 D_2$  space, and thus quite inappreciable. Some other source, or at least some compensation, must therefore be found for the interferometer interferences seen with homogeneous light.

The full discussion of the effective path-difference in terms of the diffractions occurring will be given in § 27, in order not to interrupt the progress of the experimental work here. It will then be obvious that the mere effect of changing the obliquity of the incident homogeneous rays,  $I$ , introduces no path-difference, or that the fringes observed are varied by the displacements and rotations of the grating,  $G'$ , and the mirrors  $M$  and  $N$ .

**16. Experiments continued. Analogies.**—With this possible case disposed of, it now becomes necessary to inquire into the other causes of the phenomenon, as described in paragraph 13. This is conveniently done with reference to figure 26, where  $n$  and  $n'$  are the axes of the pencil of yellow light, reflected from the opaque mirrors  $M$  and  $N$ , after arrival from the transmitting grating

*G.* It is necessary to consider the three positions of the reflecting grating  $G'$ ; viz,  $G'$ ,  $G'_1$ , and  $G'_2$ . In the symmetrical position  $G'$ , the pencils whose axes are  $n$  and  $n'$  meet at  $a$  and are both diffracted along  $r$ . In the position  $G'_1$ , they are separately diffracted at  $b$  and  $b'$  in the direction  $r_1$  and  $r'_1$ , and they would not interfere but for the objective of the telescope, or, in the other case, of the concave mirror of the grating. In the position  $G'_2$ , finally, the pencils  $n$  and  $n'$  are separately diffracted at  $c$  and  $c'$  into  $r_2$  and  $r'_2$  and again brought to interference by the lens or concave mirror, as specified.

Now it is true that the rays  $na$  and  $n'a$  (position  $G'$ ), though parallel in a horizontal plane, are not quite collimated in a vertical plane. The pencils are symmetrically oblique to a central horizontal ray in the vertical plane, and their optical paths should therefore differ. But fringes, if producible in this way here, have nothing to do with the rotation of the grating in its own plane and may here be disregarded, to be considered later.



To take the rotation of the fringes first, it is interesting to note in passing that the interferences obtained by rotation around a normal axis recall the common phenomenon observed when two picket fences cross each other at a small angle  $\phi$ . It may therefore be worth while to briefly examine the relations here involved (fig. 27) where  $S'$  and  $S$  are two corresponding pickets of the grating at an angle  $\phi$  and the normals  $D'$  and  $D$  are the respective grating spaces. The intersections of the groups of lines  $S'$  and  $S$  make the representative parallelogram of the figure ( $S$  taken vertical), of which  $B$  is the large and  $B'$  the small diagonal. The angles indicated in the figure are  $x+y=\phi$  and  $x'+y'+\phi=180^\circ$ . As the bright band in these interferences is the locus of the corners in the successive parallelograms,  $B$  is the distance between two bright bands, while  $B'$ , making an angle  $y'$  with  $S$ , is the direction of these parallel interference bands relative to the vertical. Let the free ends of  $D$  and  $D'$  be joined by the line  $E'$ ; and if  $D$  is prolonged to the left and the intercept is  $D$  in length, let this be joined with the end of  $D'$  by  $E$ . Then the triangle  $DED'$  and  $S'BS$ ,  $DE'D'$  and  $S'B'S$ , may be shown to be similar by aid of the following equations:

$$SD = S'D' \quad D' \sin \phi = E \sin x \quad S' \sin \phi = B \sin y \quad \frac{D'}{S'} = \frac{E \sin x}{B \sin y}$$

If  $E$  is expressed in terms of  $D$  and  $D'$ , and  $B$  in terms of  $S$  and  $S'$ , and the first equation is used, then

$$\frac{S}{S'} = \frac{\sin x}{\sin y} = \frac{D'}{D}$$

from which, in the fourth equation,

$$B = \frac{E}{\sin \varphi} = \frac{\sqrt{D^2 + D'^2 + 2DD' \cos \varphi}}{\sin \varphi}$$

Similarly,

$$B' = \frac{E'}{\sin \varphi} = \frac{\sqrt{D^2 + D'^2 - 2DD' \cos \varphi}}{\sin \varphi}$$

Again, the angle  $y'$  is given from

$$\frac{\sin (180 - (\varphi + y'))}{\sin y'} = \frac{D'}{D}$$

or on reduction

$$\tan y' = \frac{D \sin \varphi}{D' - D \cos \varphi}$$

If  $D = D'$ , or  $S = S'$ , then

$$B_0 = \frac{D}{\sin (\varphi/2)} \quad B'_0 = \frac{D}{\cos (\varphi/2)}$$

$$\tan y' = \frac{\sin \varphi}{\sin (\varphi/2)} = \cos (\varphi/2) / \sin (\varphi/2), \text{ or } \tan y' \tan \varphi/2 = 1$$

Thus if  $\varphi = 0$ ,  $\tan y' = \infty$ ,  $y' = 90^\circ$ , or the fringes are horizontal and  $B = 2S$ . If  $y'$  is nearly zero

$$\tan y' = \varphi / (\varphi^2/2) = 2/\varphi$$

changing very rapidly with  $\varphi$ .

If one grating of a pair, with identical grating spaces  $D$ , is moved parallel to itself, in front of the other, the effect to an eye at a finite distance is to make the grating spaces  $D$  virtually unequal; or

$$B = B_0 \frac{\sqrt{1 + (D'/D)^2 + 2(D'/D) \cos \varphi}}{2 \cos (\varphi/2)}$$

so that for an acute angle  $\varphi$ , the fringe breadth is increased. Thus  $B_0$  is a minimum in case of coincident gratings.

The analogy is thus curiously as follows: The fringes just treated rotate with the rotation of either grating in its own plane and pass through a minimum size with fore-and-aft motion; whereas in the above results the optical grating showed a passage through a maximum of size with the rotation of either grating in its own plane and a rotation of fringes with fore-and-aft motion of the grating.

Returning from this digression to figure 26, if the grating  $G'$  is not quite symmetrical, but makes a small angle  $\varphi$  with the symmetrical position as at  $g'$ , the fore-and-aft motion will change the condition of path-excess on the right (position  $g'_2$ ,  $M$  path larger) to the condition of path-excess on the left

(position  $g'_1$ ,  $N$  path larger); and if the motion is continuous in one direction,  $g'_2$ ,  $g'$ ,  $g'_1$ , the path-difference will pass through zero. No doubt the angle  $\varphi$  is rarely quite zero, so that this variable should be entered as an essential part of the problem. The resulting conditions are complicated, as there are now two angles of incidence and diffraction and it will therefore be considered later (§ 28). It is obvious, however, that if for a stationary grating  $G'$ , figure 26, the angle  $\varphi$  is changed from negative to positive values, through zero, the effect must be about the same as results from fore-and-aft motion. In both cases excess of optical path is converted into deficiency, and *vice versa*. Hence, as has been already stated, the effects both of the fore-and-aft motion and of the rotation of the grating  $G'$  around a vertical axis parallel to its face conform to the interference fringes of figure 21,  $a$  to  $e$ .

It is common, moreover, if a concave grating is used (with parallel rays) at  $G'$ , to find the two sodium doublets due to reflection from  $M$  and  $N$  approaching and receding from each other in the field of view of the ocular when the grating  $G'$  is subjected to fore-and-aft motion. This means that although the axes of incident rays are parallel in two positions, whenever  $i$  varies (as it must for a concave grating and fore-and-aft motion), the diffracted rays from  $M$  and  $N$  do not converge in the same focus in which they originally converged, but converge in distinct foci. For if  $\sin i - \sin \theta = \lambda/D$  or  $\cos idi = \cos \theta d\theta$ , suppose that for a given  $i$ ,  $\theta = 0$ ; then  $\cos idi = d\theta$ . But the deviation,  $\delta$ , of the diffracted ray from its original direction is now  $di + d\theta$ , or

$$\delta = di(1 + \cos i) = 2di \cos^2 i/2$$

Similarly, the principal focal distance  $\rho'$ , for varying  $i$ , is not quite constant. From Rowland's equation, if parallel rays impinge at an angle  $i$  and are diffracted at an angle  $\theta = 0$ ,

$$\rho' = \frac{R}{1 + \cos i} = \frac{R}{2 \cos^2 i/2}$$

If  $i = 20^\circ$ , then  $\cos^2 i/2 = .976$ , and  $\rho' = R/2$ , nearly but not quite.

I have not examined into the case further, as both the sodium doublets are distinctly seen if the ocular follows them (fore and aft), and the lateral displacement of doublets is of minor interest.

With the plane reflecting grating this discrepancy can not enter, since for parallel rays the angles of incidence remain the same throughout the fore-and-aft motion, and therefore the angles of diffraction would also be identical.

Two outstanding difficulties of adjustment have still to be mentioned, though their effect will be discussed more fully in the next chapter. These refer to the rotation of the grating  $G'$ , around a vertical axis and around a horizontal axis, in its own plane or parallel to it. The rotation around the vertical axis was taken up in a restricted way above, in figure 13, Chapter II. The effect (rotation of  $G'$ ) is to change the inclination of the fringes passing from inclination to the left through zero to inclination towards the right. The effect is thus similar to the fore-and-aft motion, as shown in figure 21.

It was here, with the ocular thrown much to the right (near  $M$ ), that I again encountered the arrow-shaped fringes of figure 2,  $D$ , Chapter I. Though they are rarely quiet, the observation can not be an illusion. As seen with white light and a fine slit they are merely an indication of fringes which, when viewed with a broad slit and homogeneous light, will be horizontal.

Rotation around a horizontal axis parallel to the face of the grating must also destroy the parallelism of the rulings. The usual effect was to change the size of fringes (distance apart, etc.); but I was not able to get any consistent results on rotating  $G'$ , owing to subsidiary difficulties. On rotating the grating  $G$ , however, a case in which fine rotation around a horizontal axis was more fully guaranteed, the fringes passed with continuous rotation through a vertical maximum, as in figure 22.

In figure 26, the central region  $a$  of the grating  $G'$  is found, on inspection, to be yellow in the position  $G'$ , red in the position  $G'_1$ , and green in the position  $G'_2$ . The slit in this case must be very fine. For a wide slit and homogeneous light, the continuous change in the obliquity of pencils is equivalent to the continuous change of wave-length in the former case. It is therefore interesting to make an estimate of the results to be expected, if the vertical fringes for the cases  $bb'$  or  $cc'$  were Fresnellian interferences, superposed on whatever phase-difference arrives at these points. In the usual notation, if  $c$  is the effective width at the concave grating,  $F$  its principal focal distance,  $x$  the deviation per fringe,  $d\theta$  the corresponding angle of deviation,  $\lambda$  the wave-length of light,

$$x = \lambda F / c \text{ or } d\theta = \lambda / c$$

If  $c = 1.6$  cm.,  $\lambda = 6 \times 10^{-5}$  cm., then  $d\theta = 3.7 \times 10^{-5}$ , or about  $7''$  of arc.

The corresponding deviation  $d\theta D$  equivalent to  $d\lambda D$  of the  $D_1 D_2$  lines would be (if the grating space is  $D = 173 \times 10^{-6}$  cm.,  $\theta = 20^\circ$ , nearly, the normal deviations for yellow light),

$$d\theta_D = \frac{d\lambda_D}{D \cos \theta} = \frac{6 \times 10^{-5}}{173 \times 10^{-6} \times \cos 20^\circ} = 3.7 \times 10^{-4}$$

Thus  $\frac{d\theta}{d\theta_D} = 0.1$ , or, in this special case, there would be ten hair lines to the  $D_1 D_2$  space. As  $c$  is smaller or larger, there would be more or less lines. This is about the actual state of the case as observed. Finally, if  $c$  is very small, the fringes are large, since

$$\frac{d\theta}{d\theta_D} = \frac{\lambda D \cos \theta}{c d\lambda_D}$$

Thus conditions for practical interferometry would actually appear, the fringes being of  $D_1 D_2$  width for  $c = 0.17$  cm., provided a wide slit and homogeneous light of at least  $D_1$  or  $D_2$  grade is used. Such an interferometer seems to differ from other forms, inasmuch as the fringes remain of the same size and distribution, from their entrance into the field to their exit; or for a motion of the opaque mirror  $M$  of about 6 mm.

To resume the evidence thus far obtained, we may therefore assert that in the case of homogeneous light and a wide slit, or the absence of a slit, the field would either be bright or dark, as a whole. There is a single enormous horizontal fringe in the field. Hence the pronounced flickering with half wave-length displacements of any part of the apparatus. With the slit narrowed until the Fraunhofer lines are seen sharply, the linear phenomenon in question (Chapter I) appears. This may become ladder-like, but it always remains very narrow ( $\frac{1}{3} D_1 D_2$ ) when the rulings of the two gratings are not quite parallel.

**17. Subsidiary diffractions.**—The behavior of the linear phenomena sometimes suggests probable relations to the Fresnellian interferences, produced, however, not within the telescope, as in §§ 27, 28, Chapter III (for the interferences are seen together with the Fraunhofer lines in the principal focal plane), but outside of it, at the grating, as suggested by figure 26. If the concave grating  $G'$  is screened off, until a width of strip parallel to the rulings and not more than 5 mm. wide is used, the linear phenomenon is much enhanced, being both broader and stronger, without losing its general character. Here the  $D$  lines are still visible. The ladder-like patterns show an equally pronounced coarsening. So far as these phenomena go, it is obvious that the resolving power of the grating must be in question, seeing that the total number of rulings has been greatly reduced. The use of screens with narrower slits carries the process farther; but after the opening is less than 2 mm. in width the available light is insufficient for further observation. If a small lens is used, the phenomena can still be seen over 2 meters beyond the principal focus of the grating.

A screen was now made as in figure 28 *a*, with two slits about 2 mm. wide and 2 mm. apart (*b*), and placed over the effective part of the grating. The result, after careful trial as to position, was noteworthy. Oblique fringes were widened to many times the  $D_1 D_2$  space and coarsened, showing a definite grid-like design, as in figure 28 *b*, whereas, on removing the screen, the original pattern of a regular succession of brilliant dots (fig. 28 *c*) again appeared.

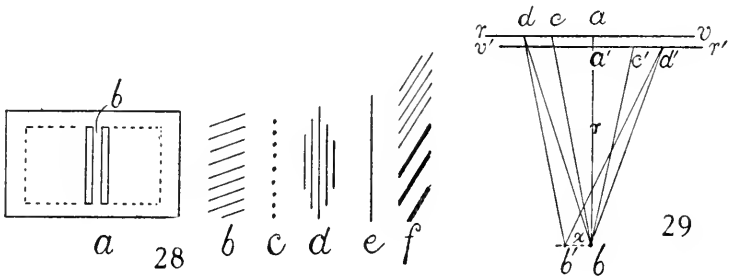
It was with the linear fringes, however, that the evidence obtained was most striking; for these now showed all the Fresnellian interferences (fig. 28 *d*). On removing the screen, the brilliant linear phenomenon (fig. 28 *e*), which in all the experiments made had thus far resisted manifolding, appeared at once. The pattern, *d*, moreover, when viewed with a small lens, within a meter in the direction of the rays, showed very definite enlargement with distance. Though a fine slit was needed, the resolving power of the grating was now too small to show any Fraunhofer lines. Similar results were obtained for a wire 1 or 2 mm. in diameter. With the screen, figure 28 *a*, and a bar, *b*, 1 mm. wide, the fine interference grid due to the bar, and the coarse grid due to the spaces (the fine lines being about twice as narrow as the coarse, but all of the same inclination) were often obtained together (fig. 28 *f*). A space 1 cm. wide intersected by a bar 2 mm. wide gave similar results, fine grids or

thick lines, according as one or both spaces were used. If either mirror, *M* or *N*, is screened, the whole phenomenon vanishes.

It follows, then, if *rv* and *v'r'*, figure 29, represent the two reversed, overlapping spectra at the grating, *b* the focus and *aa'b* the direction of the homogeneous diffracted rays condensed at *b*, that about 0.5 cm. of the spectrum, *d'a'* and *ad* on either side of *a*, is chiefly active in modifying the resulting diffraction pattern. Within this the homogeneous rays, *cc'* and *dd'*, are capable of interference. Although the wave-fronts entering *b* are slightly spherical, their radius is about *r* = 1 meter, and they may therefore be regarded plane. In such a case the angular width *dx* of the illuminated strip at *b*, for a width of screen *dd'* = 1 cm., between two extinctions, may be written

$$d\theta = \frac{dx}{r} = \frac{\lambda}{dd'} = \frac{60 \times 10^{-6}}{1} = 6 \times 10^{-5}$$

whereas the angular breadth of the *D<sub>1</sub>D<sub>2</sub>* doublets is about  $37 \times 10^{-5}$ ; *i e.*, the rays from *d* and *d'*, if in phase, should cease to illuminate *b* at a breadth of about one-sixth the distance between the sodium lines. The rays within



*dd'* would correspond to greater widths; those from *cc'*, for instance, 0.5 millimeter apart, would illuminate twice the estimated width, so that a strip at *b*, with a breadth of one-third the interval *D<sub>1</sub>D<sub>2</sub>*, is a reasonable average. All rays, however, would produce illumination at *b*. As the screens are narrower, not only would the fringe be broader, but more lines would appear, because there is less overlapping. All this is in accord with observation. Excepting the occurrence of independent half wave-fronts, the phenomena do not differ from the ordinary diffraction.

With regard to waves of slightly different lengths, focussed at *b'*, each is there superposed on a wave of different length from its own, and appreciable interference ceases for this reason. If the slit is widened, the phenomenon (with white light) also vanishes by overlapping. The case of the screen with two spaces has already been treated in relation to figure 26. In general, these are cases of the diffraction of a rod, or of a slit, which are possible only if the colors,  $\lambda$ , are symmetrically distributed to the right and to the left of it. Thus they require *both* spectra and can not appear if single spectrum only is present. To reveal the nature of the phenomenon, a wide slit and homogeneous light must be resorted to, as has been done in the present paper, even if white light and the fine slit totally change the aspect of the fringes.

**18. Conclusion.**—To return, finally, to the original inference, it appears that beating wave-trains have not been observed, but that the striking scintillations are due to an exceptional susceptibility of the apparatus to laboratory tremors, when exhibiting the phenomenon in question. Of this I further assured myself by observations made at night and on Sunday, though there is some doubt in my mind. What has certainly been observed is the interference of a  $D_1$  or  $D_2$  line with a reversed  $D'_1$  or  $D'_2$  line, both having the same source and longitudinal axis. One can only assert, therefore, that light of the wave-length interval of the breadth of these lines is capable of interference, when the line is reversed.

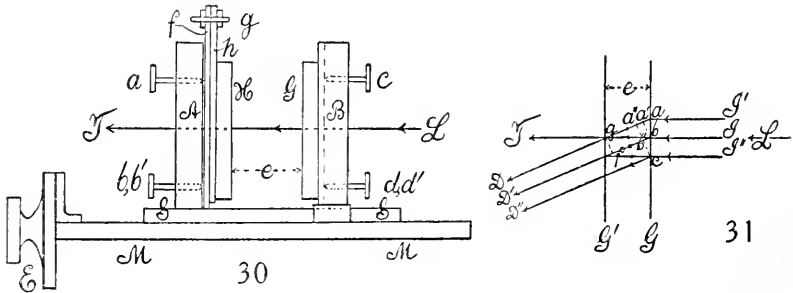
The phenomena, as a whole, are to be treated as diffractions of symmetrical *half wave-fronts*, each of which may be separately controlled by the corresponding micrometer.

## CHAPTER III.

### THE INTERFERENCES OF THE NON-REVERSED SPECTRA OF TWO GRATINGS, TOGETHER WITH AN INTERPRETATION OF THE PHENOMENA IN CHAPTERS I AND II.

**19. Introduction. Method.**—The chief purpose of the present paper is the search for phenomena similar to those of Chapter II, but in which the two spectra brought to interference are not inverted relatively to each other. Incidentally the strong interferences may have a value on their own account. It has been shown that the totality of the phenomena with spectra reversed on a transverse or a longitudinal axis are quite complicated, and a series of companion researches in which similar results are aimed at, in the absence of inversion, is thus very desirable.

The apparatus (fig. 30) is a modification of that shown in figure 50, in the next section, *MM* being the base of the Fraunhofer micrometer, *SS* the slide, *E* the micrometer screw. The brass capsules *A* and *B* are securely mounted on the slide *S*, free from the base *M*, and on the base *M* free from the slide



*S*, respectively. Each capsule is provided with three adjustment screws relative to horizontal and vertical axes *a*, *b*, *b'*, and *c*, *d*, *d'*, together with strong rearward-acting springs, by which the gratings *G* and *H* at a distance *e* apart may each be rotated slightly around a vertical or a horizontal axis (plane dot slot mechanism). The two gratings *G* and *H* must be identical, or very nearly so, as to the number of lines per inch, and with their ruled faces toward each other. These faces, as well as the ruled lines, are to be nearly in parallel. To secure the latter adjustment a bolt, *g*, normal to the face of the grating *H*, serves as an axis, and an available tangent screw and spring (not shown) is at hand for fine adjustment. This device is of great importance in bringing the longitudinal axes of the two spectra due to *G* and *H* into coincidence, and a fine wire must be drawn across the slit of the collimator to serve as a guiding-line through the spectrum. Any lack of parallelism in slit and rulings rotates the fringes.

The beam of light,  $L$ , either white or homogeneous, as the experiment may require, is furnished by a collimator (not shown), which, with the telescope at  $T$  (placed in plan, in figure 31, at  $T$  or  $D$ ), are the usual parts of a spectro-scope. The collimator with slit is always necessary for adjustment. It may then be removed if the phenomenon is to be studied in the absence of the slit. The telescope is frequently replaced to advantage by a lens. White light is to be furnished by the arc lamp (without a condenser), by sunlight, or by an ordinary Welsbach burner. Both spectra are naturally very intense. A sodium flame suffices for the work with homogeneous rays.

The adjustments in case of white light are simple and the interferences usually very pronounced, large, and striking. Brilliant spectra, channeled with vertical narrow black lines, are easily obtained when the longitudinal axes are placed accurately in coincidence by rotating the plate  $h$  carrying the grating  $H$ , on the plate  $f$ , around the axis  $g$ . If the gratings are quite identical the sodium lines will also be in coincidence. Otherwise the two doublets,  $D_1D_2$  and  $D'_1D'_2$ , of the two spectra (nearly identical in all their parts and in the same direction) are placed in coincidence by rotating either grating around a vertical axis. Thereupon the strong fringes will usually appear for all distances,  $e$ , less than 2 cm. These fringes are nearly equidistant and vertical and intersect the whole spectrum transversely. They are not complicated with other fringes, as in the experiments of the next section. They increase in size till a single shadow fills the field of view, in proportion as the distance  $e$  is made smaller and smaller to the limit of complete contact. With the two adjustments carefully made, finally, by aid of the fringes themselves, further trials for parallelism are not necessary. Two film gratings, or even films, give very good fringes. During manipulations great care must be taken to keep the angle of incidence,  $i$ , rigorously constant; *i.e.*, to avoid rotating both gratings together or the apparatus as a whole, as this displaces the sodium doublets relative to each other and seriously modifies the equations.

**20. White light. Colored fringes.**—The two sodium doublets seen in the arc spectrum are usually equally brilliant, and but one set of strong fringes is present in the field of the telescope. Relatively faint fringes may sometimes occur, due, no doubt, to reflection, as investigated in the next section.

If both gratings are rotated, changing the angle of incidence from  $0^\circ$  to  $i^\circ$ , the fringes disappear from the principal focal plane, but reappear strongly in another focal plane (ocular forward or rearward). In such a case the  $D$  lines are no longer superposed. To be specific, let  $i$  and  $i'$ ,  $\theta$  and  $\theta'$ , be the angles of incidence and diffraction at the two gratings in question, the angle between their ruled faces being  $i-i'$ . Let  $D$  and  $D'$  be the two grating constants, and nearly equal. Then for a given color,  $\lambda$ , in relation to the individual normals of the two gratings,

$$\sin \theta - \sin i = \lambda/D \qquad \sin \theta' - \sin i' = \lambda/D'$$

Now if  $\theta'$  is referred to the original normal it becomes  $\theta'' = \theta' + i - i'$ ,  
or

$$\sin(\theta'' - i + i') - \sin i = \lambda/D'$$

If the sodium lines are to coincide,  $\theta = \theta''$ , or approximately

$$\sin(\theta - (i - i')) - \sin i' = \sin \theta - \cos \theta \cdot (i - i') - \sin i' = \lambda/D'$$

or on eliminating  $\sin \theta$

$$\sin i - \sin i' - (i - i') \cos \theta = \frac{\lambda}{D} - \frac{\lambda}{D'}$$

which is nearly

$$(1) \quad \frac{i - i'}{D - D'} = \frac{\lambda}{D^2(1 - \cos \theta)}$$

In case of the Wallace grating below

$$D = 1.75 \times 10^{-4} \quad \lambda = 58.93 \times 10^{-6} \quad i - i' = 10^4 \times 3.29 (D - D')$$

Thus if the inclosed angle  $i - i'$  between the plates is 1 degree, or 0.0175 radian,  $D - D' = 5.3 \times 10^{-7}$ , about 0.3 per cent of  $D$  and equivalent to about 43 lines to the inch. With adequate facilities for measuring  $i$ , this method may be useful for comparing gratings, not too different, in terms of a normal or standard, practically, since the finite equations may also be expanded. In a similar way the slight adjustments of the longitudinal axes of the two spectra may be made by rotating one grating around a horizontal axis; but this correction is less easily specified. Finally, one should bear in mind that with film gratings there is liable to be an angle  $i - i'$  between the adjusted plates. Fortunately this has very little bearing on the method below.

The range of displacement of grating within which the fringes may be used with an ordinary small telescope extends from contact of the two gratings to a distance of  $e = 2$  to 3 cm. beyond.

In figure 31, which is a plan of the essential planes of the apparatus,  $G, G'$  being the ruled faces of the gratings in parallel,  $I, I', I''$ , three impinging rays of white light diffracted into  $D, D'$ , the points  $a, b, c, a', a'', b$  are in the same phase, so that the path-difference of the rays from  $b$  at  $g$  and  $f$  is easily computed. If the single ray  $I$  is diffracted into  $D$  and  $D'$  or  $I$  and  $I'$  into  $D$ ,  $I$  and  $I''$  into  $D'$ ,  $I'$  and  $I''$  into  $D$  and  $D'$ , the equations for these fringes should be (if  $\Delta P$  is the path-difference),

$$\Delta P = e(1 - \cos \theta) = e(1 - \sqrt{1 - \lambda^2/D^2})$$

where  $D$  is the grating space,  $e$  the distance apart, and  $\lambda$  the wave-length. Thus the micrometer value of a fringe for a color  $\lambda$  should be, under normal incidence,

$$(2) \quad \delta e = \frac{\lambda}{1 - \cos \theta} = \frac{\lambda}{1 - \sqrt{1 - \lambda^2/D^2}}$$

For two colors  $\lambda$  and  $\lambda'$

$$n\lambda = e(1 - \cos \theta) = eM \quad (n + n')\lambda' = e(1 - \cos \theta') = eM'$$

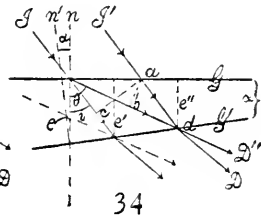
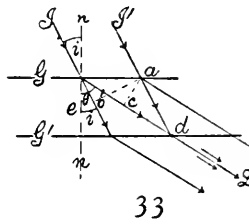
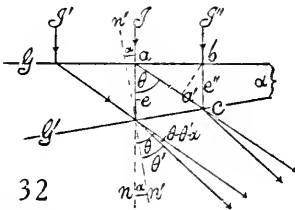
if  $n'$  is the number of fringes between  $\lambda$  and  $\lambda'$ . Thus

$$(3) \quad n' = e \frac{M'\lambda - M\lambda'}{\lambda\lambda'}$$

or the number of fringes increases as  $e$  is greater.

Equation (2) does not, as a rule, reproduce the phenomenon very well. Since the grating space  $D$  of the two gratings is rarely quite the same, the air-plate inclosed, in case of apparent coincidence of the sodium lines, is slightly wedge-shaped, as in figure 32. Hence the two diffractions take place at incidences  $0^\circ$  and  $\alpha^\circ$ , respectively, and the corresponding angles of diffraction will be  $\theta$  and  $\theta'$ . If we consider the two corresponding rays  $I$  and  $I''$ , diffracted at the first and second face, respectively, and coinciding at  $c$  in the latter, the points  $a$ ,  $b$ , and  $a'$  ( $ba'$  normal to  $ac$ ), are in the same phase, and we may compute the phase-difference at the coincident points at  $c$ . Since the distance  $bc$  is

$$e' = e \frac{\cos \alpha \cos \theta}{\cos (\theta - \alpha)}$$



the path-difference is

$$n\lambda = \frac{e \cos \alpha \cos \theta}{\cos (\theta - \alpha)} (1 - \cos \theta)$$

whence

$$(4) \quad \delta e = \frac{\lambda \cos (\theta - \alpha)}{\cos \theta \cos \alpha \cdot (1 - \cos \theta)}$$

which changes into equation (2) when  $\alpha = 0$  and  $n = 1$ . Fortunately this correction is, as a rule, small. In case of the Wallace gratings ( $D = 1.75 \times 10^{-4}$  cm.), for instance, if  $\lambda = 58.93 \times 10^{-6}$ , then  $\theta = 19^\circ 40'$  or  $\delta e = 1.01 \times 10^{-3}$ ; whereas if  $\alpha = 5^\circ$ , then  $\delta e = 1.04 \times 10^{-3}$ ; if  $\alpha = 10^\circ$ , then  $\delta e = 1.07 \times 10^{-3}$ , etc.

If the incidence is at an angle  $i$  and the plates are parallel, figure 33, the inquiry leads in the same way to an equation of more serious import. If the gratings  $G$  and  $G'$  are at a distance  $e$  apart and the incident rays are  $I$  and  $I'$ , the points  $a$ ,  $b$ ,  $c$  are in the same phase. Hence the two rays leaving  $d$  and diffracted along  $D$  correspond to a path-difference

$$(5) \quad \frac{e}{\cos i} (1 - \cos (\theta - i))$$

whence

$$\delta e = \frac{\lambda \cos i}{1 - \cos (\theta - i)}$$

Table 1 and fig. 35 show the variation of fringes with the angle of incidence  $i$ , equation (5). Hence if the angle of incidence is changed from  $-5^\circ$  to  $+5^\circ$ ,  $\delta e$  increases to nearly 3 times its first value. This, therefore, accounts for the large discrepancies of  $\delta e$  found in the successive data below. To secure increased sensitiveness and to make the apparatus less sensitive to slight changes of  $i$ , this angle should be about  $25^\circ$ , in which case  $\delta e$  is about three wave-lengths per fringe. But normal incidence is frequently more convenient.

Finally, in figure 34, if the angle of incidence is  $i$  and the two faces  $G$  and  $G'$  make an angle  $\alpha$  with each other and are initially at a distance  $e$  apart, changing successively to  $e'$  and  $e''$ , the points  $a, b, c$ , being in the same phase, the two rays  $D$  and  $D'$  leaving at  $d$ , at an angle  $\theta - i$ , will have a path-difference at  $d$  equal to

$$e \frac{\cos \theta \cos \alpha}{\cos i \cos (\theta - \alpha)} (1 - \cos (\theta - i))$$

whence

$$(6) \quad \delta e = \frac{\lambda \cos i \cos (\theta - \alpha)}{\cos \alpha \cos \theta (1 - \cos (\theta - i))}$$

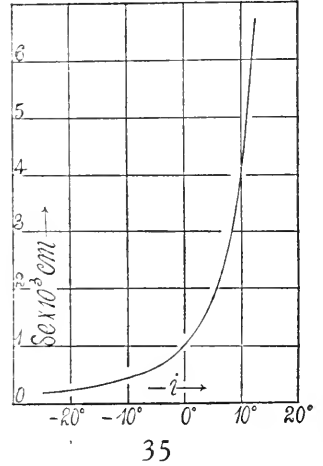


TABLE 1.—Wallace gratings.  $D = 10^{-4} \times 1.75$ .  $\lambda = 10^{-6} \times 58.93$ .

| $i$         | $10^3 \times \delta e$ | $i$         | $10^3 \times \delta e$ |
|-------------|------------------------|-------------|------------------------|
| $+19.040'$  | $\infty$               | $-5^\circ$  | 0.643                  |
| $+15^\circ$ | 16.740                 | $-10^\circ$ | 0.443                  |
| $+10^\circ$ | 4.090                  | $-15^\circ$ | 0.321                  |
| $+5^\circ$  | 1.840                  | $-20^\circ$ | 0.240                  |
| $= 0^\circ$ | 1.012                  | $-25^\circ$ | 0.185                  |

This equation reproduces the preceding equation (5) if  $\alpha = 0$  and the original equation (2) if  $\alpha = i = 0$ . It shows that a discrepancy or angle between the plates is of minor importance. Hence the change of this angle may be used to bring the sodium lines in coincidence when the gratings differ slightly in their grating constants  $D$ . On the other hand, changes of incidence  $i$  are of extreme importance.

Experiments made with the film grating showed that equation (2) not only fits very badly, but that  $\delta e$  per fringe is a fluctuating quantity. Table 2 gives some results obtained by measuring the successive values obtained for  $\delta e \times 10^3$ , corresponding to 10 fringes. Fringes were distinctly seen within 3 cm. of displacement by an ordinary telescope.

TABLE 2.

Gratings 15,050 lines to inch; computed values  $10^3 \delta e = 0.94$  cm. per fringe.

|                            |                            |                       |
|----------------------------|----------------------------|-----------------------|
| First sample:              | Second sample:             | } (normal incidence)  |
| $10^3 \delta e = 1.22$ cm. | $10^3 \delta e = 0.98$ cm. |                       |
| 1.07                       | 1.21                       | } (oblique incidence) |
| 1.16                       | 1.06                       |                       |
|                            | 1.11                       |                       |

TABLE 2.—Continued

Wallace gratings 14,050 lines to inch; computed value  $10^3\delta e = 1.01$  cm. per fringe.

|   |      |
|---|------|
| $10^3\delta e = 1.22$ cm. (large fringes); $10^3\delta e = 1.35$ (different $i$ ) |      |
| 1.24  | 1.32 |
| 1.25  | 1.30 |
| 1.23  | 1.35 |
| 1.23 (small fringes)  | 1.33 |
| 1.23  | 1.33 |
|   | 1.32 |
|   | 1.34 |

The reason for lack of accord is given in equations (5) and (6) and table 1. Any wedge effect of the glass plate is probably negligible. To show that the irregularity of the above results is to be sought in the accidental variations of the angle of incidence  $i$  at both gratings, the rough experiments in table 3 suffice.

TABLE 3.

|  |   |
|--|---|
| $i$ , negative (less than $10^\circ$ ),<br>Ocular drawn in,<br>focus changing, }<br><hr/>          | $\delta e \times 10^3 = 0.77$ cm.<br>.78<br>.74 |
| $i = 0$ ; ocular set for<br>principal focal plane. Na lines<br>in field and coincident, }<br><hr/> | $\delta e \times 10^3 = 1.18$ cm.<br>1.12       |
| $i$ , positive (less than $10^\circ$ ),<br>ocular drawn out, }                                     | $\delta e \times 10^3 = 1.69$ cm.<br>1.66       |

Thus, as equation (6) implies, small variations of  $i$  produce relatively large variations of  $\delta e$ , and if  $i$  passes continuously through zero, from negative to positive incidence,  $\delta e$  increases continually and may easily be more than doubled. If the phenomenon is in focal planes in front of the principal plane (ocular in),  $\delta e$  is small, and *vice versa*. Moreover, this enormous discrepancy is quite as marked for thin glass (2 mm.) as for thick glass plates (8 mm). Again, the rather stiff screw of the micrometer, which twisted the whole apparatus slightly, was sufficient to introduce irregularity. Placing the telescope close to the grating or far off made no difference. Hence the position of the optical center of the objective does not affect the result.

An additional result was obtained by placing a plate of glass between the two gratings  $G$  and  $G'$ . The effect was an unexpected *enlargement* of fringes, increasing with the thickness of the glass plate (0.6 cm. or more). The reason for this is given by equation (3), in paragraph 2, for the number of fringes  $n'$  between two colors  $\lambda$  and  $\lambda'$ ,

$$n' = \frac{e(M'\lambda - M\lambda')}{\lambda\lambda'}$$

where  $M = 1 - \cos\theta$ ,  $M' = 1 - \cos\theta'$ . Since  $n'$  is a number, the glass plate can be effective only in changing  $\theta$  and  $\theta'$ . As both are diminished by refraction, the cosines are increased and  $1 - \cos\theta$ ,  $1 - \cos\theta'$  are both decreased. Hence  $n'$  is decreased or the number of fringes is decreased, and their distance apart is thus larger.

It is obvious that when the sodium lines are not superposed the fringes can not lie at infinity, but are found in a special focal plane, depending on

the character of coincidence; *i.e.*, whether the rays are convergent or divergent. Finally, a slight rotation of the slit around the axis of the collimator rotates the fringes in the opposite direction to the sodium lines, and it is rather surprising that so much rotation of slit ( $10^\circ$  or  $20^\circ$ ) is permissible without fatally blurring the image. The slightest rotation of one grating relatively to the other destroys the fringes.

Naturally, the colored fringes vanish when the slit is widened or when it is removed. To give them sharpness, moreover, the beam passing through the grating must be narrow laterally. It is possible to see these colored fringes with the naked eye; but the transverse and longitudinal axes must in this case be slightly thrown out of adjustment, so that the fringes are no longer visible in the telescope. To the eye they form a somewhat fan-shaped set of colored fringes; *i.e.*, narrower below than above. Neither are the lines quite straight. If the collimating lens is removed, a slit about 0.1 cm. wide across a white flame will also show (to the telescope or to the eye) fine, strong lines rotating in opposite direction to the slit, according as the transverse and longitudinal axes are differently placed. As has been already stated, it is with the latter condition that the focal plane in which the fringes lie varies enormously.

Finally, when the sodium lines are superposed but the longitudinal axis of the spectra not quite so, a second class of fringes appear, which, however, are always more or less blurred. They rotate with great rapidity over  $180^\circ$  when one grating rotates over a small angle relatively to the other and the angle between the longitudinal axes of spectra passes through zero. In the latter position the regular fringes appear in full strength in the principal focus. To see the secondary interferences, the ocular must be drawn inward (toward the grating), and these fringes increase in size with the displacement of the ocular away from its position when regarding the principal focal plane. This secondary set of fringes is always accompanied by another very faint set, nearly normal to them and apparently quivering. The quiver may be due to parallax and the motion of the eye. These are probably the vestiges of the regular set of fringes, out of adjustment.

**21. Homogeneous light. Wide slit. Transverse axes coincident.**—If there is no color-difference, fringes of the same kind will nevertheless be seen in the telescope, on widening the slit indefinitely. Path-difference is here due to differences of obliquity in the interfering rays. As in the preceding case, accurate adjustments of the longitudinal and transverse axes (in case of sodium,  $D_1$  and  $D'_1$  or  $D_2$  and  $D'_2$  coincide horizontally and vertically) of the homogeneous color-field are essential if strong fringes are to appear in the principal focus. These fringes are, as a rule, well marked, and widening the slit merely increases the width of the channeled, homogeneous field of view. If, owing to slight differences of grating space, the sodium lines are not quite superposed automatically, this may be corrected by rotating either grating, or else the apparatus as a whole, until the fringes are strongest. The



If the grating  $G'$  is displaced  $\delta e$  parallel to itself, however, the path-difference will again be increased by  $\lambda$  whenever

$$\delta e = \frac{\lambda \cos i}{1 - \cos(\theta' + i)}$$

Since  $i$  is small, this equation will not differ appreciably from equation (2), with which it coincides for the central fringes.

If the sodium lines are not superposed, these fringes may still be seen, but they are not in the principal focal plane and the new focal plane changes continually, as the fringes grow in size. Examples are given in table 4. The large values of  $\delta e$  show that  $i$  was not actually negligible. Experiments similar to the above, bearing on the reason for the discrepancy (equation 6), were tried with the thin Wallace gratings, and the results are given in table 5.

TABLE 5.—Thin Wallace grating.

|                                   |                                   |                                   |                   |                   |
|-----------------------------------|-----------------------------------|-----------------------------------|-------------------|-------------------|
| $i$ negative (within $10^\circ$ ) | $\delta e \times 10^3 = 2.60$ cm. | $\delta e \times 10^3 = 2.40$ cm. |                   |                   |
| Ocular in,                        | 2.34                              | 2.45                              |                   |                   |
|                                   | 2.57                              |                                   |                   |                   |
| $i = 0$ , normal incidence,       | $\delta e \times 10^3 = 1.48$ cm. | $\delta e \times 10^3 = 1.37$ cm. | } (small fringes) |                   |
| Ocular set for principal          | 1.50                              | 1.37                              |                   |                   |
| focal plane,                      | 1.37                              | 1.32                              |                   | } (large fringes) |
|                                   |                                   | 1.19                              | } (small fringes) |                   |
| $i$ positive (within $10^\circ$ ) | $\delta e \times 10^3 = 0.86$ cm. | $\delta e \times 10^3 = 0.96$ cm. | } (small fringes) |                   |
| Ocular out,                       | .88                               | .86                               |                   |                   |
|                                   |                                   | .85                               |                   | } (large fringes) |
|                                   |                                   | .87                               |                   |                   |
|                                   |                                   | .96                               | } (large fringes) |                   |

As before, the effect of  $i$  passing from negative (through zero) to positive values is enormous,  $\delta e$  increasing nearly threefold for a change of  $i$  estimated as within  $20^\circ$ . Here, however, the drawn-out ocular (towards the observer) corresponds to the small values of  $\delta e$ , whereas above the reverse was the case. This depends upon which of the spaces  $D$  or  $D'$  is the greater.

**22. Homogeneous light. Fine slit. Transverse axes not coincident.**—To obtain this group of interferences, the two sodium lines from a very fine slit are thrown slightly out of coincidence; *i.e.*, by not more than the  $D_1D_2$  distance. In the principal focal plane, therefore, these doublets are seen sharply, while if the ocular is drawn sufficiently forward or rearward, an interesting class of fringes soon appears which resemble Fresnel's fringes for two virtual slits. These fringes may be seen, however, on both sides of the focal plane and increase in size with the distance of the plane of observation (focus of ocular) in front or behind the principal focal plane. In figure 37 the two gratings,  $G$  and  $G'$ , are struck by parallel pencils from the collimator at different angles of incidence ( $0^\circ$  and  $i^\circ$ ). The two diffracted pencils of parallel rays are caught by the objective  $L$  of the telescope and condensed at the principal foci,  $F$  and  $F'$ , appearing as two bright yellow lines. In front and behind the plane  $FF'$ , therefore, are two regions of interference,  $I$  and  $I'$ , throughout which the Fresnellian phenomenon may be seen in any plane parallel to  $FF'$ , observed by the ocular. When the electric arc is used with a very fine

slit, these sodium fringes often appear at the same time as the colored fringes, and, though they are usually of different sizes, their lateral displacement with a change of distance apart of the gratings,  $\delta e$ , is the same. The fringes in question appear alone when the sodium burner is used. They may then (at times) be observed with the naked eye, with or without a lens, and they fail to appear in the telescope unless the objective is strengthened by an additional lens. They are always vertical, but finer in proportion as the  $D_1D_2$  and  $D'_1D'_2$  doublets are moved farther apart. They become infinite in size, but still strong, when the doublets all but coincide, showing a tendency to become sinuous or possibly horizontal. Rotation of either grating  $G$  around an axis normal to itself and relative to the other produces greatly enhanced rotation of the fringes, as in all the above cases, but they soon become blurred.

Only in the case when the horizontal axes of the field coincide (parallel rulings, etc.) do they appear strong. When the angle of incidence (or non-coincidence) is increased for both gratings, the size of the fringes increases; but when the  $e$  distance is increased by the micrometer, the fringes are apparently constant as to size. However, after displacement of 4 mm. they are liable to become irregular and stringy, though still moving. A fine slit is not essential, particularly when  $e$  is small. They vanish gradually when the slit is too wide. If a telescope with a strong objective is used, these fringes may be seen, retaining their constant size long after those of the next paragraph vanish. Examples of data are given in table 6, and  $\delta e$  is too low in value as compared with the computed datum for  $i = 0^\circ$ . With the Wallace gratings, these fringes were best produced by the aid of the sodium lines, in the ordinary electric arc, simultaneously with the colored fringes and for the case of a very fine slit. They were apparent both with an ocular drawn out or drawn in. In the former case several successive groups were observed. Beginning with the sharp sodium lines in principal focus ( $D_2$  and  $D'_2$  coincident), a slight displacement of the ocular outward showed the first group, this resembling a grid of very fine striations. Further displacement outward produced a second set, equally clear but larger. A third displacement of the ocular outward showed the third set, and these now coincided with, and moved at, the same rate as the colored fringes in the same field. Other groups could not be found. No doubt, for these four successive steps the interference grids of  $D_1$  and  $D'_1$ ,  $D_2$  and  $D'_2$  are coincident and superposed, until they finally find their place in the colored phenomenon.

TABLE 6.—Ives grating. Homogeneous light. Fine slit. Sodium lines not coincident.

|                               |
|-------------------------------|
| $\delta e \times 10^3 = 0.87$ |
| .77                           |
| .83                           |

**23. Homogeneous light. Slit and collimator removed.**—Fringes similar to those seen with the wide slit above may be observed to better advantage by removing the slit altogether. The sodium flame is then visible as a whole; and if the adjustments are perfected it is intersected with strong, vertical black

lines, visible to the naked eye or through a lens or a suitably strengthened telescope. They decrease rapidly with increase in  $e$ , but vanish to the eye before the preceding set in paragraph 22. The sodium lines need not be in adjustment, but the longitudinal axes of the field must be, as usual. If diffuse white light is present, faint colored fringes may be seen at the same time. If the collimator only partly fills the field of view, these diffuse light fringes and the preceding set may occur together. Both rotate markedly for slight rotation of either grating in its own plane. There seems to be a double periodicity in the yellow field, but it is too vague to be discerned. When magnified with a lens, they admit of a play of  $e$  within about 0.6 cm. from contact. When the sodium lines are not coincident, the focal plane continually changes with  $e$ . Otherwise it remains fixed.

Some data are given in table 7.

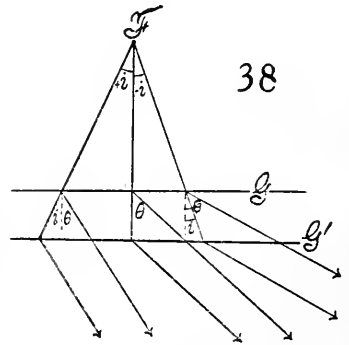
TABLE 7.—Ives grating. Homogeneous light. Collimator and slit removed. Focus continually changing.

|   |   |                                   |
|---|---|-----------------------------------|
| Large fringes; ocular out; lens on        | { | $\delta e \times 10^3 = 0.95$ cm. |
|   |   | 1.01                              |
| Ocular in, lens on                        |   | 1.04                              |
| Very small fringes, lens off              | { | 1.02                              |
|   |   | 0.96                              |
| Wallace grating. Sodium lines coincident. |   | 1.01                              |
| Principal focal plane                     |   | $\delta e \times 10^3 = 1.08$ cm. |
|   |   | 1.18                              |
|   |   | 1.20                              |

These data are similar to the above and subject to the same discrepancy whenever slight variation of the angle of incidence accidentally occurs. In figure 38 the case of three rays from a given flame-point  $F$  is shown corresponding to the equation

$$\delta e = \frac{\lambda \cos i}{1 - \cos(\theta + i)}$$

when  $i$  passes from positive to negative values. If either of the gratings is displaced and if they are parallel, the focal plane will not change; but if  $G$  and  $G'$  are not parallel, the focal plane differs from the principal plane and now moves with the grating.



**24. Inferences.**—The above data show that the equation underlying all the interferences observed is the same. The interferences themselves may result from different causes, but their variation in consequence of the motion of the grating,  $\delta e$ , is due to one and the same cause. This is best seen by producing them simultaneously in pairs. As a means of finding an accurate comparison of the number of lines per centimeter on any grating, in comparison with those on the given grating, the method used in paragraph 20 deserves consideration.

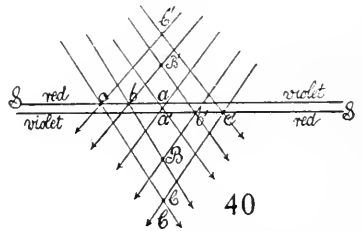
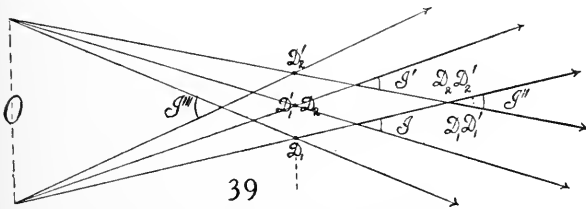
If the fringes are to be used for practical purposes, great care must be taken to keep the angle of incidence of the impinging light constant. This was not done in the present paper, where the purpose is merely an identification of the phenomena. Moreover, a micrometer with the screw running easily is essential, as otherwise the frame is liable to show appreciable twist (change of incidence) during displacement of the fringes.

The fringes are not of the sensitive type, but they admit of a large range of displacement and are therefore adapted to special purposes.

With regard to their bearing on the behavior of reversed spectra, for the interpretation of which the present experiments were undertaken, it is obvious that the interferences with homogeneous light and a wide slit (paragraph 21), or in the absence of a slit (paragraph 23), are of analogous origin in both cases. It makes no difference, therefore, whether one of the spectra is reversed or not, except, perhaps, that in the former case (inversion), the coincidence of longitudinal and transverse axes is a more insistent condition. The colored fringes of paragraph 20 obviously can not be produced with reversed spectra. There remain the fringes with the fine slit and homogeneous light (paragraph 22); in other words, the occurrence of a sort of generalized Fresnellian interferences, within the telescope, modified by causes which lie outside of it. Thus  $D_1$  and  $D'_1$  or  $D_2$  and  $D'_2$  may be placed sufficiently close together to produce a region of interference before and behind the principal plane in which the sodium lines are in focus. If the  $D_1D'_1$  lines are 0.01 cm. apart and the fringes seen likewise at 0.01 cm. apart, their position, measured from the principal plane, will be at

$$R = \frac{XC}{\lambda} = \frac{10^{-4}}{6 \times 10^{-5}} = \frac{5}{3} \text{ cm.}$$

or less than 2 cm. The ocular would then have to be displaced forward or rearward by this amount. But there are two sodium doublets, each pair of which is to interfere. Suppose that  $D_2$  and  $D'_1$  are in coincidence so that the



scheme is  $D_1 : D_2 D'_1 : D'_2$ , as in figure 39, where  $o$  is the principal plane of the objective and  $D_1$  to  $D'_2$  the principal focal plane. We should then have the separate regions of interference  $I$  and  $I'$  and the combined regions  $J''$  and  $J'''$ . When the breadth of the latter is the whole number of fringes, the two patterns clearly merge into a single pattern. The experiments show several of these stages, terminating outermost in the focal plane of the colored fringes under the given conditions. Since the fringes lie on hyperbolic loci the problem

itself is beyond the present purposes; but it appears that the colored fringes will not appear until the corresponding  $D_1$  and  $D_2$  lines are shared by the whole of the two continuous spectra.

The final question at issue is the bearing of the present Fresnel phenomenon on the reversed spectra. If in figure 40,  $s$  and  $s'$  represent the traces of two reversed spectra in the principal focal plane, superposed throughout their extent (*i.e.*, in longitudinal coincidence), the rays  $a_1a'_1B$ , through the line of symmetry  $a, a'$ , are at once in a condition to interfere with a given difference of phase; but so are all the symmetrically placed pairs of colors,  $c, c', b, b'$ , of the two spectra (the distances  $cc', bb'$ , being arbitrary), provided the corresponding rays meet. As they do not meet in the principal focus, they can interfere only outside of this— $b$  and  $b'$  at  $B, c$  and  $c'$  at  $C$ , etc. Similar conditions must hold at  $B'$  and  $C'$  within the principal focal plane. The linear interference is thus successively transferred to different pairs of wave-lengths. The phenomena of this paper can not, therefore, be detected in case of reversed spectra, because in the principal focal plane *different* wave-lengths are everywhere superposed, except at the narrow strip  $aa'$ , which experiment shows to be about one-third of the width of the sodium doublet, in apparent size. Beyond the principal focus the corresponding conditions in turn hold for the rays at  $B, C$ , etc.,  $B', C'$ , etc. Hence there can not be any Fresnellian interferences (paragraph 22), for there are not two virtual slits, but only a single one, as it were, and the interferences are laid off in *depth* along the normal  $C'C$ . The phenomenon may, in fact, be detected along this normal for 2 or 3 meters.

**25. Rotation of colored fringes. Non-reversed spectra.**—When the slit is oblique, it effectively reproduces the wide slit, locally, and therefore does not destroy the colored fringes. At every elevation in the field the slit is necessarily linear, though not vertical. In figure 41, let the heavy lines,  $H$ , denote the colored fringes for a fine vertical slit and white light, showing nearly the same distance apart, throughout. Let the light lines,  $L$ , denote the fringes for a wide vertical slit and homogeneous light,  $\lambda$ . These fringes are due to the successively increased or decreased obliquity of the rays in the horizontal plane. Now let  $acb$  be the image of the oblique slit in homogeneous light. It is thus merely an oblique strip, cut from the area of light lines or striations, as it were, and consists of an alternation of black and bright dot-like vertical elements in correspondence with the original striated field. We may suppose  $ab$  to have rotated around  $c$ , so that the vertical through  $c$  is its position on the colored field (white light and fine vertical slit).

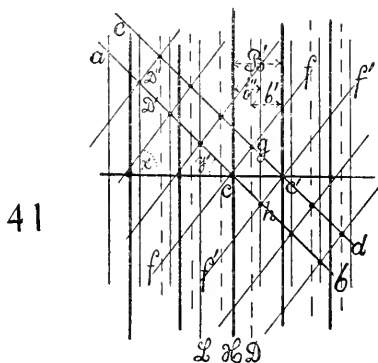
A color,  $\lambda'$  (near the one  $\lambda$ ), corresponding to the field of the lines  $L$  in case of a wide slit and homogeneous light  $\lambda'$ , will supply nearly the same grid, so far as the distance apart of fringes is concerned. But the grid is displaced laterally, in consequence of the different angle of diffraction,  $\theta$ . This is shown by the dotted lines  $D$  in figure 41, the effect being as if the slit had been displaced laterally. If the wide slit for homogeneous light  $\lambda'$  is now narrowed and

inclined as before, an alternation of bright and dark elements will appear in the image of the slit  $ed$ , corresponding to  $\lambda'$ . If we suppose that for white light and the fine vertical slit the position of the fringe ( $\lambda'$ ) was at  $c'$ , we may again regard  $c'$  as an axis of rotation. To find the fringes such as  $ff$ , it is then only necessary to connect corresponding black elements on  $ab$  and  $ed$ . Their inclination is thus opposite to  $ab$  and  $ed$ , or they have rotated in a direction opposite to that of the slit. If, for instance, the slit image  $ab$  or  $ed$  is gradually moved back to the vertical, the points  $g$  and  $h$  will move with great rapidity and in both directions toward infinity and the fringes  $ff$  and  $f'f'$  become vertical lines through  $c$  and  $c'$ , respectively.

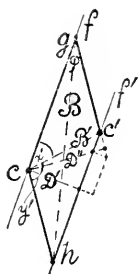
It is interesting to inquire into the frequency of fringes,  $n$ , when the angle of diffraction,  $\theta$ , is changed. From the original equation  $e = n\lambda / (1 - \cos \theta)$ , since  $d\lambda/d\theta = D \cos \theta$ , the rate of change

$$\frac{dn}{d\theta} = \frac{e}{D} \frac{1}{1 + \cos \theta} = \frac{e}{D + 1} \frac{1}{D^2 - \lambda^2}$$

where  $e$  is the distance apart of films and  $D$  the grating space. Since  $\cos \theta$  varies but slowly with  $\theta$  and is additionally augmented by 1,  $dn/d\theta$  is nearly constant and about equal to  $e/2D$ .



41



42

The fringes and slit images are thus given by the two sides of the parallelogram  $cgc'h$  for the two colors  $\lambda$  and  $\lambda'$ . The diagonal  $cc'$  represents  $d\theta$ ; the diagonal  $gh$  has no signification. On the other hand, the normal distances apart,  $D'$  and  $D''$ , of  $ff$  and  $f'f'$  and  $ab$  and  $ed$  are both important.

If  $D'$  and  $D''$  are the normal distances apart of the fringes and the slit images, respectively,  $B$  and  $B'$ , the two diagonals of the rectangle  $cgc'h$ , modified for convenience in figure 42,

$$D' = D'' (\cos \varphi + \sqrt{B'^2/D''^2 - 1} \sin \varphi)$$

which may be obtained from the two small triangles below  $c'$ . If  $B = D''$ ,  $D' = D'' \cos \varphi$ ; and if  $\varphi = 0$ ,  $D' = D'' = d\theta$ , remembering that  $c$  and  $c'$  lie on two consecutive colored fringes obtained with white light and a fine slit. If the slit images and fringes are symmetrical, each is at an internal angle,  $90 - \varphi/2$ , to the longitudinal axis of the spectrum.

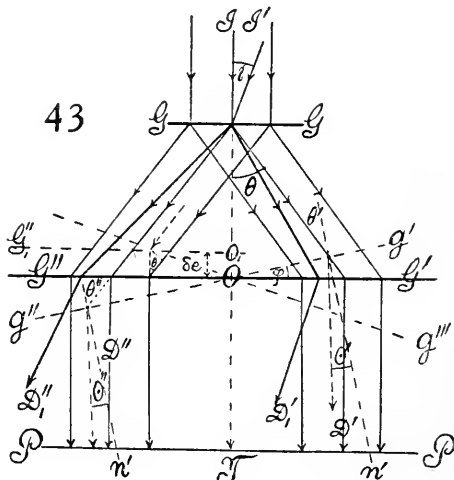
But these equations, though useful elsewhere, have very little immediate value here, because the experimental variables, figure 41, are  $B'$ , the distance between two consecutive colored fringes and  $b''$  and  $b'$  the corresponding distance between the fringes in case of homogeneous light in each case  $\lambda, \lambda'$ ; and the angle  $\gamma'$ , which indicates the inclination of the slit. Thus  $B'b'b''$  are given by computation and  $\gamma'$  is specified at pleasure. Obviously, if parallelograms are to be obtained, figure 41,  $b' = b''$ , appreciably. This is the case in experiment. Hence if we evaluate the height in the triangle  $cgc'$  for each angle it follows easily that

$$\sin x' = \frac{\tan \gamma'}{\sqrt{(B'/b' - 1) + \tan^2 \gamma'}}$$

If  $B' = b'$ ,  $x' = 90^\circ$  for all values of  $\gamma'$ ; *i.e.*, the fringes remain vertical. If  $B'$  is equal to  $2b'$ ,  $x' = \gamma'$ , the fringes and slit are symmetrically equiangular with the longitudinal axis of the spectrum. This is nearly the case in figure 41 and frequently occurs in experiment. If  $b'$  differs from  $b''$ , the fringes would not be straight. This also occurs, particularly when the thickness  $e$  of the air-film is very small.

**26. Final treatment of reversed spectra. Hypothetical case.**—To obtain an insight into the cause of the interferometer fringes as obtained with reversed spectra and two gratings, it is convenient to represent both gratings, figure 43,  $GG$  and  $G''G'$ , as transmitting, and suppose both diffracted beams,  $ID'$  and  $ID''$ , subsequently combined in view of the principal plane  $PP$  of an objective or a lens. It is clear that this simplified device can apply only for homogeneous light. In the case of white light, the opaque mirrors  $M$  and  $N$  (of the interferometer, above) return a divergent colored beam or spectrum, so that only for a single color can the second incidence be the same as the first. Again, if the constants of the two gratings are different, it is the function of these mirrors to change the incidence at the second grating correspondingly, so that for homogeneous light the rays issue in parallel. Finally, no reference to the lateral displacement  $OG''$  and  $OG'$  of rays need be made because, as more fully shown in the next paragraph, this is eliminated by the theory of diffraction.

The motion of the opaque mirrors  $M$  and  $N$  (above), on a micrometer, merely shortens the air-paths  $GG'$  or  $GG''$  in its own direction, and consequently the same fringe reappears for an effective displacement of half a wavelength, as in all interferometers.



The case of a single grating, moreover, is given if the planes of the grating  $GG$  and  $G'G''$  and their lines are rigorously parallel, the planes  $OG'$  and  $G''O$  being coplanar. To represent the interferences of the two independent gratings and with homogeneous light for the case of oblique incidence, it is necessary to suppose the grating  $G'G''$  cut in two halves at  $O$ , parallel to the rulings, and to displace the parts  $OG'$  or  $OG''$  separately, normally to themselves. Figure 43 shows that for normal incidence  $i=0$ , the displacement per fringe,  $\delta e$ , would be

$$\delta e = \frac{\lambda}{1 - \cos \theta}$$

or the fringes are similar to the coarse set of the present chapter.

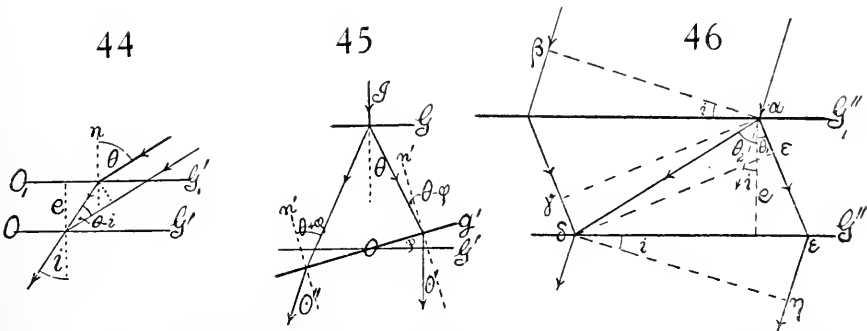
If the rays impinge at an angle  $i$ , figures 43 and 46, they will be parallel after the two diffractions are completed; for it is obvious that the corresponding angles of incidence and diffraction are merely exchanged at the two gratings. Hence the homogeneous rays  $I'$ , impinging at an angle  $i$ , leave the grating at  $D'_1$  and  $D''_1$  in parallel, at an angle of diffraction  $i$ , and the rays unite into a bright image of the slit. If, however,  $OG'$  be displaced to  $O_1G'_1$ , parallel to itself, as in figure 44, the paths intercepted are

$$\frac{e}{\cos i}, \text{ and } \frac{e}{\cos i} \cdot \cos(\theta - i)$$

and the path-difference per fringe, therefore,

$$\delta e = \frac{\lambda \cos i}{1 - \cos(\theta - i)}$$

which reduces to the preceding equation if  $i=0$ . Hence a series of interference fringes of the color  $\lambda$  must appear in the principal focus of the telescope or lens, on either side of  $i=0$ . The theory of diffraction again annuls the apparent path-difference between  $GG$  and  $G'G''$ .



As to the number of fringes,  $n$ , between any two angles of incidence  $i$  and  $i'$ , it appears that for homogeneous light of wave-length  $\lambda$ ,

$$n = \frac{e}{\lambda} \left( \frac{1 - \cos(\theta - i)}{\cos i} - \frac{1 - \cos(\theta - i')}{\cos i'} \right)$$

where  $e$  is the distance apart of the two parallel halves of the grating  $G''O$ ,  $OG'$ . Hence  $n$  vanishes with  $e$ , or the fringes become infinitely large. Lateral displacements are here without signification, as stated above.

If the grating  $G'$  is rotated over an angle  $\varphi$ , figure 43, and  $e = b\varphi$  where  $2b$  is half the virtual distance apart at the grating  $G'$  of the two corresponding rays impinging upon it (Chapter II, fig. 26), the rotation of the grating per fringe is thus

$$\delta\varphi = \frac{\lambda}{b} \frac{\cos i}{1 - \cos(\theta - i)}$$

or  $n$  (above) passes through zero as  $\varphi$  or  $b$  decreases from positive to negative values. If  $b$  is considered variable there is a wedge-effect superposed on the interferences.

It is this passage of  $n$  through zero that is accompanied by the rotation of the fringes, as above observed.

In case of two independent gratings,  $GG$  and  $G'G''$  ( $G'G''$  to be treated as consisting of identical halves,  $OG'$  and  $G''O$ ), nearly in parallel, fringes may be modified by rotating  $G'G''$  around the three cardinal axes passing through the point of symmetry  $O$ . The rotation of  $G'G''$  around an axis  $O$  normal to the diagram is equivalent to the fore-and-aft motion of  $G'G'$  when mirrors are used (fig. 26, Chap. II). The rotation around  $OT$  in the diagram and normal to the face of the grating requires adjustment at the mirrors around a horizontal axis to bring the spectra again into coincidence. This is equivalent to rotation around  $G''OG'$ . Both produce enlargement, and rotation of fringes is already explained.

Let the grating  $G'G''$  be rotated over an angle  $\varphi$  into the position  $g'g''$ , figure 45. Then the angle of incidence at the second grating,  $\theta$ , on one side is increased to  $\theta' = \theta + \varphi$  and on the other decreased to  $\theta'' = \theta - \varphi$ . In such a case the diffracted rays are no longer parallel. If  $\theta'$  and  $\theta''$  are two angles of diffraction on the right and on the left,

$$\sin \theta' + \sin(\theta - \varphi) = \sin(\theta + \varphi) - \sin \theta'' = \lambda/D$$

whence

$$\sin \theta'' + \sin \theta' = 2 \sin \varphi \cos \theta$$

or if  $\theta$  is the mean value of  $\theta'$  and  $\theta''$

$$\theta = \varphi \cos \theta, \text{ nearly.}$$

Similarly, since  $\sin \theta = \lambda/D$ , for  $i = 0$ ,

$$\sin \theta' - \sin \theta'' = 2\lambda (1 - \cos \varphi)/D$$

Hence only so long as  $\varphi$  is very small, are the rays appreciably parallel on rotating  $G'G''$  around  $O$  normal to the diagram; but this is usually the case, as  $\varphi = 0$  is aimed at, and fringes are thus seen in the principal focus.

To the same degree of approximation it is clear that on rotating the grating into a position such as  $og''$  the rays emerge parallel to  $IT$ , figure 43.

The next question at issue is the rotation of fringes with fore-and-aft motion, or rotation around an axis  $O$  normal to the diagram, as shown in figure 26,

Chapter II. In other words, when  $e$ , the virtual distance apart, is zero, since  $n \propto e/\lambda$ , the fringes are infinitely large horizontally. The collimator, however, furnishes a pencil of rays which are parallel in a horizontal sectional plane only. They are not collimated or parallel in the vertical plane (parallel to the length of the slit). Hence when the fringes are reduced to a single one of infinite size horizontally, this is not the case vertically; *i.e.*, from top to bottom of the spectrum the path-difference still regularly varies. The adjustment around an axis through  $O$ ,  $G'OG''$ , normal to the rulings, is still outstanding. It does not seem worth while to enter the subject further because much of the rotational phenomenon will depend upon whether the axes used are, in fact, truly vertical or parallel to the slit. In my apparatus this was not quite guaranteed, and the quantitative results obtained may therefore be due to mixed causes. Also, a rotation around an axis normal to  $O$  always requires an adjustment for superposition of the longitudinal axes of the spectra, and this introduces path-difference.

Finally, the case of figure 21, Chapter II, or the rotation around an axis parallel to  $IT$  in the present figure 43, is to be considered. This has already been given in terms of colored fringes (white light), but it occurs here for homogeneous light, in which case the above explanation is not applicable. Seen in the principal focal plane with telescope and wide slit, the *non-reversed* spectra would require careful adjustment of longitudinal and transverse axes; otherwise they vanish. Nothing will rotate them.

Figure 43 shows that if  $G'G''$  is rotated about  $IT$ , the effect is merely to destroy the fringes, since the coincidence of the longitudinal axes of the spectra is here destroyed. No effect is produced so far as path-difference is concerned. To restore the fringes, therefore, either of the opaque mirrors  $M$  or  $N$  of the apparatus must be rotated on a horizontal axis until the two spectra are again longitudinally superposed. It is this motion that modifies the path-difference of rays in a vertical plane. In other words, when the fringes corresponding to any virtual distance apart,  $e = b \varphi$ , of the halves of the grating  $G'G''$ , have been installed, the rays *as a whole* may still be rotated at pleasure around a horizontal axis. In this way a change in the number of fringes intersected by a vertical line through the spectrum is produced. The number of intersections will clearly depend on the obliquity of the rays (axes of vertical pencils), and will be a minimum when the center of the field of view corresponds to an axis of rays normal to the grating  $G'G''$ . In other words, the vertical maximum in figure 22 occurs under conditions of complete symmetry of rays in the vertical plane. If, therefore,  $e$  or the virtual distance apart of the half gratings,  $G''O$  and  $OG'$ , is also zero, the field will show the same illumination throughout.

In conclusion, therefore, to completely represent the behavior of fringes, it will be sufficient and necessary to consider that either grating,  $G'G''$  for instance, is capable of rotation, not only around a vertical axis through  $O$ , but also through a horizontal axis through  $O$  parallel to the grating. The last case has been directly tested above, Chapter II, § 16. But a rotation

around these two axes is equivalent to a rotation around a single oblique axis, and the fringes will therefore in general be arranged obliquely and parallel to the oblique axis.

Thus if  $\varphi_v$  and  $\varphi_h$  are the angles of rotation of the grating (always small) around a vertical and a horizontal axis, respectively, and if  $x'$  is the angle of the interference fringes with the horizontal edge or axis of the spectrum

$$\tan x' = \frac{\varphi_v}{\varphi_h}$$

so that if  $\varphi_v = 0$ ,  $x' = 0$ ; if  $\varphi_h = 0$ ,  $x' = 90^\circ$ . This recalls the result obtained above for the interferences of two coarse grids. In other words, for a rotation of grating around a vertical axis (parallel to slit) the fringes of maximum size will be horizontal (Chapter II, fig. 21), because the adjustment around the horizontal axis remains outstanding and the residual fringes (large or small) are therefore parallel to it. For a rotation of grating around a horizontal axis, the fringes of maximum size will be vertical (Chapter II, fig. 22), for the vertical adjustment is left incomplete. When both adjustments are made, a single fringe fills the whole infinite field, and this result follows automatically if but a single grating is used to produce the fringes, as in the original method (Chapter I).

To deduce equations it is convenient to regard both gratings as transmitting and to suppose one of them to be cut into independent but parallel halves, either by a plane through its middle point and parallel to the rulings (vertical axis of rotation), or by a plane through the same point and normal to the rulings (horizontal axis of rotation). The parallel halves of the grating are then displaced along the normal,  $e$ , to both.

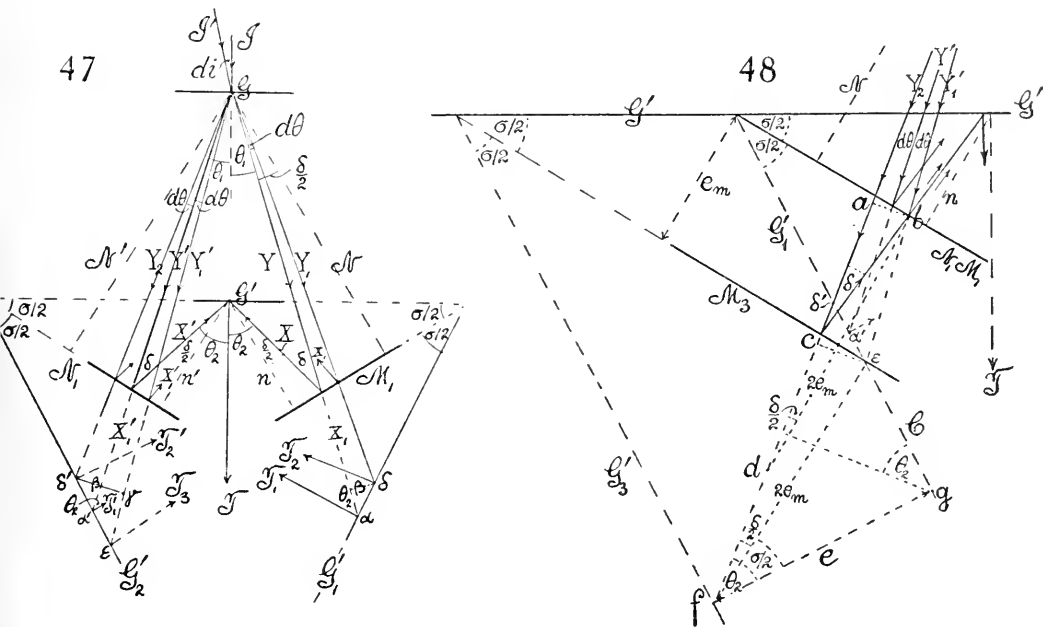
**27. Case of reflecting grating. Homogeneous light.**—The results exhibited in figure 43 for transmitting gratings are shown in figures 47 and 48 for the combination of one transmitting grating  $G$  and one reflecting grating  $G'$  (the adjustment used in Chapter II), for which the direct path-lengths of rays were computed (cf. figs. 23 and 24, Chapter II). The path-differences obtained were inadmissible. It is now necessary to completely modify the demonstration.

In figure 47 the rays are shown for the case of complete symmetry of all parts, gratings at  $G$  and  $G'$  vertical and parallel, opaque mirrors at  $M_1$  and  $N_1$ , telescope or lens at  $T$ . The incident ray  $I$  at normal incidence is diffracted and reflected into  $Y$ ,  $X$ ,  $T$ , and  $Y'$ ,  $X'$ ,  $T$ , respectively; the incident ray  $I'$  at an angle of incidence  $di$  into  $Y_1$ ,  $X_1$ , etc., and  $Y'_1$ ,  $X'_1$ , etc., respectively; both at a mean angle of diffraction  $d\theta$  (nearly) to the right, corresponding to  $di$ .

The angles of diffraction ( $di = 0$ ) are  $\theta_1$ , and  $\theta_2$ ; the double angles of reflection, therefore,  $\delta = \theta_2 - \theta_1$ , on both sides; the double angles of the grating  $G'$  with the mirrors  $M_1$  and  $N_1$ , symmetrically,  $\sigma = \theta_1 + \theta_2$ .

The normal from the point of incidence at  $G$  and at  $G'$ ,  $N$ , and  $n$  makes angles  $\delta/2$  with  $Y$  and  $X$ , respectively, on both sides. The method of treat-

ment will consist in reflecting  $G'$  in  $M_1$  and  $N_1$ , producing the planes  $G'_1$  and  $G'_2$  (virtual images), and then rotating  $M_1$  and  $G'_1$   $180^\circ$  around  $IT$  (axis of symmetry) into coincidence with  $N_1$  and  $G'_2$  (interference). Then the rays prolonged into  $\alpha$  and  $\beta$  coincide with the rays prolonged into  $\alpha'$  and  $\delta'$  and the (virtual) diffracted rays  $T_1$  and  $T_2$  become  $T'_1$  and  $T'_2$ . The ray on the left, prolonged into  $\varepsilon$ , is diffracted into  $T_3$ . Then the interferences will all be given by discussing the left half of this diagram, which is amplified in figure 48.



Since the distance  $GG'$ , figure 47, is very large, the rays are nearly parallel. Thus the arc  $\delta'\gamma$ , with its center at  $G$ , is practically a plane wave-front, perpendicular to the rays in  $\delta', \beta', \gamma$ , and the diffracted rays  $T', T'_2$ , and  $T'_3$  are also practically parallel. Hence in the case of symmetry and coincidence of  $M_1$  and  $N_1$  the points  $\delta', \beta', \gamma, \delta', \alpha',$  and  $\varepsilon$  are in the same phase (diffraction). In other words, there is no path-difference between  $Y+X$  and  $Y'+X'$ , whether the angle of incidence is zero or not ( $Y_1+X_1$  and  $Y'_1+X'_1$ ). The whole field in the telescope must therefore show the same illumination (homogeneous light, wide slit) between the maximum brightness and complete darkness. Interference fringes can occur only when the opaque mirror,  $M_1$ , is displaced parallel to itself out of the symmetrical position. If  $M_1$  and  $N_1$  are symmetrical, as in figure 47, the displacement of  $G'$ , fore and aft, parallel to itself, is without influence.

This reduces the whole discussion to the normal displacements of the system  $G', M_1, N_1$ , given in figure 48. Let the mirror  $M_1$  be displaced over a normal distance  $e_m$  to the position  $M_3$ ,  $N_1$  remaining in place. Then the image of  $G'$  will be at  $G'_3$ , at a perpendicular distance,  $e$ , from its original posi-

tion  $G'_1$ . The path-difference so introduced, since  $a$  and  $b$  ( $ab$  normal to the ray  $Y_2$  impinging on  $M_3$  at  $c$  and reflected to  $b$ ) are in the same phase, is

$$2e_m \cos \delta/2$$

and the displacement per fringe<sup>1</sup> will be

$$\delta e_m = \frac{\lambda}{2 \cos \delta/2}$$

which is nearly equal to  $\lambda/2$ , as in most interferometers, remembering that  $e_m$  and  $\delta e_m$  refer to the displacement of the mirror  $M_1$ . Two interfering rays will be coincident at  $b$ .

In the next place  $e$  and  $\delta e$  may be reduced from the corresponding displacements  $e_m$  and  $\delta e_m$  of the mirror  $M_1$ . In figure 48 the figure  $fdbe$  is approximately a parallelogram with the acute angles  $\delta/2$ . Hence, since  $\theta_2 = (\delta + \sigma)/2$

$$2e_m \cos \sigma/2 = e$$

as is also otherwise evident. Thus per fringe, if the length  $\varepsilon g = c$

$$\lambda = \delta e \cos \theta_2 + \delta c \sin \theta_2$$

since  $\delta c = 2\delta e_m \sin \sigma/2$ .

If  $G'$  is displaced parallel to itself,  $\delta e$  will not be modified, since each virtual image  $G'_1$  and  $G'_3$  moves in parallel, in the same direction, by the same amount. If then the grating  $G'$  is rotated around an axis at  $G'$ , perpendicular to the diagram, figure 47, over a small angle,  $\varphi$ , the result (apart from the superposed rotational effect) is equivalent to a displacement of the mirrors  $M_1$  and  $N_1$  in opposite directions, producing a virtual distance apart  $e$  and the corresponding interference fringes. In other words, the rotational effects may be explained here in the same way as in the preceding paragraph.

The angle  $2d\theta$ , within which the interference rays lie, per fringe, is subtended by  $\delta e_m$ , and this may be put roughly ( $N = 162$  cm., normal distance)

$$2d\theta = (2\delta e_m \sin \delta/2)/N = (\lambda \tan \delta/2)/N$$

This angle is very small, scarcely  $10^{-8} \times 3.2$  radians, or less than 0.01 second of arc. Hence all pencils consist of practically parallel rays.

An important result is the angular size of the fringes; *i.e.*, if  $e_m$  and  $\lambda$  are given

$$-\frac{d\theta_2}{dn} = \frac{\lambda}{e_m \sin \delta/2} = \frac{D_2 \sin \theta_2}{e_m \sin \delta/2}$$

$D_2$  being the grating space.

Thus they become infinitely large when  $e_m$  passes through zero. The angular size is independent of the distance between the gratings. It ought, therefore, to be easy to obtain large interference fringes, which is not the case. The reason probably lies in this: that the two opaque mirrors are not quite

<sup>1</sup>The differential symbol  $\delta$  is unfortunately also used to designate the double angle of reflection  $\delta$ . But it is improbable that this will lead to confusion.

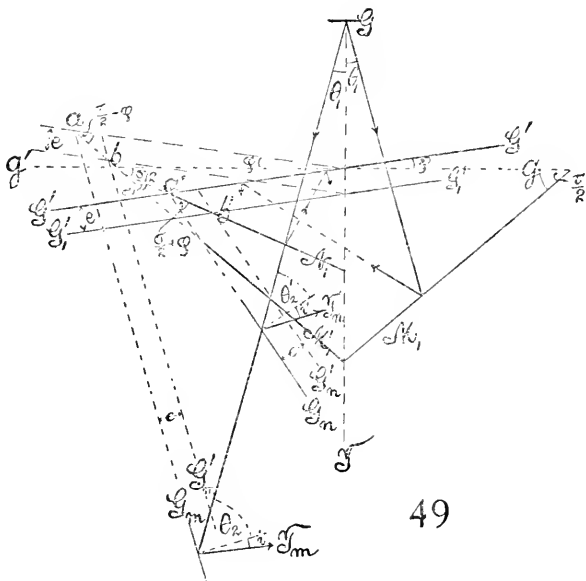
symmetrical, so that in figure 47, on rotation of  $M_1$   $18^\circ$  on  $GG'$ , the trace of  $M_1$  crosses  $N_1$  at an angle. If  $d\theta/dn = 3.7 \times 10^{-4}$ , the distance apart of the sodium lines, and  $D_2 = 173 \times 10^{-6}$  cm.,

$$e = 1.8 \text{ cm., about}$$

*i.e.*, path-lengths on the two sides should differ by about 2 centimeters, if the mirrors were quite symmetrical.

**28. Non-symmetrical positions. Fore-and-aft motion.**—It remains to account for the marked effect produced on displacing the grating  $G'$  in a direction nearly normal to itself.

If the displacement is symmetrical, or even if the grating and mirrors are reciprocally non-symmetrical (*i.e.*, the former at an angle  $\varphi$  to the transverse line of symmetry  $gg'$ , the latter inclosing an angle  $\alpha$ , fig. 49), no effect results from the displacement of  $G'$ , if the mirrors  $M_1$  and  $N_1$  are so placed that the virtual images  $G_m$  and  $G_n$  are parallel and the diffracted rays, therefore, also parallel. In such a case  $G_m$  and  $G_n$  are displaced by the same amount, normally, their distance apart is constant, and the intercepts of rays equal.



If, however, this compensation does not occur; if the grating  $G'$ , the mirrors  $N_1$  and  $M_1$  make angles  $\varphi, \sigma/2, \tau/2$ , respectively ( $2\alpha = \tau - \sigma$ ), with the transverse line of symmetry  $gg'$ , the fore-and-aft motion of  $G'$  is more effective as the angle  $\alpha - \varphi$  is greater. The diffracted rays are then no longer parallel, but make angles of incidence at the second grating,  $\theta'_2$  for the  $N_1$  side and  $\theta_2$  for the  $M_1$  side, and of diffraction  $i'$  and  $i$ , respectively, as shown in figure 49, at  $T_n$  and  $T_m$ . The following relations between the angles are apparent:

$$\sigma = \theta'_1 + \theta'_2 - \varphi \qquad \tau = \theta_1 + \theta_2 + \varphi$$

If at the first grating  $\theta_1 = \theta'_1$  and  $\alpha$  is the angle between the mirrors,

$$2\alpha = \tau - \sigma = \theta_2 - \theta'_2 + 2\varphi$$

The images are at an angle  $\beta$ , where

$$\beta = 2(\alpha - \varphi) = \theta_2 - \theta'_2$$

If  $G'G'$  is displaced to  $G'_1G'_1$  over a normal distance  $e$ , or  $e/\cos \varphi$  along the line of symmetry  $GT$ , the virtual images  $G_m$  and  $G_n$  will be displaced to  $G'_m$  and  $G'_n$  over the same normal distance  $e$ . This is obvious, since the quadrilaterals  $ab$  and  $a'b'$  are rhombuses by the law of reflection, and hence the perpendicular distances  $e$  between the (equal) sides all identical.

If  $D_2$  is the grating space of  $G'$ ,

$$(1) \quad \sin \theta_2 + \sin i = \lambda/D_2 \quad \sin \theta'_2 + \sin i' = \lambda/D_2$$

or if  $i$  and  $i'$  are very nearly equal and both small, as in the experiment,

$$(2) \quad \cos \theta_2 d\theta = -\cos i di$$

Again, in case of the displacement  $e$  of  $G'$ , the paths are shortened at  $G_m$  by  $e/\cos \theta_2$ , at  $G_n$  by  $e/\cos \theta'_2$ , resulting in the path-difference  $\Delta P$ , or

$$(3) \quad \Delta P = e(\sec \theta_2 - \sec \theta'_2)$$

Since  $\theta_2$  and  $\theta'_2$  are nearly the same, this may be adequately simplified by differentiation. Putting

$$(4) \quad d\theta = \theta_2 - \theta'_2 = 2(\alpha - \varphi) \quad \Delta P = 2(\alpha - \varphi)e \tan \theta_2 \sec \theta_2$$

Hence per fringe, apart from sign,

$$(5) \quad \delta e = \frac{\lambda \cos^2 \theta_2}{2(\alpha - \varphi) \sin \theta_2}$$

Thus, if

$$\lambda = 6 \times 10^{-5} \quad \alpha - \varphi = 1^\circ = 0.0175 \quad \theta_2 = 20^\circ$$

then

$$\delta e = \frac{6 \times 10^{-5} \times 0.88}{2 \times 0.0175 \times 0.342} = 0.004,4 \text{ cm.}$$

per fringe for each degree of arc of non-symmetry,  $\alpha - \varphi$ .

The effectiveness of the fore-and-aft motion, according to this equation, is evidence of a residual angle,  $\alpha - \varphi$ , of non-symmetry. This is not improbable, as my apparatus was an improvised construction, lacking mechanical refinement. Further, the wedge effect due to  $\alpha$ , which makes  $e_m$  variable, would be superposed on the interferences, and hence these could not be increased in size above a certain maximum. This is also quite in accord with observation.

If  $\alpha = \varphi$ ,  $\beta = 2(\alpha - \varphi) = 0$  and  $\theta_2 = \theta'_2$ ; *i.e.*, the virtual images  $G_m$  and  $G_n$  and the diffracted rays are parallel and  $\delta e = \infty$ . In other words, the fore-and-aft motion has no effect. If  $\alpha = 0$ ,  $\beta = 2\varphi$ ; or if  $\varphi = 0$ ,  $\beta = 2\alpha$ . In either case  $\delta e$  is finite, and fore-and-aft motion is effective. If the mirrors and grating were rotated in counter-direction so that  $\varphi$  is negative,  $\delta e$  will depend on  $\alpha + \varphi$ , and the fore-and-aft effect will be correspondingly marked. Moreover, the interference will not in general appear in the principal focus, but usually sufficiently near it for adjustment.

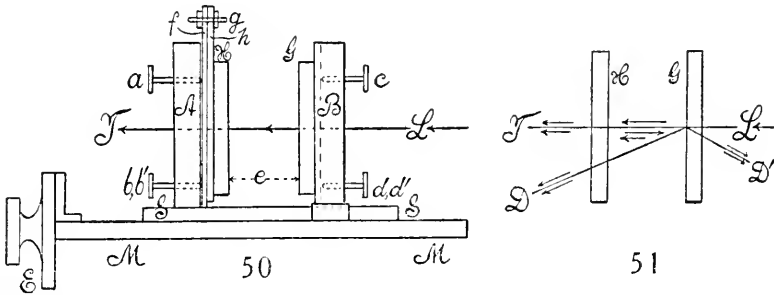
If  $\delta e_\theta$  is the actual displacement of the grating  $G'$  in the line of symmetry,  $\delta e_\theta = \delta e / \cos \varphi$ , so that the angle  $\varphi$  enters equation (5) again, but only to a small extent.

## CHAPTER IV.

### THE DISTANCE BETWEEN TWO PARALLEL TRANSPARENT PLATES.

**29. Introductory.**—The problem of finding the distance separating two parallel glass disks, as well as their degree of parallelism, is frequently one of practical importance. Thus, in my work on the repulsion of two such disks, it would enter fundamentally, and it has long been my intention to repeat that work with two half-silvered glass disks, for comparison with the case of metallic disks. It has since occurred to me that the method devised by my son, Mr. Maxwell Barus, and myself\* would probably be ideal for the purpose, both for very small distances (within 0.1 mm.) as well as for distances ten or more times larger. This method admits of use of the film grating, and there are three types of interferences of successive orders of fineness, the first virtually involving the colors of thin plates (resolved spectroscopically), the other two being dependent on diffraction. To measure the thickness of the air-space it would be necessary to count the number of fringes between two definite Fraunhofer lines only, supposing the constants of the grating to be given.

**30. Apparatus.**—The apparatus has been designed for transmitted light, in preference, though the case of reflection is also available.



*MM*, figure 50, is the base of a Fraunhofer micrometer, firmly attached below to a massive tripod (not shown). *SS* is its raised slide, and *E* the head of the micrometer screw, reading to  $10^{-4}$  cm. The open case *A* is screwed to the slide *SS* and contains the glass plate *H* half-silvered on the right. *H* is attached to a plate of brass, on the plane-dot-slot principle, and may therefore be rotated around the vertical and horizontal axis by aid of a rearward spring mechanism (not shown) and the adjustment screws *a*, *b*, *b'* (the last not visible). The grating *G*, with a ruled face on the left, is similarly carried by the open rectangular case *B*, screwed down to the base *M* of the micrometer. Thus *B* is stationary, while *A* moves. Three adjustment screws, *c*, *d*, *d'* (*d'* not shown), and a spring pulling to the right suffice to rotate *G* around the

\* C. Barus and M. Barus, Carnegie Inst. Wash. Pub., No. 149, Part I, Chapters II and III, 1911.

vertical and horizontal axis. The thickness of the efficient air-film is thus  $e$ - and  $H$  and  $G$  may be brought to touch or to recede from each other several centimeters.  $L$  is the collimator (slit and lens), furnishing intense white sun, light or arc light, and the beam, after traversing the system, is viewed by the telescope  $T$  (direct beams, fig. 51), or  $D$  (diffracted beams).

The plate  $H$  is half-silvered, but the grating  $G$  is left clear. In this case, however, only the fine fringes are seen strongly on transmission. The others appear on reflection at  $G$ , preferably in the second order of spectra. Fine fringes are not well reflected, but the medium and coarse fringes are very strong and clear, and the first observations were made by means of them.

Thereafter the ruled face of the grating was half-silvered. This largely destroys the reflected field,  $D'$ , except the fine fringes, but the transmitted field  $D$  is now strong, particularly in the second order of spectra, for all the three sets of fringes in question. Mr. Ives's direct-vision prism grating shows the fine fringes well in the direct beam  $T$ . The lines are always rigorously straight, so far as they can be observed; *i.e.*, it is impossible to bring  $H$  and  $G$  rigorously in contact, not only because of dust, but since the grating (at least) is not optical plate. The fine fringes may always be found in the principal plane of a telescope, but the medium and coarse fringes usually lie in other focal planes differing from each other. By placing the ocular it is thus possible to eliminate any of the interferences or to show a single set in the field only.

To find the fringes, the direct white-slit images are made to coincide throughout their extent, and the same may be done with a pair of spectrum lines in the superposed spectra. The proper  $e$  is then to be sought. Owing to imperfect plane parallel plates, it may be necessary to correct this by the adjustment screws on the mirror until sharp, strong fringes are seen in the corresponding focal plane.

**31. Equations.**—The equations for the three useful interferences in question are for  $r < \theta_m$  and a similar group for  $r > \theta_m$

$$\begin{aligned} (1) \quad & n\lambda = 2e\mu \cos r \\ (2) \quad & n\lambda = 2e\mu \cos \theta'_m \\ (3) \quad & n\lambda = 2e\mu(\cos r - \cos \theta'_m) \end{aligned}$$

where  $\lambda$  is the wave-length of the color used,  $n$  the order of the interference,  $e$  the thickness of the sheet to be measured, and  $\mu$  index of refraction, if  $i$  is the angle of incidence of the white light on the grating,  $r$  the angle of refraction in the plate ( $\mu$ ), and  $\theta'_m$  the angle of diffraction of the  $m$ th order of spectra therein. If the sheet is an air-space, these equations become simplified, since  $\mu = 1$  and  $r$  is replaced by  $i$ ,  $\theta'_m$  by  $\theta_m$ , the angle of diffraction in air. Thus, since positive values are in question,

$$\begin{aligned} (4) \quad & n\lambda = 2e \cos i \\ (5) \quad & n\lambda = 2e \cos \theta_m \\ (6) \quad & n\lambda = 2e(\cos i - \cos \theta_m) \end{aligned}$$

In the present apparatus I have made  $i=r=0$ , a more convenient plan of testing the method, though not necessary and, in fact, often inconvenient in practice. The equations are, finally,

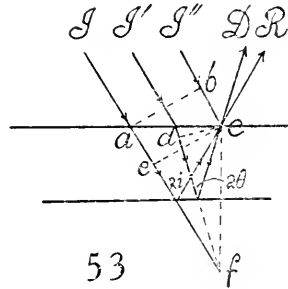
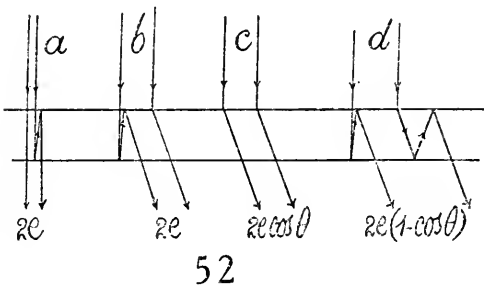
$$(7) \quad n\lambda = 2e$$

$$(8) \quad n\lambda = 2e \cos \theta_m = 2e\sqrt{1 - (m\lambda/D)^2}$$

$$(9) \quad n\lambda = 2e(1 - \cos \theta_m) = 2e(1 - \sqrt{1 - (m\lambda/D)^2})$$

if  $D$  is the grating space, and the interference in question is due to the grating spectrum of the  $m$ th order.

The meaning of the equations (7), (8), and (9) is given in figure 52. The case of equation (7) may be seen in the direct white ray, figure 52 *a*, provided the light of the focussed slit-image is resolved by direct-vision spectroscope. For this purpose Mr. Ives's grating with attached direct grating prism may conveniently be placed in front of the telescope *T*, figure 50, focussed on the slit. After adjustment these fringes appear strong. Of course, *H* and *G*



must be parallel and all but touch. Under the same conditions the fringes may be seen laterally in any order of spectrum, as in figure 52 *b*. Figure 52 *c* illustrates equation (8) and figure 52 *b* equation (9). Figure 53, finally, illustrates the general case of incidence,  $i$ .

The first and second orders of spectra are alone intense enough to produce marked effects. In case of  $i=0$ , a double diffraction of the first order,  $\theta'$  reinforces a single diffraction of the second order,  $\theta_2$ , since

$$\lambda/D = (\sin \theta' - \sin \theta) = \sin \theta_2/2, \\ (\sin \theta' - \lambda/D) = (2\lambda/D)/2 \text{ or } \sin \theta' = 2\lambda/D$$

Probably for this reason they are visible. The general case, equations (4), (5), and (6), is illustrated in figure 53, the rays *I*, *I'*, and *I''* being incident, *R* reflected, and *D* diffracted. The retardations are *ef* and *df*, respectively. If the diffractions differ by a whole number of wave-lengths the total diffraction is obtained. One would be tempted to resolve the case by aid of a wave-front *ab*, in which case the equations would be different; but they do not reproduce the phenomenon.

**32. Method.**—Suppose, now, two Fraunhofer lines,  $\lambda$  and  $\lambda'$  of the spectrum, are selected as the rays between which interference fringes are to be counted. Then, in case of equation (7), if  $n'$  is the number of interference rings between  $\lambda$  and  $\lambda'$ ,

$$\begin{aligned} (10) \quad & n\lambda = (n+n')\lambda' = 2e \\ (11) \quad & n = n'\lambda'/(\lambda - \lambda') \\ (12) \quad & 2e = n'\lambda\lambda'/(\lambda - \lambda') = Cn' \end{aligned}$$

In order to measure  $e$ , therefore, it is necessary to count the number of fringes  $n'$  between  $\lambda$  and  $\lambda'$ , and  $e$  varies directly as  $n'$ .

If the mean  $D$  and magnesium  $b$  lines be taken as limiting the range,  $10^6\lambda = 58.93$  cm.,  $10^6\lambda' = 51.75$  cm.,  $C_1 = 10^{-4} \times 4.25$ ; then

$$\begin{array}{ll} n' = 1 & 10^3e = 0.21 \text{ cm.} \\ = 10 & = 2.1 \\ = 100 & = 21 \quad \text{etc.} \end{array}$$

As it will not be convenient to count more than 100 lines ordinarily, the method is thus limited to air-spaces below 0.2 mm. and becomes more available as the film is thinner. Of course, in case of plates which contain specks of dust or lint, or are not optically flat on their surfaces, it is extremely difficult to get  $e$  down below 0.002 cm., so that ten fringes between  $D$  and  $b$  would require very careful preparation.

If equation (8) is taken,  $\lambda$  is to be increased to

$$L = \lambda / \cos \theta_m = \lambda / \sqrt{1 - (m\lambda/D)^2}$$

where  $m$  is the order of the grating spectrum, whose rays interfere. Thus equations (11) and (12) now become, since  $nL = (n+n')L' = 2e$

$$\begin{aligned} (13) \quad & n = n'L/(L-L') \\ (14) \quad & 2e = n'LL'/(L-L') = C_2n' \end{aligned}$$

If first order of diffractions are in question,  $m = 1$ ,  $10^6L = 59.11$ ,  $10^6L' = 52.33$ ,  $C'_2 = 10^{-4} \times 4.20$ . Thus for

$$\begin{array}{ll} n = 1 & 10^3e = 0.21 \text{ cm.} \\ 10 & 02.1 \\ 100 & 021. \end{array}$$

scarcely differing from the preceding case, so that one would not know in which series one is working.

If the diffractions occur in the second order,  $m = 2$ ,

$$10^6L_2 = 62.56 \quad 10^6L'_2 = 54.15 \quad C''_2 = 10^{-4} \times 4.03$$

thus again differing but slightly from the above.

If we inquire into the condition of coincidence and opposition of these fringes, the following results appear: Let the spectrum distance between the  $G$  and  $b$  line be taken as unity, and let there be  $n_1$  and  $n_2$  first-order fringes in this distance. Then in  $\frac{1}{n_1} - \frac{1}{n_2}$  is the difference of distance per fringe. Let

$x$  be the number of long fringes, to restore the original coincident phase; *i.e.*, let  $x$  longer fringes gain one long fringe on the  $x$  shorter fringes. Then

$$x(1/n_1 - 1/n_2) = 1/n_1 \quad x = C_1/(C_1 - C_2)$$

that is,  $x$  fringes constitute a new period. From the above data

$$x = 4.25 \times 10^{-4} / 4.4 \times 10^{-6} = 96.5$$

It follows that the length of coincident strips is subject to

$$e = C_1(n_1 - 1) = C_2 n_2 = C n_2 / x \text{ or } C = \frac{C_1 C_2}{C_1 - C_2}$$

where  $C$  is the new constant. This would place the fringes beyond the coarse group below, but naturally  $C$  is enormously dependent on small errors in  $C_1$  and  $C_2$ .

Finally, if equation (9) be taken, the  $\lambda$  is to be increased to

$$M = \lambda / (1 - \cos \theta_m) = \lambda / (1 - \sqrt{1 - (m\lambda/D)^2})$$

in order that equations similar to the above may apply. Thus

$$n = \frac{n'M}{M' - M} \quad 2e = \frac{MM'}{M' - M} = C_3 n'$$

In the diffractions of the first order of spectra  $m = 1$  and  $10^3 M = 4.150$ ,

$$10^3 M' = 4.747 \quad C'_3 = 0.0330$$

These are the coarse order of fringes, so that

$$\begin{array}{ll} n = 1 & 2e = 0.033 \\ 10 & 0.33 \\ 100 & 3.3 \text{ , etc.} \end{array}$$

Fringes are thus still strongly available, even if the distance apart of the plates is over 2 cm.

If the diffractions are of a second order of spectra,  $m = 2$ ,

$$10^3 M = 1.016 \quad 10^3 M' = 1.165 \quad C''_3 = 10^{-3} \times 7.85$$

These fringes are therefore of intermediate order, since

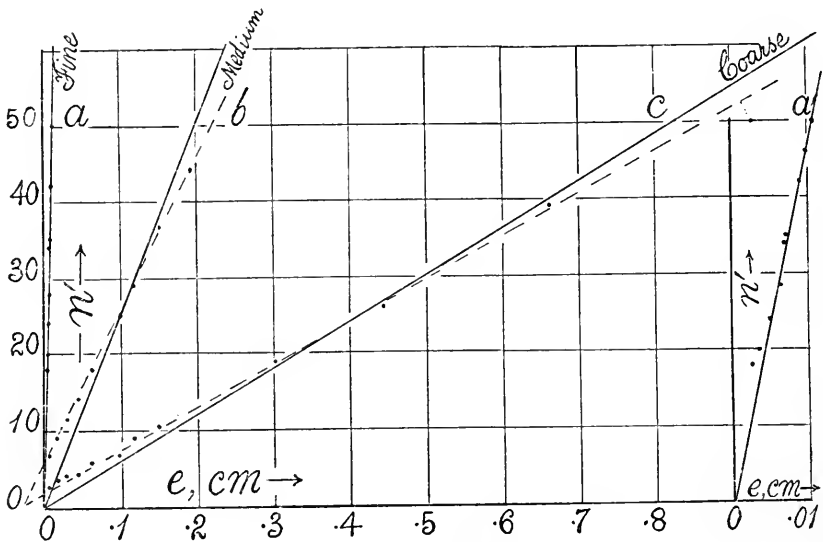
$$\begin{array}{ll} n = 1 & 2e = 0.0078 \text{ cm.} \\ 10 & 0.0785 \\ 100 & 0.785 \end{array}$$

They would be enhanced, since they cooperate with the double diffractions of the first order.

**33. Observations and corrections. Preliminary work.**—The following work was done merely with a view to testing the equations and with no attempt at accuracy. The grating was left unsilvered, so that the ruled sur-

faces confronted the half-silvered surface on ordinary plate glass. Consequently, the fine fringes were observed by transmitted light behind, and the medium and coarse fringes by reflected light in front. The micrometer was a good instrument for general purposes, but hardly equal to the present work, where the slightest rocking of the slide introduces annoyances.

To count the number of fringes between  $D$  and  $b$ , since the fringes were not generally seen in the principal focal plane of the telescope, it was considered sufficient to rotate the cross-hair into an oblique position, until its ends terminated in the  $D$  and  $b$  lines, respectively, and then to count the number of fringes on running the eye down the wire from end to end. When there are many fringes, 25 to 50, the eye is apt to tire before reaching its destination, so that several counts must be made and the mean taken.



54

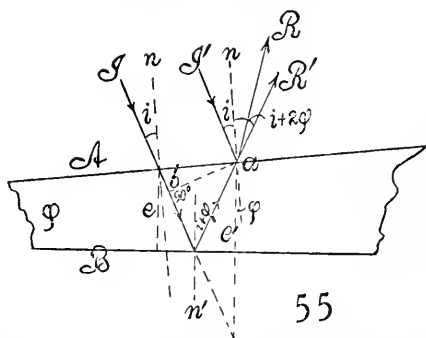
The results are given as a whole in figure 54, where the distance between plates, measured in centimeters on the micrometer, beginning at an approximate zero, is laid off horizontally and the number of fringes vertically, in case of each of the three series. The computed line  $e = Cn'/2$  is drawn in full and the observations laid off with regard to it. The zeros do not quite correspond, as very small distances here are significant. With the fine fringes I did not spend much time, as they are virtually colors of thin plates seen by diffraction. The chief difficulty with these small distances is that the plates touch and a complete readjustment is necessary. After touching, the micrometer acts like a forcing screw and its reading is too low. This is the meaning of the data in the curves  $a$  and  $a'$ , the latter with its horizontal scale magnified ten times. The object of this series is chiefly to locate the position of the line in relation to the other lines.

The observations for medium and fine fringes were made together, so that a single micrometer reading suffices. Beginning with very small distances apart, called zero, this was rapidly increased to nearly 1 cm. The fine fringes soon vanished, later the medium fringes vanished, finally (when  $e$  is several centimeters) the coarse fringes also vanish. The three together, therefore, cover with accuracy a relatively enormous range of displacement for measurements of this kind.

The curves  $b$  and  $c$  show that the observations are not completely reproduced by the line. Mean lines drawn through the observations indicate that the zeros do not correspond sufficiently for the two lines  $b$  and  $c$  to locate the common zero. This is inevitable, since the micrometer begins to count at a small distance as specified, which is otherwise arbitrary. In fact, it should be noticed, as an accessory property of this interferometry, that the two lines for finding the zero determine the absolute reading of the micrometer, mutually, and these readings are here 0.22 mm. too large. But even if the zeros were horizontally to coincide, the observations would not adequately conform to the computed lines. All that can be affirmed is that the angle between the observed and computed loci is about the same.

The main reason for the divergence is referable to the fact that the air-space is not quite plane parallel, but slightly wedge-shaped, so that the effect of the angle of the wedge is superposed on the interferences. Any slight unsteadiness of the micrometer slide, for instance, would already introduce the wedge discrepancy, without necessarily interfering with the sharpness of visibility, while any attempt to readjust would destroy the continuity of measurement. There will also be many secondary reasons for divergence, as, for instance, the three separate focal planes in which the fringes lie and the fact that the glass plates which limit the air-space are themselves wedge-shaped; other, but fainter, fringes are marching through the spectrum, such cases as coincidence and opposition, for instance, as were pointed out above, etc. But the adequate reason for the discrepancies in this paper is the incidental change of the angle of incidence,  $i$ .

If the film is wedge-shaped, very little disturbance results; but the correction to the second order of small quantities is unfortunately somewhat cumbersome. Let the edge of the wedge of air be vertical and subtend a small angle,  $\varphi$ , figure 55, between the two faces  $A$  and  $B$ . Let  $I$  and  $I'$  be the two corresponding rays incident at the angle  $i$  at the first face and at the angle  $i + \varphi$  at the second face,  $n$  and  $n'$  being the normals. Let  $e$  and  $e'$  be the consecutive thicknesses of the air-plate, taken normal to  $B$  for convenience. Then the  $I$  rays  $R'$  will issue at the  $A$  face, after reflection, at an angle  $i + 2\varphi$ , and will interfere with the  $I'$  rays  $R$ , if the objective of the telescope is sufficiently



large to converge both to the same point of the image, spectroscopically resolved. If the wave-front  $ab$  is drawn and  $e'$  prolonged, it follows at once that

$$n\lambda = 2e \cos(i + \varphi) \quad e' = e \left( 1 + 2 \frac{\sin(i + \varphi) \sin \varphi}{\cos i} \right)$$

Hence

$$n\lambda = 2e \left( \cos(i + \varphi) + \frac{\sin(i + \varphi) \sin \varphi}{\cos i} \right)$$

If  $i = 0$  and  $\varphi$  very small, this becomes

$$n\lambda = 2e \left( 1 - \frac{\varphi^2}{2} + 2\varphi^2 \right) = 2e \left( 1 + \frac{3}{2}\varphi^2 \right)$$

If in the first equation  $i$  is replaced by the angle of diffraction  $\theta$ , the equation for the diffracted fringes, as far as  $\varphi^2$ , may be reduced to

$$n\lambda = 2e \left[ \cos \theta + \varphi \sin \theta - \frac{\varphi^2}{2} \left( \frac{4}{\cos \theta} - 7 \cos \theta \right) \right]$$

so that  $\varphi \sin \theta$  is the chief correction.

Finally, the equation for the coarse fringes becomes

$$n\lambda = 2e \left[ 1 - \cos \theta - \varphi \sin \theta + \frac{\varphi^2}{2} \left( 3 + \frac{4}{\cos \theta} - 7 \cos \theta \right) \right]$$

with a similar equation for the medium fringes.

If we neglect the second order of small quantities ( $\varphi^2$ ), the last equation for the medium fringes may be put in another form, since

$$2\lambda/D = \sin \theta \text{ and } \lambda/L = 1 - \cos \theta \quad \sin \theta = \frac{2L}{D} (1 - \cos \theta)$$

whence

$$2e = \frac{nL}{1 - 2\varphi L/D} = \frac{(n+n')L'}{1 - 2\varphi L'/D}$$

$D$  being the grating space and  $\lambda$  the wave-length. Hence if  $n$  be eliminated,

$$2e = n' \frac{LL'}{L - L' - (2\varphi/D)(LL' - LL')} = n' \frac{LL'}{L - L'}$$

In other words, if  $\varphi$  is small so that  $\varphi^2$  may be neglected, the relation of  $e$  and  $n'$  is independent of  $\varphi$ ; or a slightly wedge-shaped air-film will show the same result as a plane-parallel film. Experiments made by turning the adjustment screws seem to bear this out, provided the mean thickness remains unchanged.

To give the whole subject further study, I have since half-silvered the grating as specified, so that all the fringes may be seen by transmitted light, preferably in the second order, since there is an abundance of light available. The apparatus in such a case takes a good shape and is convenient for manipulation. But these details will have to be given at some other time, and it is the chief purpose of this paper to exhibit the phenomenon as a whole.

In conclusion, I may recall that if we regard 100 fringes between the *D* and *b* lines as still available for counting under proper facilities, the successive ranges of measurements will be roughly as follows:

|                         | $e=0.021$ cm. | $e=0.392$ cm. | $e=1.65$ cm. |
|-------------------------|---------------|---------------|--------------|
| Fine fringes. . . . .   | $n'=100$      | .....         | .....        |
| Medium fringes. . . . . | $n'=54$       | $n'=100$      | .....        |
| Coarse fringes. . . . . | $n'=1.3$      | $n'=23.8$     | $n'=100$     |

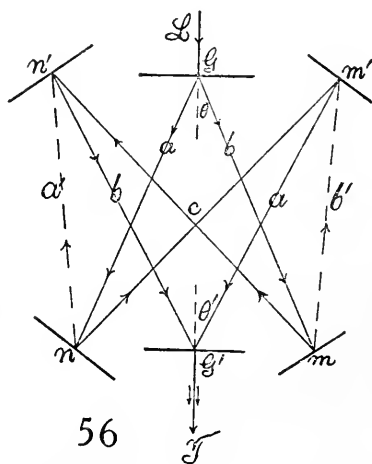
The transition from fine fringes to medium is a little abrupt. Otherwise, in cases where manual interference is not permissible, all thickness of air-films, from a fraction of a wave-length of light to nearly 2 cm., may be adequately measured in this way to advantage. It is probable, moreover, that it would be advisable to observe the fine fringes by transmitted light, but to leave the grating (which may be a film grating) clear, and to observe the medium and coarse fringes by reflected light. A concave mirror and lens (reflecting telescope) should be used for this purpose, as this will put the observer behind the plates in all cases.

## CHAPTER V.

### INTERFEROMETERS FOR PARALLEL AND FOR CROSSED RAYS.

**34. Introduction. Methods.**—To exchange the component beams of the interferometer, to mutually replace the two pencils which interfere, is not an unusual desideratum, for instance, in the famous experiment of Michelson and Morley. To replace two pencils of component rays, traveling more or less parallel to each other, by pencils moving more or less normal to each other, or to be able to operate upon pencils of corresponding rays (from the same source, crossing each other at any angle) at their point of intersection, may be of interest in a variety of operations to which the interferometer lends itself, or may even suggest novel experiments. The facility with which this may be done, or at least partially done, with the above types of spectrum interferometers, particularly when homogeneous light is used, has tempted me to investigate a number of cases.

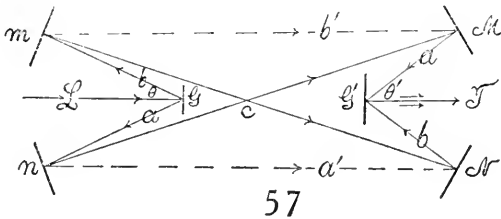
Let us begin with the above diagrammatic method, using two transmitting gratings,  $G$  and  $G'$ , figure 56, with the same (or in general with different) grating constants. Let  $L$  be the incident beam of collimated homogeneous light,  $m, n, m', n'$ , four opaque mirrors on vertical and horizontal axes parallel to their faces. The ruled faces of the gratings are to be toward each other. Then the beams  $Gm$  and  $Gn$  may be reflected either *across* each other, as shown at  $mn'$  and  $nm'$ , thence along  $n'G'$  and  $m'G'$ , and, after a second diffraction at  $G'$ , unite to enter the telescope at  $T$ ; or they may be reflected along  $m, m',$  and



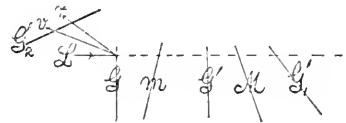
$n, n'$ , parallel to each other, and thereafter take the same course. In the first case homogeneous light is apparently not necessary. It will be seen that the path of the rays is the same, except for the branches  $mn'$  and  $nm'$ , and  $mm'$  and  $nn'$ , respectively normal and parallel to each other; moreover, that the rays are exchanged,  $a$  and  $b$  left and right combining at  $G'$  in one case,  $b$  and  $a$  left and right in the other. The rays cross at  $c$  in free space and are available there for experiments. Direct light is to be screened off. The question is whether the mirrors  $m$  and  $n, m'$  and  $n'$ , can be adjusted mechanically to move symmetrically toward each other on a vertical axis with sufficient precision to guarantee replacement. This is a matter of trial, though a successful issue is, of course, problematical. It would be advantageous to arrange the experiment so that only one pair of mirrors—*e.g.*,  $m$  and  $n$ —need

be moved, whereas the others,  $m'$  and  $n'$ , are ends of the same rigid plate. Gratings of different constants may advantageously contribute to this end. Beyond this, the paths  $mm'$  and  $nn'$  and  $mm'$  and  $nn'$  may be increased to any length, either directly or by multiple reflections from a special system. Many other modifications are suggested. If white light is used, the phenomenon is confined to a narrow strip of spectrum and the fringes must be horizontal.

As I did not have two ruled transmitting gratings and as film gratings seemed unpromising for work of this kind, the method of figure 57 represents a simple disposition of reflecting gratings, of which several were available. The ruled faces of the gratings  $G'$  and  $G$  face away from each other.



57



58

The former receives the collimated pencil of homogeneous light,  $L$ , and after diffraction the partial beams pass to the pair of opaque mirrors  $m$  and  $n$  (symmetrically placed), and thence by reflection to a similar pair of mirrors,  $M$  and  $N$ . From here the pencils reach the second grating,  $G'$ , where each is again diffracted into the common ray  $G'T$ , entering the telescope  $T$ . The grating  $G'$  may be concave with the lens at  $T$  beyond the principal focus. If the mirrors  $M$  and  $N$  are symmetrically rotated, the parallel component pencils  $Nn$  and  $Mm$  may be replaced by the pencils  $Mn$  and  $Nm$ , crossed at any angle. Homogeneous light is preferable. Simultaneously the rays are exchanged. The pencils,  $Mm$ , etc., may be of any length, and in general the remarks in the preceding paragraph apply.

A more flexible design also suggests itself, with four fixed mirrors,  $m, n, m', n'$ , four movable mirrors,  $M, N, M', N'$ , rotating symmetrically around vertical axes parallel to the faces of the gratings  $G$  and  $G'$ , these being parallel to each other, as in figure 57. On rotating  $M, N, M', N'$ , the rays may be exchanged. Here  $M . . . N'$  should be a near system,  $m . . . n'$  a fixed and far system of mirrors. Other methods will presently be described.

**35. Experiments. Reflecting gratings. Parallel rays.**—The experiments were begun with the apparatus as in figure 57,  $G$  being a Michelson grating and  $G'$  a Rowland grating, each with somewhat less than 15,000 lines to the inch. The distance of  $G$  from the mirrors  $m$  and  $n$  was about 22 cm., of  $G$  from  $G'$  about 60 cm., and of  $G'$  to the focal point just ahead of the lens (or the line of mirrors  $M$  and  $N$ ) about 90 cm. The latter were about 50 cm. apart. In the absence of sunlight, the arc lamp was used, and the fringes for reversed spectra were found without great difficulty. It was also easy to

erect them by rotating  $G'$  on an axis normal to its face. A difficulty, however, existed in retaining the fringes with a flickering arc. It will be seen that in this case the line  $LG$  moves over a small angle in all directions with the bright spot on the positive carbon, so that the angle of incidence is varied, and with it the angle of diffraction  $\theta$  at  $G$ . All this is magnified by reflection from the mirrors. Moreover, unless the collimator lens is very near  $G$ , the illuminated part or bright line on  $G$  is displaced right and left. Path-difference between  $GnNG'$  and  $GmMG'$  is thus modified. If the faces of the mirrors are not all quite in a vertical plane or parallel to the same plane, the up-and-down play of the arc will mar the longitudinal coincidence of the two superposed spectra, and hence the interferences will vanish. Thus they appear and disappear periodically, depending on the accidental position of the bright spot of the arc; and if this annoyance is to be avoided, sunlight or a steady light must be used. The phenomenon and the spectra were not nearly so bright as when observed with the transmitting grating, a result probably due both to the additional reflections (particularly those at the grating) and to the high dispersion.

In other respects the behavior was the same as that described in Chapters I and II, though the strip of fringes for reversed spectra seemed to be somewhat broader, probably owing to the increased dispersion and hence the greater breadth of adequately homogeneous spectrum light. The linear phenomenon, moreover, consisted of two or more black lines alternating with bright, whereas a single black line was the characteristic feature above. When different strips of the grating  $G$  are used (the illumination should not be more than 0.5 cm. wide), considerable fore-and-aft displacement at the mirror  $M$  is necessary.

The adjustment for crossed rays  $Mn$  and  $Nm$ , figure 57, is subject to new conditions. In case of white light and a narrow slit, the dispersion produced by  $G$  is at least partially annulled by  $G'$  instead of being incremented; for the change of the angle of incidence here compensates the changes of the angle of diffraction. Thus if  $\sin i_v - \sin \theta_v = \lambda_v/D$  for violet and  $\sin i_r - \sin \theta_r = \lambda_r/D$  for red, and if  $\sin i_v = \lambda_v/D$  and  $\sin i_r = \lambda_r/D$ , then  $\sin \theta = \sin \theta_r = 0$ .

A sharp, white image of the slit may thus be seen for the reflection from each mirror  $M$  and  $N$ , or the images may be colored if but a part of the spectrum is reflected from  $M$  and  $N$ . The system of two gratings,  $G$  and  $G'$ , tends to become achromatic. It would seem to follow, therefore, that in general homogeneous light and a wide slit would have to be used, but this introduces additional annoyances, inasmuch as the transverse axes of the spectra (sodium lines), which are to coincide, are not visible, but must be replaced inadequately by the edges of the slit. The experiment is thus (particularly in view of the faint illumination seen in the telescope) difficult, and in a laboratory not free from agitation, or in the absence of a good mercury lamp of intense homogeneous light, it did not seem worth while to spend much time on it. Moreover, a similar investigation will presently be made with a transmitting grating.

In other words, in case of the rays  $nM$ , the violet is incident at a larger angle at  $G'$  than the red, and but one color (yellow) can be diffracted along  $G'T$ , whereas in case of the rays  $mN$  violet is incident at  $G'$  at a smaller angle than red, and  $G'$  may thus be so placed that all rays are diffracted along  $G'T$ , supposing the two gratings to be nearly identical as to dispersion. Figure 58, presently to be described, suggests the inclination of the successive vertical planes in figure 57.

One curious result deserves special mention. Each separate spectrum ( $a$  or  $b$ , fig. 57, without superposition) shows very definite coarse stationary interferences; *i.e.*, the usual appearance of channeled spectra. The cause of this long remained obscure to me, but will be explained in Chapter VI. The gratings being of the reflecting type and the mirrors silvered on the *front* face, there is no discernible cause for interferences. No film or set of parallel plates enters into the experiments. If in figure 57 the grating  $G'$  is reflected at  $M$  into  $G'_1$ , and this image reflected in  $m$  into  $G'_2$ , the phenomenon may be treated as if the gratings were transmitting in a manner shown in figure 58. Here the direction of the traces of the grating  $G$  and  $G'$ , the mirrors  $m$  and  $M$  only are given, together with the direction of the reflected images of  $G'$  in  $M$  ( $G'_1$ ), and in  $m$  ( $G'_2$ ). Then the violet ( $v$ ) and red ( $r$ ) rays from  $G$  impinge on  $G'_2$  virtually with a greater angle for  $v$  and a smaller one for  $r$ , as already suggested. An enhanced spectrum must be produced beyond  $G'_2$ . This second spectrum is channeled.

**36. Experiments. Transmitting grating. Parallel rays.**—The chief difficulty in the preceding experiments was the absence of sufficiently intense homogeneous light. This may be obviated by using the transmitting grating. But as two samples were not available (as in fig. 56), the simplified method of figure 59 was tested, where but a single grating  $G$  is used. Here the light  $L$  from collimator and slit impinges on the grating  $G$  and is diffracted to the opaque mirrors  $M$  and  $N$ . From here it is reflected to the corresponding opaque mirrors  $m$  and  $n$ , to be again reflected to the grating  $G$ , and finally diffracted along the line  $GT$ . The interferences are observed by the telescope at  $T$ . In order that the undeviated white beam may not enter the telescope annoyingly, the diffraction  $LG$  takes place in the lower half of the grating and the mirrors are slightly inclined upward, so that the second diffraction  $GT$  may occur in the upper half of the grating. To obviate glare in the field, the beam  $LG$  is carried to the grating in an opaque tube and all undeviated light is suitably screened off. The distances  $mn$  to  $G$  and  $G$  to  $MN$  were about a meter each.

The interferences were easily found. They are usually at an angle to the vertical, but may be erected by rotating the grating on an axis normal to its face. They were linear and exactly like the cases of Chapter I, probably in consequence of the low dispersion of the grating used. Considerable magnification at the telescope is thus admissible.

The horizontal fringes traveling up or down are available for interferometry,

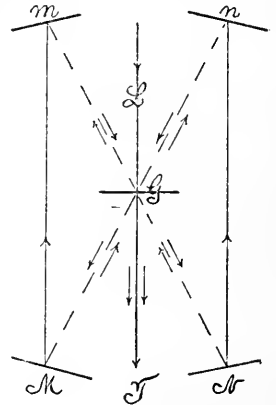
and the independent and separated component beams  $Mm$  and  $Nn$  are conveniently accessible.

The experiments with homogeneous light (sodium arc) gave perfectly regular striations covering the whole of the wide slit image, *uniformly*. With glass compensators 0.6 to 0.1 cm. or more thick on both sides, the striations became somewhat smaller, as was to be anticipated. Fringes could be erected and enlarged by rotating the grating on an axis normal to its face and by other corresponding rotations. The fringes, as a whole, were large and splendid and suitable for general purposes in interferometry.

**37. Experiments. Transmitting grating. Crossed rays.**—The second position of this apparatus was now tested, the rays passing along the diagonal of the rectangle (fig. 59) and crossing at  $G$  in the grating. The interfering pencils were thus  $GNGmG$  and  $GMGnG$ . The slit should be quite wide. Seen in the telescope at  $T$ , therefore, the dispersion is reduced in virtue of double diffraction, the tendency being toward white slit images, as already explained. A variety of very interesting results were obtained after the interferences had been found. The outgoing and returning paths are coincident, and both component rays pass through the grating two times, the ruled face being towards the telescope.

The adjustment is at first somewhat difficult. Having made a rough setting of the mirrors as to distance, etc., by the aid of sunlight or arc light, so that the spectra may be seen, two wide slit images will appear in the telescope  $T$ , but they will usually be differently colored. The mirrors  $m$  and  $n$  are then to be rotated around vertical axes (fine-screw motion) until both slit images are identically colored and coincide. After this, homogeneous light (sodium arc) must be used and the rotation of mirrors on the vertical and horizontal axes repeated until both fields are identically yellow on coincidence. The sharply focussed edges of the wide slit are now the vertical and horizontal guide-lines for adjustment. All corresponding lines must coincide if the phenomenon is to be obtainable. Thereafter the micrometer at  $M$ , actuating the mirror fore-and-aft parallel to itself, is manipulated till the fringes appear.

Two types of interference may be observed. The first are variations of nearly equidistant fringe patterns, obtained with homogeneous light only and covering the whole wide slit image on good adjustment. They would appear equally well in the absence of the slit. The second type is obtained in the presence of white light, or of the mixture of white light with the homogeneous light. It is a linear phenomenon, identical in appearance with the one described in Chapter I, though occurring here in the case of a *wide slit*. Both are very vivid, and the latter particularly, when at its best, in violent tremor.



59

It is convenient to describe the homogeneous fringes first. White light must be absent, the wide field full yellow, and the longitudinal and side edges of the two slit images sharply superposed. When the fringes appear they will usually be oblique; but they may be made vertical by rotating the grating on an axis normal to its face. If the grating is in the symmetrical position of figure 59, the size of fringes is an intermediate minimum. To enlarge them, curiously enough, the grating must be slightly rotated, either way, on a *vertical* axis. The fringes then pass through a maximum of size at a definite angle on either side of the minimum. In such a case they also appear rapidly to become irregular and their perturbation is naturally enhanced. They contain a double periodicity, which will presently be carefully examined.

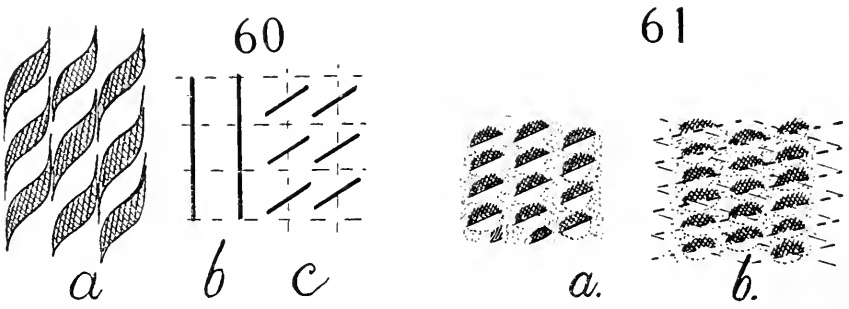
Fore-and-aft motion of the grating has no effect. In displacing the mirror at *M* on the micrometer, the fringes remain visible for an excursion of at least 0.7 cm. In fact, in case of a strong telescope and wide slit they were not lost for a micrometer displacement of over 1 cm., *i.e.*, much over 30,000 wavelengths of path-difference. As a rule, the fringes are strong only in part of the yellow field, and in such a case the center of intensity moves with the displacement of *M* across the slit image, to disappear at the edges, as in the usual cases of displacement interferometry. Slight non-coincidence of the horizontal edges of the slit images slightly rotates the fringes, but they soon vanish completely. Slight rotation of the grating around the vertical axis distributes the fringes more evenly over the field, the proper setting being determined by trial. Displacement by aid of a compensator of glass gave the usual results.

Later I returned to the experiments with sodium light and with the grating rotated around a vertical axis to the right or left and out of the symmetrical position of figure 59. In each case the fringes passed through maximum size at an angle of asymmetry of about  $5^\circ$  or  $10^\circ$  from a normal position. Beyond or below this they diminish in size. Naturally, to bring the fringes to the center of the field, the micrometer screw at *M* or *N* had to be adjusted for path-difference, as in displacement interferometry generally.

The details of the interference patterns obtained were in astonishing variety. Suppose that by rotating the grating around an axis normal to its face the fringes are made nearly but not quite *vertical* at the beginning. Then on rotating the grating around a vertical axis into the position for maximum size just specified, the standard type of large fringes seen are of the appearance shown in figure 60a. In other words, they look and behave like independent, thick, twisted cords, hung side by side. The evolution of these independent parallel striations of fringes may be detected on rotating the mirror *M* or *N* around a vertical axis, thus moving one slit image in definite amounts, micro-metrically, over the other, horizontal edges remaining superposed. As the one slit image passes in this way across the other, the original type, figure 60b, apparently continuous, breaks up and enlarges into the type *c* by the rotation of its parts. Thus the successive lengths of the continuous fringe *b* behave like a series of magnetic needles, each rotating on its own pivot. These may

again correspond and appear as a single striated field; but more frequently the form figure 60a is in evidence, though sometimes quite irregular. In fact, there are many variations of this design. Families of curves, intersecting each other nearly orthogonally, may even appear.

If the fringes are originally quite vertical, there seems to be no rotation, but two sets of vertical fringes apparently pass through each other as the mirror *M* is rotated micrometrically on a vertical axis. These fringes at intervals again unite into an apparently simple striation. One slit image may be broader than the other. Fringes of different sizes then appear, so long as the smaller is within the larger, and are most intense when the vertical edges meet. In general, therefore, the interference patterns of originally nearly vertical fringes consist of a succession of *strands*, nearly in parallel, which behave alike but independently.



If the grating is rotated on an axis normal to its face until the fringes are nearly horizontal, a correlative series of interesting phenomena may be observed. When the grating is normal to the incident pencil, the fringes are usually arranged in parallel strands. They are equidistant in each strand; but these strands are separated by a narrow band of even color, so that the phenomenon looks as if thick, twisted, yellow cords were hanging apart, side by side. Usually the central or the two central cords are more intense, and there may be four to six in all, filling the whole of the wide-slit image. On rotating the mirror, *M* or *N*, micrometrically, on a vertical axis, the fringes of the strand may be made to correspond, so as to fill the field with uniform striations and without apparent vertical separation. This is particularly the case when the fringes are very fine.

On rotating the grating to the right or to the left about 20°, on the vertical axis from the symmetrical position of figure 58, the fringes reach a maximum of size, after which (on further rotation to about 30°) they diminish indefinitely. These maximum cases are shown in figure 61, *a* and *b*, and their appearance is now that of a string of elongated beads, hung vertically and equidistant. On rotating *N* about a vertical axis, slightly, the nodules become quite horizontal. They are continually in motion, up and down, and quiver about the horizontal position like small disturbed magnetic needles. At times the field appears reticulated (indicated in the figure), as if two sets of nearly horizontal fringes intersected at a small angle. It is now difficult to obtain

continuous striations on rotating  $N$ , but the whole field may easily be filled with nodules. The occurrence of two maxima is probably an incidental result, as in other adjustments but a single one appeared. Naturally the rotation of the grating or of the mirrors  $M$  and  $N$  changes the path-difference of the pencils crossing within it, so that the micrometer screw at the mirror  $M$  must be moved in compensation. Thus this is another method of displacement interferometry and the usual equation suffices.



62

The following rough experiments were made: Placing the strong fringes in the center of the field (slit image), the reading of the micrometer was taken. Then a thick glass plate,  $e=0.71$  cm., was inserted in one beam, nearly normally, and the micrometer displacement,  $\Delta N$ , was found when the fringes were brought back to the center of the field again. The results were (for instance)

$$\Delta N = 0.375 \quad 0.393 \text{ cm.}$$

The displacement equation is ( $\mu$  being the index of refraction of the plate)

$$\mu = 1 + \Delta N / e - 2B / \lambda^2$$

where the correction for dispersion may be put  $2B / \lambda^2 = 0.026$ . Hence  $\mu = 1.50, 1.52$ , as was anticipated. On using white light, where there is but a single strand, a cross-hair, and greater care as to the normality of the plate compensator, etc., there is no reason why results of precision should not be obtained.

**38. The same. The linear phenomenon.**—The occurrence of the linear phenomenon reciprocally with the fringes for homogeneous light is interesting. It usually appears when there is a flash of the arc lamp, *i.e.*, a displacement of the crater, introducing white light into the sodium arc. It is thus undoubtedly due to the reversed spectra for white light and may, in fact, be produced by using the white arc or sunlight in place of the sodium arc. When the mirror  $M$  is displaced on the micrometer parallel to itself, the linear pattern moves through the wide-slit image from right to left; or the reverse. It does so also when either mirror,  $M$  or  $N$ , is slightly rotated on a vertical axis. The change in appearance during this transfer is very striking. In the middle, between the extreme right and left positions, the linear phenomenon is exceptionally strong and fairly tumbling in its mobility. Toward the right or left from the center it becomes gradually less intense, and on one side merges into the homogeneous striations which then appear. On the other side it seems merely to vanish. Doubtless the linear phenomenon is found, as usual, at the line of symmetry of two reversed spectra; but, as both spectra are shrunk to very small lateral dimensions, many colors probably adequately coincide. In an achromatic reproduction of the slit all colors will coincide.

It is thus not necessary that the edges of the slit images should be superposed to produce the linear phenomenon. What is still more curious is the

result that not even the longitudinal axes of the spectra need be quite in coincidence, though, of course, the phenomenon appears most intensely for the case of precise superposition. The angle of admissible separation of longitudinal axes is, however, much larger here than in the usual cases above, so that one of the longitudinal guide-lines of the two spectra may be appreciably above the other.

The last result and the fact that the linear phenomenon appears here with an indefinitely wide slit are new features. The cause of the latter has just been referred to the exceptionally reduced width of spectrum resulting from the double diffraction. If the dispersion were quite reduced to zero, all colors in a definite narrow, transverse strip of the white slit image would be in a condition to interfere. This strip contains the superposed images of an indefinitely fine slit. The slit in any other position, right or left, would have two non-coincident images. Hence, when one wide-slit image moves over the other, there is also a shift of the linear phenomena.

To produce the linear phenomenon with sunlight is difficult. The interferences should first be produced with the sodium arc, strongly, and the arc thereafter replaced with sunlight entering the slit at the same angle. Furthermore, the pencil leaving the collimator should be a narrow, vertical blade of light, and at the mirrors,  $M$  and  $N$ , red and green light should be screened off, retaining only a narrow strip of yellow light for each. Finally, to avoid glare, the slit is not to be too broad nor too narrow to cut off the yellow field of the telescope.

Under these circumstances of completed adjustment, the linear phenomenon usually appears strongly. Its form may be greatly modified by rotation of either mirror,  $M$  or  $N$ , micrometrically, around the vertical axis, as already suggested. The types are given in figure 62, quite fine, nearly vertical lines,  $q$ , changing to moving, coarser forms,  $m$ , and these into the tumbling variety,  $t$ , very coarse and nearly horizontal. The latter change by rotation and diminution into  $m'$  and  $q'$ , while  $N$  is being continually rotated over a very small angle, sliding one slit image continuously over the other. In the condition  $t$ , the fringes rotate with astonishing rapidity, and this rotation is nearly  $180^\circ$ ; *i.e.*, if the angle between  $m$  and  $m'$  is  $\alpha$ , the angle of rotation has been  $180^\circ - \alpha$ , so that between  $q$  and  $q'$  there is about  $180^\circ$  of rotation. At the stage  $t$ , with fine micrometric adjustment, the fringes may be made quite horizontal, and they are then relatively large and square, or at times shaped like blunt arrow-heads. This rapid rotation of fringes near  $t$  accounts for their turbulence, since tremors have the effect not merely of raising and lowering them, but also of producing the rotary motion in question. They may also be rotated, of course, on slightly tilting the grating about an axis normal to its face. Rotating the latter on an axis parallel to its face places the phenomenon in different parts of the superposed yellow field.

Since a preponderance of yellow homogeneous light is present in the whole of the superposed wide-slit images in the telescope, it is not difficult to suggest the cause for the variations of the interference pattern when one image passes

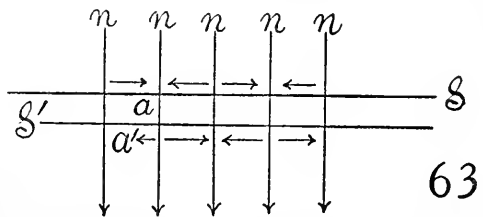
horizontally over the other. The forms,  $t$ , correspond to minimum path-difference, remembering that in accordance with figure 59 all rays pass the plate of the grating twice.

Further experiments were made with sunlight to detect the changes which befall the phenomena in different focal planes. The ocular of the telescope was gradually drawn out from an inner extreme position to an outer extreme position, through the normal position for principal focal plane. In this case a variation of form corresponding closely to figure 62 was also observed. The characteristic feature, however, was the prevalence of arrow-head or caret-shaped lines, both in the case of the extremely fine striations and of the coarser nodules. In the former case these roof-like designs were closely packed from end to end of the phenomenon and usually pointed upward. They recall the top edges of extremely eccentric ellipses in displacement interferometry, and in view of their lateral motion with the micrometer  $M$  and the decreased dispersion due to double diffraction, their origin may be similar.

**39. The same. Inferences.**—When the pencils,  $Mm$  and  $Nn$ , figure 59, are parallel and sodium light is used, the whole field is uniformly striated, whether the striations are made fine or coarse. I have found it impossible, on placing plate compensators (0.5 to 1.5 cm.) in both beams and rotating these to any degree whatever, to produce any suggestion of a secondary periodicity in the field. The fringes for a thick compensator, slightly wedge-shaped, merely become a little finer. Films of mica are liable to blur the field. In general, moreover, reflections would be relatively weak and thus inappreciable. They would require a separate adjustment for coincidence and not appear with the principal phenomenon. Hence the strands of interferences obtained in case of crossed rays are in a measure unique. The second periodicity is not stationary, but a part of the phenomenon. The glass plate of the grating produces an effect in virtue of its thickness, precisely as in the case of the displacement interferometry of my earlier papers.

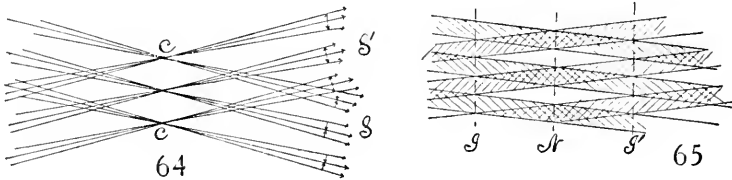
Experiments made with polarized light proved to be entirely negative. The phenomenon appears between a polarizer and an analyzer so long as sufficient light is present to exhibit it. Observation with a nicol, in the absence of the polarizer, showed nothing but the obvious effect of reflection.

The occurrence of these parallel strands for crossed rays and homogeneous light is thus difficult to explain. I have tried a great variety of methods of superposing special interferences, etc., to produce the nodules with parallel rays,  $mM$  and  $nN$ , or to break them with crossed rays,  $mN$  and  $nM$ , without avail. There is no focal plane effect, nor any polarization effect. It is therefore necessary to confront the case at its face value, as in figure 63. Here  $S$



and  $S'$  are the traces of two longitudinally coincident reversed spectra, drawn apart for distinction, the region of the  $D$  lines only being used. The light is homogeneous to this extent and the slit wide, so that there is oblique incidence. Then every point of  $S$  should (on adjustment) interfere with every point of  $S'$ , the result showing a uniformly striated field in the telescope. This is emphatically the case for the parallel rays,  $mM$ ,  $nN$ ; but with the crossed rays,  $mN$ ,  $nM$ , the interference is confined to the rays in the equidistant positions,  $n$ , in figure 63, and midway between them the field is a neutral yellow. In other words, between the rays  $n$  the rays are displaced, as shown by the arrows, recalling the arrangement of nodes in acoustics.

Corresponding rays  $a$  and  $a'$  (for instance) do not coincide and hence can not interfere, the region  $aa'$  remaining neutral. In figure 64 the rays crossing at  $c$  (fig. 57) have been shown for three nodes and the transverse arrows indicate the directions in which the rays have been urged laterally. Naturally, I am merely stating the case as immediately suggested by the results. One may argue that there may be a secondary periodicity in the grating. But why



does it not appear at all in the case of parallel pencils, when it is so obtrusive in the case of crossed pencils of rays? Again, the interferences are unquestionably due to  $D_1$  and  $D_2$  light, simultaneously. If the grids for these two wavelengths should be at a slightly different angle to each other, their superposition would give something like the observed phenomenon, apart from details. Thus in figure 65 the two grids due to  $D_1$  and  $D_2$ , intersecting at a small angle, may be interpreted as appearing strand or cord like at  $N$ , and neutral at  $I$  and  $I'$ . With white light the linear phenomenon would eventually become achromatic.

But, again, why should lines so close together as  $D_1$  and  $D_2$  show any appreciable difference of angle or rotational phase-difference in their interference pattern? Intersecting grids, moreover, can be produced by other methods and nearly always betray their origin. The final inference is that suggested by figures 63 and 64, that homogeneous rays on crossing (here in a medium of plate glass) may exert a lateral influence on each other, to the effect that identical rays emerging from the crossing are arranged in equidistant nodal planes according to figure 63.

**40. Experiments. Reflecting grating. Crossed rays.**—In the preceding experiments the remarkable phenomenon of double interferences was obtained with glass-plate apparatus. It is improbable that any secondary interference can have been produced by the presence of reflected light, since the reflected pencils will be weak as compared with the primary pencils and

differently situated. It is nevertheless necessary to forestall all misgivings by avoiding glass plates altogether and adapting the methods of figure 57, where reflecting surfaces (front faces) only are present, to the experiment for crossed rays  $mN$  and  $nM$ .

In the apparatus as finally perfected,  $G$ , figure 57, was a Michelson plate grating and  $G'$  a Rowland concave grating, each with about the same grating constant. A strong lens was placed at  $T$  for observation at the focus of the concave mirror of  $G'$ . The latter was capable of fore-and-aft motion, of rotation about a vertical axis in its own plane and about an axis normal to that plane;  $G$  was capable of rotation about a horizontal axis parallel to its plane. Thus the possibility of fore-and-aft motion and the three cardinal rotations for the gratings, together with a micrometric fore-and-aft motion of  $M$ , was at hand, as well as the rotation of  $M$  and  $N$  about horizontal and vertical axes.

The interferences were found after establishing the coincidence of the yellow homogeneous fields, in the manner described in the preceding paragraph. The fringes were at first small and apparently single, but they could be enlarged at pleasure and the two definite systems separated by fore-and-aft motion of  $G'$ . They occupied only a part of the wide yellow slit image, the sodium arc being used. On actuating the micrometer at  $M$  there was displacement of the interference pattern as a whole, so that the conditions of displacement interferometry are here also implied, though the equations are liable to be different. On rotating  $M$ , micrometrically, about a vertical axis, the structure of the interference reticulations changed and was at times reduced to a single set.

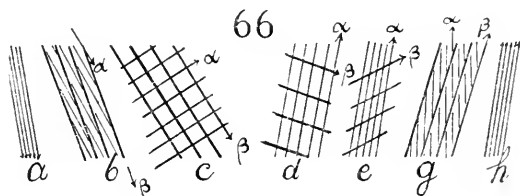
Whenever the arc flashed, or when white light was used, the linear phenomenon appeared alone, either cross-hatched or longitudinal, depending upon the character of the reticulated pattern for homogeneous light. With sunlight, even after narrowing the blade from the collimator and screening off red and green light, the phenomenon was faint and hard to find, unless it was produced alternately with sodium arc.

With the arc freshly charged with sodium, but a single set of interferences or else the linear phenomenon appears, since the broadened sodium lines are equivalent to a continuous spectrum in this region. Not until the excess of sodium has all been evaporated and the sodium lines are normal does the true reticulation show itself. It is interesting to describe two cases of this double-interference pattern, obtained by gradual and successive fore-and-aft motion of the grating  $G'$ , between limits, while the edges of the two wide-slit images, respectively horizontal and vertical, are kept in contact throughout.

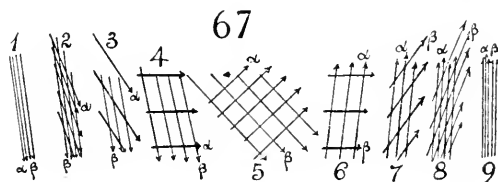
Suppose the original fine fringes to be nearly vertical; then the apparently simple fringes,  $a$ , figure 66 (their appearance, however, would lead one to suspect their simplicity), change to the cord-like strands  $b$ , appearing like helices of a very large pitch. Both interference fringes are still nearly parallel, and they cover the whole wide-slit image uniformly. These eventually pass into the square or rectangular reticulation,  $c$ , with both systems equally strong. Probably intermediate forms have here been skipped. The system,  $e$ , occurs

very soon afterward, in which the difference in size of fringes has become enormous. Following *e*, the procession is reversed in *g*, *h*.

Both systems ( $\alpha$  and  $\beta$  systems, say) have passed through maxima, but not at the same time, or not for the same fore-and-aft adjustment. Both systems have rotated, the rotation being very rapid near the maximum. The reticulations quiver and look precisely like capillary waves in a rectangular trough of mercury, except that they are usually at an angle to the bounding edges of the superposed slit images.



In this quivering system of two identically strong fringes it is difficult to make out the rotations, but after considerable revision the sequence in figure 67 was definitely ascertained. Beginning with the



extreme fore-and-aft position of  $G'$ , and moving it successively forward in steps of 1 or 2 millimeters, the apparently single grid, 1 changes to 2, where the two systems  $\alpha$  and  $\beta$  can be disentangled,  $\alpha$  expanding and rotating more rapidly, so that 3 and 4 follow. Here  $\alpha$  is horizontal and probably of maximum size,  $\beta$  is still nearly vertical and but slightly expanded. Therefore, while the  $\alpha$ -effect wanes the  $\beta$ -effect waxes, and the squared or orthogonal type, 5, is produced. The lines are here equally strong and it is the symmetrical figure of the series. Thereafter in 5, 6, 7, 8, and 9 the chief expansion and rotation is transferred to the  $\beta$  system, with which the  $\alpha$  system has changed functions. Hence both systems rotate nearly  $180^\circ$  in the same direction and pass through maximum size; but the maximum is retarded in rotational phase for one as compared with the other. Rotation and growth are accelerated near the maximum. The total displacement of the grating  $G'$  between the cases 1 and 9 (fig. 67) was about 2 cm.; but this depends upon the obliquity of the grating and incidental conditions, as explained above.

Suppose, in the second place, that the original fringes, 1, figure 67, were nearly horizontal; in such a case the evolution is much the same, but the symmetrical form number 5 becomes smaller and more and more flatly rhomboidal horizontally. Probably the scheme of rotation is the same, but is much harder to ascertain in view of the flat forms. On the other hand, the field now abounds in vertical strands of interferences, like those of the preceding paragraph, and nodules are often in evidence, as before.

If the original lines are quite vertical, they do not seem to rotate with fore-and-aft motion of  $G'$ , but form intersecting, vertical, apparently simple systems throughout the motion. Slight departure from the vertical produces rhomboids very long vertically and often very coarse.

**41. The same. Compensators.**—A compensator of ordinary plate glass, at the intersection  $c$ , figure 57, produces no effect, if symmetrical to both beams. If not symmetrical, the interferences are displaced to right or left in the field of the telescope, as in any case of displacement interferometry, depending on which component beam receives the longer glass-path. Thus this adjustment corresponds to the grating in the preceding paragraph, the difference being that in the latter case the same ruling is used for both diffractions. Hence the interference figures obtained are simpler, showing vertical strands only. In the present case strands occur in all directions. The maxima for oblique positions of the glass plate were not found with reflecting gratings.

If the compensator is within 1 inch in thickness, its introduction occasions no difficulty. The interference pattern may be changed, but it remains the same during the rotation of the compensator; but if the latter is thicker than 2 inches, the figure is usually so small as to be found with difficulty, unless the grating  $G'$  is brought forward, to allow for the mutually inward refraction of the rays. If this is done, the same figure may be reproduced. On advancing the grating, plate compensators much over 3 inches thick were tested without the slightest annoyance. Lenticular compensators require special adjustment and are very difficult of use.

The effects of rotating the grating about the three cardinal axes have all been considered above. In the present instance two sets of fringes are symmetrically rotated, subject to the same conditions. Rotation of  $G'$  around a horizontal axis requires an elevation or depression of the arc lamp, if the fringes are to remain in the field. Rotation around a vertical axis separates the slit images, and a readjustment for superposition is necessary. Results so obtained are therefore complicated and were not studied.

**42. Miscellaneous experiments. Fringes with mercury light.**—A few random experiments made with the sodium arc, in the presence and absence of the magnetic field, showed no results; nor was this to be expected, as a reasonably strong field would blow out the arc. Again, the insertion of a glass compensator, 0.7 cm. thick, in one of the component beams, developed no maximum on rotating the compensator about a vertical axis. Thus with reflecting gratings the peculiar behavior of the transmitting grating, showing a maximum on either side of a symmetrical minimum (§36, 37), is not reproduced.

The effect of rotating the first reflecting grating  $G$  on a vertical axis is only to throw the sodium light out of one side or the other of the (superposed) slit images. No available means of enlarging the fringes indefinitely was found. It is probable that this would require fine adjustment for symmetry. The field of interference, as a whole, is within a spot-like area which may be moved up and down, or right and left, by the vertical and horizontal adjustment screws on the mirror  $M$ . Coincidence at the two sides of the slit favor different interferences. The case is always as if, at a single point of the field only, there were actual coincidence, and that the interference pattern is grouped closely around it.

With the use of an ordinary glass mercury lamp (27 storage cells, 5 ampères) the fringes are found with difficulty when the beam at the first grating is wide. On using a vertical blade of light the definition was improved. The fringes are faint, very susceptible to motion, and at times even absent. They occur, however, as a *single* set, as was anticipated, showing that the above duplicated fringes are actually due to the two sodium lines. The mercury fringes are easily rotated and pass through a horizontal maximum with fore-and-aft motion. Rotating  $G$  about a normal axis may further increase this maximum size to a limit at which the fringes appear irregular or sinuous. A displacement of the mirror  $M$  over 0.7 cm. was easily permissible, without destroying the fringes. They occur, as above stated, within a certain adjusted spot area of the field of view. An attempt was again made to detect a Zeeman effect by placing the poles of an electromagnet on the two sides of the lamp; but here again no difference was discernible on opening and closing the electric circuit. The field, however, for incidental reasons, could not be made strong enough for a critical experiment.

**43. Inferences.**—After these experiments (made with the apparatus figure 57, free from glass plates and depending on reflections only) the cause of the phenomenon is no longer obscure. Obviously one of the paired grids in figure 66 or 67 belongs to each sodium line. The retardation of one phenomenon, rotationally, as compared with the other, is due to the difference in wave-length between  $D_1$  and  $D_2$ . The phase-difference between numbers 4 and 6 (fig. 67) is thus equivalent to 6 Ångström units. If the displacement of  $G'$  is about 0.3 cm., there should be about 0.5 mm. displacement, fore and aft, for 1 Ångström unit. If the grating,  $G'$ , is on a micrometer, this should be a fairly sensitive method of detecting small differences of wave-length, or give evidence of doublets lying close together. The sensitiveness clearly increases with the length of path of the component rays and may thus be increased.

With this definite understanding of the phenomenon, it is desirable to deduce the equations, which in the occurrence of parallel rays would not differ essentially from those of Chapter II or III. It is useful, however, to treat the new case of crossed rays. In figure 69 the angles of diffraction are  $\theta_1$  and  $\theta_2$ , if the incidence of light,  $L$ , is normal at  $G$  and at an angle  $i_2$  at  $G'$ ,  $G$  and  $G'$  being parallel. The mirrors are set symmetrically at angles  $\sigma_1$  and  $\sigma_2$  to the normal in question, and the diffracted rays are reflected at angles  $\alpha_1/2$  and  $\alpha_2/2$ , respectively. The reflected rays cross the normal at an angle  $\beta$ . Then

$$\sin \theta_1 = \lambda/D_1 \qquad \sin \theta_2 = \lambda/D_2 - \sin i_2$$

where  $D_1$  and  $D_2$  are the grating constants. From the figure

$$\alpha_1/2 = \theta_1 + \sigma_1 - 90^\circ \qquad \alpha_2/2 = \theta_2 + \sigma_2 - 90^\circ \qquad \theta_1 = \alpha_1 + \beta \qquad \theta_2 = \alpha_2 + \beta$$

From these equations,

$$D_2 \sin i = D_2 \sin (2\theta_2 + 2\sigma_2 + \beta) - D_1 \sin (\dots)$$

If  $D_1 = D_2$ , then  $\theta_1 = \theta_2$ ,  $\sigma_1 = \sigma_2$ , and therefore  $i_2 = 0$ .

Thus the relations are quite complicated, but if  $D_1=D_2$ , or the gratings have the same constant, rays of all wave-lengths should, after double diffraction, issue normally to the grating  $G'$ , and the arrangement is therefore achromatic. If  $D_1$  is not quite the same as  $D_2$ , but nearly so, an adjustment of  $\sigma$  would probably meet the case approximately. If the original incidence is at an angle  $i_1$ ,  $D_1 \sin i_1$  would have to be subtracted from the first member, but the diffractions would now differ on the two sides of the apparatus.

The relations of the rotations of the striations of  $D_1$  and  $D_2$  light to the fore-and-aft motion is next to be considered. It will be convenient to make use of figure 68 for this purpose, the notation being the same as in figure 69. The two rays, 1 and 2 ( $D_1$  and  $D_2$ ), have both been introduced, and the position of  $G'$  is such that the  $D_2$  rays intersect in its face and are diffracted into  $T_2$ . In such a case the combined pencil is divergent,  $D_1$  rays will undergo an earlier intersection, and consequently be separately diffracted into  $T_1$  and  $T'_1$ . Hence  $D_1$  and  $D_2$  are differently circumstanced in relation to the fore-and-aft motion, and the rotation produced will thus be advanced in one case, as compared with the other, for the reason discussed in Chapter III, paragraph 26. It is also clear that the difference of phase in the two rotations will be greater, as the total path of rays between  $G$  and  $G'$  is greater, so that the large distances used in the present experiments (nearly 3 meters) account for the astonishing sensitiveness of the phase of rotation to the wave-length difference. In fact,  $D_2$  will be in the same phase as  $D_1$ , if the grating is moved forward from  $G'$  to  $g'$ , figure 68, since in both cases the rays intersect in the normal. Hence if  $R$  is the total path  $GmNG'$ , and if the angle of dispersion between  $D_1$  and  $D_2$  is  $d\theta$ ,  $\theta_2$  the angle of diffraction at  $G'$ , and  $h$  the displacement from  $G'$  to  $g'$ ,  $D$  the grating space,

$$Rd\theta = h \sin \theta_2$$

or

$$d\theta = \frac{h\lambda}{DR}$$

and the resolving power

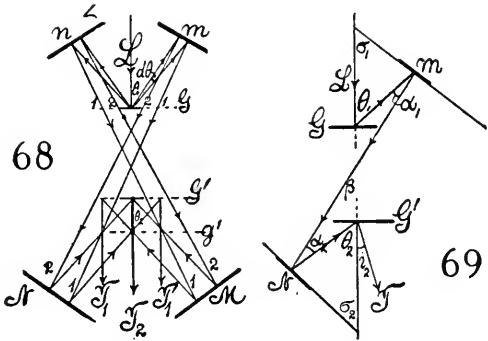
$$\frac{d\lambda}{\lambda} = \frac{h}{R \cos \theta_2} = \frac{Dh}{R\sqrt{D^2 - \lambda^2}}$$

In the given adjustment, roughly,

$$d\theta = 3.7 \times 10^{-4} \quad R = 300 \text{ cm.} \quad \theta_2 = 20^\circ$$

whence

$$h = \frac{3 \times 10^2 \times 3.7 \times 10^{-4}}{0.34} = 0.3 \text{ cm.}$$



As the resolving power is, roughly,  $h/R$ , and if  $h = 0.003$  cm. is still appreciable,

$$d\lambda/\lambda = \frac{3 \times 10^{-3}}{3 \times 10^2} = 10^{-5}$$

*i.e.*, lines  $1/100$  of the distance apart of the sodium lines should be rotationally separated.

Again, the displacement, fore and aft, between like rotational phases of  $D_1$  and  $D_2$  should be about 3 mm., and this agrees fairly well with the order of values found.

The case of the transmitting grating (fig. 59) is thus also elucidated, though it is not clear to me why the duplication of fringes is so efficiently concealed in the nodular forms observed. The reason for the minimum of size, for the symmetrical position  $i = 0$ , and the two maxima for oblique positions of the grating ( $i = \pm 20^\circ$  about), suggests an explanation similar to that given in Chapter II. In other words, in the oblique position the short path-length is compensated by the increased thickness resulting from the greater obliquity of grating, whereas the long path-rays traverse the plate of the grating more nearly normally. In this way the path-difference is reduced as compared with the symmetrical position, and the fringes are therefore larger. The oblique grating acts as a compensator in both of the component beams, and the fringes may be visible, even if in the original position (fig. 59) they are all but invisible. If, however, the apparatus (fig. 57) is used with a plate-glass compensator symmetrical at  $c$ , there are no maxima or minima for any obliquity. Hence the tentative explanation for the case of figure 59 is not warranted.

The fore-and-aft motion of the plate grating (fig. 59) produces no effect, since the rays are reflected back so as to retrace their paths. They are also reflected between parallel mirrors  $N, m$  and  $n, M$ . Thus the path-difference is not modified. The result is merely a decrease of the distance  $M, N$ , and a corresponding increase of  $m, n$ , and *vice versa*.

The marked effects produced by rotating the transmitting grating around a normal axis, finally, follow the explanations given for the rotation of fringes of non-reversed spectra in Chapter III, paragraphs 25 and 26.

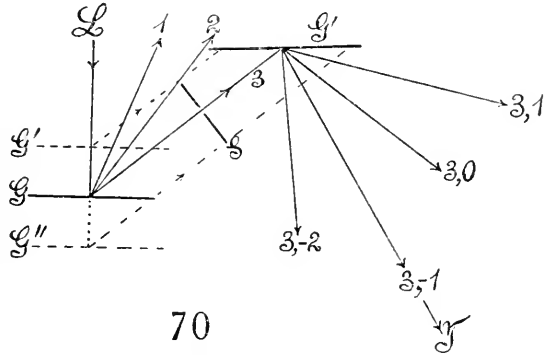
In conclusion, an interesting application of the apparatus (fig. 56) or the other similar types may be suggested. By half-silvering the mirrors and providing a similar opaque set *beyond* them, there should be no difficulty (in the case of homogeneous light) of bringing the interferences due to crossed rays,  $c$ , and to parallel rays,  $a'b'$ , into the field of the telescope *together*. Strictly homogeneous light (mercury arc) would be needed to obviate the duplication of the sodium arc. In such a case, therefore, the parallel fringes could be used after the manner of a vernier on the crossed fringes, with a view to a repetition of the experiment of Michelson and Morley, if this experiment had not been so thoroughly carried out by the original investigators. However, the plan would be to rotate the apparatus, as a whole, so that the two crossed rays would be alternately in and at right angles to the earth's motion, whereas the two parallel rays would preserve the same relation to that motion. Naturally, the parallel and crossed paths would in such a case have to be lengthened by multiple reflections.

## CHAPTER VI.

### CHANNELED SPECTRA OCCURRING IN CONNECTION WITH THE DIFFRACTIONS OF REFLECTING GRATINGS.

**44. Introductory.**—Throughout the preceding work I had noticed that the spectrum due to either of the component beams, after successive reflection from two reflecting gratings, was often regularly furrowed by transverse black bands, before the two spectra were brought to interfere. As these fringes are stationary, they do not modify the phenomenon investigated; but questions now arise as to whence these reflected fringes of a *single beam* come. They are not strong, as a rule, and I was therefore inclined to attribute them to some imperfection of the silvering of the opaque mirrors, but this proved not to be the case, so that it seemed worth while to examine them by special experiments.

**45. Apparatus.**—The apparatus for this purpose, as one beam only is wanted, is quite simple. In figure 70,  $L$  is a vertical blade of parallel rays of white light from a collimator and slit. These rays impinge on the plane grating  $G$ , whence the orders 1, 2, 3, etc., of spectra are reflected. Either of these pencils may be received by the second grating  $G'$ , plane or concave, from which spectra of any order are available. If  $\circ$  denotes the reflected pencils, the groups from two gratings may be distinguished as (3, 1), (3, 0), (3, -1), (3, -2), etc., as in the figure. Any of these two



different pencils is to be examined at  $T$  by a lens or telescope, for instance, and the latter (with strengthened objective where needed) is more convenient, even when the concave grating is used. A wide slit  $S$ , revolvable about  $G$ , is often useful for screening off spectra or parts of spectra. In some experiments the grating  $G'$  may be replaced by an opaque mirror.

The gratings are provided with the usual adjustments for parallelism of rulings and slit.  $G'$  and  $T$  must be capable of considerable right-and-left motion, and  $G$ , in particular, of controllable fore-and-aft motion.

**46. Scattering.**—An interesting result of this work is the evidence and spectroscopic quality of scattered rays, incidentally encountered. For instance in figure 70, if the slit  $S$  is narrow, it cuts off all the rays but the orange yellow of the third order, and the reflected spectra (3, 1), (3, -1), etc., will largely

consist of orange-yellow light. Associated with each of these reddish-yellow patches, however, are vividly violet-blue patches, each separated from the reddish yellow by an almost total absence of green, relatively speaking. If the light is very intense, the connecting part of the spectrum also appears, but it is always far less vivid than the ends of the spectrum in question.

Inasmuch as all violet radiation proper has been screened off at  $S$ , it is obvious that violet light must have been scattered in all directions from  $G$ , a part of which, therefore, passes the slit and is resolved by the second grating  $G'$ . Moreover, as the scattering lines of the grating are equidistant, the scattered light has a regular wave-front. (Cf. Carn. Inst. Wash. Pub. No. 229, 1915, pp. 100-102.)

The correlative experiment of detecting the reddish light transmitted after scattering was also tested. For this purpose the reflecting grating  $G$  may be replaced by a transmitting grating, slit  $S$  placed beyond, and the light then analyzed by a second grating  $G'$  behind the slit and diffracting toward it on one side. But no results of value were obtained.

**47. Fringes with white light.**—The experiments with the apparatus (fig. 70) were commenced with sunlight and (what is essential) a fine slit. Fringes are found in all combinations of doubly diffracted pencils (3, +1), (3, -1), (3, -2), etc.; (2, 1), (2, -1), etc.; (1, -1), (1, 1), etc., but none in the reflected pencils (3, 0), (2, 0), (1, 0), etc., as a rule. Whether the grating  $G'$  be concave or plane, it is best to use a telescope at  $T$ , because (when provided at the objective with an auxiliary concave or a convex lens) it more easily offers a wide range of observation along its axis than an ocular. The latter must be wide and has to be shifted bodily; but both methods were used. A concave grating at  $G$  and plane grating at  $G'$  gave no results. The concave grating is usually more free from channeled spectra.

Of the great variety of fringes obtained, I shall give only two typical examples. The second order of spectra for  $G$  (plane) was separated from the others by the slit  $S$  and diffracted into  $G'$  (fig. 70). The successive fringes appear as the ocular is drawn *outward* from the principal focus.

Combination  $G_2, G'_0$ : Only a good sodium doublet, which became washed on drawing out the ocular of  $T$ , was obtained; no fringes appeared.

Combination  $G_2, G'_{-1}$ : Just outward from the principal focus a large, coarse, irregular set of fringes appeared; next (ocular farther out) a large regular set, somewhat diffuse, possibly double and superposed; then a finer, half-size, very regular set, possibly decreasing. After this the mottled surfaces of the gratings were successively in focus. A weak spectacle lens was now added to the objective of  $T$ , whereupon very large regular fringes were seen when the ocular was far out.

Combination  $G_2, G_{-2}$ : The ocular moving outward from the principal focus, the fringes seen in succession were as follows: large, regular, vague; half-size sharp; surfaces vertically striated; (lens on) fine regular set in red; doubled regular set in green.

Combination  $G_2, G-3$ : Fine set just before the surfaces appeared, which were delicately striated; fine regular set; coarse set, both close to surface; (with lens on) fine regular set; doubled, strong regular set.

Different distances between  $G$  and  $G'$  had very little influence on the size of the phenomena. A few examples may be given, which are observed when the ocular is moved outward.

$G_3, G_1$ : Distance 10 cm.—Fringes, faint regular; strong irregular; faint regular; flat field; surfaces visible; faint regular.

Distance 25 cm.—Strong irregular; faint regular; small regular; large (double) irregular; lines slit into fine fringes; large faint regular.

Distance 46 cm.—Large strong, with two absorption bands; fine regular; double-sized faint; surfaces with fine striations; alternations of fine and coarse lines; faint, regular, large, etc.

Fringes of different color are often in different focal planes. When a lens is used with the concave grating, observations must sometimes be made 2 meters off to get the large regular fringes. Red fringes may be narrower than the corresponding violet set.

If the grating  $G$  is moved fore and aft, parallel to itself, the fringes are shifted across the stationary sodium line, as in displacement interferometry.

Whereas in the positive combination (3, 1), (3, 2), etc., the spectra widen, they tend to close up for the negative combinations (3, -1), (3, -2), etc. With two identical plate gratings they may image the white slit. But this seems to have little effect on the fringes seen as a whole when the ocular is out of focus.

When *white* light is used and the grating  $G'$  replaced by an opaque mirror, or in case of combinations which involve direct reflection (2, 0; 3, 0; etc.) at  $G'$ , there seem to be no fringes.

**48. Fringes with sodium light.**—While there is some difficulty in obtaining the fringes with white light, fringes with homogeneous light are obtained at once, provided the light is sufficiently intense. A sodium arc lamp, or a mercury lamp, with a fine slit, must therefore be used. In this case, moreover, the grating  $G'$  may often be replaced by an opaque mirror, or the fringes of the order  $G_2G_0, G_2G_0$ , etc., may be produced with entire success. On moving  $G$  fore and aft, they again travel across the sodium line. Often, in fact, two sets of fringes seem to be shifted. A few examples again may be given of the great variety in this display while the ocular is being drawn out:

$G_1, G'-2$ : Sodium lines  $D_1D_2$  single size; large strong fringes, lines split.

$G_1, G'-1$ : Closed spectrum; striations continuous.

$G_1, G'0$ : Reflection;  $D_1D_2$  single size; surfaces of gratings finely striated.

$G_1, G'_1$ :  $D_1D_2$  double size; strong grid seen very near the surface of  $G'$ .

$G_1, G'_2$ :  $D_1D_2$  treble size, out of reach.

$G_2, G'0$ : Reflection; no fringes.

- $G_2, G' - 1$ : Distance 12 cm.—Coarse irregular; with lens fine regular set, near and beyond the surfaces.
- $G_2, G' - 1$ : Distance 45 cm.—Surfaces with doubled fine striations; with lens finally strong and regular.
- $G_2, G' - 1$ : Distance 60 cm.—Regular faint; irregular double, very strong; surfaces striated; with lens strong double irregular; finally regular small.
- $G_3, G' 1$ : Regular; regular line split; irregular coarse; surfaces finely striated,  $G$  coarser; fringes grow continually larger without vanishing.

On moving  $G$  fore and aft, two grids seem to travel through each other in opposite directions. This probably accounts for the occurrence of irregular fringes. The size of fringes seems to be a minimum for a conjugate focus near the surfaces. The whole phenomenon is continuous. Irregular fringes, probably superpositions, become regular in other focal planes.

- $G_3, G' 2$ : About the same; minimum size at the surfaces, increasing about three times as the ocular is drawn either way.
- $G_3, G' 0$ ; also  $G_3$ , mirror: About the same results, only brighter and better. Hence in case of large dispersion two gratings are not needed. The two sodium lines, when the ocular is drawn out of focus, multiply themselves at regular intervals, so that the grids are sometimes distinct, sometimes partially superposed. Thus the classic diffraction phenomena of a slit suggest themselves as the starting-point for an explanation of the present phenomena as a whole.
- $G_3, G' 0$ , produced alternately with sodium light and sunlight, showed the same sequence of fringes (the large ones with a tendency to split) in the former case, while nothing appeared in the case of white light.

**49. Grating on a spectrometer.**—It seemed necessary, therefore, to consider the diffraction of a fine slit, when seen in the telescope, somewhat in detail. In Chapter III the production of beautiful Fresnellian interferences from two identical slit images and homogeneous light was demonstrated; but an equally clear manifestation of the diffraction of a slit image, when the ocular is out of focus, does not seem to occur. The broad image of the slit out of focus shows a stringy structure only, but no separation is easily obtainable. Fringes, as such, are quite absent when the ocular is drawn out.

The light of the sodium arc was now passed through a very fine slit and collimator and reflected from a plate grating. The above intermittently regular and irregular fringes were strikingly obtained with the ocular out of focus. As this is successively more and more drawn out, fine lines become coarser, and then seem to subdivide, giving the structure a fluted appearance, frequently regular. There is, in other words, a double periodicity. In

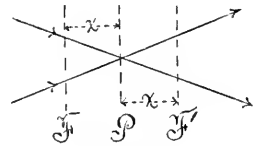
the case of highly diffracting grating ( $D = 10^{-6} \times 175$ ), the results appear best in the second order.

The same beautifully duplicated fringes were obtained with a transmitting film grating of about the same dispersion, particularly well in the first order.

The sodium flame gives too little light for the present purposes, but the phenomenon is seen.

Believing that some irregularity might be introduced by the double-sodium line, I installed a mercury lamp for comparison. In the first experiment a film grating ( $D = 173 \times 10^{-6}$ ) was used, the ocular traveling outward from the principal focus. Both the green and the double yellow mercury lines enlarged and showed fringes of increasing size and number together. The green field had a darker band, the yellow a bright band in the middle. As the fringes enlarged, each split up into secondary fringes, 4 or 5 eventually, and this again occurred for both green and yellow fields.

Rotating the grating around a vertical axis seemed to shift the primary fringes laterally over the stationary secondary fringes. A concave lens for positions anterior to the principal focus and a convex lens for posterior positions (toward the eye) were successively added to increase the range of observation. On both sides of the principal focal plane (fig. 71) fringes occur, which enlarge with the distance  $x$  from that plane. As they enlarge, each fringe splits up into secondary fringes, which in turn enlarge.



Sometimes the arrangement is irregular. Green and yellow fields may overlap, but they do not do so conformably.

The undeviated ray, however fine the slit may be, merely shows a stringy field, sometimes suggesting structure, but never showing clear-cut fringes.

The same kind of results were obtained with a reflecting grating of about the same dispersive power. In the second order the fringes were particularly clear and regular. Primary fringes, finally, carried three to four secondary fringes each.

Next, a ruled transmitting grating of less dispersive power (grating constant  $352 \times 10^{-6}$  cm.) was adjusted for mercury light. Here in the undeviated ray and in the first order no clearly separated fringes were obtained. In the second and third orders, however, they were very perfect, and followed the above rules, showing sharp secondary fringes.

It follows, therefore, that a certain degree of dispersion is needed to resolve the fringes, which is inadequate in amount in the order zero, in this case, and scarcely so in the first order. In the higher orders the conditions are met. Using a very fine slit, however, I later just succeeded in separating the fringes in the first order.

Finally, I returned to the endeavor of detecting diffraction fringes in the undeviated image, using a micrometer slit, a good achromatic lens (or no lens), and a distant (2 meters), moderately strong telescope. In this case separated and distinct diffraction fringes, white throughout, were undoubtedly obtained. They moved with the eye so as rarely to be stationary and in the same direc-

tion if the ocular is drawn out, or the reverse if it is thrust in. On close examination two sets, in different focal planes, seemed to be present, one stationary and the other moving as described, and accounting for the observed pronounced parallax. Suggestions of movable fringes accompanying the stationary are also present when the latter are produced by the grating. In this case the stationary fringes are strong; in the case of simple diffraction the movable fringes are more prominent.

**50. Inferences.**— There can be no doubt that the great variety of channeled spectra obtained, when white light is successively diffracted by two gratings, is referable to the fringes obtained in the diffraction of homogeneous light, observed outside the principal focal plane, on a spectrometer. In other words, if light of a given pure color (sodium, mercury) is used, a single grating suffices. Each line of the spectrum is resolved into well-defined groups of fringes, if it is observed either in front of or behind the principal focal plane. The arrangement of fringes varies in marked degree with the distance of the plane observed from the latter ( $x$ , fig. 71). If reflecting gratings are used, there is no other possible source of interferences; but reflecting and transmitting gratings show the phenomenon equally well.

After finding how easily the Fresnellian interferences of two virtual slits could be reproduced in the telescope (Chapter III) and observed on either side of (before or behind) the sharp images, it seemed reasonable to suppose that the diffraction of a slit could also be produced and exhibited in this way; but the availability of this anticipation is attended with much greater difficulty. The image of a very distant slit does indeed show separated diffraction fringes on either side of the principal focal plane in the observing telescope. But they move right and left with the eye, in the same direction if the ocular is drawn outward from the principal focal plane, and in the direction opposite to the eye if the ocular is thrust in. Hence, in this respect, the fringes do not at once recall the phenomena under consideration. Usually the blurred image, out of focus, is stringy, without definite structure. It is resolved in a single focal plane only.

To obtain sharp stationary fringes from an image of the slit, this image must be produced by the diffraction of a grating having a dispersing power above a certain minimum. Thus in a grating of about 7,000 lines to the inch the undeviated slit image and the image of the first order are not clearly resolved, unless the slit is very fine. In the second and higher orders, however, the resolution is very pronounced and the fringes stationary.

The resolution of fringes is equally manifest in front of or behind the principal focal plane, so that if a weak convex lens is added to the objective of the telescope, the succession of fringes is found with an outgoing ocular; if a weak concave lens is added to the objective, the succession is found with an ingoing ocular, starting in each case near the principal focus. As the fringes increase in size they in turn subdivide, sometimes irregularly, as if each fringe were a new slit image, capable of undergoing secondary diffraction. Beyond these secondary fringes no further resolution was detected.

Returning to the work with two successive gratings and white light, the channeled spectra obtained are too complicated for concise description. A very interesting result, however, is the passage of the fringes across the stationary sodium line, when the first grating  $G$  is moved fore and aft in a direction normal to its plane. The region of the  $D$  line is thus alternately dark and bright. The direction of these rays remains unaltered while the illumined strip is shifted horizontally across the ruled space (fig. 70) of the second grating. Usually it is difficult to see the  $D$  line in the focal plane of the fringes. When homogeneous light is used this fiducial mark is necessarily absent and the cross-hairs of the ocular must be supposed to replace it. The shift of the fringes is then equally obvious, and sometimes (sodium light) different groups seem to travel in opposite directions while the grating  $G$  moves in one direction. In case of homogeneous light and two gratings, moreover, the fringes seem to be of minimum size in the conjugate focal plane of the gratings. They increase in size and in turn split up in focal planes before and behind this.

An insight into these occurrences was finally obtained in observation with homogeneous light in the spectrometer by shifting the grating (transmitting) in its own plane, right and left. The fringes in such a case move *bodily* across the field of the telescope, new groups entering on one side for those which leave on the other. These fringes, even if quite distinct, are differently arranged in coarse and fine series and are frequently accompanied by dark or bright bands. This probably also accounts for the effect of the fore-and-aft motion of the grating, mentioned above. Moreover, it would be interesting to search for repetitions of given groups of fringes while the grating is being shifted parallel to itself, from end to end, as this might indicate the residual imperfections of the screw with which the grating was ruled. If the ocular is drawn and set outward from the principal focal plane (at which the slit image is quite sharp) into a different position, the fringes move in a direction opposite to the grating. If the ocular is set inward from the principal focal plane, they move in the same direction as the grating. This would not be unexpected; but secondary fringes or something else in the field seem to remain stationary. Successive fields may be quite different as to arrangement of fine and coarse lines, but all plane gratings exhibit the same phenomena. Thus it is obvious that the fringes of the present paper result from a residual irregularity in the rulings of the grating. Micrometrically, the successive strips of a slit image, however fine, are of unequal intensity. Between these there is diffraction, as may be tested by examining the clear glass at the edge of the ruled space.

To attempt a theory of these phenomena seems premature; but it is obvious that in the otherwise indistinguishable images of a slit in homogeneous light, however sharp or however narrow, the nature of its origin still persists and may be detected by observations outside of the principal focal plane. A fine slit is in all cases presupposed, and all the phenomena vanish for a wide slit. On the other hand, the width of the pencils of parallel rays may be far greater than is necessary to show the strong Fraunhofer lines, if indeed there is any limitation to this width.

## CHAPTER VII.

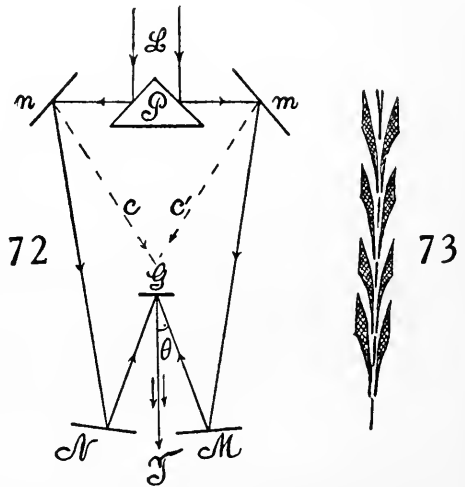
### PRISMATIC LONG-DISTANCE METHODS IN REVERSED AND NON-REVERSED SPECTRUM INTERFEROMETRY.

**51. Purpose.**—It is preliminarily the object of the present paper to examine a variety of new methods for the production of interferences with spectra, with a view to the selection of as simple a design as possible for practical purposes. Some interesting differences appear in the results, so that the simplicity of construction does not necessarily recommend the apparatus for use.

In the second place, the endeavor will be made to assemble appurtenances in such a way that the extremely mobile phenomena may be under control, even in a moderately agitated laboratory. In case of the early interferometer experiments, the interferences disappeared on merely touching the apparatus, and are rarely or never at rest; whereas it is, of course, necessary that they should remain visible while the micrometer is being moved. These experiments are now nearly completed, but will preferably be described in a succeeding report.

**52. Methods and apparatus.**—Some prismatic methods were tested in the earlier volume, but not developed; for the plan of using a transmitting grating twice, or two gratings in succession, seemed to contain greater promise. The prism method is, however, more simple than any of the others and therefore deserving of special study.

In figure 72 the large right-angled prism  $P$ , with its faces silvered, receives the pencil of parallel white rays,  $L$ , on its orthogonal faces and reflects them to the plane opaque mirrors  $n$  and  $m$ . From here the rays are further reflected, either nearly in parallel, as in the figure, or crossed, as at  $c, c'$ , to the remote opaque mirrors  $N$  and  $M$ , which in turn reflect them to the plane or concave grating  $G$ . If the rays converge at the appropriate angle of diffraction,  $\theta$ , a selected color will be diffracted in the direction of the normal to  $G$  in each case. If the two paths are nearly equal, these rays will therefore interfere in the axis  $GT$  and the results may be observed by a telescope or a lens at  $T$ . In my apparatus the distances  $mM$  and  $nN$  were of the order of 2 meters. In consequence of the three successive reflections, it is somewhat difficult to



obtain spectrum lines normal to the axis of the spectrum, so that if the latter are superposed the lines will be at an angle. But if this is small, it does not seriously interfere with the occurrence of fringes, as they extend from top to bottom of the spectrum.

The appearance in general is of the linear character heretofore described. They pass symmetrically from extreme fineness, through a maximum size, to fineness again, with the fore-and-aft motion of the grating  $G$ , and they usually rotate near the maximum.

If the mirror  $M$  is displaced nearly in a direction normal to itself, on a micrometer, the fringes undergo the same evolution, and in this respect differ from the case where the primary differentiator,  $P$ , was also a grating. In this case the displacement of  $M$  showed no discernible modifications of the size or character of the fringe pattern. The fringes merely moved. In figure 72 the effect of moving  $G$  or  $M$  fore and aft is similar, since it throws the point of convergence of the rays  $NG$  and  $MG$  in front of or behind the grating. The result is therefore different when white light impinges on  $G$  from what it is when the light is already nearly homogeneous.

The limit of visibility is also inferior to the double-grating method heretofore used, for the fringes passed between the limits of visibility through the maximum size, for a displacement of  $M$  of only about 3 mm. Smaller ranges may occur. On limiting the incident beam at  $L$  to a breadth of about 0.5 cm., the fringes became much broader and relatively intense.

There is, of course, an abundance of light, so that the screening of the incident beam is not disadvantageous. In this case, when the fore-and-aft position (illuminated strips on the grating coincide, as in figure 72) and the position of the grating relative to its normal axis were carefully adjusted, large arrow-headed fringes, as in figure 73, were obtained, usually less closely packed vertically. Apart from tremors, these move slowly up and down (breathing), as a result, no doubt, of changes of temperature in the air-paths. A mica film inserted into one beam and slowly rotated produced similar motion, besides introducing its own grid of vertical and parallel fringes. The reason for the occurrence of these arrows is not quite clear to me, though they are associated with horizontal fringes and homogeneous light, the doubly inflected forms belonging to inclined fringes and homogeneous light.

In the endeavor to reproduce these fringes with the sodium arc, I failed after long trials. The reason may be sought in the flicker of the arc, whereby the beam passes from one side to the other of the edge of the prism  $P$ , but it is probably due to the inadmissibility of a wide slit.

**53. The same. Crossed rays.**—The present method, using four mirrors, has, nevertheless, the advantage of admitting the use of either parallel or crossed rays. Inasmuch as these rays are white until they leave the grating, the method is interesting. On being tested it showed the same peculiarities as the preceding. The crossed rays ( $cc'$ , figure 72) are more nearly normal to the mirrors  $M$  and  $N$ ; nevertheless the range within which the interfer-

ences are visible is not above 2 mm. of displacement of  $M$ . The fringes may, as usual, be made as large as possible, by first superposing the two illuminated strips on the grating  $G$  (by fore-and-aft motion) and then rotating the grating on an axis normal to its face until the best conditions appear. Both spectra are very bright, but liable to be in different focal planes from inadequate planeness of the reflecting system. If work of precision is aimed at, this condition is of foremost importance.

**54. Another method.**—If the opportunity of using crossed pencils of white light is to be dispensed with, the prism method may be simplified, as shown in figure 74. Here  $P$  is a prism with silvered sides and a prism angle of less than  $30^\circ$ . It receives horizontal white rays  $L$  from a collimator, which, after reflection from the opaque mirrors  $M$  and  $N$ , impinge on the grating  $G$ , plane or concave, and are observed at  $T$  by a telescope or lens.

If  $\varphi$  is the prism angle and  $\theta$  the angle of diffraction, it is easily seen that the angle between the rays reflected at  $M$  or  $N$  is

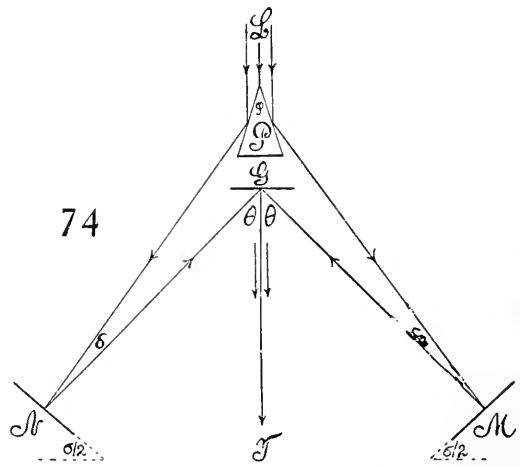
$$\delta = \theta - \varphi$$

Hence, if  $P$  is a  $30^\circ$  prism, the observations can be made only in the second-order spectra. If observations in the first order

are desired because of the greater illumination,  $\varphi$  must be less than  $20^\circ$ , as a rule, for a grating of about 15,000 lines to the inch. The mirrors  $M$  and  $N$  make an angle of  $\sigma/2 = (\varphi + \theta)/2$  with the line  $MN$ .

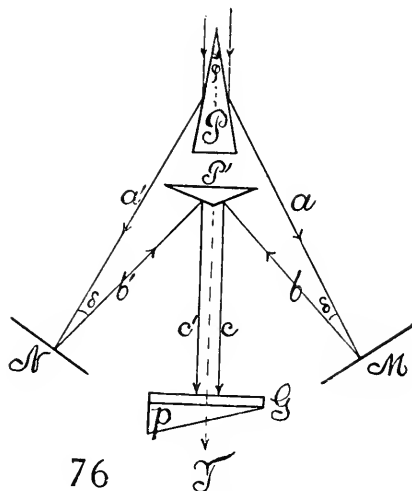
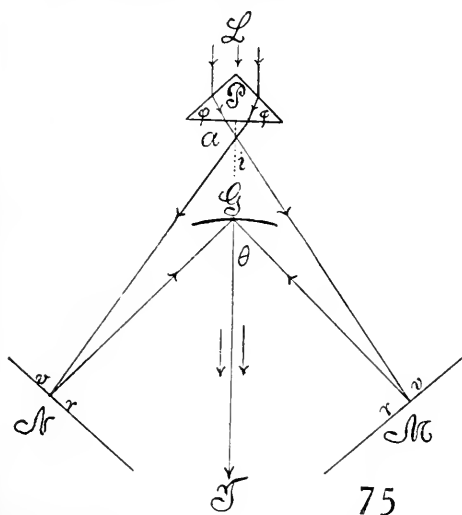
The first experiments were made with a  $30^\circ$  prism and second-order spectra from a concave grating ( $D = 177 \times 10^{-6}$  cm.). Sunlight was used. The two superposed spectra were magnificent, with abundance of light and high dispersion; but the spectra were of unequal intensity and in different focal planes, so much so that the images of the guiding horizontal thread of the spectra could scarcely be seen together. This made the adjustment for coincident longitudinal axes very difficult, and the interferences were not found until after long trial. The reason for this is the probable concavity or convexity of one or more of the reflecting surfaces. Another difficulty was the distance apart of the mirrors  $M$  and  $N$  (roughly, 150 cm. for a distance of about 2 meters from  $P$  to  $T$ ), so that it was inconvenient to observe and actuate the mirror micrometer at  $M$ . Further attempt at improvement was therefore abandoned.

This prism was now replaced by one of less angle than  $\varphi = 20^\circ$ , also well silvered. In the first experiments the adjustment did not admit of a coincidence of light, except near the  $C$  line of the red; but  $M$  and  $N$  were now less than 90 cm. apart, while the distance between  $G$  and  $T$  was about 110 cm., and



between  $G$  and  $P$  about 10 cm. In this case the focal planes were nearly identical and the interferences easily found in the red region between the two  $C$  lines. They appeared as small red pearls, very vivid on limiting the lateral extent of the pencil  $L$  to about 5 mm., but, to my astonishment, they very soon vanished on displacing  $M$  in a direction normal to itself 1 or 2 mm.

**55. Methods using prismatic dispersion.**—The small range of displacement available in the prismatic reflection methods induced me to devise corresponding refraction methods, to see whether these would show any advantage in this respect. Accordingly the interferometer (fig. 75) was installed and the fringes found without much difficulty. Here  $P$  is the symmetrical prism, receiving the collimated beam of incident white light on the faces meeting at the obtuse edge and refracting them in relation to the smaller prism angle  $\phi$ . This must be less than  $45^\circ$ , for convenience in observation, as otherwise the dispersed beams meeting the opaque mirrors  $M$  and  $N$  will



be too far apart for manipulation, supposing, of course, that the distance  $PM$  and  $PN$  are over a meter. I used an equilateral  $90^\circ$  prism for want of a better. The spectra reflected from  $M$  and  $N$  respectively impinge on the grating  $G$ , concave or plane, and are viewed at  $T$  with a lens or telescope. In consequence of the large angle  $\theta$ , second-order spectra were used, without apparent disadvantage. The dispersion of  $P$  and  $G$  being summational, the total is very large.

To return to the angles again, if  $\phi$  denotes the obtuse prism angle, and  $r$  the angle of refraction, the angle of incidence is  $90^\circ - \phi/2$ , or

$$(1) \quad \cos \phi/2 = \mu \sin r$$

Again,

$$(2) \quad \sin i' = \mu \cos (\phi/2 + r)$$

when  $i'$  is the angle of emergence. Hence

$$\sin i' = \cos \phi/2 (\sqrt{\mu^2 - \cos^2 \phi/2} - \sin \phi/2)$$

If  $\phi = 90^\circ$ , then  $\sin i = (1/2)(\sqrt{2\mu^2 - 1} - 1)$ . Thus if  $\mu = 1.55$ , then  $\sin i' = 0.475$ , and  $i' = 28.4^\circ$ . Now, since  $i + \delta = \theta$ , the angle  $\theta$  will obviously have to be in the second order of the spectra of the grating  $G$ .

Although the two spectra obtained in this way were highly dispersed and very brilliant, the interference phenomenon itself was not much superior to the case where reflection from the (silvered) faces of the prism was employed. The fringes disappeared, in fact, for a displacement of 1 or 2 mm. of the mirror  $M$ , showing the usual inflation of form just before vanishing. The details also were of the same nature, the large arrow-shaped forms being obtained when illuminated strips on the grating were superposed and the latter slightly rotated until the maximal conditions appeared.

To increase the range, the angle  $\delta$  must be reduced, as far as practicable. This is possible in the present method, since the points of intersection at  $a$  and  $G$  may be made to all but coincide. Reflection from the mirrors  $M$  and  $N$  would then be normal. To attain this end it will be necessary either to have the grating constant or the prism angle  $\phi$  predetermined, or to use rays of suitable divergence at  $L$ .

**56. Methods with paired prisms.**—White light (fig. 76,  $L$ ) from a collimator is reflected in turn from the silvered sides of the sharp prism  $P$ , from the opaque mirrors  $M$  and  $N$ , and from the silvered blunt prism  $P'$ , as shown by the component beams  $abc$  and  $a'b'c'$ . Thereafter the white beams are diffracted by an Ives film grating  $G$ , with attached prism  $p$ , and observed in a telescope at  $T$ . Interference, therefore, takes place in the focal plane of the telescope and would not (for the case in fig. 76) occur in its absence. Very interesting results were obtained with this apparatus. The spectra are non-reversed or else (if slit and grating are rotated  $90^\circ$ ) inverted. The work, however, is still in progress and will be described elsewhere. I will merely add, in this place, that the work with prisms is important, inasmuch as it shows the essential part played by the diffraction of the slit of the collimator, in its bearing on the phenomena of the present report. It is the function of the prism  $P$  to cleave the diffracted field which leaves the collimator. For this reason pencils identical in source are found on both sides of  $P$ . The experiments thus furnish the final link in the theory of the phenomena.

Furthermore, as the above results already show, the range of displacement of either opaque mirror ( $M, N$ ) within which interference fringes are visible, increases in marked degree with the dispersion to which the white ray is subjected on separation and before the resulting partial rays reach their final recombination. These ranges increase from a fraction of a millimeter to almost a centimeter, while the width of the strip of spectrum carrying the interference fringes, *caet. par.*, remains the same. This also has a fundamental bearing on the phenomenon and is under investigation. The question at issue is whether increase of range of displacement results simply from the geometry of the optic system, or whether wave-trains are actually uniform throughout greater lengths, in proportion as they have been more highly dispersed.

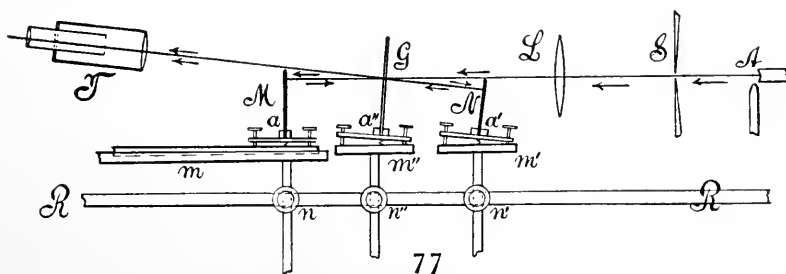
## CHAPTER VIII.

### THE LINEAR TYPE OF DISPLACEMENT INTERFEROMETERS.

**57. Introductory.**—This apparatus will be referred to in various places in this book and presents certain interesting features. The incidence of the grating is normal ( $I=R=0$ ), and both component rays in their vertical projection lie strictly in the same plane. To make the horizontal projection also collinear is not quite possible in practice, because the direct or unreflected rays and the corresponding spectra would overlap with the spectra of the interferometer. As the former are much more intense, the interference patterns would scarcely be visible in the combination. To avoid this, the rays diverge slightly (a few degrees, depending on the distance between grating and opaque mirrors) in a vertical plane. But this is of no consequence, as the horizontal projections only are used in the measurements. One may note, in passing, that this avoidance of coincidence with undesirable spectra secured by tilting the grating and the corresponding opaque mirror in the same direction is, in general, one of the essentials of the adjustments.

The advantage of the linear displacement interferometer is this: that it can be built on a rail and mounted along a wall or a pier. If the rail is tubular, a current of water may be passed through it from the middle toward both ends, to insure constancy of temperature.

**58. Apparatus.**—The apparatus was constructed as follows and gave good results at once, showing strong interferences. The ellipses were, in fact, oblate in the red, circular in the yellow, and prolate in the blues, but clear throughout.



Light enters from an arc lamp, *A*, or Nernst burner, or the sun, at the slit *S*, and is collimated by the lens *L*. Then the parallel rays pass the grating *G* with its ruled side toward *L*. From the grating the reflected beam returns to the opaque mirror *N*, and is then reflected into the auxiliary or adjustment telescope, *T*. The component beam transmitted at *G* is reflected from the opaque mirror *M*, returned to the ruled side of *G*, and thus also reflected into *T* coincidentally with the other beam.

Figure 77 shows that the entering undivided beam  $LG$  passes just above the mirror  $M$ , and is reflected just below this from the top of  $N$ . Similarly, the reunited beam  $GT$  passes just above  $M$ , but is reflected from the top of  $M$ , the object being to make the vertical angle at  $G$  as small as possible.

The mirrors  $M$  and  $N$  and the grating  $G$  are on adjustable bases,  $a, a', a''$ , each controlled by three leveling screws on a plane-dot-slot arrangement in the tablets  $m, m', m''$ , the axis of rotation being horizontal and normal to the diagram. The tablets, furthermore, may be revolved and raised or lowered by the rods  $n, n', n''$ , which are attached by ordinary clamps to the large, tubular, horizontal rail,  $RR$ , in question, admitting of a circuit of water. The latter is secured to the pier.

The angles of inclination of the figure are much exaggerated, since the distance  $MG=GN$  (nearly) is from one-half to several meters in extent.

The mirror  $M$  is on a Fraunhofer micrometer suggested at  $m$ . The bases,  $a, a', a''$ , are drawn to the tablets,  $m, m', m''$ , by firm springs, preferably running into the tubes below them.

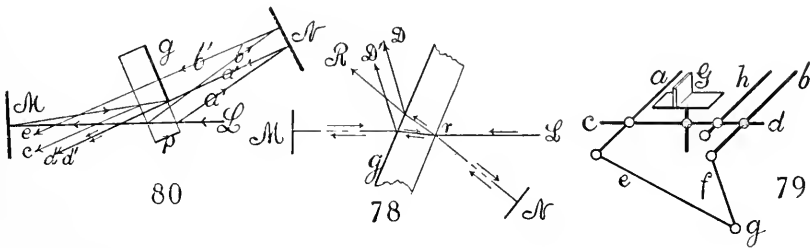
The axis of the adjustment telescope,  $T$ , lies in the plane of the figure and serves the purpose of bringing the direct slit images into horizontal and vertical coincidence. When this is done it may be removed, if desirable, as the ray  $GT$  is not thereafter used.  $T$  should not be attached to the rail, but placed on an independent table, or standard, so as not to be an integrant part of the interferometer. The telescope,  $T$  (not shown), for the observation of the interferences, should be independently mounted on the same table. This telescope lies outside of the diagram, to the right or the left of it, to catch either of the two diffraction spectra selected. It will be seen that these lie quite above the direct diffraction spectra of the ray  $LGM$ . Otherwise, as this is much more intense, it would completely wipe out the interference spectra and their combination. The latter, when seen alone, are very brilliant, black and colored patterns, running through the spectrum when the micrometer,  $m$ , is manipulated. If the distance  $GN$  is large and the grating  $G$ , as usual, slightly wedge-shaped, the superfluous rear reflection from  $G$  may be blotted out at  $N$  by a small screen. It is easily recognized, as it is brown from scattered light.

The installation is simple. The parts being adjusted nearly symmetrically, the undivided ray from a wide slit is brought to the top of  $M$  by raising or lowering the lamp. This should first be done roughly with the lens and slit removed.  $N$  has at the same time been placed just below the beam, and this passes through the middle part of  $G$ . The latter is then inclined by the adjustment screws until the component beam  $GN$  strikes the top of  $N$ , symmetrically. Next  $N$  is inclined and rotated (vertical axis) until the reflected beam enters the telescope,  $T$ . Finally,  $M$  is inclined and rotated (vertical axis) until the reflected rays  $MG$  and  $GT$  also enter the telescope, the final sharp adjustment being made with a narrow slit and the eye at the telescope. The mirror  $M$  must also have a fine vertical adjustment (not shown). If the

distances  $NG$  (face toward the light) and  $MG$  are equal, the interferences are then easily found by moving the mirror  $M$  on the micrometer toward the grating.

As compared with the other non-linear interferometers used under like conditions, the present instrument, even when mounted on a  $\frac{1}{4}$ -inch gas-pipe,  $RR$ , showed itself remarkably steady, so that rings could be observed in spite of the tremors of the hill on which the laboratory is built.

**59. Film-grating adjustment. Michelson's interferometer.**—If the grating  $G$  is a film grating, like those in the market, with 14,000 lines to the inch, it should be mounted smoothly on the unruled side, on a *thick* glass plate, with Canada balsam, and without a cover plate for the ruled side. It is to be adjusted with the glass side toward the source of light, so that the reflection taken may be from this side only (see  $r$ , fig. 78). In the telescope,  $T$ , directed toward the reflected beams, two slits (one for each component beam) only appear, as the glass plate does not reflect on the side covered by the grating ( $g$  in fig. 78). The slits placed in coincidence will then show the elliptic inter-



ferences in the diffracted beam  $D$  at the proper distances. With so large a dispersion as the above, the ellipses are usually too large. They should then be reduced in size by a compensator placed in the beam on the ruled side of the grating; or, preferably, the grating may be mounted on a plate of glass fully 1 cm. (or more) thick, as in figure 78. This thick plate has the additional advantage of eliminating the stationary interferences due to the front and rear faces of the grating. In case of thin glass plates (2 or 3 mm.), these stationary interferences are very strong, coarse, vertical lines and exceedingly annoying.

If the film grating is carefully mounted in this way, it is nearly as good as a ruled grating. There is, however, one insuperable objection, inasmuch as the ruled face, though it does not reflect sharply, does diffract, and this more strongly than the other. Thus there are always 3 superposed spectra in the telescope, the third coming from the film side only, whereas the other two are produced by the rays coming coincidentally from  $r$  on the unruled side of the grating. Hence the velvety blackness of the interferences in case of the ruled gratings can not be reproduced by the film grating, since the interferences are spread out on a colored ground. They are, however, quite strong enough for all practical purposes, and the lines are sharply and symmetrically

traced. A vertical wire 2 or 3 mm. thick, placed symmetrically in front of the objective of the telescope, makes the interference relatively strong and sharp, by blotting out the third spectrum partially; but it at the same time diminishes the light available. A wide slit in front of the objective subserves the same purposes better.

If the distance apart of the mirrors  $M$  and  $N$  and the grating  $G$  is large, it is best to *dispense with the rail RR* altogether, and to mount the mirrors and grating *directly on the pier or wall*. This has the additional advantage of a large free space between  $M$  and  $G$  or  $G$  and  $N$ , so that spacious apparatus like a fog-chamber may be independently mounted there. This was the case in the optic experiments on the thermal coefficients of the refraction of air, etc., below, where the distance between  $MG$  and  $GN$  was nearly 2 meters. In such a case, moreover, in addition to the usual three adjustment screws of the mirror  $M$  at the micrometer, it is desirable to have two others bearing on the rigid parts of the support, so that the final adjustment may be made elastically. By devising a tetrahedral plan of bracing  $M, G, N$ , independent of each other, using short rods and clamping all parts on relatively short stems, I eventually obtained a mounting which was almost free from tremors, even amid the disturbances of the surrounding laboratory. In figure 79 one of these mountings is suggested:  $a$  and  $b$  are  $\frac{1}{4}$ -inch gas-pipes (about a foot long), sunk into the wall of the pier at their rear ends;  $cd$  is a cross-rod of same size and material, clamped in place, and supporting the grating (or a micrometer)  $G$ . The screw  $h$  abutting against the wall gives the horizontal elastic adjustment. The braces  $e$  and  $f$ , which may be adjusted by rotation (screw) abutting in  $g$  at the wall, give the grating vertical elastic adjustment. Thus  $h, e$ , and  $f$ , rotate  $G$  around vertical and horizontal axes, respectively.

**60. Michelson's interferences.**—If the collimator,  $SL$ , is removed and replaced by a strong sodium flame provided with a condenser, Michelson's interferences will appear at  $T$  when the instrument is in adjustment. It is rather surprising that, even in case of a film grating adjusted as above, they are well-defined circles covering the whole field of the telescope. If the collimator  $SL$  is retained and the sodium light introduced from the side by aid of a reflecting mirror, placed between the grating  $G$  and the collimating lens  $L$ , both interferences may be observed at the same time in corresponding telescopes. The mirror introducing the homogeneous light should in such a case be provided with a clear space (silver removed), through which the white beam,  $SL$ , may pass without obstruction. In a vertical plane the interferences have the same size and character at the sodium line. Horizontally the spectrum interferences vary with the dispersion.

If an apparatus constructed of gas-pipe is employed, however, it is far too frail for the practical use of the Michelson interferences. Vibrations within the apparatus are excited on merely touching it. For the purpose of displacement interferometry, however, such an apparatus is quite adequate; for the measurements are taken when the tremors have vanished.

**61. Film grating. Another adjustment.**—The supernumerary spectra may be gotten rid of altogether by using the method shown in figure 80. Here the impinging vertical sheet of white light,  $L$ , from the collimator, falls upon the clear or unruled part  $p$  of the plate of the grating, the film extending out as far as shown at  $G$ . If  $M$  and  $N$  are the opaque mirrors, the reflected rays  $a$  and  $b$  passing  $G$  are additionally reflected into  $a'$  and  $b'$ , and thence, after leaving the grating, into  $c$  and  $d$ . As both of the latter pass through the film, both produce spectra; but  $b'$  and  $e$  may be blotted out by a screen at the mirror  $N$ . This leaves only  $d$  beyond the grating. Again, the transmitted ray from  $L$ , after reflection at  $M$ , is again reflected into  $c$  and  $d'$ , which is made coincident with  $d$ . But  $c$ , being reflected from the unruled side, has no spectrum. Thus the spectra due to the two rays  $d$  alone interfere.

Had the grating been reversed, *caet. par.*, then the ray  $c$  would have produced the strongest spectrum, and superposed on the other two it would have greatly diminished the clearness.

In the telescope, whereas the ray  $a'$  prolonged is white, the ray  $d'$  from  $M$  and reflected from the film is strongly azure blue, due to regularly scattered light. This blue image is apt to be less sharp, unless very flat parts of the film are found. The two spectra, however, are good and the interferences satisfactory. The sodium line is sufficiently indicated, though, like the blue image, not quite sharp.

This method of using the unruled edge of the plate of the grating for reflection is, of course, equally applicable and advantageous in the case of the ruled grating. Only the two interfering spectra and no diffused light are present in the field of the telescope, and if sunlight is used the Fraunhofer lines are beautifully sharp.

**62. Equations.**—The equations for  $N_c/e$ , for normal incidence  $I=R=0$ , takes its simplest form as

$$(1) \quad N_c/e = \mu - \lambda d\mu/d\lambda = A + 3B/\lambda^2, \text{ nearly}$$

where  $N_c$  is the coördinate of the center of a given ellipse on the micrometer  $M$ , for the thickness of glass grating  $e$ , index of refraction  $\mu$ , and color of wavelength  $\lambda$ .

Hence if two different wave-lengths,  $\lambda$  and  $\lambda'$ , are in question ( $\delta$  refers to differences),

$$(2) \quad \delta N_c/e = \delta\mu - \delta \frac{d\mu}{d\lambda} \lambda$$

$\delta N_c$  being the displacement of the micrometer to pass the center of ellipses from line  $\lambda$  to line  $\lambda'$ .

If  $\mu = A + B/\lambda^2$  and  $\lambda d\mu/d\lambda = -2B/\lambda^2$ , then

$$(3) \quad \delta N_c = 3eB \left( \frac{1}{\lambda^2} - \frac{1}{\lambda'^2} \right)$$

from which  $B$  may be obtained without further measurements. If greater approximation is necessary, so that two constants,  $B$  and  $C$ , enter the dispersion equation,

$$(4) \quad \delta N_c = 3eB \left( \frac{1}{\lambda^2} - \frac{1}{\lambda'^2} \right) + 5eC \left( \frac{1}{\lambda^4} - \frac{1}{\lambda'^4} \right)$$

so that observations at three spectrum lines,  $\lambda$ ,  $\lambda'$ ,  $\lambda''$ , would be necessary.

The amount of displacement corresponding to the thickness  $e$  of glass is, at a given spectrum line  $\lambda$ ,

$$\Delta N_c = e \left( \mu - 1 - \lambda \frac{d\mu}{d\lambda} \right) = e(\mu - 1) + \frac{2Be}{\lambda^2} = e(A - 1) + \frac{3Be}{\lambda^2}$$

where  $2B/\lambda^2$  is constant for all values of  $e$ , or

$$A = \frac{\Delta N_c}{e} - \frac{3B}{\lambda^2} + 1 \quad \mu = \frac{\Delta N_c}{e} - \frac{2B}{\lambda^2} + 1$$

It is therefore not possible to obviate the term in  $B$ , determined as shown, if  $\mu$  is to be measured.

If equal distances are cut off at  $M$  and  $N$ , the interference pattern, of course, remains stationary in the spectrum. It is interesting to inquire to what degree this may be guaranteed. Equation (3) is available for the purpose, and, since  $\lambda$  and  $\lambda'$  are nearly the same,  $\lambda' - \lambda = \delta\lambda$  and

$$\delta N_c = 3eB \frac{2d\lambda}{\lambda^3} = \frac{6eB}{\lambda^3} d\lambda$$

Let  $\delta\lambda$  be the width of the sodium lines:

$$\delta\lambda = 6 \times 10^{-8} \text{ cm.} \quad \lambda = 59 \times 10^{-6} \text{ cm.} \quad e = 0.68 \text{ cm.} \quad B = 4.6 \times 10^{-11}$$

data for the above grating and sodium light. Hence

$$\delta N_c = \frac{6 \times 0.68 \times 4.6 \times 10^{-11} \times 6 \times 10^{-8}}{(59)^3 \times 10^{-18}} = 5.5 \times 10^{-5} \text{ cm.}$$

*i.e.*, about a half of  $10^{-4}$  cm. This would be equivalent to the space on a grating with about 20,000 lines to the centimeter, or 50,000 to the inch. The ellipses can not be set as closely as this, but the order of sensitiveness is within that of a good micrometer.

It is interesting to inquire whether the sensitiveness will change markedly for larger angles of incidence  $I$ . If  $\mu$  is the index of refraction, the largest angle  $R$  obtainable at grazing incidence,  $I = 90^\circ$ , would be  $\sin R = 1/\mu$ . It may then be shown that

$$\frac{dN_c}{d\lambda} = \frac{2eB}{\lambda^3} \frac{2B/\lambda^2(\mu^2 - 1) + 3\mu}{\sqrt{\mu^2 - 1}}$$

Putting  $\mu = 1.5$  and the other data as above, where  $d\lambda = 6 \times 10^{-8}$  cm.,

$$dN_c = \frac{1.34 \times 4.6 \times 10^{-11}}{(59)^3 \times 10^{-18}} \frac{9.2 \times 10^{-11} / (59)^2 \times 10^{-12} + 4.5}{1.12} = 7.7 \times 10^{-5} \text{ cm.}$$

The datum is of the same order as above, so that the sensitiveness changes but very little for different angles of incidence. Thus there is no disadvantage in using  $I = 0$ .

## CHAPTER IX.

### THE USE OF COMPENSATORS, BOUNDED BY CURVED SURFACES, IN DISPLACEMENT INTERFEROMETRY.

**63. Introduction.**—The method of increasing the sensitiveness of the displacement interferometer by increasing the dispersion of the grating readily suggests itself, but unfortunately the interference pattern loses sharpness in the same ratio and ultimately becomes too diffuse for practical purposes. Similar sensitiveness is secured when the air-paths and the glass-paths of the component beams of light are respectively identical, with the same inadequacy in the huge mobile figures, for the purpose of adjustment. In fact, if for simplicity we consider the incidence normal ( $I=R=0$ , linear interferometer), the sensitiveness becomes

$$d\theta/dn = \lambda^2 / [2eD \cos \theta \cdot ((\mu + 2b/\lambda^2) - N)]$$

where  $\theta$  is the angle of diffraction for the wave-length  $\lambda$ ,  $e$  the thickness of the plate of the grating,  $\mu$  its index of refraction,  $D$  the grating space,  $n$  the order of the fringe, and  $b$ ,  $N$ , constants. Hence, other things being equal,  $d\theta/dn$  increases as  $D$  and  $e$  grow smaller, where  $e=0$  is obtained by a compensator counteracting the thickness of the plate of the grating.

It occurred to me that the difficulty of diffuse interference patterns might be overcome, in part, by the use of compensators with curved faces, when the case would become similar to the conversion of the usual interference colors of thin plates into Newton's rings. Naturally a cylindrical lens with its elements normal to the slit is chiefly in question, though an ordinary lens also presents cases of interest, chiefly because of the easy conversion of elliptic into hyperbolic patterns, and the lens is more easily obtained.

Other methods were tried. For instance, on using a Fresnel biprism with its blunt edge normal to the slit, two sets of interference patterns, one above the other in the spectrum, are obtained. When the blunt edge is parallel to the slit, either side of the prism gives its own interferences, but they can not be made clearly visible at the same time. A doubly reflecting plate or a *thin* sheet of mica covering one half of the beam will produce two intersecting patterns, but these also are of little use for measurement.

**64. Lens systems.**—If but a single compensator is to be used, *i.e.*, compensation in one of the component beams only, the lens in question must be of very small focal power; otherwise the adjustment will be impossible, as the two direct images of the slit will be in very different focal planes. Moreover, the focal power should be variable. All this makes it necessary to use a *doublet*, preferably consisting of lenses of the same focal power, respectively convex and concave. If these lenses are themselves weak, say 1 meter in focal distance, both slit images may easily be seen in the telescope and be

sufficiently sharp for adjustment. If the lens first struck by light is convex and the second concave, their focal distances  $f_1$  and  $f_2$ , respectively, and their distances apart  $D$ , the focal power  $1/F$  of the combination used is

$$(1) \quad D/f_1f_2 = D/f^2$$

since  $f_1=f_2=f$ . The position of the equivalent lens is  $d=DF/f_1=f_2=f$ .  $D$ ,  $d$  are both measured from the second or concave lens to the convex lens, and  $D$  would always be smaller than  $f$ . If the lens system is reversed,  $F$  remains the same as before for the same  $D$ , the system being again convex, but  $d$  is reversed. The equivalent lens again lies toward the convex side of the system. In other words, the equivalent lens generally lies on the same side of the doublet as the convex lens.

In the actual experiment, however, the rays go through the lens system twice. In this case it is perhaps best to compute the distances directly. Of the two adjustments, the one with the concave lens toward the grating and the convex lens toward the mirror has much the greater range of focus relative to the displacement  $D$ . Supposing the mirror appreciably in contact with a convex lens, therefore, if  $b$  is its principal focal distance measured from the concave lens,  $b+D=M$  its principal focal distance from the convex lens or mirror,

$$(2) \quad \frac{1}{b} = \frac{2/f_2 - 1/(f_1+D)}{1 - D(2/f_2 - 1/(f_1+D))} - \frac{1}{f_1}$$

where  $f_1$  is the (numerical) focal distance of the concave and  $f_2$  that of the convex lens. If we now write

$$(3) \quad b = B(1 - D(2/f_2 - 1/(f_1+D)))$$

equation (2) is easily converted into

$$(4) \quad \frac{1}{2B} = \frac{1}{f_2} - \frac{1}{f_1} + \frac{D}{f_1f_2}$$

so that the usual value of the principal focal distance has been halved relatively to the new position of the equivalent lens. If, as in the present case,  $f_1=f_2=f$

$$2B = f^2/D \quad b = \frac{f}{2D} \frac{f^2 - 2D^2}{f+D} \quad M = b+D = \frac{f^3 + 2D^3}{2D(f+D)}$$

The following table shows roughly the corresponding values of  $D$  and  $M$  in centimeters:

| $D$ | $M=C+D$ | $2B$ | $d$ |
|-----|---------|------|-----|
| 2   | 2450    | 2500 | 49  |
| 5   | 950     | 1000 | 47  |
| 10  | 455     | 500  | 45  |
| 15  | 292     | 333  | 41  |
| 20  | 212     | 250  | 38  |
| 25  | 165     | 200  | 35  |

As  $b$  is smaller than  $B$  by equation (3), the equivalent lens is on the side of the convex lens and at a distance

$$B - M = (f^2 - 2D^2) / 2(f + D)$$

behind the mirror, or

$$B - b = f(f + 2D) / 2(f + D)$$

behind the concave lens.

If the system is reversed,  $f_1$  and  $f_2$  are to be replaced by  $-f_1$  and  $-f_2$ , whereas  $D$  remains positive. Thus the equations become successively

$$\frac{1}{b} = \frac{1/(f_1 - D) - 2/f_2}{1 - D(1/(f_1 - D) - 2/f_2)} + \frac{1}{f_1}$$

$$b = B(1 - D(1/(f_1 - D) - 2/f_2))$$

$$\frac{1}{B} = -\frac{2}{f_2} + \frac{1}{f_1} + \frac{2D}{f_1 f_2}$$

If  $f_1 = f_2 = f$ , then

$$B = f^2 / 2D \qquad b = \frac{f}{2D} \frac{f^2 - 2D^2}{f - D} \qquad M = b + D = \frac{1}{2} \frac{f^2 + 2D^2}{D(f + D)}$$

$$B'' - b = -\frac{f}{2} \frac{f - 2D}{f - D} \qquad B'' - M = -\frac{1}{2} \frac{f^2 - 2D^2}{f - D}$$

Hence the equivalent lens has the same focal distance as before, but it is now placed in front of the system, at a greater distance than it was formerly behind it. Measured from the mirror (mirror distances,  $M$ ) the data (in millimeters) are roughly as follows:

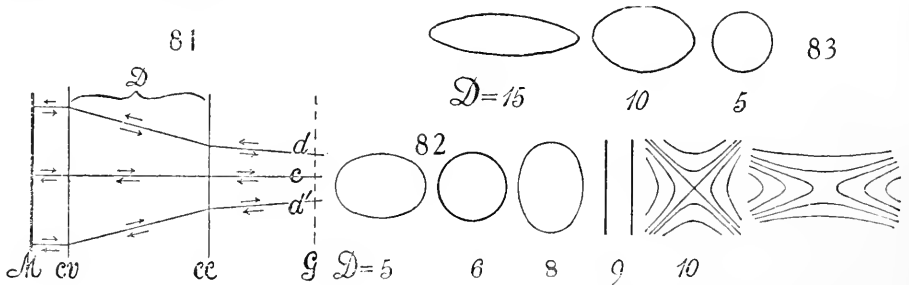
| $D$ | $2B$ | $B - M$ |
|-----|------|---------|
| 2   | 2500 | -51     |
| 5   | 1000 | -52     |
| 10  | 500  | -54     |
| 15  | 333  | -56     |
| 20  | 250  | -57     |
| 25  | 200  | -58     |

The total displacement of the equivalent lens on reversal is about 1 meter, falling off to 96 cm. in the extreme case. The image is larger if the convex lens is nearer the grating and the concave lens nearer the mirror.

**65. Effective thickness of the lenticular compensator.**—The compensator with curved faces may change the interference pattern in two ways; viz, by changing the angle of incidence and refraction of the rays at the grating, and by changing the path-difference of successive rays passing through it. Both conditions are virtually the same, or at least occur simultaneously. If there is but one compensator, as above, the two effects must be small, since the rays reflected from each of the opaque mirrors,  $M$  and  $N$ , of the interferometer, must eventually enter the telescope, to unite in two nearly identical images of the slit. It was rather unexpected to observe that the interferences are still obtained, even when the two slit images are quite appreciably different in size, but they are then confined to a single plane, as will be shown in § 69.

Since the beam of light coming out of the collimator and traversing the grating is a vertical ribbon of light, several centimeters high vertically, but very thin in comparison (a few millimeters) horizontally, it is relative to the vertical plane that the marked effect must be expected. In figure 81,  $G$  is the grating,  $cc$  the principal plane of the concave,  $cv$  that of the convex lens,  $M$  the opaque mirror. If the beam consists merely of the axial pencil  $c$ , the distorting effect due to the introduction of the lens doublet is slight for any value of their distance apart,  $D$ . The two lenses are practically equivalent to a plate. If a broad beam  $dd$  is in question and the rays retrace their path, the same is still true. But if, on changing  $D$ , the rays do not retrace their path, so that the equivalent lens is convergent or divergent, then the rays after leaving  $M$  re-impinge on the grating at different angles than before and the interference pattern is correspondingly changed, principally in its vertical relations.

Thus it is the lens system which changes the obliquity of rays lying in a vertical plane and passing through the grating, to the effect that the axial rays may represent a case of either maximum or minimum path-difference. The latter will be the case when the divergent pencil which usually traverses the grating becomes convergent in consequence of a sufficiently large value of the  $D$  of the lens system.



**66. Observations largely with weak lenses and short interferometer.**—The film grating used (Wallace, 14,500 lines to the inch) was cemented with canada balsam to a thick piece of plate glass, so that the total thickness of plate at the grating was 1,734 cm. This introduces a large excess of path in one of the component beams; but it is generally necessary, if the stationary interferences, due to the reflection at the two faces of the plate of the grating, are to be obviated and if the ellipses produced are to be reasonably large for adjustment (cf. § 69). The lens doublet was to be added on the same side as the glass specified, so that the excess of glass thickness on one side was further increased by about 0.19 cm., on the average. Under these circumstances the ellipses were strong, but (in view of the large dispersion) with inconveniently long horizontal axes.

On inserting the doublet (convex and concave lens, each 1 meter in focal distance) with its concave lens at the mirror and gradually increasing the distance  $D$  by moving the convex lens toward the grating, a series of forms

was obtained which passed from the initial horizontally long ellipse, through circles, vertically long ellipses, vertical lines, into hyperbolic forms of increasing eccentricity, as recorded in figure 82.

On reversing the system, keeping the convex lens fixed near the mirror and increasing the distance  $D$  by moving the other lens toward the grating, the original ellipse usually flattened out further, as shown in figure 83. Moving the lenses sideways parallel to themselves had no definite effect; moving them fore and aft together ( $D$  constant) produced results similar to the above. The vertical lines of figure 82 are liable to be sinuous or to resemble the grain of wood around a knot. In case of figure 82, as the equivalent lens lies in front of the mirror, the rays reaching the grating are thus necessarily converging. In figure 83 the equivalent lens lies behind the mirror, so that the rays at the grating are more convergent. Both positions furnish essentially convergent rays.

If corresponding to figure 82, the convex lens is kept fixed near the grating and the concave lens gradually moved up to it, the order of forms is reversed, but not quite completely. They usually terminate in long, vertical ellipses, before reaching which the wood-grained forms are sometimes passed. The same is similarly true for the case of figure 83.

With cylindrical lenses (respectively convex and concave, each 1 meter in focal distance) very little effect was observed when the axes of the cylinders were parallel to the slit. With the axes perpendicular to the slit, the effects of spherical lenses were virtually reproduced, except that the central fields partook of a more rectangular character.

To carry out the purposes of the present paper with strong lenses, respectively convex and concave, the vertical sheet of light from the slit must be diverged into a wedge by the concave lens and then collimated by the convex lens. The mirror, normal to the rays, reflects them, so that they retrace their path and become a sheet of light before the final reflection and diffraction at the grating. The following experiments were made with strong lenses:

At first lenses of double the preceding focal power,  $f = \pm 50$  cm., were tried, but with no essential difference in the results. Thereupon strong lenses of focal distances  $f_1 = -73$  cm. and  $f_2 = 13.1$  cm. were used together, the convex lens being, as usual, near the mirror. For  $D = 7.5$  cm., about, these gave fairly clear images of the slit and it was easy to find the ellipses, which were now very eccentric, almost spindle-shaped in form. They could be obtained strong and clear without difficulty, and the nearly horizontal lines filled the whole spectrum. Reversal of lenses practically failed to give results, the rays after reflection being too divergent.

On the large interferometer, where the distances between mirror and grating are nearly 2 meters, adjustment was more difficult and the result (if parallel rays are retained) less satisfactory, because the slit images are not in focus at the same time. This is particularly the case when the convex lens is nearest the mirror and the concave lens toward the grating. Thus when  $f = \pm 100$  cm. and  $D = 15$  cm., the modified slit image may be twice as large as the other and

the interferences in the principal focal plane of the telescope are only just seen. At  $D = 5$  cm., however, the results are acceptable. When the concave lens is nearest to the mirror and the convex lens toward the grating, the modified slit image is smaller than the other. Adjustment is then easier and the usual elliptic and hyperbolic forms may be observed without trouble. In both cases the flickering of the arc lamp used passes the rays through different parts of the lenses relatively to the center, and the adjustment is thus easily destroyed.

If the spectra from  $M$  and  $N$ , however, are observed, not in the principal focal plane but in advance of it (toward the eye), interferences of great interest will be observed, to be discussed in § 69.

**67. Remarks.**—A few explanatory observations may here be inserted. The occurrence of the elliptic or oval and the hyperbolic type of fringes may be most easily exhibited by laying off the order of the fringe in terms of the distance (in arbitrary units) above and below the center of the image of the slit. If we call the latter  $y$  and consider the allied colors of thin plates, for instance,

$$n = 2e\mu \cos r/\lambda \text{ or more generally } n = (e\mu/\lambda)f(y, r)$$

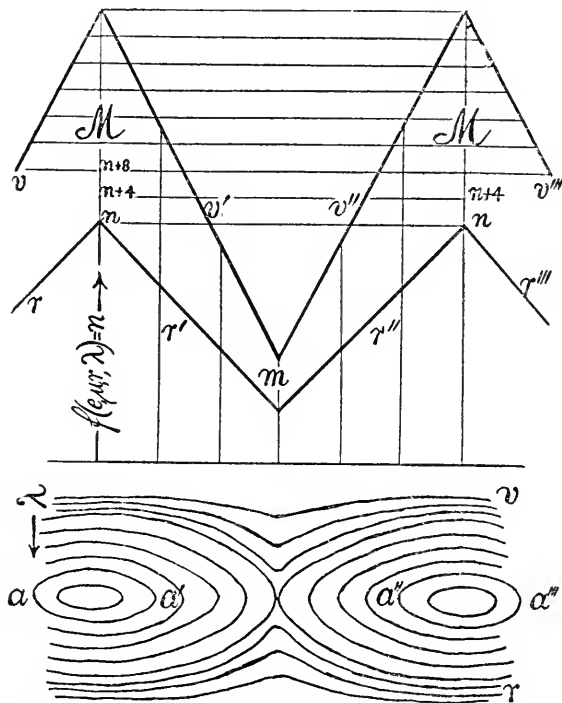
(where  $e$  is the thickness of the plate,  $\mu$  its index of refraction,  $\lambda$  the wave-length of light in case of a dark locus of the order  $n$ ) is to be expressed in terms of  $y$ , which itself determines  $e \cos r$ ,  $r$  being the angle of refraction in the plate of the grating. The phenomenon will thus be coarser for red light than for violet light, since  $\mu$  decreases when  $\lambda$  increases, and any two curves,  $r$  and  $v$ , figure 84, may be assumed as the loci of the equation in question. If, now, horizontal lines be drawn for  $n = 1, 2, 3$ , etc., they will determine the number of dark bands in the spectrum for any value of  $y$ .

If the central ray is also a line of symmetry and intersects the grating normally, it must correspond to a maximum or a minimum of  $n$ . These conditions are shown in the diagram at  $M$ , where the maximum number of bands occurs, and at  $m$ , where the reverse is true. The question is thus referred to two sets of loci,  $rr'$  and  $vv'$ , or  $r'r''$  and  $v'v''$ , etc. In the former case  $e \cos r$  varies with  $y$  in the same sense as  $\mu/\lambda$ ; in the latter in the opposite sense and is preponderating in amount. Both may vary at the same rates in the transitional case, in which, therefore, the two curves  $r$  and  $v$  are at the same distance apart for all values of  $y$ .

Suppose, furthermore, that the same phenomenon is exhibited in terms of wave-length  $\lambda$ , as in the lower part of the diagram, the spectrum being now equally wide for all values of  $y$ , while at any given  $y$  the upper diagram still shows the number of dark points (bands) between  $r$  and  $v$ . If now, we suppose that under any conditions these dark points are grouped symmetrically with reference to any given color (which is probable, for a maximum or a minimum of any value of  $y$  will be so for all values), and that the successive dark points have been connected by a curve, the interference pattern will be of the elliptic type in case of  $aa'$ ,  $a''a'''$ , and of the hyperbolic in the case of  $a'a''$ .

The other features of the phenomenon are secondary and therefore left out

of the diagram. Thus, for instance, the distance apart of the bands shrinks from red to violet, and the ovals, etc., are only appreciably symmetric, because they occupy so small a part of the spectrum. The horizontal distribution of dark bands around the center is determined by variations  $e \cos r$  and is not linear. Whether the long axes of the ellipses are horizontal or vertical depends



84

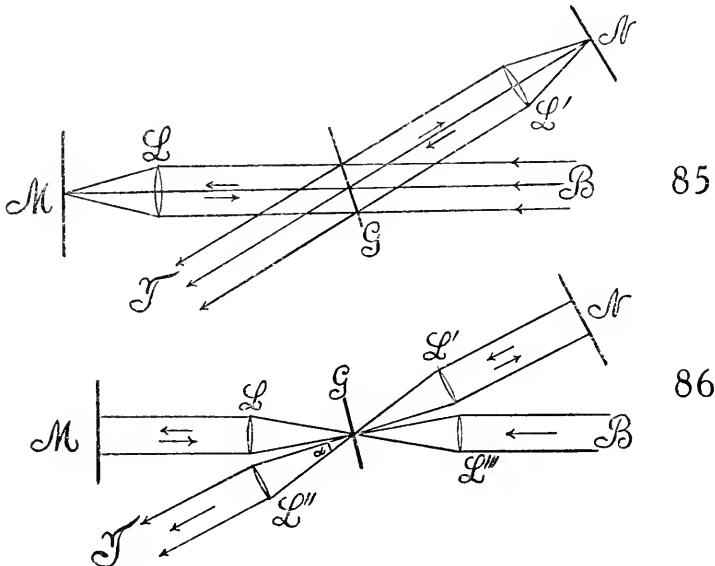
upon the slope of the lines  $r$  and  $v$ . Maxima and minima will not, as a rule, occur close together, though in certain wood-grain-shaped patterns this seems to be the case.

In conclusion, therefore, the main feature in modifying the type of interference pattern is the varying thickness of the compensator. For oval types the preponderating lens is convex; for the hyperbolic type it is concave. Neither of these lenses is here appreciably affected in modifying the horizontal distribution of path-difference, because the dispersion of the grating requires a horizontally parallel system of rays.

**68. Observation with lens systems on both sides.**—The method shown in plan in figure 85 ( $L$  and  $L'$  convex lenses,  $G$  grating,  $M$  and  $N$  mirrors, telescope at  $T$ ) was tested. The outcome can not at once be foreseen, since the focal distances for different colors is different and since slight displacements of either lens must greatly modify the interference pattern. The latter, however, as obtained in every case, proved to be exceedingly fine lines, tipping in the

usual way with the motion of the micrometer and indicating a center of ellipses very distant in the field of the spectrum. In other words, the interference pattern is no longer automatically centered and is therefore useless.

A modification of this plan is the method shown in figure 86 (horizontal section), where  $B$  is the beam from the collimator,  $L, L', L'', L'''$ , four condensing lenses of the same power ( $f = 50$  cm.),  $G$  the grating,  $M$  and  $N$  opaque plane mirrors,  $T$  the telescope. In all the above cases the horizontal rays from the collimator traverse the grating in parallel and eventually condense to a single point in the field of the telescope. The same is true of all rays having the same angle of altitude. These rays, therefore, act as a whole, since they pass through the plate of the grating at the same angle of incidence. On the other hand,



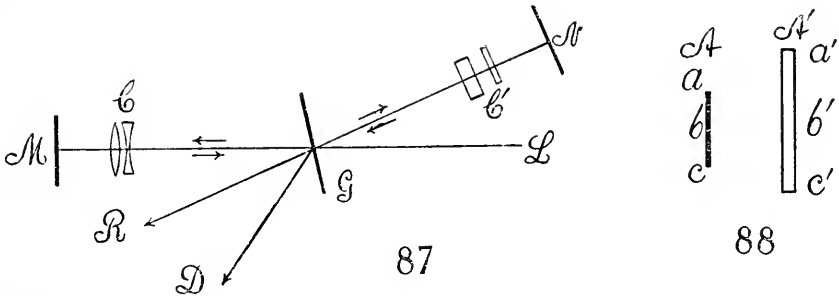
relative to a vertical plane, the rays traverse the grating at different angles, each angle corresponding to a horizontal strip of the spectrum. It is by the easy modification of this obliquity that the curved compensator becomes effective. In figure 86 the rays are also oblique relative to a horizontal plane; but the result, unfortunately, is not available, since each of these oblique rays must have its own complete spectrum. Consequently the diffracted pencil will consist of an infinite number of overlapping spectra, the extreme cases lying within the same angle  $\alpha$  shown in the figure. A large telescopic objective would then reunite these spectra into a white image of the slit, while a small objective will show colored slit images, passing from impure red to impure violet. Naturally, the interferences will also overlap, and therefore vanish.

**69. Telescopic interferences.**—If interference patterns of small angular extent are to be obtained, it is essential that the rate at which obliquity increases from ray to ray be made as large as practicable. Probably, therefore,

an opportunity for realizing these conditions will be found within the telescope; *i.e.*, after the rays pass the objective. The endeavor would therefore be directed to bringing two spectra, focussed in two planes, one of which is behind the other and consequently of different sizes, both vertically and horizontally, to eventual interference.

The experiment was made on the long interferometer (fig. 87), the distances between mirror *M* and grating *G* and from the latter to the mirror *N* being nearly 2 meters each. *C* is the lenticular compensator, consisting of two lenses, respectively concave and convex, each having the same focal distance,  $f = \pm 50$  cm. The distances apart, *D*, of the lenses may be varied. The glass plate *C'*, which is revolvable about the vertical, is thick enough to exactly counterbalance, if necessary, the thickness of the glass plate of the grating and of the lens system *C*. A sharp wedge sliding transversely may also be used. It is best to replace *C'* by two plates of glass, one thick and the other thin, so that the latter may be removed.

The telescope directed along the axis *R* will therefore, in general, see two white slit images, *A* and *A'* (fig. 88), not both in focus at once, *A'* coming from



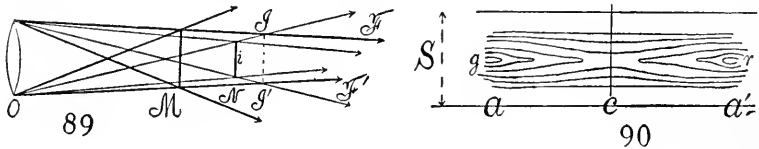
*M* being larger, *A* from *N* (parallel rays) smaller. The focal plane of *A'* will be towards the grating as compared with *A*, and *A'* is larger than *A*, in proportion as the distance apart of the lenses *C* is larger. Similarly, the two spectra are observed along the diffraction axis, *D*, not in focus at once and of different areas.

To obtain the interferences the slit image *A* must be placed anywhere within *A'*, and they will occur at the top of the spectrum if *a* and *a'* are vertically in coincidence; in the middle if *b* and *b'* coincide, etc.

The plane of the new interferences is no longer the principal focal plane, containing the Fraunhofer lines, but lies in front of it; *i.e.*, towards the eye of the observer and away from the grating. This distance, measured along *D* for the given small telescope used, was fully 1 cm. The focal planes of the two spectra are usually not so far apart. *A'* corresponds to a virtual object behind the observer.

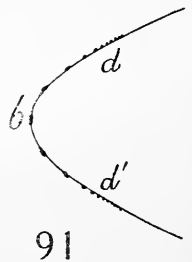
If the vertical plane in which the interferences lie be taken as the image, the object would be situated about 3 meters beyond the objective of the telescope used. This would place it 30 cm. in front of the mirror *M* or *N*, where there is but a single beam in each case. In fact, the telescope may be brought quite

up to the grating. Hence interference is produced in the telescope itself, where rays are relatively very divergent, a condition which accounts for the smallness of the interference pattern. This understanding of the case is tentatively shown in figure 89, where  $O$  is the objective of the telescope,  $M$  the larger image from the mirror with the lens compensator, and  $N$  the image from the other mirror (parallel rays). If the corresponding rays be drawn through the extremity of  $M$  and  $N$ , their fields of interference,  $F$  and  $F'$ , would begin in the plane  $I$  and  $I'$ . For axial rays it would be at  $i$ . Thus the locus as a whole would not be a plane, and this seems to be the case. If the telescope moves toward the grating,  $II'$  moves toward the right in the figure, as though the virtual object beyond the grating were fixed in position. At all events, the problem is to find the interference diagram of two symmetrical plane parallel spectra, of different areas and placed at definite distances apart.



The appearance of the fringes is indicated in figure 90, where  $S$  is the height of the spectrum, usually quite out of focus. There are many more lines than could be drawn in the sketch. The ends  $a$  and  $a'$  seem to surround small ellipses, but these are not quite closed on the outer edge. The center of symmetry is at  $C$ . The demarcations are stronger and broader vertically if the distance apart of the lenses  $C$  (fig. 87) is small; fainter, but nevertheless clear and narrower, if this distance is large. Horizontally the fine lines thread the spectrum. The best results were obtained when the lenses  $C$  are less than 1 cm. apart, the middle band being about half as high as the spectrum. Two contiguous lenses gave a design which nearly filled the spectrum vertically. For practical purposes the lens compensator  $C$  is to be attached to the mirror  $M$ , just in front of and moving with it. It makes little difference here whether the concave lens or the convex lens of the doublet  $C$  is foremost.

If the micrometer  $M$  is moved, or if the telescope is slid to the right or left, or forward, so as to take in other parts of the spectrum, the nearly closed lines at  $a$  and  $a'$  become finer and finer crescent-shaped lines, always open outward, till they pass beyond the range of vision. The whole phenomenon remains on the same level of the spectrum. On moving the telescope forward as far as  $G$  (fig. 87), the ocular has to be drawn outward (towards the eye) till it is fully 2 cm. beyond the position of the principal focal plane. The whole spectrum is now seen with the interferences from red to violet (no ellipses), but having the same relative position as before. The central horizontal band measures about one-fifth the height of the spectrum, while the fine parallel horizontal lines extend to the upper and lower edges. The



appearance is now curiously like a blunt wedge (fig. 91), with a band at  $b$  nearest the eye, and the lines  $dd$  extending quite to the rear. This impression is probably an illusion, due to the shading; the lines grow finer and are more crowded toward the bottom and top of the spectrum. The illusion of a reëntrant wedge is not possible.

To use this interference pattern for measurement, the cross-hair is supposed to pass through the region  $c$  (fig. 90) symmetrically. Very slight motion of the micrometer mirror  $M$  then throws  $c$  either to the right or the left of the cross-hair. In this case the lens doublet,  $C$ , is attached to the mirror and moves with it, as stated. To obtain the extreme of sensitiveness, the path-difference of  $NG$  and  $GM$  must be all but zero; *i.e.*, the grating plate  $G$  and the lens doublet  $C$  (fig. 87) must be all but compensated for equal air-distances by the compensator  $C'$ . In this case of full compensation, the interference pattern, in the absence of a doublet  $C$ , would be enormous and diffuse, seen preferably in the principal plane of the telescope, but useless for measurement. The introduction of a lenticular compensator, balanced by a compensator in  $GN$ , transforms the huge pattern into the small interference fringes in question, with the advantage that the high mobility of the coarse design has been retained. In other words, an index suitable for adjustment has been found, compatible with extreme sensitiveness. In fact, it is difficult to place the micrometer mirror  $M$  so that the region  $c$  (fig. 90) is exactly bisected. As the plane in which these interferences are seen most distinctly is 1 cm. or more anterior to the principal focal plane, the Fraunhofer lines are unfortunately blurred and a cross-hair is needed as a line of reference.

I may in conclusion refer to a similar series of experiments now in progress, in which the compensators placed in the  $M$  and  $N$  pencils (fig. 87,  $C$ ,  $C'$ ), instead of being of different shapes as above, are plates of different kinds of glass (crown and flint, for instance). Here the successive differences of dispersive power, from wave-length to wave-length, produce effects closely resembling those discussed, with the advantage that difficulties inherent in the curved system are avoided.

# CHAPTER X.

## THE DISPERSION OF AIR.

**70. Introduction.**—In view of the long-armed interferometer available, it seemed interesting to test the refraction of air at different wave-lengths,  $\lambda$ . An iron tube of inch gas-pipe, 138 cm. long, was therefore placed in one or the other of the component beams. The tube was closed at both ends by glass plates, about one-eighth of an inch thick, kept in place with resinous cement. A lateral tube communicated with an air-pump and drying train, so that the tube could be alternately exhausted and refilled with air. By using sunlight, the different lines of the spectrum were obtained with sufficient clearness, and the method consisted in finding the reading of the micrometer for successive Fraunhofer lines, both for the case of a plenum of air and for a vacuum. If  $\Delta N$  is the (monochromatic) displacement of micrometer corresponding to the latter difference of pressure,  $\mu$  being the index of refraction of air,  $e$  the thickness,

$$(1) \quad \Delta N_{\lambda} = e \left( \mu_{\lambda} - 1 - \lambda \frac{\partial \mu_{\lambda}}{\partial \lambda} \right)$$

To determine  $\mu_{\lambda}$ , we must know  $\partial \mu_{\lambda} / \partial \lambda$ . It has been omitted above, because it enters differentially and because of its small value. It appears as a constant decrement of  $\Delta N_{\lambda}$ , as  $\lambda$  is constant and  $\partial \mu_{\lambda} / \partial \lambda$  is negative. In the present case, where  $\mu$  is actually to be measured,  $\partial \mu_{\lambda} / \partial \lambda$  enters directly and is essential; but it follows from any two experiments when  $\mu$  is found for different colors.

TABLE 8.—Values of  $B$ . Inch iron gas-pipe, 138.0 cm. long.  $D$  line.

| $t$<br>Bar   | $p$       | $10^3 \Delta N$   |
|--|-----------|---|
| $\left. \begin{array}{l} 22.0^{\circ} \\ 76.20 \\ 20^{\circ} \end{array} \right\}$ | 75.0      | 38.0  |
| $\left. \begin{array}{l} 22.3^{\circ} \\ 75.83 \\ 20^{\circ} \end{array} \right\}$ | 74.5      | $\left. \begin{array}{l} 37.9 \\ 37.7 \\ 37.6 \\ 37.9 \\ 37.7 \\ 37.6 \\ 37.6 \\ 37.7 \\ 37.5 \\ 37.7 \end{array} \right\}$ |
| Mean . . . . .   | . . . . . | 37.69   |

**71. Observations with arc lamp.**—In table 8 results are given as obtained with the electric arc, in which the sodium line usually appears with sufficient distinctness in the spectrum to be available as a line of reference for measure-

ment. Disregarding earlier results, the following are mean values of the ten independent data for  $\Delta N$  (each comprising a reading for vacuum and for plenum):

$$10^6\lambda = 58.9 \text{ cm.} \quad t = 22.3^\circ \quad p = 74.5 \text{ cm.} \quad 10^3\Delta N_D = 37.69 \text{ cm.} \quad l = 138.0 \text{ cm.}$$

Thus

$$(2) \quad \mu - 1 = \frac{\Delta N}{e} + \frac{\lambda \partial \mu}{\partial \lambda} = (\mu_0 - 1) \frac{p}{76} \frac{273}{\tau}$$

where  $\mu_0$  refers to normal pressure and absolute temperature ( $\tau$ ). If  $\mu_0$  is given for the  $D$  line,  $\partial \mu / \partial \lambda$  is determinable. It will be sufficient for the present purposes to put  $\mu_0 = A + B/\lambda^2$ , or  $\lambda. \partial \mu / \partial \lambda = -2B/\lambda^2$

$$(3) \quad \frac{\Delta N}{e} - (\mu_0 - 1) \frac{p}{76} \frac{273}{\tau} = \frac{2B}{\lambda^2}$$

$B$  referring to  $\tau$  and  $p$ . Mascart's\* value for  $\mu_0 - 1$  (agreeing with Fabry's) is  $10^{-6} \times 292.7$ , whence

$$B = 10^{-14} \times 1.34 \text{ at } \tau \text{ and } p$$

If the value  $B$  be computed from Mascart's observations between  $C$  and  $E$ ,  $D$  and  $F$ , respectively,

$$B_{CE} = \frac{2.1 \times 10^{-6}}{1.28 \times 10^{-8}} = 1.64 \times 10^{-14} \quad B_{DF} = \frac{2.3 \times 10^{-6}}{1.39 \times 10^{-8}} = 1.65 \times 10^{-14}$$

so that the mean value  $10^{14}B = 1.65$  may be taken. Since the last decimals of  $\mu$  are in question, it will not be correct to more than 5 to 10 per cent.

The value found above ( $10^{14}B = 1.34$ ) is therefore somewhat too small. True, since from equation (3)

$$(4) \quad \frac{\partial B}{\partial(\Delta N)} = 10^{-14} \times 1260$$

an error of  $10^{-4}$  cm. in  $\Delta N$  is an error of  $0.13 \times 10^{-14}$  or 10 per cent in  $B$ . Very close agreement can not therefore be expected in either result. One is tempted to refer the present low value of  $B$  to flexure of the glass end plates of the tube, which, when the tube is exhausted, become slightly saucer-shaped and introduce a sharp concentric wedge of glass into the component beam, whereby the interference pattern is changed, probably in the direction of smaller values, as found. But the direct experiments below do not show this. In any case, the measurement of  $B$  lies at the limits of the method. An advantage may possibly be secured by using two identical tubes, one in each component beam, the tubes to be exhausted alternately. The sensitiveness would then be doubled.

**72. Observations with sunlight. Single tube.**—These observations are given in table 9, the exhaustion throughout being 75 cm. and the temperature about  $16^\circ$ . In the first set sunlight was used without a condensing lens; in

\* See excellent summary in Landolt and Boernstein's Tables, 1905, p. 214.

the second set the sun was focussed with a weak lens (0.5 meter in focus) at the point formerly occupied by the electric arc. The spectrum (particularly in the second case) was brilliant and the lines clear. The focus of sunlight is to be placed just outside the focus of the collimator lens, in order that a nearly linear pencil may be available to penetrate the long refraction tube twice. The distance of the collimator lens to the grating was about 2 meters. The spectrum is then a bright band in the telescope, the width being limited by the height of the ruled part of the grating. The strip of white light on the grating should not be more than a few millimeters wide. It must therefore be narrowed by an opaque screen (wide slit of the given width) in the path of the beam (see fig. 92 below).

TABLE 9.—Dispersion of air. Tube  $l=138.0$  cm. Bar. 77.25 cm. at  $19.5^\circ$ .  $p=75.0$  cm

| Line.                                  | Temp.        | $10^3\Delta N$ | $10^{+14}B$ |
|--|--------------|----------------|-------------|
| <i>C</i>                               | $16.0^\circ$ | 38.5           | 1.5         |
| <i>D</i>                               | "            | 39.            |             |
| <i>b</i>                               | "            | 39.4           |             |
| <i>C</i>                               | $16.0^\circ$ | 38.5           | 1.4         |
| <i>D</i>                               | "            | 38.9           |             |
| <i>b</i>                               | "            | 39.3           |             |
| Improved seeing, weak condensing lens. |              |                |             |
| <i>C</i>                               | $16.4^\circ$ | 38.8           | 1.51        |
| <i>D</i>                               | "            | 39.2           |             |
| <i>C</i>                               | $16.4^\circ$ | 38.9           | 1.65        |
| <i>D</i>                               | "            | 39.1           |             |
| <i>b</i>                               | "            | ?39.3          |             |
| <i>F</i>                               | "            | 40.1           |             |
| <i>C</i>                               | $16.4^\circ$ | 38.8           | 1.61        |
| <i>F</i>                               | "            | 40.1           |             |

The equation for  $B$  in this case, if the symbol  $\delta$  refers to differences for two given values of  $\lambda$ , is

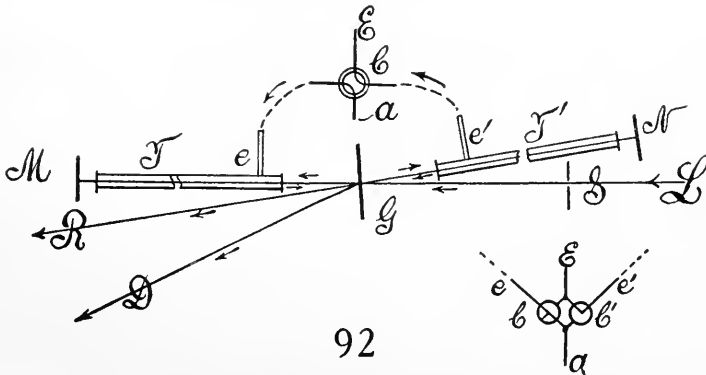
$$3B_0 = \frac{\delta\Delta N/e}{\delta \frac{1}{\lambda^2}} \frac{76}{p} \frac{\tau}{273}$$

if the value of  $B$  is to hold for normal conditions.

The data are shown in table 9, series 1 and 2 being obtained without condensing lens. These are inferior, as regards definition of lines, to the subsequent set, in which condensed sunlight was used. In all cases there is sometimes an irregularity (marked by ? in table 9) in which the observation is obviously discordant, but the reason could not be found. Possibly values of  $\tau$  and  $p$  taken were not the actual values. The data for  $B \times 10^{14}$  given in the table are mean values. Some of these are low. Later values, where the  $F$  line is included, come out larger, the range being from 1.3 to 1.8 or 1.5, on the average. It is desirable to use the whole of the available range of the spectrum (sufficiently luminous from  $C$  to  $F$ ) to obtain an acceptable value of the coefficient  $B$  and additionally to improve the method by using two

identical tubes, alternately exhausted as suggested above. The attempted *B* measurement is at the limits of the method, as has already been instanced in the discussion of errors in the preceding paragraph, and it is not to be concluded that data which happen to agree with Mascart's result from a correct application of the present method. In fact, there is no reason for excluding the exceptional values, and the present results are to be regarded as preliminary.

**73. Two (differential) refraction tubes.**—In the following experiments two identical iron tubes (138 cm. long, of inch gas-pipe) were installed, one being placed in each of the component beams of light, which subsequently interfered, and the tubes were exhausted alternately. There are apparently three advantages in this arrangement. In the first place, the sensitiveness is doubled; in the second, the flexure of glass plate should be the same at each tube, in each experiment, and thus fail to disturb the interference pattern. Furthermore, by using the tubes in parallel (*i.e.*, exhausting both at the same time), any irregularity of flexure effect, etc., should be determinable, as the air in both tubes will be identically circumstanced. Finally, the air being inclosed in a thick metallic envelope at both beams is not subject to incidental disturbances. An unexpected difficulty, however, was encountered; for there is reflection of direct spectra from the eight glass surfaces, and this must be specially met. The direct spectrum is easily eliminated by inclining the grating until the reflected interference spectra are at a different level; but reflections of this spectrum are not so easily dealt with. Fortunately they are weak. Even so, they are very annoying, as they overlap the interference pattern and dull it. They could be eliminated by attaching the glass plates obliquely to the axis of the pipes, but this remedy was not thought of at the outset.



92

Figure 92 is a diagram of the disposition of the parts of the apparatus. *L* is the beam of white sunlight from the collimator limited laterally by the wide slit ( $\frac{1}{8}$  inch) *S*. *G* is the grating, *T* and *T'* the two refraction tubes, *M* (micrometer) and *N* the opaque mirrors, *R* the refracted and *D* the diffracted (spectrum) beam of light. *C* is virtually a four-way stopcock (or two 3-way glass stopcocks) leading respectively to the exhaust pump *E* and dry

air supply  $A$ , from the tubulures  $e$  and  $e'$  of both refraction tubes  $T$  and  $T'$ . These are therefore alternately exhausted.

Preliminary results are given in table 10, the arc lamp with its sodium line being used in the absence of sunlight. It will be seen that  $\Delta N$ , apart from temperature (which is here higher than above), has been doubled. The deflections were symmetrical within  $0.15 \times 10^{-3}$  cm.

TABLE 10.—Dispersion of air. Differential tubes, each 138 cm. long.  $D$  line in electric arc.  $p=74$  cm.

| Barometer.       | Temp. | $10^3 \Delta N$ | $(\mu_0 - 1) \times 10^8$ | $B_0 \times 10^{14}$ |
|------------------|-------|-----------------|---------------------------|----------------------|
| 75.93 cm., 22°   | 21.5° | 75.4            | 291.6                     | 1.47                 |
|                  |       | 75.3            |                           |                      |
|                  |       | 75.4            |                           |                      |
| 76.02 cm., 19.5° | 18.0° | 76.3            | 291.8                     | 1.49                 |
|                  |       | 76.4            |                           |                      |
|                  |       | 76.4            |                           |                      |
| (Single tube)    | 23.0° | 37.8            | 293.6                     | 1.80                 |

The values of  $B$  found in the first two series of this table, if the standard value of  $\mu_0 - 1 = 0.0002927$  is assumed, is somewhat small, but as near to the true values as may be expected. Again, if  $B \times 10^{14} = 1.65$  is assumed, the  $\mu_0 - 1$  values given in the table are similarly small, being 0.3 per cent short of standard values. A single-tube experiment made for comparison (series 3), similarly, came out too large in each case. It follows from this that  $p$  and  $t$  observations are not sufficiently guaranteed. It is hardly probable, however, that with a micrometer reading to  $10^{-3}$  cm. and estimated to  $10^{-4}$  cm. (vernier) the precision can be much enhanced; for since

$$B_0 = \frac{\lambda^2 \Delta N}{2} \frac{76}{e} \frac{\tau}{273 p} (\mu_0 - 1)$$

$$\frac{\partial B_0}{\partial p} = -\frac{\lambda^2 \Delta N}{2} \frac{76}{e} \frac{\tau}{273 p^2} \quad \frac{\partial B_0}{\partial \tau} = \frac{\lambda^2 \Delta N}{2} \frac{76}{e} \frac{1}{273 p}$$

or at the  $C$  line and  $D$  lines, respectively,

$$\delta p = 1 \text{ cm.} \quad \delta B = 0 \begin{cases} 0.8 \times 10^{-14} \\ 0.7 \times 10^{-14} \end{cases} \quad \delta \tau = 1^\circ \quad \delta B_0 = \begin{cases} 0.2 \times 10^{-14} \\ 0.2 \times 10^{-14} \end{cases}$$

Now, unless the measurement can be made in terms of rings, it is difficult to detect a few millimeters of pressure difference by displacement only.

The interesting question now occurs whether the two tubes, if identical for a plenum of air, remain identical (no shift of the interference pattern) throughout all the stages of identical exhaustion. On trial, nothing could be detected, the fringes remaining stationary during the whole period of exhaustion, or during the influx of air following a high vacuum. Hence there is no perceptible difference effect of flexure of the glass ends, and the ultimate question of accuracy depends on the measurement of  $\tau$  and  $p$ . To eliminate the possible effect of flexure, an air column of negligible length, in which the glass effect only is present, will have to be tested; otherwise there is no possibility of separating the air and glass effect.

**74. Differential and single refraction tubes. Sunlight.**—The direct experiments for the coefficient  $B$  were now resumed and conducted with sunlight, with the results given in table 11. The first two series were made with the two identical tubes specified, exhausted alternately, one tube containing a plenum of air, while the other was nearly empty in each experiment. The  $C$  and  $F$  lines alone were used for measurement. In spite of the large displacement ( $\Delta N = 0.076$  to  $0.078$  cm.), the results were not as satisfactory as was expected, owing to the fact that sharpness of vision is made difficult by the stray reflected spectra to which reference has already been made. But the data for  $B$  obtained with one exception (No. 2 in the first series) are consistent and reasonably good. In every other respect the work was satisfactory and could have been improved by using oblique cover-glasses. The values of  $B$  obtained are therefore disconcerting.

TABLE 11.—Dispersion of air. First and second series, Differential Tubes, each 138.0 cm. long.  $C$  and  $F$  lines. Third and fourth series, Single Tube, good adjustment.

| Barom.         | $p$  | Line | $10^3\Delta N$ | $10^{14}B$ | Temp. | Barom.         | $p$  | Line | $10^3\Delta N$ | $10^{14}B$ | Temp. |
|----------------|------|------|----------------|------------|-------|----------------|------|------|----------------|------------|-------|
| 77.05 }<br>22° | 74.0 | C    | 76.4           | 1.0        | 17.4  | 77.22 }<br>21° | 74.0 | C    | 38.4           | 0.99       | 18.0  |
|                |      | F    | 78.0           | ....       | ....  |                |      | F    | 39.2           | ....       | ....  |
|                | 74.0 | C    | 76.1           | 1.3        | 17.4  |                | 74.0 | C    | 38.2           | 1.11       | 18.0  |
|                |      | F    | 78.2           | ....       | ....  |                |      | F    | 39.3           | ....       | ....  |
|                | 74.0 | C    | 76.3           | 1.1        | 17.4  |                | 74.0 | C    | 38.3           | 1.18       | 18.0  |
|                |      | F    | 78.0           | ....       | ....  |                |      | F    | 39.3           | ....       | ....  |
| 74.0           | C    | 76.2 | 1.1            | 17.4       | 74.0  | C              | 38.2 | 1.06 | 18.0           |            |       |
|                | F    | 78.0 | ....           | ....       |       | F              | 39.0 | .... | ....           |            |       |
| 76.27 }<br>23° | 74.0 | C    | 75.8           | 1.0        | 21.4  | 77.22 }<br>21° | 76.0 | C    | 39.3           | 0.99       | 18.1  |
|                |      | F    | 77.4           | ....       | ....  |                |      | F    | 40.1           | ....       | ....  |
|                | 74.0 | C    | 75.4           | 1.1        | 21.4  |                | 76.0 | C    | 39.2           | .99        | 18.1  |
|                |      | F    | 77.2           | ....       | ....  |                |      | F    | 40.0           | ....       | ....  |
|                | 74.0 | C    | 75.4           | 1.1        | 21.4  |                | 76.0 | C    | 39.0           | .99        | 18.2  |
|                |      | F    | 77.1           | ....       | ....  |                |      | F    | 40.0           | ....       | ....  |
|                |      |      |                |            |       | 76.0           | C    | 39.2 | .99            | 18.2       |       |
|                |      |      |                |            |       |                | F    | 40.0 | ....           | ....       |       |

I then went back to the single-tube experiments (in series 3 and 4), and these are the smoothest results obtained. The  $C$  and  $F$  lines were used as before. In the last series, for instance, the micrometer reading is the same to  $10^{-4}$  cm. throughout. In spite of this satisfactory behavior, the value of  $B$  obtained is again of the same low order, all the data, both for double and single tubes, being consistent throughout in this respect. Series 3 and 4 agree, although  $p$  is changed from 74 cm. to 76 cm. of mercury.

In table 12 I have summarized the data in comparison with the standard results, computing  $\mu_0 - 1$  and  $B_0$ , for each of the cases, reducing all values to  $0^\circ\text{C}$ . and 76 cm. of mercury. The difference of  $\mu_0 - 1$  for the  $F$  and  $C$  lines, which is  $3.2 \times 10^{-6}$  for the standard data, is but  $2.3 \times 10^{-6}$  on the average in the present results. Similarly, the mean values of the latter are  $10^{-6} \times 4.1$  and  $10^{-6} \times 3.2$  larger for the  $C$  and  $F$  lines, respectively, than the standard results.

These conditions are particularly puzzling, since in §73, with the use of the arc lamp, both results were nearly normal. I therefore endeavored to detect the causes for this difference of behavior.

TABLE 12.—Summary of Table 11. "St." refers to standard data.  $A = (\mu_0 - 1)$ .

| Line, etc.                           | $\lambda \times 10^6$ | St.<br>$10^6 A$ | Series.         |                 |                 |                 | Ser.<br>(1) to (4)<br>$B_0 \times 10^{14}$ | $(\mu_0 - 1)$ St.      |                        |
|--------------------------------------|-----------------------|-----------------|-----------------|-----------------|-----------------|-----------------|--|------------------------|------------------------|
|                                      |                       |                 | (1)<br>$10^6 A$ | (2)<br>$10^6 A$ | (3)<br>$10^6 A$ | (4)<br>$10^6 A$ |  | $B_0 \times 10^{14} C$ | $B_0 \times 10^{14} F$ |
| <i>C</i> .....                       | 65.63                 | 291.8           | 295.0           | 296.0           | 296.3           | 296.5           | 1.18                                       | 1.85                   | 1.33                   |
| $10^6$ Diff. from St.                | .....                 | .....           | -3.2            | -4.2            | -4.5            | -4.7            | 1.20                                       | 2.37                   | 1.56                   |
| <i>F</i> .....                       | 48.61                 | 295.0           | 297.3           | 298.0           | 298.7           | 298.6           | 1.28                                       | 2.22                   | 1.70                   |
| $10^6$ Diff. from St.                | .....                 | .....           | -2.3            | -3.3            | -3.7            | -3.6            | 1.08                                       | 2.55                   | 1.50                   |
| $10^6$ Diff. <i>F</i> and <i>C</i> . | .....                 | 3.2             | 2.3             | 2.3             | 2.4             | 2.1             | .....                                      | .....                  | .....                  |

The standard of length was first compared with a normal meter, showing that the  $\tau = 138.0$  cm. for the *M* tube should be replaced by 137.75 cm. and for the *N* tube by 137.59 cm. As this correction affects all the results,  $\mu_0 - 1$  and *B*, in the same ratio, it contributes nothing to modify the discrepancy in question. The correctness of the micrometer screw was assumed, as it was of good manufacture.

The test next was made to see if the lines taken as *C* and *F* actually had the accepted wave-lengths. A revolvable arm, with its axis at the grating and 125.5 cm. long, was therefore installed for the direct measurement of the diffraction of the grating. The results obtained for the wave-lengths of the lines taken showed that no mistake had been made in their selection.

To endeavor to obtain further evidence, the values of *B* were computed for the mean data of table 11, by using the standard values for  $\mu_0 - 1$  in case of the *C* and *F* lines and the  $\Delta N/e$  given by the observations. The results so obtained are given in the last columns of table 12, for each of the four series and the *C* and *F* lines at normal temperature and pressure. The mean results are thus—

$$B_0 \times 10^{14} = 1.19 \text{ from observations with sunlight directly} \\ \text{between } C \text{ and } F \text{ lines.}$$

$$B_0 \times 10^{14} = 2.25 \text{ from standard } \mu_0 - 1 = .0002918 \text{ at } C \text{ line.}$$

$$B_0 \times 10^{14} = 1.52 \text{ from standard } \mu_0 - 1 = .0002950 \text{ at } F \text{ line.}$$

The *B* values of table 10 show a march to be referred to temperature and pressure. So the present unsatisfactory differences are probably pressure-temperature effects beyond the discrimination of the method.

One reason for this discrepancy which suggests itself is the possible distortion of the glass plates at the end of the exhaust tubes during the exhaustion. There may be a residual temperature effect due to the heating of the air by the beam which passes twice through it, above the indicated temperature of the surrounding tube of iron. But as  $\mu_0 - 1$  is already too large compared with standard values, this would make the case worse. Similarly, a larger thermal coefficient than the normal value ( $1/273$ ) would further increase

the data for  $\mu_0 - 1$ . For the case of the *F* lines, the *B* values found by comparison with the standard  $\mu_0 - 1$  (last column of table 12) might be taken as correct within the error of method. Nothing, however, has been found to account for the correspondingly large values of *B*<sub>0</sub> for the *C* line.

**75. Distortion of glass absent.**—To test the effect of possible distortion of the end plates of the tube, a shallow cell was constructed but 0.8 cm. deep, closed by plates of the same glass. The diameter of the tube was identical with that of the long refracting tubes. Tests made with the electric arc and sodium line gave the mean values

|                  |                         |         |
|------------------|-------------------------|---------|
| Plenum . . . . . | $10^3 \Delta N = 5.47;$ | 6.6 cm. |
| Vacuum . . . . . | 5.25;                   | 6.4 cm. |

Thus the effect of exhaustion is 0.00021 cm. The long tube gave, on the average, 0.039 cm. for 138 cm. of length. Hence the air effect should be

$$0.039 \times 0.8 / 138 = 0.00022$$

which is practically identical with the value found. Hence there is no perceptible distortion referable to the glass plates.

TABLE 13.—Dispersion of air. *D* and *F* lines. Single Tube, length 138 cm. Barom., 75.40 at 28°. *p* = 7.4 cm. Temp. 20°. St. refers to standard data. *A* =  $\mu_0 - 1$ .

| Line.    | $10^3 \Delta N$    | $10^6 \frac{\Delta N_0}{e}$ | $10^{14} B_0$ | Line, etc.                         | $\lambda \times 10^6$ | St.<br>$10^6 A$ | Mean<br>$10^6 A$ | St. $\mu_0 - 1$  |                  |
|----------|--------------------|-----------------------------|---------------|------------------------------------|-----------------------|-----------------|------------------|------------------|------------------|
|          |                    |                             |               |                                    |                       |                 |                  | $10^{14} B_0, F$ | $10^{14} B_0, D$ |
| <i>F</i> | <i>cm.</i><br>39.4 | 312.8                       | 2.24          |                                    | <i>cm.</i><br>48.61   | 295.0           | 304.0            | 2.10             | 19.2             |
| <i>D</i> | 38.2               | 303.8                       | ....          | $10^6$ Diff. from St.              | ....                  | ....            | -9.0             | ....             | ....             |
| <i>F</i> | 39.0               | 310.1                       | 1.38          |                                    |                       |                 |                  |                  |                  |
| <i>D</i> | 38.3               | 304.6                       | ....          | <i>D</i>                           | 58.93                 | 292.7           | 299.4            | 1.78             | 2.06             |
| <i>F</i> | 39.0               | 310.5                       | 1.49          | $10^6$ Diff. from St.              | ....                  | ....            | -6.7             | ....             | ....             |
| <i>D</i> | 38.3               | 304.6                       | ....          | $10^6$ Diff. <i>F</i> and <i>D</i> | ....                  | 2.3             | 4.6              | 1.83             | 2.06             |

**76. Further observations with sunlight.**—In the absence of other than inferential reasons to account for the difficulties met with, a final series of observations was made between the *D* and *F* lines and a single tube, with the results given in table 13. The mean value of *B*<sub>0</sub> found directly, viz,  $1.70 \times 10^{-14}$ , would be admissible; but the corresponding values of  $\mu_0 - 1$  as compared with the standard values are again too large and worse than above. The same is true of the values of *B*<sub>0</sub> found by comparison of  $\Delta N/e$  with the standard values of  $\mu_0 - 1$ , and their coefficients come out differently for the *C* and *F* lines. In fact, the discrepancy of  $\mu_0 - 1$  is now about 3 per cent, whereas observations for  $\Delta N/e$  should not be in error more than  $(2 \times 1/400 = 0.0025)$  0.5 per cent. There is thus something variable at the limit of application of the present method which has persistently escaped detection. I have thought that a distortion associated with the form of the interference pattern in passing from *C* to the *F* line may be in question, as the discrepancy

varies in different, otherwise satisfactory experiments; or the failure to completely exhaust the tube may leave a small error which becomes appreciable in  $B$ .

**77. Conclusion.**—If allowance is made for the fact that  $\Delta N$  at the micrometer is measured for air, at barometric pressure  $p'$  and absolute temperature  $\tau$ , the equation for  $\mu_0 - 1$  at normal conditions would be

$$\mu_0 - 1 = \frac{\Delta N}{e} \frac{76}{p} \frac{\tau}{273} \frac{1}{1 - p' \Delta N / ep} - \frac{2B_0}{\lambda^2}$$

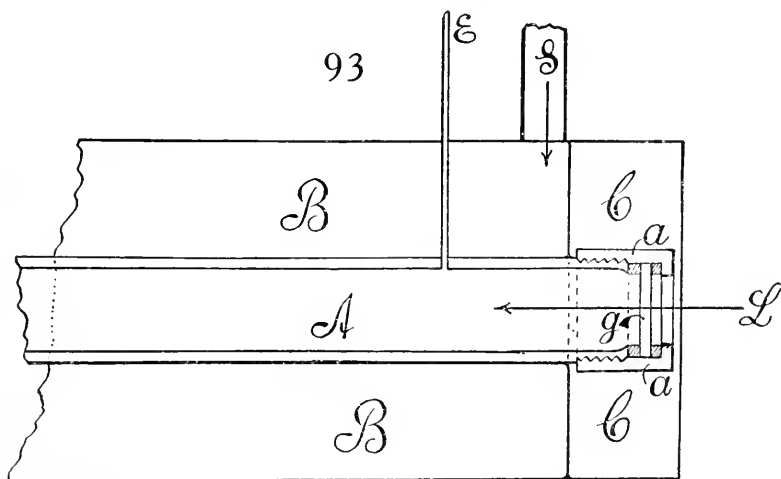
where the correction factor  $1 - \Delta N p' / ep$  would not appreciably modify the results.

It is difficult to see, therefore, why the promising results of §4, which are quite as near the standard data as the method warrants, did not bear consistent fruit in the sequel. The direct values of  $B_0 \times 10^{14}$  are usually too small, sometimes too large, and range from 1 to 2. On the other hand,  $\mu_0 - 1$  usually comes out too large, whereas it should be correct to a few tenths percentage. None of the causes examined, temperature, pressure, thermal coefficient, flexure of glass, etc., quite account for such a result. If  $B_0 \times 10^{14}$  is computed from standard results for  $\mu_0 - 1$  and observed at different spectrum lines, the data are nearly correct for some lines, but too large for other lines, so that a single constant does not reduce the series. It does not seem probable, however, that equation (1) is inadequate; for the results obtained with equal care at different times for the same  $\mu_0 - 1$  or  $B_0$  are not in accord. The discrepancies, in other words, are not persistent in value and are therefore due to some incidental cause which has not been detected. It has seemed to me that the change in shape of the interference pattern on passing from red to violet, which in case of ordinary glass mirrors is marked, may be responsible for some of the difficulties encountered. This pattern, which for optically flat surfaces would remain elliptical, becomes more and more irregular as the distances,  $e$ , of the mirror and grating are increased. The distorted image shrinks laterally from red to violet fully one-half, so that it is not certain that the center of figure is actually a fiducial point. The question, however, would have to be tested.

## CHAPTER XI.

### THE CHANGE OF THE REFRACTION OF AIR WITH TEMPERATURE.

78. **Apparatus.**—In the earlier report (Carnegie Inst. Wash. Pub. 149, III, Chap. 15, p. 223) I began some experiments on the change of the refractive index of air with rise of temperature. The question is interesting, inasmuch as the temperature coefficient has not in most investigations been found identical with the coefficient of expansion of air, as Lorentz had obtained it and as would otherwise be anticipated; but a value, over 3 per cent larger, first put forward by Mascart, seems preferable. My earlier work was left unfinished, however, because the design of the apparatus, in which the refraction tube was heated in an independent annular steam-bath, was unsatisfactory. It seemed to be impossible to reach the temperature of the steam in that way, even after half a day's waiting. In the present work, therefore, the apparatus is modified, so that the steam may play directly on the long refraction tube. In this way the temperature difficulty was quite eliminated.



The tube containing the air column was made of inch brass gas-pipe, 71.7 cm. long (between windows) and 2.5 cm. in internal diameter (*A*, fig. 93, which shows one end of the apparatus). The ends were closed with the usual brass caps *a*, in which round windows, about 2 cm. in diameter, had been cut on the lathe. The ends were closed by plates of glass *g*, secured between two jackets of rubber and "vulcanized" fiber. *L* shows the axis of the beam of light.

*BB* is the steam chamber, steam entering at *S* and leaving by a similar tube at the other end of the apparatus. Steam is thus directly in contact with the tube. The projecting end of *A* is inclosed by a recess packed with wadding,

CC. As the walls of the brass pipe were thick and the ends relatively short, there seemed to be no objection to this arrangement. Care was taken to conduct the escape steam and hot gases away from the interferometer.

The displacement interferometer was of the linear type described above, the mirrors  $M$  and  $N$  and the grating  $G$  being attached directly to the wall of the pier and without an intervening rail. Unfortunately the pier in a large city is also in incessant vibration, so that the interference patterns quiver. It is this insuperable difficulty which has prevented me from reaching results as accurate as were anticipated. A few of the data, however, will be added as an example of the efficiency of the method.

TABLE 14.—Refraction of air at different temperatures. Tube, 71.7 cm. long, 2.5 cm. in diameter.

| Barometer.             | Temp. | $p$ . | $10^3 \times \Delta N$ | Barometer.                | Temp.  | $p$ . | $10^3 \times \Delta N$ |
|------------------------|-------|-------|------------------------|---------------------------|--------|-------|------------------------|
| 77.04 cm.<br>22°<br>I  | 19.7° | 75.3  | 19.3                   | 75.12 cm.<br>20°<br>VI    | 19.9°  | 74.3  | 19.3                   |
|                        |       |       | 19.4                   |                           |        |       | 19.1                   |
|                        |       |       | 19.3                   |                           |        |       | 19.2                   |
| 76.25 cm.<br>20°<br>II | 21.7° | 75.5  | 19.1                   | 76.98 cm.<br>18.7°<br>VII | 100.4° | 75.5  | 15.0                   |
|                        |       |       | 19.3                   |                           |        |       | 15.0                   |
|                        |       |       | 19.2                   |                           |        |       | 15.0                   |
|                        |       |       | 19.4                   |                           |        |       | 15.0                   |
|                        |       |       | 19.4                   |                           |        |       | 15.0                   |
| 77.22 cm.<br>20°<br>IV | 19.1° | 75.7  | 19.3                   | 76.55 cm.<br>23°<br>III   | 100.2° | 75.3  | 15.0                   |
|                        |       |       | 19.8                   |                           |        |       | 15.0                   |
|                        |       |       | 19.7                   |                           |        |       | 15.4                   |
|                        |       |       | 19.8                   |                           |        |       |                        |
|                        |       |       | 19.7                   |                           |        |       |                        |
| 76.25 cm.<br>20°<br>V  | 22.2° | 75.5  | 19.7                   | 75.12 cm.<br>20°<br>VIII  | 99.7°  | 74.3  | 15.0                   |
|                        |       |       | 19.1                   |                           |        |       | 15.0                   |
|                        |       |       | 19.2                   |                           |        |       | 14.9                   |
|                        |       |       | 19.4                   |                           |        |       | 15.0                   |
|                        |       |       | 19.6                   |                           |        |       | 15.1                   |
|                        |       |       | 19.5                   |                           |        |       |                        |

**79. Observations.**—The data are given in table 14, where the temperature and barometric pressure are shown in the first column, the differences in the pressure  $p$  between the plenum of air and the exhausted air in the refraction tube in the second column, while the third shows the values of  $\Delta N$ , the displacement of the micrometer corresponding to  $p$ , as found in successive independent experiments at the temperature given. For such long distances between grating and mirrors the ellipses are visually distorted, and much depends on finding a satisfactory sharp interference pattern. This was the case, except in series 3 and 5, when for incidental reasons (outside tremors) the patterns were disagreeably flickering. The observations are usually for room air, as the special drying of air in series 3 and 5 made no perceptible difference. At 100° care must be taken to obviate convection currents of air, so far as possible. The endeavor was made to keep  $p$  as nearly as possible at the same value, apart from the barometer pressure, which does not enter into the equations. In series 4 the values of  $\Delta N$  are relatively large,

but quite consistent with each other. The reason for this could not be made out. But for the inevitable tremors the observations would all have been acceptable.

**80. Computation.**—Since the ends of the air-tube are perpendicular to the beam of light

$$(1) \quad \Delta N = e \left( \mu - 1 - \lambda \frac{\partial \mu}{\partial \lambda} \right)$$

where  $\Delta N$  is the difference of the displacements of the micrometer in the presence and absence of air in the tube,  $e$  the effective length of the air column, and  $\mu$  the index of refraction of the air for the given wave-length  $\lambda$ . The equation presupposes a knowledge of the dispersion of air  $\partial \mu / \partial \lambda$ ; but, as this is small, the term may be temporarily omitted. If  $\lambda$  is constant, it corresponds to a constant correction of  $\Delta N$  throughout the experiments.

Again, if we have an equation of the form of Mascart's,  $\mu_{76}$  referring to  $0^\circ$  C. and normal barometer, and  $N_0$  to the absence of air in the tube,

$$(2) \quad \frac{\mu - 1}{\mu_{76} - 1} = \frac{p}{76} \frac{1 + \beta(p - 76)}{1 + \alpha t} = \frac{N_p - N_0}{N_{76} - N_0} = \frac{\Delta N_p}{\Delta N_{76}}$$

where  $\alpha$  and  $\beta$  are two constants. If the tube is not quite exhausted ( $\delta B$  remaining), the observations for a plenum (barometric pressure,  $B$ ) and exhausted air being made at the same temperature,

$$\frac{\delta B}{B} (1 - \beta(B - \delta B)) = \frac{N_{\delta B} - N_0}{N_B - N_0}$$

or nearly

$$\frac{B - \delta B (1 - \beta B)}{B} = \frac{N_B - N_{\delta B}}{N_B - N_0} = \frac{\Delta N_{B - \delta B}}{\Delta N_B}$$

Thus if one neglects the small correction  $1 - \beta B$  of  $\delta B$

$$(3) \quad \Delta N_B = \Delta N_{B - \delta B} \frac{B}{B - \delta B}$$

the micrometer displacement  $\Delta N_B$  in case of complete exhaustion at the barometric height,  $B$ , and the displacement  $\Delta N_{B - \delta B}$  corresponding to partial exhaustion  $B - \delta B$ , are proportional to those pressures. Since  $\delta B$  was quite small, this equation was assumed, and  $p - \delta B$  is thus nearly the height of the mercury column of the partially exhausted tube. In the table this is briefly called  $p$ , and differs from the barometric height.

Finally, for two partial pressures  $p$  and  $p'$  and temperatures  $t$  and  $t'$  of the air

$$(4) \quad \frac{p}{p'} \frac{1 + \alpha t'}{1 + \alpha t} (1 + \beta(p - p')) = \frac{\Delta N}{\Delta N'}$$

$\Delta N$  and  $\Delta N'$  being the micrometer displacement corresponding to  $p$ ,  $t$ , and  $p'$ ,  $t'$ , respectively. Hence if care be taken to make  $p = p'$ , nearly,

$$\frac{1 + \alpha t'}{\Delta N} = \frac{1 + \alpha t}{\Delta N'} = \frac{\alpha(t' - t)}{\Delta N - \Delta N' N \delta}$$

if, for brevity,  $t' - t = \delta t$  and  $\Delta N - \Delta N' = \delta N$ ; or

$$(5) \quad \frac{1}{\alpha} = \Delta N \left( \frac{\delta t}{\delta N} - \frac{t'}{\Delta N} \right)$$

If  $p$  is not quite equal to  $p'$ ,  $\beta(p' - p)$  may still be neglected, but  $\Delta N/p$  and  $\Delta N'/p'$  must replace  $\Delta N$  and  $\Delta N'$ , or  $\Delta N(1 - \delta p/p)$  replace  $\Delta N$  where  $\delta p = p - p'$ .

On applying equation (5) to series 1, 2, 3, for which  $p$  is nearly constant,

$$\delta t = 79.5^\circ \quad \delta N = 0.00423 \quad \alpha = 0.00380$$

applying it to series 4, 5, 7, similarly,

$$\delta t = 79.8^\circ \quad \delta N = 0.00404 \quad \alpha = 0.00404$$

The mean value is thus  $\alpha = 0.00392$ . The reason of this difference is found in series 4, where  $\Delta N$  is excessive. In fact, if we compare percentage errors of  $\alpha$  and  $\delta N$

$$(6) \quad \frac{d\alpha/\alpha}{d(\delta N)/\delta N} = \alpha \frac{\Delta N}{\delta N} \delta t = 1.4$$

so that an error of 5 per cent in  $\delta N$  would be an error of over 5 per cent in  $\alpha$ . For the case where the fringes tremble this is inevitable. If the mounting were without tremor, however,  $\delta N$  should be guaranteed to  $5 \times 10^{-5}$  cm., corresponding to the evanescence of a single interference ring, so that  $\alpha$  should be determinable to 1 per cent, even in case of a tube of the length 71.7 cm. given.

If  $\delta t$  is small or  $t'$  small, equation (5) becomes, approximately,

$$\frac{\delta N}{\Delta N} = \alpha \delta t \text{ or } \Delta N' = \Delta N(1 - \alpha \delta t)$$

This equation may be used to find the successive values of  $\Delta N$  in the table, if the second, for instance, is supposed to be correct. It appears that the first and fifth differ about equally ( $\pm 0.0001$  cm.) from the second, but the error of the fourth ( $-0.00028$ ) is excessive. Hence if this second datum be taken as the mean of series 1, 2, 5, and combined with the two data for  $100^\circ$ ,

$$\Delta N = 19.28 \quad \delta N = 0.421 \quad \delta t = 78.6^\circ \quad t' = 100.3^\circ \quad \alpha = 0.00385$$

This is the more probable result of table 14 and would agree with Mascart's value, 0.00382.

Somewhat later, the independent series of observations 6 and 8 were carried out. The interference pattern at  $99.7^\circ$  was exceptionally quiet and clean, but at lower temperatures this was not better than usual. The results are

$$10^3 \delta N = 4.15 \quad \delta t = 79.8^\circ \quad \alpha = 0.00372$$

somewhat below the preceding value.

**81. Final experiments at  $100^\circ$ .**—Somewhat later, at a time when the laboratory was relatively quiet and after the same effective improvements had been made in the mounting of the interferometer mirrors, the experiments

at 100° were repeated. The optical measurements were satisfactory, or at least just short of the counting of interference rings for measurement. The arc lamp, moreover, which is unsteady, would scarcely suffice for this purpose. The results obtained were as follows (table 15):

TABLE 15.—Refraction of air at different temperatures.

| Bar.      | Temp. | $p$  | $10^3\Delta N$ | Bar.      | Temp.  | $p$  | $10^3\Delta N'$ |
|-----------|-------|------|----------------|-----------|--------|------|-----------------|
| 75.6 cm.  | 21.8° | 74.0 | 19.3           | 76.72 cm. | 100.3° | 74.0 | 15.1            |
|           |       |      | 19.2           |           |        |      | 15.4            |
|           |       |      | 19.3           |           |        |      | 15.0            |
|           |       |      | 19.1           |           |        |      | 15.1            |
| 76.65 cm. | 21.8° | 74.0 | 19.6           | 20.5°     |        |      | 15.5            |
|           |       |      | 19.4           |           |        |      | 15.0            |
|           |       |      | 19.5           |           |        |      | 15.2            |
|           |       |      | 19.2           |           |        |      | 15.4            |
|           |       |      | 19.3           |           |        |      | 15.2            |
|           |       |      |                |           |        |      | 15.3            |
|           | 15.2  |      |                |           |        |      |                 |

If the mean values of  $\Delta N$  and  $\Delta N'$  be taken and  $\alpha$  computed

$$10^3\Delta N = 19.22$$

$$10^3\Delta N' = 15.22$$

$$\delta N = 4.00$$

$$\delta t = 78.5^\circ$$

the result is

$$\alpha = 0.00361$$

As these experiments were the smoothest and were made under the most satisfactory conditions, they are probably the most trustworthy. I have not, therefore, been able to obtain evidence for a value of  $\alpha$  (between 0° and 100°) greater than the coefficient of expansion of gases, though it must be confessed that the method in its present surroundings is not sufficiently sensitive to furnish a definite criterion.

Later results at low temperatures (series 3) like the above series 4, table 14, again gave a high result for  $\Delta N$ , in each case consistently. It is probable that the interference pattern changes between the case of a plenum and of highly exhausted air, owing either to flexure of the glass ends or to some other cause, or possibly depending only on the form of the pattern which happens to appear. In such a case the lines of symmetry for  $N$  (plenum) and  $N$  (exhaustion) would differ, introducing a systematic error very difficult to obviate. Thus different values of  $\Delta N$  often follow a difference of adjustment of the mirror at the micrometer, while all cases for the same adjustment are practically identical.

**82. Experiments at red heat.**—To investigate the feasibility of such experiments, an inch steel tube (bicycle tube), 68 cm. long, with flanges brazed on at the ends, and an exhaustion tube near the middle, was heated in an organic combustion furnace to low red heat. The ends just projected outside the furnace and were closed by plate-glass windows with a jacket of asbestos between (applied wet and dried); or, finally, with a jacket of aluminum cement, clay, plaster, etc. These short but relatively cold ends are, of course,

an objection to the method, but no better device was found. Even so, the windows frequently cracked and had to be replaced. Such an apparatus naturally leaks, particularly at low temperatures, where the viscosity of air is relatively small, so that the experiments as a whole are merely tentative. To maintain the exhaustion as high as 70 cm., it was necessary to keep the air-pump at work. To reduce this annoyance the exhaustions were at first not carried above 60 cm. of mercury. With the interference fringes, however, no serious difficulty was experienced after the tube had taken definite shape. Distortion of fringes was inevitable, but centers of symmetry for measurement were always available.

The first experiments were made without exhaustion, at low and high temperature (low red heat). The difference of displacement  $\delta N$  between cold ( $25^\circ$ ) and hot was (for instance) in two different experiments

|            |                       |          |
|------------|-----------------------|----------|
| $25^\circ$ | $10^3 N = 35.0$ cm.   | 35.2 cm. |
| red hot    | $10^3 N' = 28.5$      | 28.6     |
| or         | $10^3 \delta N = 6.5$ | 6.6      |

at atmospheric pressure. The  $\delta N$  so obtained makes no allowance for the change of refractive index of the hot glass ends, nor for any displacement or rotation or warping of the ends during the course of the experiment, which required a lapse of an hour or two.

In the next experiment, therefore, the method of exhaustion was attempted, the partial vacuum used being about 16.6 cm. when the full barometer read 76.64 cm. Thus  $p = 60$  cm. An example of the results obtained is given in the following data.

|                   |                        |          |      |          |
|-------------------|------------------------|----------|------|----------|
| Cold Tube.        |                        |          |      |          |
| Pressure 76.6 cm. | $10^3 N = 34.8$ cm.    | 34.7 cm. |      |          |
| Pressure 16.6     | 22.7                   | 22.5     |      |          |
| $p = 60.0$        | $10^3 \Delta N = 12.1$ | 12.2     |      |          |
| Red-hot Tube.     |                        |          |      |          |
| Pressure 76.6 cm. | $10^3 N = 24.6$        | 24.5     | 26.8 | 26.0 cm. |
| Pressure 16.6     | 20.1                   | 19.4     | 20.0 | 20.0     |
| $p = 60.$         | $10^3 \Delta N = 4.5$  | 5.1      | 6.8  | 6.0      |

In the two experiments at the end readjustment was necessary, as the red-hot tube warped during the exhaustion. In the last case the glass cracked. The first two data should therefore be taken, so that

$$10^3 \Delta N = 12.1 \text{ cm.} \quad 10^3 \Delta N' = 4.8 \text{ cm.} \quad 10^3 \delta N = 7.3 \text{ cm.} \quad t = 25^\circ \quad p = 60 \text{ cm.}$$

If equation (5) above is solved for  $t'$  the result is

$$(7) \quad t' = \frac{1}{\alpha} \frac{\delta N}{\Delta N'} + \frac{\Delta N}{\Delta N'} t$$

or if  $\alpha = 1/273$

$$t' = 478^\circ$$

This result is certainly small, as one would estimate the temperature (red heat) at several hundred degrees higher. Unfortunately the relatively cold

ends of the tube and the leakage at the windows both contribute to a low value of  $t'$ . But these do not seem to be adequate reasons. It is more probable that the longitudinal radiation of the air on the one hand and the value of  $1/\alpha = 273$  assumed (if this is too small) may be the chief causes for the low value of  $t'$ . It is not, of course, possible to come to any further decision; but the experiments are distinctly unfavorable to the large value of  $\alpha$  (small  $1/\alpha$ ) above considered.

The method is not adapted for very high temperatures, since equation (7) may be written

$$(8) \quad \tau' = \frac{1}{\alpha} + t' = \frac{\Delta N}{\Delta N'} \left( \frac{1}{\alpha} + t \right)$$

and therefore, since  $\tau' \Delta N' = \tau \Delta N$ ,

$$\frac{\partial t'}{\partial (\Delta N')} = -\tau \Delta N / (\Delta N')^2$$

where ( $\tau$  referring to absolute temperature)  $\Delta N'$  rapidly reaches the limit of accurate measurement.

**83. Further experiments at high temperatures.**—A variety of experiments were now made to obtain a more nearly tight joint at the ends, by using various clays, aluminum, etc., as cements, but without success. Finally, an improvement was obtained by using plaster of paris in the way shown in figure 94. *A* is the end of the hot tube in the combustion furnace *F*. The flange *f* is set somewhat back, so that packing of plaster *p* may secure the window *g* to the end of the tube. The plaster is put on wet and allowed to dry thoroughly. Lying outside of the furnace, it is never heated to redness. The joint is at first fairly good, though it gradually deteriorates at high temperatures, and must be replaced. In this way the following results were found:

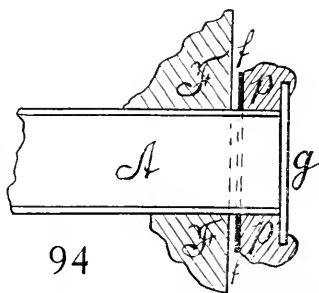


TABLE 16.

|                     | <i>p.</i> | $10^3 \Delta N$ |                 | <i>p.</i> | $10^3 \times \Delta N$ |              | <i>p.</i> | $10^3 \Delta N$ |
|---------------------|-----------|-----------------|-----------------|-----------|------------------------|--------------|-----------|-----------------|
| Just below red heat | 74.5      | 12.4            | Cold tube (22°) | 74.0      | 17.6                   | Low red heat | 73.5      | 8.9             |
|                     |           | 12.5            |                 |           | 17.7                   |              |           | 8.5             |
|                     |           | 12.0            |                 |           | 17.8                   |              |           | 8.6             |
|                     |           |                 |                 |           | 18.1                   |              |           | 8.8             |
|                     |           |                 |                 |           | 17.8                   |              |           |                 |

Thus, from the first and second series,  $t' = 154^\circ$ ; from the first and third series,  $t' = 330^\circ$ . As in the first experiments tried, both of these data are much too low. Here they can hardly be referred to the leak, since this was smaller. The ends are exposed not more than 1 or 2 cm. each, or a total length of about 70 cm. of tube.

Some adjustment is needed at the mirrors, to place the slit images in coincidence for the case of an exhaustion, as compared with a plenum of air. This adjustment is slight, but unfortunately its effect on  $\Delta N'$  can not be estimated.

Cooling of gas as resulting from longitudinal radiation might be suggested, but, as it was not encountered in the case of the steam tube, it would not seem to be menacing here.

Finally, it will be seen from equation (8) that the effect of a leak is to make  $\Delta N'$  too small. It will be larger as the vacuum is more perfect. Hence  $t'$  should be too large for this reason. A small  $t'$  can not be due to a leak. The exhaustion effect, since the gas expands into a vacuum, can not be serious. None of these incidental difficulties seem adequate to account for the large temperature discrepancies consistently obtained. All things considered, it seems to me most probable that the temperature coefficient, as the gas enters the region of red heat more fully, continually decreases, and that this is the real explanation of the low temperature values obtained.

The apparatus was now taken apart and provided with a fresh jacket. After drying, the cold apparatus again appeared in good condition. The results with the barometer at 75.55 cm. were

| Cold ( $22^\circ$ ) $p$ | $10^3 \Delta N$ | Red hot $p$ | $10^3 \Delta N'$ |
|-------------------------|-----------------|-------------|------------------|
| 73.0                    | 17.7            | 73.0        | 8.0              |
| ....                    | 17.8            | ....        | ....             |
| ....                    | 17.8            | ....        | ....             |

Unfortunately the glass cracked after the first experiment at red heat. The data for  $\Delta N$  (cold) agree almost exactly with the preceding results. The high temperature would be  $t' = 383^\circ$ , again enormously too low. Nevertheless, if the values of  $\alpha$  were in question, as the temperature must have been at least  $850^\circ$ , this would come out as low as  $\alpha = 0.0015$ . The misgivings already enumerated apply here as before. As the experiments are very laborious they were abandoned at this point, for it did not seem that further work would materially enhance the result; nor was it thought necessary to actually measure the high temperatures.

**84. Flames.**—In the earlier report on the refraction of flames an abnormally low result of  $\mu$  was obtained for the ignited gases. I have since repeated this work with additional improvements. It appears that it is quite possible to look through the peak of the blue case (symmetrically) without destroying the interference pattern as a whole, though this naturally quivers excessively. The last of the new results showed for the presence ( $N'$ ) and ( $N$ ) of the flame the micrometer readings:

|              |       |       |       |       |       |
|--------------|-------|-------|-------|-------|-------|
| $N'$ , flame | 0.029 | 0.029 | 0.029 | 0.029 | 0.029 |
| $N$ , air    | .0297 | .0295 | .0294 | .0296 | .0296 |

Hence the mean difference is 0.00056 cm., or per centimeter of breadth (2.3 cm.),

$$\delta N = 0.00024 \text{ cm.}$$

If the space occupied by flames were vacuum, the difference would have been 0.000268 per linear centimeter. Thus  $\Delta N' = 0.00002$  cm., which lies within the error of observation, but is otherwise quite of the order to be expected for the hot gases in question.

**85. Conclusion.**—Though the experiments made are of a tentative character, the inference seems warranted that, so far as my work goes, the temperature coefficient  $\alpha$  of air at low temperature is identical with the coefficient of expansion of gases. At high temperatures the value of  $\alpha$  seems to decrease rapidly, in proportion as the gas is more highly ionized at red heat.

It has occurred to me that such ionization might load the gas in relation to the light-wave passing through it, and that the observed excess of index of refraction over the value anticipated at high temperatures might be explained in this way. But air ionized by the X-rays shows no such effect. Neither does the refraction of flames at high temperatures, so far as can be made out, show a large value of the refractive index of the ignited gases.

It is difficult to see how the experiment at red heat can be improved, unless a quartz tube is made for the purpose. But even here the difficulty of obtaining adequately plane parallel ends and a tube of sufficient breadth is formidable. The attempt to grind in reëntrant glass cylinder-like stoppers at the end of the tube was thought of, but did not succeed.

## CHAPTER XII.

### ADIABATIC EXPANSION OBSERVED WITH THE INTERFEROMETER.

**86. Introductory.**—In the preceding report<sup>1</sup> I tested a number of receivers in which air was expanded adiabatically, by passing one of the component beams of the displacement interferometer through the air contained. The vessels then used were not very satisfactory, being, as a rule, not long or capacious enough to insure trustworthy results. Moreover, the interferometer did not at that time admit of the introduction of long or bulky apparatus, whereas in the new form a length of almost 150 cm. is available. The main purpose of the research will thus be to ascertain how long and thin a tube may be made to be serviceable for expansion experiments. Furthermore, it seemed worth while to repeat the work preliminarily with a large, staunch tank since found in the laboratory. This was a heavy cylinder of cast brass, about 27.1 cm. (inside) and closed by plates of heavy glass, each 0.56 cm. thick and 20.3 cm. apart (inside), the whole containing a volume of air of about 11,713 cubic centimeters, to be increased to 12,800 cubic centimeters, because of the efflux pipe. The expansion pipe was 2 inches in diameter and closed by a 2½-inch brass stopcock, with a plug practically floating in oil to prevent the ingress of air from without. The glass plates were secured by iron bolts, a layer of resinous cement (equal parts of beeswax and resin) between glass and the flat end faces of the cylinder being introduced to prevent leakage.

To expand the gas in the receiver, the 2-inch pipe communicated with a tall, galvanized iron boiler used as a vacuum chamber, 29.4 cm. in diameter and 147 cm. high, thus containing a volume of 99,800 cubic centimeters, or 100,200 cubic centimeters with the influx pipe. It was in communication with a large air-pump and provided with a mercury gage for the measurement of the partial vacuum produced by the pump. The air flowing into the air-chamber after exhaustion was dried in the usual way and the influx controlled by a fine screw stopcock. There was a special opening for a thermometer. Vacuum and air-chamber were rigidly connected by a brass union with a rubber washer. There was no appreciable leakage so far as the atmosphere without was concerned. The 2-inch stopcock, however, was not quite tight within, so that air passed very slowly from the air to the vacuum chamber, in proportion as their pressures were different; but as the air-chamber is in service, either at atmospheric pressure (the influx cock being open) or, after exhaustion, at approximately the same pressure as the vacuum chamber, this leakage was of no appreciable consequence. Otherwise the interference pattern would not have been stationary.

While this apparatus was not long enough to fully realize the advantages of the method of displacement interferometry for the purposes in question,

---

<sup>1</sup> Carnegie Inst. Wash. Pub. 149, Part II, Chapter IX, 1912.

it was useful for testing the ring method in comparison with the former. The equivalent of a vanishing interference ring is here not immediately given in terms of the wave-length of light, since the rings move through the spectrum.

With the exception of a few incidental experiments of my own, optic methods of the present kind have not hitherto been used. They are here particularly applicable, since the number of the rings vanishing in a given region of the spectrum has merely to be counted after the sudden exhaustion and during the period of slow influx of air.

Succeeding parts of the chapter will refer to other available forms of apparatus with similar ends in view, and the additional purpose of ascertaining how long and narrow an apparatus may be shaped, without seriously interfering with the adiabatic measurements; for if the apparatus is increased indefinitely in length and diameter, it is obvious that the suddenness of the exhaustion through any available pipe will be more and more impaired. The same is true if the apparatus, for a given (sufficient) length, is too narrow, though for a different reason.

TABLE 17.—Values of  $\gamma$ . Bulky air chamber,  $V=99,800$  cub. cm.,  $v=11,620$  cub. cm.  $(V+v)/V=1.116$ .  $C=952.6$ ;  $1+x=1.0341$ ;  $e=20.3$  cm.

| Series. | $t$                 | $p_0$      | $p$        | $10^3\Delta N$ | $\gamma$ | Number of rings. | $\gamma'$ |
|---------|---------------------|------------|------------|----------------|----------|------------------|-----------|
|         | $^{\circ}\text{C.}$ | <i>cm.</i> | <i>cm.</i> | <i>cm.</i>     |          |                  |           |
| I       | 22.4                | 75.88      | 56.38      | 1.15           | 1.15     | 30               | 1.49      |
|         | ....                | .....      | 56.88      | .95            | 1.39     | 29               | 1.50      |
|         | ....                | .....      | .....      | .92            | 1.44     | 29               | 1.50      |
|         | ....                | .....      | .....      | 1.02           | 1.28     | 29               | 1.50      |
| II      | 22.4                | 75.88      | 47.68      | 1.53           | 1.29     | 46               | 1.58      |
|         | ....                | .....      | .....      | 1.33           | 1.53     | 46               | 1.58      |
|         | ....                | .....      | .....      | 1.45           | 1.38     | 46               | 1.58      |
|         | ....                | .....      | .....      | 1.47           | 1.36     | 46               | 1.53      |
| III     | 22.8                | 75.70      | 38.50      | 1.95           | 1.38     | <sup>1</sup> 61  | 1.54      |
|         | 23.2                | .....      | .....      | 2.25           | 1.14     | <sup>1</sup> 60  | 1.54      |
|         | 23.6                | .....      | .....      | 2.05           | 1.29     | 61               | 1.53      |
|         | 24.0                | .....      | .....      | 1.91           | 1.42     | 62               | 1.50      |
| IV      | <sup>2</sup> 22.5   | 76.75      | 30.35      | 2.65           | 1.28     | 77               | 1.58      |
|         | <sup>2</sup> 22.5   | .....      | .....      | 2.20           | 1.65     | 76               | 1.59      |
|         | 23.6                | .....      | .....      | 2.73           | 1.21     | 78               | 1.54      |
|         | 23.6                | .....      | .....      | 2.49           | 1.39     | 78               | 1.54      |

<sup>1</sup> Count broken owing to flicker of arc; obtained from rhythm. <sup>2</sup> Sunlight.

87. Experiments with short, bulky air-chambers.—An example of the data obtained is given in table 17, where the ratio of specific heats,  $\gamma$ , computed directly both from displacement of ellipses and  $\gamma'$  from interference rings, is shown in detail. The original pressure of the air-chamber is that of the barometer,  $p_0$ . The pressure of the vacuum chamber is given under  $p$ . The displacement,  $\Delta N$ , from four independent observations in each case and the number of interference rings vanishing from exhaustion to plenum are the data chiefly of interest. It has not been possible, according to the table, to

\* Carnegie Inst. Wash. Pub. 149, Part II, § 83, p. 129; § 85, p. 135. 1912.

place the micrometer with an accuracy of more than 0.0002 cm. or 0.0003 cm. in successive cases,  $\Delta N$  being the difference of two readings, each uncertain to  $10^{-4}$  cm. But the effect of this is to throw out  $\gamma$  by about the same number of tenths, so that the roughness of values in the table is inevitable. On the other hand, however,  $\gamma$  obtained by displacement is usually too small, whereas the value computed from the evanescence of rings is always much too large. Thus in the first series there should have been an evanescence of 31 rings, in the second of about 50 rings, in the third of 64 rings, in the fourth of 85 rings. The reason for this discrepancy is very hard to determine, but will be considered in the next paragraph. The mean values of  $\gamma$  from displacement and from rings are usually more nearly correct than either, as if the errors were equal and opposite in the two cases. The error is, in some way which has not been made out, associated with the placing of the micrometer. Thus, without apparent cause, the micrometer reading with a *plenum* of air may differ by several  $10^{-4}$  cm., so that if these discrepancies are in opposite directions the value of  $\gamma$  shows such large divergences as in series 4, for instance. In other words, the error appears to be extraneous to the method of experiment.

It has been suggested that the number of vanishing rings observed is approximately about 10 per cent too small throughout, and that the corresponding data for  $\gamma$ , though excessive, are nevertheless of the same order of value. Experiments were made to determine whether the change of wave-length,  $\lambda$ , influenced this result. This was done by allowing the center of ellipses in one case to move from the *D* line towards the red, in the other from the yellow into the *D* line. The mean wave-length would in the last case be smaller, and one may estimate the former as

$$\lambda = \lambda_D + \frac{\lambda_C - \lambda_D}{2} \frac{\Delta N}{\Delta N_0}$$

where  $\Delta N_0$  is the displacement of mirror which passes the center of ellipses from the *C* to the *D* line. This was found to be  $10^3 \Delta N_0 = 28.1$  cm. Hence

$$\lambda = \lambda_D + 3.35 \times 10^{-6} \times \frac{\Delta N}{0.0281} = 10^{-6} (58.93 + 119 \Delta N)$$

Even in the final case, therefore, where  $10^3 \Delta N = 2.5$ ,  $\lambda_D$  would not be in error by more than 0.5 per cent. Using sunlight and at

$$p_0 = 76.75 \text{ cm.} \quad p = 48.65 \text{ cm.} \quad \tau = 294.5^\circ \text{ (abs. temp.)}$$

the number of rings *R* were counted when the ellipses traveled into the *D* line and from the *D* line, respectively, with results of which the following are examples:

|                     |               |    |      |    |                      |
|---------------------|---------------|----|------|----|----------------------|
| From <i>D</i> line, | <i>R</i> = 47 | 46 | 46   |    | Mean <i>R</i> = 46.3 |
| Into <i>D</i> line, | <i>R</i> = 45 | 47 | 46.5 | 46 | Mean <i>R</i> = 46.1 |
| Indifferent,        | <i>R</i> = 46 | 46 |      |    | Mean <i>R</i> = 46.0 |

These results agree with the second series of table 17, and there is thus no appreciable difference.

One may note that the results for  $\gamma$ , when rings are counted, are consistently too large, but always of the same order. In fact, if  $R$  were increased by the reduction factor  $\tau_{076}/273p_0$ , the values of  $\gamma$  would all be nearly correct; but there is no reason for such a correction. Moreover, since the data for  $\gamma$  obtained from  $\Delta N$  (ellipses brought back to fiducial position) and from  $R$  (ellipses displaced) are each separately consistent with each other, the discrepancy can not be due to leakages of air, as these would affect both measurements in the same way. The only source of error which is not common to both (apart from the displacement of ellipses) is the possible distortion of the glass upon exhaustion; for, in case of  $\Delta N$ , measurement is made at a plenum and at maximum exhaustion only, but at varying pressures for the case of rings. Thus if the rings needed are supposed to increase in the ratio of

$$p_0/p = 1.3 \quad 1.6 \quad 2.0 \quad 2.5$$

roughly, an approximate adjustment of the two sets of observations would also be obtained. Moreover, the effect of flexure would be an increase of the path of the beam in glass and so counteract the negative effect of decreased density.

**88. Effect of strained glass.**—To detect the possible effect of the inward flexure of the two plates of glass, a metallic ring about 25 cm. in internal diameter was provided. To this, two glass plates of about the same thickness (0.8 cm. each) as in the above vessel were cemented free from leakage and kept in place by clamps. The distance apart of the two plates within was but 1.8 cm., so that the micrometer displacement due to exhaustion of air was reduced to a small value. Hence, if the flexure of the glass plates due to exhaustion and the reverse were optically appreciable, it should here be detected.

To compute the residual air effect for the lamella of air,  $e = 1.8$  cm. thick, we may write

$$(1) \quad C\vartheta_0 = p/(\mu - 1) = p_0/(\mu_0 - 1)$$

where  $C = 952.6$ ,  $\vartheta_0$  is the temperature of the isothermal experiment,  $\mu$  and  $\mu_0$  the index of refraction of air at the pressures  $p$  and  $p_0$ . Furthermore,

$$(2) \quad \mu - 1 = \mu_0 - 1 - \Delta N/e$$

if  $\Delta N$  is the micrometer displacement for the pressure difference  $p - p_0$  at  $\vartheta_0$ .

Finally, if  $n$  is the number of rings vanishing or of fringes passing at the sodium line, then

$$(3) \quad \Delta N = n \frac{58.93}{2 \times 10^6}$$

Thus if  $p - p_0 = \delta p$ , then

$$n = \frac{2 \times 10^6}{58.93} \frac{e}{C\vartheta_0} \delta p = 0.216 \delta p$$

so that  $n$  and  $\delta p$  are proportional quantities. The following results were found:

|                             | $\delta p$  | No. of rings observed. | No. of rings computed. |
|-----------------------------|---|------------------------|------------------------|
| Middle of glass plate. . .  | $\left\{ \begin{array}{l} 30 \text{ cm.} \\ 45 \\ 60 \end{array} \right.$ | 7.2                    | 6.5                    |
| 4 cm. above middle. . . . . |   | 10.0                   | 9.7                    |
| 8 cm. above middle. . . . . |   | 13.2                   | 13.0                   |
| At edge. . . . .            | 45  | 9.8                    | 9.7                    |
|                             | 45  | 10.0                   | 9.7                    |
|                             | 45  | 10.5                   | 9.7                    |

The observed data are the means of 5 or 6 trials. As it is difficult to observe the rings without interruption in an agitated laboratory, there is no doubt that observed and computed values are coincident. The first and last rings are not easily counted, and individual data were found to agree with the computed results perfectly. Finally, if the glass strain were effective (for there is actual flexure), it would be shown in the observations made by passing the beam through different parts of the plate of glass, between the center and the edge. No consistent difference was found.

Hence an appreciable strain effect is also absent, and the reason for the discrepancy in the two sets of values from  $\Delta N$  and from  $n$ , in table 17, remains outstanding.

**89. Equations.**—In the preceding report\* the equation for the value of  $\gamma$  is deduced as

$$\gamma = \frac{\log p/p_0}{\lg(1 - C\vartheta_0\Delta N/e(1+x)p_0)}$$

or

$$\Delta N = (1+x) \frac{ep_0}{C\vartheta_0} \left( 1 + \left( \frac{p}{p_0} \right)^{1/\gamma} \right)$$

Here  $p_0$  and  $p$  are the pressures in the air-chamber (barometric) and the vacuum chamber respectively, before exhaustion,  $\vartheta_0$  the original temperature of the air,  $\Delta N$  the displacement of the micrometer corresponding to the shift of the ellipses on exhaustion. If the air-chamber is quite tight,  $\Delta N$  may be taken at any time.  $C$  and  $1+x$  are the optic constants

$$C = p_0/\vartheta_0(\mu_0 - 1) = 952.6$$

for dry air, being the optic gas constant, if  $\mu_0 - 1$  replaces  $\rho_0$ , the normal density of the gas. To allow for the dispersion of air an empirical equation (convenient in the present calculation),

$$\mu - 1 = B/\lambda^x = 0.0002101/\lambda^{0.341}$$

was constructed. The deduction assumes that the centers of ellipses are brought back again to the fiducial line  $D$ , of the spectrum, the micrometer displacement in question being  $\Delta N$ .

\* Carnegie Inst. Wash. Pub. 149, Part II, pp. 166-168.

In the case where rings are counted, however, the center of ellipses leaves the *D* line by a short distance, less than one-tenth of the interval between the *C* and *D* lines. In such a case, if  $\mu_a = A_a + b_a/\lambda^2$  for air and  $\mu_g = A_g + b_g/\lambda^2$  for glass, the micrometer displacement to bring the ellipses back again from  $\lambda'$  to  $\lambda$  should be

$$\delta N = 3(e_a b_a + e_g b_g)(1/\lambda^2 - 1/\lambda'^2)$$

$e_a$  and  $e_g$  being the lengths of air and glass\* in the beam. Here

$$\begin{aligned} e_a &= 20.3 \text{ cm.} & b_a &= 10^{-14} \times 1.65 & e_a b_a &= 10^{-14} \times 33.5 \\ e_g &= 2 \text{ cm.} & b_g &= 10^{-12} \times 48 & e_g b_g &= 10^{-12} \times 96 \end{aligned}$$

so that the effect of air, where  $b_a$  is variable with pressure, is but 0.3 per cent of the glass effect and may in the first approximation be neglected. The equation may therefore be written:

$$\frac{\delta}{\lambda^2} = -\frac{2\delta\lambda}{\lambda^3} = \frac{\delta N}{3e_g b_g} \quad -\frac{\delta\lambda}{\lambda} = \frac{\delta N \times \lambda^2}{6e_g b_g}$$

If the mean data from series I be inserted ( $\delta N = 960 \times 10^{-6}$  when  $\lambda$  refers to the *D* line)

$$-\frac{\delta\lambda}{\lambda} = \frac{960 \times 10^{-6} \times 10^{-8} \times 0.3473}{6 \times 96 \times 10^{-12}} = 10^{-2} \times 0.58$$

For the case of the *C* and *D* lines  $\delta\lambda/\lambda = 3.35/58.9 = 0.057$ , roughly, about ten times the preceding distance.

In fact, the observations made for the estimate given in the preceding paragraph (semi-displacement),

$$-\frac{\Delta\lambda}{\lambda} 2(\lambda - \lambda_0) = \frac{2 \times 119}{58.9} \Delta N = 4\Delta N$$

compared with the present

$$-\frac{\delta\lambda}{\lambda} = \frac{10^{-8} \times 0.3473 \delta N}{576 \times 10^{-12}} = 6\delta N$$

are quantities of the same order, though one would have expected closer coincidence.

The discrepancy observed between the method of measurement in terms of the displacement ( $\Delta N$  to bring the ellipses back to the fiducial position) and the method of counting rings can not, therefore, be explained as the result of a change of wave-length  $\lambda$  in the latter case; *i.e.*, the equation

$$\Delta N = (n_0 - n)\lambda/2$$

where  $n_0 - n$  is the number of vanishing rings of the mean wave-length  $\lambda$ , is at fault for some other reason. Curiously enough, the ring method is essentially simple, as it reduces to  $\gamma = \frac{\log(p/p_0)}{\log(n/n_0)}$ , if  $n_0$  and  $n$  are the number of rings

---

\* Thickness of glass plates of air-chamber, 1.3 cm.; of the plate of the grating, 0.7 cm.

vanishing when a plenum of air and the adiabatically exhausted air, respectively, are introduced into one of the beams. Since

$$\mu_0 - 1 = n_0 \lambda / 2\ell = p_0 / C\vartheta_0$$

this is equivalent to

$$\Delta N = (n_0 - n) \lambda / 2$$

**90. Experiments with long tubes. Diameter, one inch.**—The difficulty encountered in the case of the preceding experiments was the small value of the displacement  $\Delta N$  obtained. As a consequence, every little incidental disturbance produced a large effect in  $\gamma$ . It is the purpose of the present experiments to remedy this defect by using long tubes by which  $\Delta N$  may be increased over ten times. It was particularly of interest, moreover, to begin with relatively thin tubes, and inch gas-pipe suggested itself for the purpose. The value of  $\gamma$  to be expected will necessarily be too small, as the air must undergo reheating before the exhaust cock can be closed. The question, however, is whether consistent values of  $\gamma$  will be found, even for these extreme conditions and for large variations of pressure. Obviously the window plates will not produce discrepancies, as has been directly shown in paragraph 88.

The gas-pipe installed was 143.4 cm. long within. To make the junction with the vacuum chamber, a straight pipe of the same diameter and about 75 cm. long was needed between the main pipe and the 2½-inch stopcock. The connecting pipe, together with the tube itself, is probably the chief cause of the resistance to flow and the low value of  $\gamma$  found, but it was not possible to shorten it.

The large stopcock inevitably leaked slightly when the pressures were different in the two chambers; but immediately after exhaustion this made no appreciable difference, as the two pressures are then nearly the same. In fact, no rings vanish from the spectrum from this cause. Just before exhaustion, however, after closing the gas-pipe by the fine influx stopcock, appreciable leakage is shown by the spectrum. Hence the exhaustion must be made immediately after the influx cock is closed. Some low results at the outset are referable to this difficulty.

The tube was, as usual, filled with dry air after exhaustion. The results are given in table 18, in the same way as in the preceding case. The experiments themselves were throughout satisfactory, no difficulty being encountered at the interferometer. The work, moreover, is equally trustworthy at low and at high exhaustions, a result which is rather surprising. In the latter case, as the total displacement,  $\Delta N$ , is over 0.0276 cm., the  $\gamma$  contained should be correct within 1 per cent.

Only one attempt was made to find  $\Delta N$  by the march of the interference fringes. Fully 276 were observed, and it is here necessary to count the fringes passing the  $D$  line, since the ellipses are displaced throughout the greater part of the length of the spectrum; but this introduces no inconvenience whatever. The difficulty is due to the time needed in counting so many evanescences; for during this interval the electric lamp is liable to flicker seriously, or some

commotion will occur in the laboratory or without, tending to make the count uncertain. The rings disappear temporarily during the tremor. In a quiet laboratory, however, and with sunlight replacing the arc light, this would be a method of precision. Thus, for instance, at the highest exhaustions used, over 900 fringes would have to pass the *D* line, a datum from which  $\gamma$  could be accurately obtained.

TABLE 18.—Values of  $\gamma$ . Iron gas-pipe, 1 inch internal diameter.  $C=952.6$ .  
 $e=143.4$  cm.  $1+x=1.0341$ .

| Series. | <i>t</i> | <i>p</i> <sub>0</sub> | <i>p</i> | 10 <sup>3</sup> $\Delta N$ | $\gamma$ | No. of rings. | $\gamma'$ |
|---------|----------|-----------------------|----------|----------------------------|----------|---------------|-----------|
| I       | °C.      | cm.                   | cm.      | cm.                        |          |               |           |
|         | 19.2     | 76.84                 | 57.84    | 8.75                       | 1.18     | 276           | 1.28      |
|         | ....     | .....                 | .....    | 8.60                       | 1.21     | ...           | ....      |
|         | ....     | .....                 | .....    | 8.35                       | 1.24     | ...           | ....      |
|         | ....     | .....                 | .....    | 8.40                       | 1.24     | ...           | ....      |
| II      | 19.1     | 76.28                 | 48.08    | 12.95                      | 1.20     |               |           |
|         | ....     | .....                 | .....    | 13.15                      | 1.18     |               |           |
|         | ....     | .....                 | .....    | 13.15                      | 1.18     |               |           |
|         | ....     | .....                 | .....    | 13.25                      | 1.17     |               |           |
|         | ....     | .....                 | .....    | 13.10                      | 1.19     |               |           |
|         | ....     | .....                 | .....    | 13.25                      | 1.17     |               |           |
| III     | 19.2     | 76.28                 | 38.98    | 18.05                      | 1.14     |               |           |
|         | ....     | .....                 | .....    | 18.10                      | 1.14     |               |           |
|         | ....     | .....                 | .....    | 17.95                      | 1.15     |               |           |
|         | ....     | .....                 | .....    | 17.80                      | 1.17     |               |           |
| IV      | 19.3     | 76.28                 | 29.78    | 22.70                      | 1.15     |               |           |
|         | ....     | .....                 | .....    | 22.80                      | 1.14     |               |           |
|         | ....     | .....                 | .....    | 22.65                      | 1.15     |               |           |
|         | ....     | .....                 | .....    | 22.80                      | 1.14     |               |           |
| V       | 19.3     | 76.28                 | 20.88    | 27.85                      | 1.12     |               |           |
|         | ....     | .....                 | .....    | 27.60                      | 1.14     |               |           |
|         | ....     | .....                 | .....    | 27.60                      | 1.14     |               |           |

If we compare the mean results for  $\gamma$  with the exhaustion used (pressure *p* in the vacuum chamber, full barometric pressure *p*<sub>0</sub> in the air-chamber), the results decrease slightly as the vacuum is higher. Thus

|      |            |        |        |        |        |        |
|------|------------|--------|--------|--------|--------|--------|
| If   | <i>p</i> = | 58 cm. | 48 cm. | 39 cm. | 30 cm. | 21 cm. |
| Then | $\gamma$ = | 1.23   | 1.18   | 1.15   | 1.14   | 1.13   |

which is what might have been expected, except that the rate of decrease is much less than would be surmised. There seems thus to be no objection to the use of high exhaustions, which in turn give a better value of  $\gamma$  from the large range of  $\Delta N$  obtained.

The low mean value of  $\gamma$  obtained has been referred to the resistance of the inch piping to the outflow of air. It is probably not due to the stop-cock, as incidental differences in the speed of opening and closing would otherwise have shown a marked effect. One may conclude that the air in the long inch gas-pipe expands adiabatically with a coefficient  $\gamma$  between 1.1 and 1.2, in case of such exhaustions as the above.

91. **The same. Diameter of tube, two inches.**—The experiments were now continued by enlarging the diameter of the tube to 2 inches. Brass gas-pipe, 1.35 cm. long, to be closed with thick glass plates, was at hand. To connect the same with the vacuum chamber, a similar 2-inch pipe, 115 cm. long, as far as the 2½-inch stopcock, was necessary. Moreover, as this was in the way of the light received from the grating, the beam was reflected by an offset consisting of two silver mirrors in parallel. No difficulty was found with this arrangement, and the sodium line was in view to give evidence if any accidental displacement should occur.

Unfortunately, the ellipses obtained were somewhat irregular open forms (*i.e.*, half ellipses), and the endeavor to secure small closed patterns did not succeed. This annoyance depending chiefly on the parts of the mirror and grating used, and on shifting accessories, is not easily controlled. The individual measurements of  $\Delta N$  are therefore not as good as those recorded in table 18, where a displacement of  $10^{-4}$  cm. was assured. They suffice, however, for the present purposes.

The new data are given in table 19,  $t$  being the temperature of both chambers,  $p_0$  the initial normal pressure of the air-chamber (2-inch pipe), and  $p$  that of the vacuum chamber.

TABLE 19.—Values of  $\gamma$ . Brass gas-pipe, 2 inches internal diameter.  
 $C=952.6$ ;  $1+x=1.0341$ .  $e=135.3$  cm.  $(V+v)/v=1.049$ .

| Series. | $t$  | $p_0$ | $p$   | $10^3 \Delta N$ | $\gamma$ |
|---------|------|-------|-------|-----------------|----------|
| I       | °C.  | cm.   | cm.   | cm.             |          |
|         | 17.0 | 75.66 | 56.46 | 7.15            | 1.35     |
|         | .... | ..... | ..... | 7.35            | 1.30     |
|         | .... | ..... | ..... | 7.25            | 1.33     |
|         | .... | ..... | ..... | 7.55            | 1.27     |
| II      | 17.0 | 75.66 | 47.36 | 10.85           | 1.33     |
|         | .... | ..... | ..... | 10.95           | 1.31     |
|         | .... | ..... | ..... | 11.10           | 1.29     |
|         | .... | ..... | ..... | 11.05           | 1.30     |
| III     | 16.1 | 75.86 | 38.36 | 14.93           | 1.31     |
|         | .... | ..... | ..... | 15.15           | 1.28     |
|         | .... | ..... | ..... | 15.10           | 1.29     |
|         | .... | ..... | ..... | 15.38           | 1.26     |
| IV      | 16.2 | 75.86 | 29.36 | 19.53           | 1.25     |
|         | .... | ..... | ..... | 19.57           | 1.25     |
|         | .... | ..... | ..... | 19.27           | 1.28     |
|         | .... | ..... | ..... | 19.75           | 1.23     |
| V       | 16.4 | 75.86 | 20.36 | 23.71           | 1.27     |
|         | .... | ..... | ..... | 23.95           | 1.25     |
|         | .... | ..... | ..... | 23.70           | 1.27     |
|         | .... | ..... | ..... | 23.75           | 1.26     |

The effective value of  $\gamma$  in these experiments is, for the lower exhaustions, above  $\gamma=1.3$ , showing a considerable improvement over the data for the inch tube, which were not much above  $\gamma=1.1$ . This was to be inferred, of course; but it was not expected that the increment of  $\gamma$  due to increased diameter

would be so rapid. It would seem to be probable, therefore, that if a 4-inch tube were used the conditions for obtaining a trustworthy value of  $\gamma$  would be nearly met.

As the exhaustions in a successive series are gradually increased (initial partial vacua from  $p = 56.46$  cm. to  $p = 20.36$  cm. in the vacuum chamber), the observed values of  $\gamma$  gradually but slowly decrease, the mean values being ( $p_0 = 75.7$  cm. to 75.9 cm.)

|                 |       |       |       |           |
|-----------------|-------|-------|-------|-----------|
| $p = 56.46$     | 47.36 | 38.36 | 29.36 | 20.36 cm. |
| $\gamma = 1.32$ | 1.31  | 1.29  | 1.25  | 1.26      |

where the fourth value is too small, for incidental reasons. This general result is also to be expected; but it is rather remarkable that with such high exhaustions as those finally used the decrease of  $\gamma$  is not more marked.

The work, as a whole, progressed smoothly throughout, the only interference with precision being the incidental occurrence of open ellipses. To obtain other patterns would have required longer additional adjustment than the work at the present stage seemed to warrant.

**92. The same. Diameter of tube, four inches.**—The first experiments made with the 4-inch tube are given in table 20. The completed apparatus showed a slight leak, which could not be detected after long searching. The tube was therefore admitted for a tentative series of experiments. The exhaust pipe here, as above, was rigid and straight, but only 2 inches in diameter, with a 2½-inch stopcock. To exhaust the air-chamber, the handle of the cock was suddenly jerked over an angle 180° between the two closed positions. The plug virtually floated in oil, as shown elsewhere.

TABLE 20.—Values of  $\gamma$ . Brass pipe, 4 inches internal diameter.  $C = 952.6$ ;  $1+x = 1.0341$ ;  $e = 126.9$ .  $(V+v)/V = 1.119$ . Small leak in apparatus.

| Series. | $t$  | $p_0$ | $p$   | $10^3 \Delta N$ | $\gamma$ |
|---------|------|-------|-------|-----------------|----------|
|         | °C.  | cm.   | cm.   | cm.             |          |
| I       | 19.9 | 76.15 | 57.00 | 5.90            | 1.42     |
|         | .... | ..... | ..... | 6.10            | 1.37     |
|         | .... | ..... | ..... | 6.23            | 1.34     |
|         | .... | ..... | ..... | 6.15            | 1.36     |
| II      | 23.0 | 75.79 | 38.39 | 12.40           | 1.36     |
|         | .... | ..... | ..... | 12.73           | 1.32     |
|         | .... | ..... | ..... | 12.60           | 1.30     |
|         | .... | ..... | ..... | 12.75           | 1.31     |
| III     | 23.2 | 75.79 | 29.39 | 15.50           | 1.40     |
|         | .... | ..... | ..... | 15.71           | 1.37     |
|         | .... | ..... | ..... | 15.77           | 1.37     |

As a whole, the results are disappointing; and they are irregular, for mean readings could not be made because of the leak. They are, nevertheless, interesting, inasmuch as with some of the above data they point out a special source of discrepancy. It will be seen that the  $\gamma$  values tend to decrease in successive measurements, beginning with a high value, which is here nearly

correct. This can not be referred to the temperature of the 4-inch tube, because the initial optic density is necessarily measured. It must therefore be due to the temperature of the vacuum chamber. It follows, therefore, that the time allowed in these experiments, between observations, though sufficient for establishing the initial temperature of the air-chamber, is not sufficient for the much larger vacuum chamber. The two chambers are thus no longer at the same temperature, a condition which the equations implicitly assume.

The apparatus was now taken apart and thoroughly overhauled. After reassembling the parts, the chamber was found free from leakage. As the exhaust pipe was in the way of the beam of light entering the telescope, the offset, consisting of two parallel mirrors firmly adjusted, was used without annoyance, here as above. The work throughout progressed smoothly, though the ellipses were again not as satisfactory in form as would have been desirable.

TABLE 21.—Values of  $\gamma$ . Data as in Table II, 4'' brass pipe.

| Series. | $t$  | $p_0$ | $p$   | $10^3 \Delta N$ | $\gamma$ |
|---------|------|-------|-------|-----------------|----------|
| I       | °C.  | cm.   | cm.   | cm.             |          |
|         | 16.5 | 75.90 | 56.80 | 6.34            | 1.33     |
|         | .... | ....  | ....  | 6.15            | 1.37     |
|         | .... | ....  | ....  | 6.27            | 1.34     |
|         | .... | ....  | ....  | 6.30            | 1.35     |
| II      | 16.6 | 75.90 | 47.60 | 9.25            | 1.38     |
|         | .... | ....  | ....  | 9.40            | 1.36     |
|         | .... | ....  | ....  | 9.30            | 1.34     |
|         | .... | ....  | ....  | 9.20            | 1.39     |
|         | .... | ....  | ....  | 9.55            | 1.33     |
|         | 16.7 | 76.19 | 47.89 | 9.31            | 1.37     |
|         | .... | ....  | ....  | 9.45            | 1.35     |
| III     | 16.9 | 76.19 | 38.69 | 12.87           | 1.34     |
|         | .... | ....  | ....  | 12.70           | 1.36     |
|         | .... | ....  | ....  | 12.80           | 1.35     |
|         | .... | ....  | ....  | 12.76           | 1.35     |
| IV      | 17.0 | 76.19 | 29.69 | 16.26           | 1.35     |
|         | .... | ....  | ....  | 16.23           | 1.35     |
|         | .... | ....  | ....  | 16.25           | 1.35     |
|         | .... | ....  | ....  | 16.04           | 1.38     |
| V       | 17.1 | 76.19 | 20.69 | 20.00           | 1.35     |
|         | .... | ....  | ....  | 19.60           | 1.40     |
|         | .... | ....  | ....  | 19.73           | 1.38     |
|         | .... | ....  | ....  | 19.69           | 1.39     |

Table 21 contains the results. Changes in the values of  $\Delta N$  in a given series are most likely referable to the form of the interference pattern, indirectly to the flickering of the electric lamp. There seems to be no evidence to associate them with the manner in which the 2½-inch stopcock is opened and closed. This was merely jerked around 180°, between the two closed positions of the plug, and, so far as can be seen, the rate of motion is adequate. The successive observations show no consistent difference, as was the case

in the preceding table. Hence this discrepancy has been eliminated. What is most interesting is that the 4-inch tube shows no consistent difference in the  $\gamma$  values for high or low exhaustion. Thus the mean values under increasing exhaustion,  $p$ , are

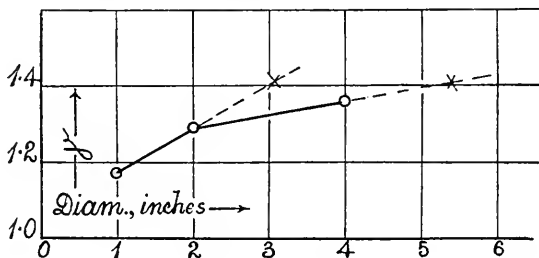
|            |      |      |      |      |      |
|------------|------|------|------|------|------|
| $p =$      | 56.8 | 47.6 | 38.7 | 29.7 | 20.7 |
| $\gamma =$ | 1.35 | 1.36 | 1.35 | 1.36 | 1.38 |

Accidentally the highest value of  $\gamma$  belongs to the highest exhaustion.

The chief anticipation of the work (*i.e.*, that with a 4-inch tube the true value of  $\gamma$  would appear) has not been fulfilled. The value obtained is still much below normal, successive results ranging as follows:

|                          |      |      |          |
|--------------------------|------|------|----------|
| Diameter of tube.....    | 2.5  | 5.0  | 10.0 cm. |
| Mean $\gamma$ .....      | 1.17 | 1.29 | 1.36 cm. |
| Diameter of exhaust pipe | 2.5  | 5.0  | 5.0 cm.  |

The relatively small increase between the tubes 5 cm. and 10 cm. in diameter is disappointing. At the rate obtained from the first two experiments (see fig. 95) a 3-inch tube should have been nearly sufficient. At the rate established by the last two observations, however, a tube at least 5.5 inches



95

in diameter would be needed to obtain trustworthy values of  $\gamma$ . These differences are possibly due to the exhaust pipe, which in case of the last observation does not increase in size. Hence a 3-inch pipe with a 4-inch stopcock may be estimated as being adequate for  $\gamma$  measurement, provided the exhaust pipe is straight and clear throughout.

The observations were broken off at this point, with the object of searching for some means of obtaining a more sensitive and regular interference pattern. If the method is to be ultimately successful, then  $10^{-4}$  cm. on the micrometer must be guaranteed. If the ellipses are not quite regular or not closed, this is not the case. A more sensitive method of defining optic density is thus in question.

## CHAPTER XIII.

### MISCELLANEOUS EXPERIMENTS.

**93. Effect of ionization on the refraction of a gas.**—It seemed interesting to test this question carefully, although a negative result was to be expected. Accordingly one component beam was surrounded by a thick iron tube, while the other was allowed to travel freely in air, along a path energized by the X-rays. For this purpose the X-ray bulb was placed near the grating and the radiation directed toward the mirror *N*, the beam *GM* being inclosed. A thick sheet of lead, 1 foot square, was placed behind the bulb to additionally screen off radiation along *GM*. Under these circumstances the ionization along *GN* must have been enormous by comparison with *GM*. Quiet ellipses were produced in the interferometer, and the effect of opening the X-ray current and closing it again, alternately, was observed. Not the slightest deformation of the ellipses or any motion of the fringes could be detected. An ionization effect is therefore wholly absent. It might have been supposed, for instance, that the ions present might load the wave of light and produce an appreciable result in the interferometer (cf. fig. 92).

Since a shift of 0.1 of a ring would probably have been detected,  $\Delta N = 0.00005$  cm. would have produced a perceptible effect. Hence, since  $\mu - 1$  is, roughly, equal to  $\Delta N/e$ , the value of the ionization effect could not exceed

$$\frac{5 \times 10^6}{2 \times 138} = 1.8 \times 10^{-3}$$

The ionization effect can not, therefore, exceed 0.01 per cent of  $\mu - 1$ .

To further test this question, the iron tube, 1 inch in diameter and 138 cm. long, was provided with a fine axial wire about 0.02 cm. in diameter, passing through central holes in the glass plates at the end. The ends of the wire were drawn tight by hard-rubber rods on the outside, so that the tube became a cylindrical condenser. All holes were sealed hermetically with resinous cement. The interference fringes were clearly producible.

The poles of an induction coil were now connected with the inner wire and the tube, respectively, to alternately change the condenser and discharge it, with the object of strongly ionizing the air within. On partial exhaustion the whole tube became luminous, on account of the discharge, in the usual way.

The best results were obtained with a plenum of air when but two storage cells actuated the coil. Under these circumstances no sparks passed from core to shell of the iron condenser tube, while the air within was intensely ionized by the silent discharge. On closing the current, from 0.5 to 1 per cent of the rings was swept inward at once. On opening it, the rings again emerged. This inward motion, however, was in the same sense as the effect of a decrease of

density, such as would result, for instance, from rise of temperature or from partial exhaustion. Hence the effect observed, though very definite, would correspond to a temperature effect due to electrical currents traversing the air. One should expect the effect of ionization, if appreciable, to be the reverse of this. With voltages high enough to produce sparks in the tube, the interference figures naturally show violent agitation or quiver. If the displacement in question is one ring and  $\delta$  denotes differences,  $\delta(\Delta N) = 30 \times 10^{-6}$  cm.

If only temperature changes, one may write, roughly,  $\Delta N \cdot \tau = \text{constant}$ ,  $\tau$  referring to absolute temperature, whence

$$\delta\tau = \tau\delta(\Delta N)/\Delta N = 293 \frac{30 \times 10^{-6}}{40 \times 10^3}$$

if results found for a similar tube, above, be taken.

Thus  $\delta\tau = 2.2 \times 10^{-7}$  degrees centigrade is the average temperature increment, for the whole length of the tube.

When but a single cell was used to energize the coil, no effect could be recognized. In case of two cells, moreover, when the plenum of air was replaced by a partial vacuum of 1 cm. or less, so that an arc was seen, no effect was observable, although the reddish light colored the field of the telescope.

There are two points of view, however, from which the assumption of a temperature effect is not admissible. If the pipe is closed, so that the density of the air contained remains unchanged, there is no difference in the phenomenon. But there should not, for the case of constant density, be any effect, unless the nature of the gas is changed. Again, the effect is instantaneous and not increased on keeping the circuit closed. The simple explanation in terms of temperature made above must therefore be taken with reservation. At all events, the effect of ionization would be small and equivalent to a dilution of the gas of but

$$\frac{1}{273} \times 2.2 \times 10^{-7} \text{ or about } 10^{-9}$$

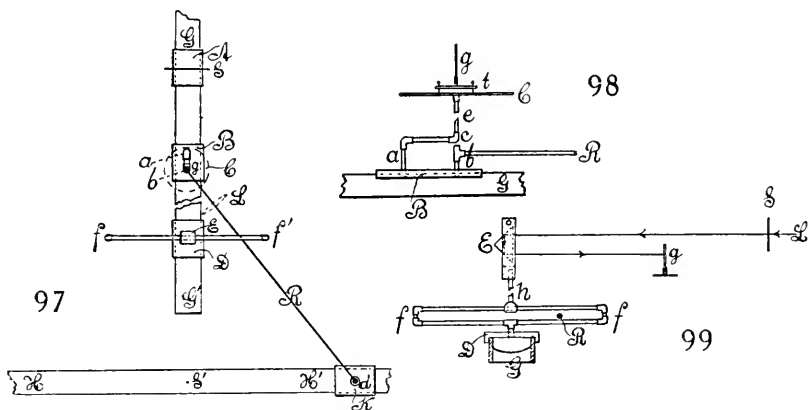
of its density, when sparks are about to occur.

**94. Mach's interferences.**—It is frequently necessary to use the interferometer in such a way that but one ray passes in a given direction; *i.e.*, the rays are not to retrace their path. Interferometers of this kind are treated above, but Mach's design offers advantages, which will be presently pointed out. As a rule, in using these interferometers, the center of the elliptic interference pattern is remote and the lines are hair-like and found with great difficulty. These annoyances are overcome when the apparatus is put together as follows:

In figure 96,  $L$  is the vertical sheet of light from a collimator impinging on the strip of plate glass  $gg$ , half-silvered on one side, toward or near the ends. The pencil  $L$  is thus reflected to the opaque mirror  $N$  and transmitted to the opaque mirror  $M$  (on a micrometer), and then reflected to the other end  $g'$  of the glass strip  $gg'$ . Thereafter, both the pencils,  $Mg'$  and  $Ng'$ , are available;



In figure 97,  $GG'$  and  $HH'$  are double slides like the carriage bed of a lathe, each about 1.5 to 2 meters long and 10 cm. wide, rigidly fastened together. They are placed at right angles to each other on a flat table, the vacant distance between  $G'$  and  $HH'$  being less than a meter. For ordinary purposes they need not be screwed down.  $A, B, D, K$ , are flat carriages, or tables, provided with screw sockets for supporting the different standards, and capable of sliding to and fro with a minimum of friction.  $A$  carries the micrometer slit  $S$ .  $B$  and  $C$  are joined by the Rowland rail  $R$ , whose length is thus equal to the radius of the concave grating to be examined, or nearly so, so that the ends of  $R$  are on vertical axes at  $b$  and  $d$ .  $B$  also supports the table  $C$  (somewhat enlarged in the side elevation, fig. 98), on which the table  $t$  of the grating  $g$  may be adjusted on its leveling screws. To secure a common axis,  $b, e$ , the rod at  $ace$  is twice bent at right angles. Moreover, if  $c$  is turned to one side, the supporting rod  $e$  may be screwed into the vacant socket  $b$  at the end of  $R$ . For the case of figure 98, the angle of diffraction  $\theta$  is varied and  $\lambda = D \sin \theta$ , where  $D$  is the grating space. For the other case ( $c$  being turned aside and  $C$  screwed into and turning with  $b$ ) the angle of incidence is varied and  $\lambda = D \sin i$ . This is much simpler in form than the early method used.



Finally, the table  $C$  carries the essentially new addition to the apparatus (shown in front elevation in fig. 99), viz, the long slot  $ff$ , adapted to support the right-angled reflecting prism  $E$  and at the same time to allow free play to the rail  $R$  within  $ff$ . Figure 99 then shows the progress of the rays (turned  $90^\circ$  to the front in a horizontal plane) from the slit or collimator,  $S$ . They are doubly reflected at  $E$ , return in a vertical plane and then impinge on the grating at  $G$ . The rays thereafter pass along the rail  $R$  (fig. 97) and are examined by a strong eyepiece at  $d$  (not shown), rigidly but adjustably attached to the near end of the rail.

The displacement of  $K$  along  $HH'$  is accurately measurable on a parallel scale with vernier (not shown). If  $x_1$  and  $x_2$  are the two symmetrical readings on opposite sides of the virtual slit image at  $S$  (fig. 97), and  $R$  the radius of the concave grating, and  $x = x_2 - x_1$

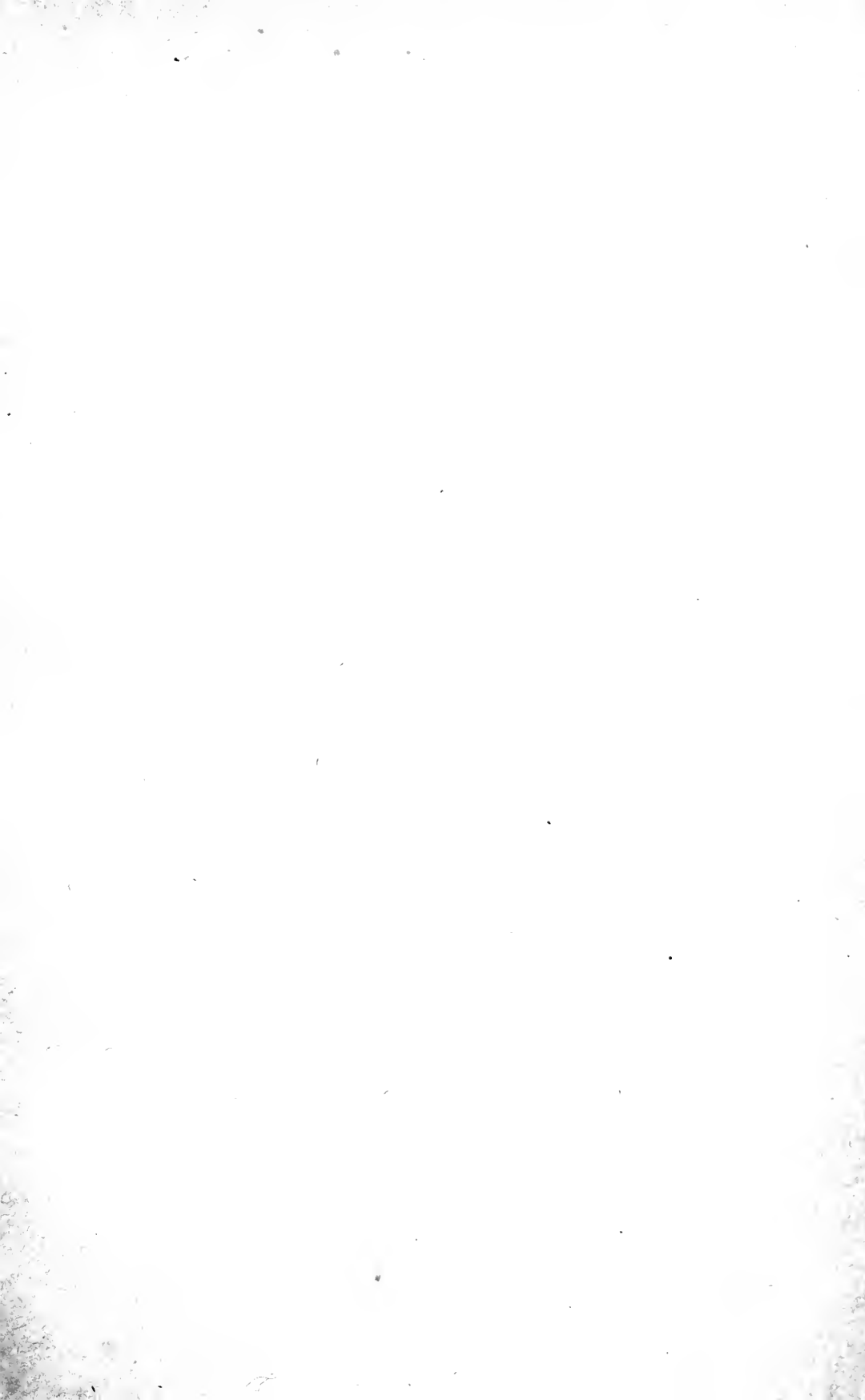
$$\sin \theta = x/2R, \text{ or } \sin i = x/2R$$

If a plane grating is used, a weak lens  $L$  is attached to the rail  $R$  and moves with it, so that its focus is in front of the ocular  $d$  (with cross-hairs). In this case  $S$  is a collimator. If a transmitting grating is examined, the collimator  $S$  (fig. 99), etc., are merely to be lowered, and the prism  $E$  is superfluous. It need not even be removed. Naturally, it is in the interest of accuracy to have all the standards like  $e$  and  $h$  as short as possible.

Finally, in the equation  $\lambda = \frac{Dx}{2R}$ , if  $D = 10^6 d$ , the values  $d$  and  $R$  are usually of the same order (175 cm.) for gratings with about 15,000 lines to the inch. In this case we may make the rail length  $R = d$ , whence

$$\lambda = x/2$$

Even in case of the concave grating, when ultimate precision is not aimed at, some variation of the distance  $SS' = 2SE$ , nearly, is admissible without destroying the definition. The carriage  $D$  with the prism  $E$  may be moved fore and aft on the slides  $GG'$  until the focus at  $d$  is sharp. The values of  $x$  are usually of the order of 100 to 125 cm., so that an accuracy of Ångström units is easily obtainable without special refinement.





MEL WHOLE LIBRARY  
  
WH 18GU I

